Characterization and Application of Mixed Mode Stationary Phases in Pharmaceutical and Biochemical Analysis using One- and Two-Dimensional Liquid Chromatography

Dissertation

der Mathematisch-Naturwissenschaftlichen Fakultät

der Eberhard Karls Universität Tübingen

zur Erlangung des Grades eines

Doktors der Naturwissenschaften

(Dr. rer. nat.)

vorgelegt von

Stefanie Bäurer

aus Donaueschingen

Tübingen

2020

Gedruckt mit Genehmigung der Mathematisch-Naturwissenschaftlichen Fakultät der Eberhard Karls Universität Tübingen.

Tag der mündlichen Qualifikation:	09.10.2020
Stellvertretender Dekan:	Prof. Dr. József Fortágh
1. Berichterstatter:	Prof. Dr. Michael Lämmerhofer
2. Berichterstatter:	Jun.-Prof. Dr. Matthias Gehringer

Table of Content

Abbreviations

^{1}D	First dimension
1D-LC	One-dimensional liquid chromatography
^{2}D	Second dimension
2D-LC	Two-dimensional liquid chromatography
ACD	At-column dilution
ACN	Acetonitrile
AEX	Anion exchange
API	Active pharmaceutical ingredient
ASM	Active solvent modulation
CAD	Charged aerosol detection
CEX	Cation exchange
CSP	Chiral stationary phase
D_{BC}	Box-counting dimension
ELSD	Evaporative light scattering detection
ERLIC	Electrostatic repulsion liquid chromatography
ESI	Electrospray ionization
FA	Formic acid
FDA	Food and Drug Administration
FPP	Fully porous particle
FSM	Fixed solvent modulation
HILIC	Hydrophilic interaction chromatography
HPLC	High performance liquid chromatography
HR MS	High-resolution mass spectrometry
HSM	Hydrophobic subtraction model
ICH	International Council for Harmonization of Technical Requirements for Pharmaceuticals for Human Use
ID	Inner diameter
IEC	Ion exclusion chromatography
IEX	Ion exchange
IR	Infrared
LC×LC	Full comprehensive 2D-LC
LC-LC	Heartcutting 2D-LC
LSER	Linear solvation energy relationship
MeOH	Methanol
mLC-LC	Multiple Heartcutting 2D-LC
MMC	Mixed mode chromatography / Multi modal chromatography
MS	Mass spectrometry
NIST	National Institute of Standards and Technologies
NMR	Nuclear magnetic resonance
Ph. Eur.	European Pharmacopoeia

pI	Isoelectric point
PQRI	Product Quality Research Institute
QSRR	Quantitative structure-retention relationship
Ref.	Reference
RID	Refractometric index detector
RP	Reversed phase
RPLC	Reversed phase liquid chromatography
SAX	Strong anion exchange
SC_G	Surface coverage after Gilar
SC_S	Surface coverage modified by Stoll
SCX	Strong cation exchange
SD	Standard deviation
sLC×LC	Selective comprehensive 2D-LC
SPAM	Stationary phase assisted modulation
SPE	Solid phase extraction
SPP	Superficially porous particle
STO	Statistical theory of peak overlap
TFA	Trifluoracetic acid
THF	Tetrahydrofuran
TOF	Time of flight
UHPLC	Ultra high performance liquid chromatography
USP	United States Pharmacopeia
UV	Ultraviolet
VEM	Vacuum-evaporation modulation
WAX	Weak anion exchange
WCX	Weak cation exchange
ZWIX	Zwitterionic ion exchange

Summary

Nowadays, the use of High-Performance Liquid Chromatography (HPLC) is indispensable in many analytical application fields. Thereby, Reversed Phase Liquid Chromatography (RP LC) is the most frequently used chromatographic mode as it is suitable for the majority of applications. However, the rising requirements in pharmaceutical quality control concerning comprehensive sample characterization as well as the increasing sample complexity rises the need of alternative, complementary chromatographic methods. Besides, the commercialization of two-dimensional liquid chromatography (2D-LC) systems further encouraged the popularity of separation methods complementary to RP LC. In this context, Mixed Mode Chromatography (MMC) gained growing importance alongside Hydrophilic Interaction Chromatography (HILIC).

MMC stationary phases show alternative selectivities due to the surface functionalization of the separation material with multiple interaction sites of different species which are involved in the chromatographic process.

In house synthesized silica gel based MMC stationary phases, namely *N*-Propyl-*N'*-2-pyridylurea and *N*-(10-undecenoyl)-3-aminoquinuclidine modified silica particles, were characterized concerning their flexible use under different elution conditions such as RP and HILIC conditions. The resulting retention data were used in order to comparatively classify the stationary phases by Principal Component Analysis (PCA) to elucidate similarities and dissimilarities. Such projections can support to make a fast-preliminary selection of potentially suitable columns before a specific sample is addressed.

Additionally, the same procedure was used for the characterization of the zwitterionic chiral stationary phases ZWIX(+) and ZWIX(-) which can also be categorized as MMC stationary phases. In order to enhance the understanding of the contribution of the distinct molecule moieties to the chromatographic process, silica particles with immobilized selector fragments of the chiral ligands were characterized in the same manner. As a complementary measure, the conformations of the immobilized ligands were examined by molecular modelling.

Furthermore, the surface charge state of the separation materials was characterized as it plays a crucial role in the separation and retention of charged analytes. In this context, ζ-potential determination as well as a chromatographic characterization proved to offer valuable information.

The characterization of the zwitterionic separation materials ZWIX(+) and ZWIX(-) and the respective fragmented selectors was further supported by the characterization of the free ligands in capillary electrophoresis.

In some cases, the use of high buffer concentrations is necessary in order to analyze multiply charged solutes. This limits the choice of compatible detection methods. Hence, the structure

elucidation of impurities in pharmaceutical drug substances and drug products involve the use of high-resolution mass spectrometry (HR MS) which constrains the tolerated buffer concentrations. In order to address this problem, on the one hand the principle of immobilized counterions was realized and on the other hand, the basicity of the ion exchange site was adjusted to influence the charge state and polarity of the stationary phase. Milder elution conditions up to a umpolung of the surface charge in case of the latter one was the result of both strategies.

Furthermore, column bleeding is an important factor in the routine analysis as well as in the field of structure elucidation as it detrimentally affects the detection sensitivity in universal detection methods and in mass spectrometry in case of ionizable ligands. Therefore, the attachment chemistry is of utmost importance also influencing the column lifetime. Previously, a new attachment chemistry was developed by Zimmermann et al. (*J Chromatogr A*, 1436 (2016) 73-83) where the chromatographic ligand is immobilized on a polysiloxane layer which is multiply linked to the silica particle. The stability of brush-type stationary phases compared to the polymer coated stationary phase was studied in a chromatographic stress test in this work.

Challenging pharmaceutical example mixtures were separated using one dimensional (1D-LC) and two dimensional HPLC (2D-LC) in order to demonstrate the advantage which resulted from the improvement strategies. In 1D-LC nucleotides and synthetic oligonucleotides were analyzed demonstrating the beneficial use of both strategies aiming at the reduction of the utilized counterion concentration.
The simultaneous analysis of fat- and water-soluble vitamins was addressed by selective comprehensive HILIC × RP with precedent optimization of the two chromatographic dimensions using design of experiments (DoE) strategy amongst others. However, the orthogonality of the two dimensions challenged their hyphenation in terms of solvent mismatch problems. Therefore, the active solvent modulation methodology was beneficially used in the 2D-LC method leading to sharp, well resolved peaks in ^{2}D.

Moreover, an impurity profiling set-up for polar analytes was developed. A set of polar stationary phases was screened under HILIC conditions analyzing proteinogenic amino acids. On the basis of these chromatograms, the most promising stationary phases for the HILIC × HILIC system were elucidated. The hyphenation of HILIC systems is challenging because of decreased refocusing possibilities in the beginning of the chromatogram as well as the comparable longer re-equilibration times. In order to prevent solvent mismatch issues, the ^{1}D elution mode eschewed water which has a high elution strength under HILIC conditions. The instrumental set-up included besides the two chromatographic dimensions, the hyphenation of multiple detectors, namely diode array detector (DAD), charged aerosol

detector (CAD) and HR MS. The UV detectors can be used to elucidate relations of compounds due to similar spectra and serve later on as an identification criterion when simpler instrumentations are used. The charged aerosol detector can be used for a quasi-universal quantification of the compound and high-resolution mass spectrometry (HR-MS and MS/MS) serves for proper identification of the peak of interest.

Zusammenfassung

Heutzutage ist die Hochleistungsflüssigkeitschromatographie (HPLC) unverzichtbar in vielen analytischen Anwendungsbereichen. Hierbei zählt die Umkehrphasenchromatographie (Reversed Phase Liquid Chromatography RP LC) zu den am häufigsten verwendeten chromatographischen Modi, da sie für die Mehrheit der Anwendungen geeignet ist. Die steigenden Anforderungen in der pharmazeutischen Qualitätskontrolle bezüglich der umfassenden Charakterisierung des Arzneistoffs und der Arzneimittel sowie die steigende Komplexität von den zu analysierenden Proben im Allgemeinen, erfordern zusätzliche, alternative chromatographische Methoden. Weiterhin fördert die Kommerzialisierung der Systeme für zweidimensionale Hochleistungsflüssigkeitschromatographie (2D-LC) die Beliebtheit der Trennmethoden, die komplementär zu RP LC sind. In diesem Zusammenhang gewinnt Mixed Mode Chromatographie (MMC) neben der Hydrophilen Interaktionschromatographie (HILIC) zunehmende Bedeutung. MMC stationäre Phasen zeigen alternative Selektivitäten aufgrund der Oberflächenfunktionalisierung des Trennmaterials mit mehrfachen Interaktionsstellen verschiedener Art, die in den chromatographischen Prozess involviert sind.

Die in house synthetisierten Kieselgel-basierten MMC stationären Phasen, *N*-Propyl-*N'*-2-pyridylurea und *N*-(10-undecenoyl)-3-aminochinuclidin modifiziertes Kieselgel, wurden hinsichtlich des flexiblen Gebrauchs der Elutionsbedingungen wie beispielsweise RP und HILIC Bedingungen charakterisiert. Um Gemeinsamkeiten und Unähnlichkeiten aufzudecken, verwendete man die erhaltenen Retentionsdaten für eine vergleichende Klassifizierung der stationären Phasen mittels Hauptkompenentenanalyse (Principal Component Analysis, PCA). Projektionen dieser Art können eine schnelle Vorauswahl potenziell geeigneter Säulen unterstützen, bevor eine spezifische Probe untersucht wird.
Dieselben Untersuchungen wurden für die Charakterisierung der zwitterionischen chiralen stationären Phasen ZWIX(+) und ZWIX(-), die ebenfalls als MMC stationäre Phasen kategorisiert werden können, verwendet. Um hierbei das Verständnis des chromatographischen Prozesses zu erweitern, wurden Kieselgel Partikel mit immobilisierten Selektorfragmenten der chiralen Liganden in derselben Art und Weise charakterisiert. Ergänzend erfolgte eine Untersuchung der Konformation der immobilisierten Liganden mittels molekularer Modellierung.
Darüber hinaus wurde der Oberflächenladungszustand des Trennmaterials beschrieben, da er eine wesentliche Rolle bei der Retention und Trennung von geladenen Analyten einnimmt. In diesem Zusammenhang erwiesen sich die Bestimmung der ζ-Potenziale als auch die chromatographische Charakterisierung als wertvolle Informationsquellen. Die Charakterisierung der zwitterionischen Trennmaterialien ZWIX(+) und ZWIX(-) und die

entsprechenden fragmentierten Selektoren wurden weiterführend durch die Charakterisierung der freien Liganden mittels Kapillarelektrophorese unterstützt.

In einigen Fällen sind hohe Pufferkonzentration nötig, um mehrfach geladene Stoffe zu analysieren, wodurch jedoch die Wahl der kompatiblen Detektionsmethoden limitiert ist. Die Strukturaufklärung von Verunreinigungen in Arzneistoffen und Arzneimitteln erfordert dagegen die Verwendung von Hochauflösender Massenspektrometrie (HR MS) wodurch die tolerierte Pufferkonzentration limitiert ist. Um dieses Problem anzugehen, wurde einerseits das Prinzip von immobilisierten Gegenionen realisiert und andererseits die Basizität der Ionenaustauschergruppe angepasst, um den Ladungszustand und Polarität der stationären Phasen zu beeinflussen. Beide Strategien führten zu milderen Elutionsbedingungen bis hin zur Umpolung der Oberflächenladung im Falle der zweiten Strategie.

Darüber hinaus ist Säulenbluten ein wichtiger Faktor in der Routineanalytik sowie im Bereich der Strukturaufklärung, da es die Detektionssensitivität von universellen Detektoren und, im Falle ionisierbarer Liganden, massenspektrometrischer Detektion nachteilig beeinflusst. Daher ist die Anbindungschemie von äußerster Wichtigkeit, da sie einen wesentlichen Einfluss auf die Lebenszeit der Säule hat. Zuvor wurde eine neue Anbindungschemie von Zimmermann et al. (*J Chromatogr A*, 1436 (2016) 73-83) entwickelt, wobei der chromatographische Ligand an einer mehrfach mit dem Kieselgel Partikel verlinkten Polysiloxan-Schicht immobilisiert ist. In der vorliegenden Arbeit wurde die Stabilität durch einen vergleichenden chromatographischen Stresstest der Bürstenphasen und der mit Polymer beschichteten Phasen untersucht.

Herausfordernde pharmazeutische Beispielmischungen wurden mittels eindimensionaler (1D-LC) und zweidimensionaler Hochleistungsflüssigkeitschromatographie (2D-LC) erfolgreich analysiert, um die umgesetzten Vorteile zu demonstrieren. Die Analyse von Nukleotiden und synthetischer Oligonukleotide demonstrierten beispielsweise die Vorteile beider Strategien zur Reduzierung der benötigten Pufferkonzentration. Die gleichzeitige Analyse von fett- und wasserlöslichen Vitaminen wurde durch eine selektive umfassende HILIC × RP Methode angegangen mit vorheriger Optimierung beider chromatographischen Dimensionen unter anderem mittels statistischer Versuchsplanung. Die Kompatibilität der mobilen Phasen beider Dimensionen bei der Kopplung beider Dimensionen erwies sich als herausfordernd aufgrund deren Orthogonalität. Durch die Verwendung der aktiven Lösungsmittelmodulation resultierten in der zweiten Dimension scharfe, gut aufgelöste Peaks.

Beispielsweise zur Erstellung von Verunreinigungsprofilen diente die Entwicklung eines speziellen instrumentellen Aufbaus. Ein Set polarer stationärer Phasen wurde unter HILIC Bedingungen zur Analyse von proteinogenen Aminosäuren getestet. Auf der Basis dieser Chromatogramme konnte die vielversprechendste Kombination der stationären Phasen für die HILIC × HILIC Trennung eruiert werden. Die Kombination von zwei HILIC Dimensionen kann

herausfordernd sein, da eine Refokussierung zu Beginn des Chromatogramms schwieriger ist und längere Reequilibrierungszeiten notwendig sind. Um Lösungsmittelinkompatibilitäten vorzubeugen, wurde in der mobilen Phase der ersten Dimension auf Wasser verzichtet, da dies eine hohe Elutionskraft unter HILIC Bedingungen besitzt. Der instrumentelle Aufbau umfasst außer den beiden chromatographischen Dimensionen ebenfalls die Kopplung multipler Detektoren wie Dioden Array Detektor (DAD), Charged Aerosol Detektor (CAD) und Hochauflösende Massenspektrometrie (HR MS). Dabei dient der DAD Detektor zur Unterstützung der Aufklärung von verwandten Verbindungen aufgrund ähnlicher Spektren und kann später als Identifikationskriterium bei einfacheren instrumentellen Aufbauten verwendet werden. Charged Aerosol Detektion ist ein quasi universeller Detektor, der zur Quantifizierung der Verbindungen verwendet werden kann. Die hochauflösende Massenspektrometrie dient der zuverlässigen Identifikation des gewünschten Peaks.

List of Publications

Publication I

Stefanie Bäurer, Aleksandra Zimmermann, Ulrich Woiwode, Orlando L. Sánchez-Muñoz, Markus Kramer, Jeannie Horak, Wolfgang Lindner, Wolfgang Bicker, Michael Lämmerhofer, Stable-bond reversed-phase/weak anion-exchange mixed-mode stationary phase obtained by simultaneous functionalization and crosslinking of a poly(3-mercaptopropyl)methylsiloxane-film on vinyl silica via thiol-ene double click reaction. *J. Chromatogr. A*, 1593 **(2019)** 110-118.

Publication II

Stefanie Bäurer, Stefan Polnick, Orlando L. Sánchez-Muñoz, Markus Kramer, Michael Lämmerhofer, *N*-Propyl-*N'*-2-pyridylurea-modified silica as mixed-mode stationary phase with moderate weak anion exchange capacity and pH-dependent surface charge reversal. *J. Chromatogr. A*, 1560 **(2018)** 45-54.

Publication III

Stefanie Bäurer, Wenkai Guo, Stefan Polnick, Michael Lämmerhofer, Simultaneous separation of water- and fat-soluble vitamins by selective comprehensive HILIC × RPLC (high-resolution sampling) and active solvent modulation. *Chromatographia,* 82 **(2019)** 167-180.

Publication IV

Stefanie Bäurer, Martina Ferri, Andrea Carotti, Stefan Neubauer, Roccaldo Sardella, Michael Lämmerhofer, Mixed-mode Chromatography Characteristics of Chiralpak ZWIX(+) and ZWIX(-) and Elucidation of their Chromatographic Orthogonality for LC×LC Application. *Anal. Chim. Acta*, 1093 **(2020)** 168-179.

Publication V

Martina Ferri*, Stefanie Bäurer*, Andrea Carotti, Marc Wolter, Belal Alshaar, Johannes Theiner, Tohru Ikegami, Carolin West, Michael Lämmerhofer, Fragment-based Design of Zwitterionic, Strong Cation- and Weak Anion-Exchange Type Mixed-mode Liquid Chromatography Ligands and their Chromatographic Exploration. *J Chromatogr A*, 1621 **(2020)** 461075.

*shared first authorship

Author Contributions

Publication I

Stable-bond reversed-phase/weak anion-exchange mixed-mode stationary phase obtained by simultaneous functionalization and crosslinking of a poly(3-mercaptopropyl)methylsiloxane-film on vinyl silica via thiol-ene double click reaction

Stefanie Bäurer
Concept and workplan
Main HPLC experiments
Data evaluation and interpretation
Classification of the stationary phases
Stress test
Writing of the manuscript

Aleksandra Zimmermann
Synthesis of the stationary phases of the MMC stationary phases
HPLC experiments
Proofreading of the manuscript

Ulrich Woiwode
Synthesis and column packing of stationary phases
Proofreading of the manuscript

Orlando L. Sánchez-Muñoz
Zeta potential determination
Proofreading of the manuscript

Markus Kramer
NMR measurements
Proofreading of the manuscript

Jeannie Horak
Discussions
Proofreading of the manuscript

Wolfgang Lindner
Scientific discussions
Proofreading of the manuscript

Wolfgang Bicker

Stress test

Proofreading of the manuscript

Michael Lämmerhofer

Scientific concept

Discussions of the results

Review and editing of the manuscript

Financing of the project

Corresponding author

Publication II

N-Propyl-*N*′-2-pyridylurea-modified silica as mixed-mode stationary phase with moderate weak anion exchange capacity and pH-dependent surface charge reversal

Stefanie Bäurer
Concept and workplan
Main HPLC experiments
Data interpretation
Classification of the stationary phase
Writing of the manuscript

Stefan Polnick
Synthesis of the stationary phase
Column packing
HPLC experiments
Proofreading of the manuscript

Orlando L. Sánchez-Muñoz
Zeta potential determination
Proofreading of the manuscript

Markus Kramer
NMR measurements
Proofreading of the manuscript

Michael Lämmerhofer
Scientific concept
Discussions of the results
Review and editing of the manuscript
Financing of the project
Corresponding author

Publication III

Simultaneous separation of water- and fat-soluble vitamins by selective comprehensive HILIC × RPLC (high-resolution sampling) and active solvent modulation

Stefanie Bäurer

1D- and 2D-LC experiments

Data evaluation and interpretation

Partial writing the manuscript

Wenkai Guo

1D-LC experiments

Data processing with MODDE

Stefan Polnick

Synthesis of the stationary phase

Proofreading of the manuscript

Michael Lämmerhofer

Scientific concept

Discussions of the results

Financing of the project

Writing and review of the manuscript

Corresponding author

Publication IV:

Mixed-mode Chromatography Characteristics of Chiralpak ZWIX(+) and ZWIX(-) and Elucidation of their Chromatographic Orthogonality for LC×LC Application

Stefanie Bäurer
Concept and workplan
main LC and LC-MS experiments
Data evaluation
Classification of the stationary phases
Writing of the manuscript

Martina Ferri
Zeta-potential determination
Proofreading of the manuscript

Andrea Carotti
Molecular modelling studies
Partial writing of the manuscript
Proofreading of the manuscript

Stefan Neubauer
LC-MS measurements
Support, advice and discussions for MS measurements and data evaluation
Proofreading of the manuscript

Roccaldo Sardella
Molecular modelling studies
Partial writing of the manuscript
Proofreading of the manuscript

Michael Lämmerhofer
Scientific concept
Discussions of the results
Financing of the project
Review and editing of the manuscript
Corresponding author

Publication V

Fragment-based Design of Zwitterionic, Strong Cation- and Weak Anion-Exchange Type Mixed-mode Liquid Chromatography Ligands and their Chromatographic Exploration

Martina Ferri* (shared first authorship)
Synthesis of the stationary phases
Zeta potential determination
HPLC experiments
Data evaluation and interpretation
Visualization
Writing of the manuscript
Review and editing of the manuscript

Stefanie Bäurer* (shared first authorship)
Data evaluation and interpretation
HPLC experiments
Supervision of experiments
Partial writing of the manuscript
Review and editing of the manuscript

Andrea Carotti
Molecular Modelling studies
Visualization
Review and editing of the manuscript,

Marc Wolter
Zeta potential determination
CE experiments
Partial writing of the manuscript

Belal Alshaar,
Synthesis of the stationary phases
HPLC experiments

Johannes Theiner
Elemental analysis

Tohru Ikegami

General scientific concept

Methodology

Supervision

Review and editing of the manuscript

Acquisition of funding

Caroline West

General scientific concept

Methodology

Review and editing of the manuscript

Michael Lämmerhofer,

General scientific concept

Methodology

Supervision, discussions of the results

Review and editing of the manuscript

Resources

Corresponding author

List of Poster Presentations

Jahrestagung der Deutschen Pharmazeutischen Gesellschaft e.V. (DphG) 2016,
München,Germany, October 4th to 7th

Characterization and Application of Stable-bond Reversed-phase/Weak Anion-exchange Mixed-mode Silica in Pharmaceutical Research

Stefanie Bäurer, Aleksandra Zimmermann, Orlando Sánchez-Muñoz, Michael Lämmerhofer

ANAKON 2017, Tübingen, Germany, April 3rd to 6th

Characterization of Stable-Bond Reversed Phase/Weak Anion-Exchange Mixed-Mode Silica

Stefanie Bäurer, Aleksandra Zimmermann, Jeannie Horak, Michael Lämmerhofer

HPLC 2017, Prague, Czech Republic, June 18th to 22nd

Comparison of Orthogonality of Commercially Available Hydrophilic Interaction Chromatography Stationary Phases and Ion Pair Reversed Phase Chromatography for the Separation of Amino Acids

Stefanie Bäurer, Stefan Neubauer, Michael Lämmerhofer

11th Balaton Symposium on High-Performance Separation Methods, 2017, Siófok, Hungary, September 6th to 8th

Characterization of Stable-Bond Reversed Phase/Weak Anion-Exchange Mixed-Mode Stationary Phases and the Benefit of Strong Acidic Co-Ligands

Stefanie Bäurer, Aleksandra Zimmermann, Jeannie Horak, Michael Lämmerhofer

Awarded with a Poster Award

ISC 2018, 32nd International Symposium on Chromatography, 2018, Cannes-Mandelieu, France, September 23rd to 27th

Influence of the Immobilization Chemistry on Chromatographic Features of Reversed Phase/Weak AnionExchange Mixed Mode Silica Gel

Stefanie Bäurer, Aleksandra Zimmermann, Jeannie Horak, Michael Lämmerhofer

Awarded with a Genzo Shimadzu Best Poster Award

HPLC 2019, 48th International Symposium of High-Performance Liquid Phase Separations and Related Techniques, Milan, Italy, June 16th to 20nd

Mixed Mode Stationary Phases and their Benefit in LC × LC

Stefanie Bäurer, Stefan Neubauer, Michael Lämmerhofer

Awarded with an Agilent Technologies Best Poster Award

12th Balaton Symposium on High-Performance Separation Methods, 2019, Siófok, Hungary, September 11th to 13th

Mixed Mode Stationary Phases and their Benefit in Two-Dimensional Pharmaceutical Analysis

Stefanie Bäurer, Stefan Neubauer, Michael Lämmerhofer

Awarded with a Poster Award

List of Oral Presentations

29th Doktorandenseminar 2019, Hohenroda, Germany, January 6th to 8th

Mixed Mode Stationary Phases and their Benefit in Pharmaceutical and Biochemical Analysis

Stefanie Bäurer, Stefan Polnick, Aleksandra Zimmermann, Jeannie Horak, Michael Lämmerhofer

1. Introduction

1.1. Pharmaceutical Background

The development of new drugs substances and the respective drug product necessitates the characterization of its efficacy and safety. However, the safety of a drug product is not only determined by toxicity and adverse effects of the drug substance, but also of the degradation products and impurities. Therefore, it is of utmost importance to characterize the drug substance as well as the drug product comprehensively [1-3]. The approved guidelines are offered by the International Council for Harmonization of Technical Requirements for Pharmaceuticals for Human Use (ICH), which categorizes organic impurities, inorganic impurities and residual solvents [2]. Albeit, especially in case of complex drug substances, very low, but harmless levels of impurities may result out of an economical production which arises the need of a thorough monitoring [4]. In this context, there are guidelines for the calculation of three threshold levels namely reporting, identification and qualification thresholds, as defined by the ICH [2, 3, 5]. The comprehensive characterization should be started already in the early stages of the development of the new drug product facilitating the understanding of the origin of eventually occurring impurities [6-8]. The stability testing comprises besides time coursed studies also stress tests characterizing the influence of temperature, ultraviolet (UV) light exposure, humidity, acid/base treatment and oxidation [2, 3, 9]. Thus, deviations in the manufacturing process can better be identified and evaluated with the help of the comprehensive knowledge about the impurity profile of the active pharmaceutical ingredient (API) and the drug product. Also the impurity profile of approved drugs need to be updated regularly [6].

Nowadays, High Performance Liquid Chromatography (HPLC) is state of the art in the quality control of pharmaceutical drugs and formulations [8]. The comparably uncomplicated hyphenation of this technique with numerous detection methods such as diode array detection (DAD), charged aerosol detection (CAD), evaporative light scattering detection (ELSD), refractive index detector (RID) and mass spectrometry (MS) counts to its major benefits [10]. The most popular technique in pharmaceutical quality control is by far Reversed phase liquid chromatography (RP LC) [8]. However, the structural similarity of the API and the degradation product is given in many cases and the concentration of the degradation product might be very small compared to API. Therefore, a co-elution of the API and the degradants cannot be excluded. In order to identify co-eluting peaks, the need for complementary analytical methods arises [11]. Hydrophilic interaction chromatography (HILIC) and Mixed mode chromatography (MMC) gained in this context increasing attention. They offer alternative retention profiles to

the well-known RP chromatography. Stationary phase classification procedures can help to narrow down suitable alternatives.

The chromatographic methods can be combined on the one hand in traditional approaches where either the full sample or the peak of interest is manually collected and subjected to the second chromatographic method. On the other hand, the second chromatographic dimension can be hyphenated using a special 2D-LC interface for online two-dimensional chromatography (2D-LC). Herein, the drug substance is analyzed in the first dimension (^{1}D) and either the peak of interest or the complete first dimension is fully automated transferred to the second complementary dimension with comparatively low effort [1, 12, 13]. Alongside biopharmaceuticals and biosimilars [14], complex mixtures can be generated by complex drug matrices or multi drug mixtures. Due to the combination of two chromatographic dimensions, the resolving power is significantly increased [15], and such samples can be comprehensively addressed as well. This underlines the potential of the use of 2D-LC in pharmaceutical analysis either for complex mixtures or in case of supposed co-elution.

1.2. Silica Particle Morphology and Ligand Attachment Strategy

1.2.1. Kinetic Performance and Silica Particle Architectures

Stationary phases based on silica possess outstanding good properties in terms of the chemical and mechanical stability, loading capacity as well as the solvent compatibility. Therefore, these support materials are used commonly in almost every chromatographic mode in HPLC [16].

Silica materials experienced a development concerning the chromatographic performance. In this connection, the Van-Deemter equation plays an important role describing the dependency of the parameters influencing the chromatographic efficiency. The plate height H is expressed in dependence of the linear flow velocity u.

$$H = A + \frac{B}{u} + C \cdot u \qquad (1)$$

Hereby, the different multiple possible flow paths through the packed bed of the silica particles, the so-called Eddy diffusion, are represented by the A-term. Smaller and homogeneous particles result in better column packing quality and thus reduces the contribution of this term. The compound diffusion along the column from the concentrated analyte zone into the less concentrated, adjacent sectors (band broadening) is called longitudinal diffusion and characterized by the B-term. An increased flow velocity decreases the influence of this phenomenon. Furthermore, the diffusion of the analyte into the pores of the particles can be observed influenced by the diffusion coefficient of the analyte. This causes a migration delay as the flow velocity is decreased in the pores (flow gradient) and is described by the C-term, the so-called mass transfer resistance. The increase of the flow rate promotes this phenomenon [17].

On the one hand, the silica particles were optimized concerning the contribution of the A-term and C-Term by decreasing the particle size from 10 µm over 5 and 3 µm down to sub-2-µm fully porous particles (FPP) [18]. The improved efficiency at higher flow rates results in ultrafast separations using particles smaller than 2 µm. (Fig. 1). Hence, the resulting backpressure stemming from the compact column bed encouraged the development of Ultra High-Performance Liquid Chromatography (UHPLC) instruments as the use of standard HPLC instruments is constrained due to pressure limits. UHPLC instruments tolerate high pressures up to 1200-1300 bar and are optimized in terms of extra column dispersion effects and detector sampling rates [18].

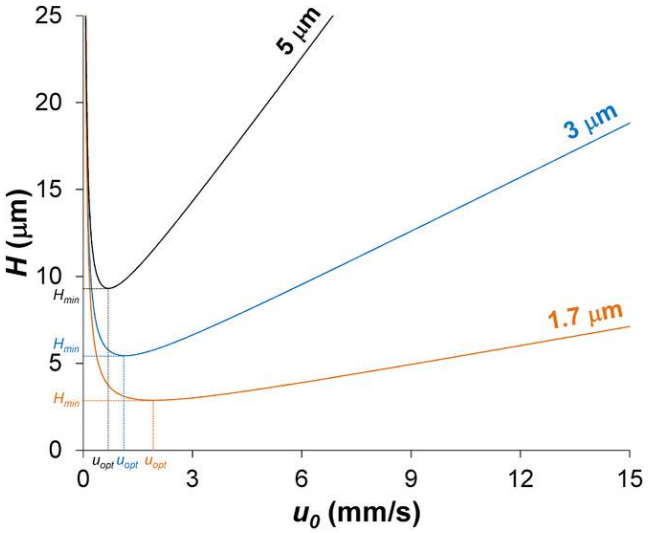

Fig. 1: Comparison of the chromatographic performance of 5, 3 and 1.7 µm silica gel particles. The smaller particles offer higher optimum flow velocities and suffer less of mass transfer resistance as the flow velocity is increased. Reprinted with permission from John Wiley and Sons from J.L. Dores-Sousa, J. De Vos, S. Eeltink: Resolving power in liquid chromatography: A trade-off between efficiency and analysis time, Journal of Separation Science, 42 (2019) 38-50 (Ref. [17]), Copyright 2018 WILEY-VCH Verlag GmbH & Co. KGaA, Weinheim

Additionally, the high pressure causes frictional heating effects meaning axial and radial temperature gradients in the column which can result in efficiency loss [19].

On the other hand, the particle design was optimized in order to improve the chromatographic performance [20, 21]. Particles consisting of a solid core and a surrounding porous shell, were developed, also known as superficially porous particles (SSP), core-shell or pellicular particles. After the introduction, or better renaissance (such materials were already proposed by Cs Horvath as pellicular particles decades ago), of the first commercially available materials in 2006, these support materials gained rising popularity [18, 22]. Due to the production process the particle size distribution is narrow leading to less heterogeneously packed columns. Consequently, the A-term (Eddy diffusion) is reduced [23]. The solid core hinders the diffusion of the analytes in regard of limiting the number of diffusion paths and constraining the diffusion into the particle pores. This decreases the influence of the A-, B- and C-term [22].
In consequence, the use of coreshell particles (inner diameter (ID) 2.7 µm, for example) leads to separations with comparable performance like fully porous particles of lower particle size (e.g. sub 2 µm) while showing significantly lower backpressures at the same conditions [24]. This offers the possibility to use standard HPLC instruments [24]. Moreover, the heat dissipation is improved by the solid core. Band broadening effects caused by frictional heating are therefore reduced [19].

1.2.2. Modification of Silica Particles with Special Attention to Column Bleeding

Bare silica is often modified in order to introduce additional interaction sites at the surface of the particles which can alter the chromatographic selectivity. The stability of the attachment chemistry must be taken into account since the ligand coverage influences the column selectivity and peak shape [25-27]. Furthermore, the detachment of ligands, the so-called column bleeding, can be measured as background signal in various detection methods [28, 29]. Ultraviolet/vis (UV) detection shows generally decreased sensitivity for column bleeding, though, depending on the used wavelength and the presence of a UV chromophore in the ligand [29]. Thus, the detection sensitivity can be significantly influenced when mass spectrometry (MS) or universal detectors like charged aerosol detector (CAD) and evaporative light scattering detector (ELSD) are used [28, 29].

Although silica particles allow the use of a wide range of pH values, the solubility of the silica support is prone to dissolve under alkaline conditions (pH>7.5) [30] and acidic conditions promote the hydrolysis of siloxane bonds [25-27]. Furthermore, metal contaminations, present in a significant degree in type A silica, catalyze the detachment especially at low pH values [31]. Therefore, nowadays, the silica type B is preferred with low metals contents [25].

Alternatively, organic/inorganic hybrid materials which introduce alkyl bridges such as ethyl bridges into the silica network, are used for stabilization of the silica support [32].

The removal or hindered accessibility of surface siloxane bonds are alternative strategies which were followed. The former includes the silanization of type B silica particles replacing silanol groups with silica hydride groups at the surface (silica type C, hydride materials) [33]. Alternatively, bulky side chains were used in order to shield sterically the attachment sites [34-36].
Furthermore, the increase of the number of the attachment sites per chromatographic ligand leads theoretically to an improved stability. Following this approach, siloxane based stationary phases like bidentate silica [34, 37], horizontally polymerized silica [38], polymer coated [39-41] and the hydrophobization of the silica surface followed by functionalization via polymer coating [42] were proven to have a superior column life time.

1.3. Chromatographic Modes and Functional Surface Modifications

1.3.1. Reversed Phase Liquid Chromatography (RP LC)

Reversed phase (RP) liquid chromatography is a well-established, popular chromatographic technique [8] which is especially suitable for non-polar and moderately polar analytes. Besides other support materials, silica gels modified with alkyl chains of different lengths (e.g. C1, C4, C8 and C18) are used [43, 44]. The selectivity range can be altered by the use of aryl- [45], perfluorinated- [46] or cyano- ligands [47], for example. The mobile phases usually consist of pure organic solvents such as methanol (MeOH), acetonitrile (ACN) or tetrahydrofuran (THF), or mixtures with water [48]. The retention of the investigated compounds increase with the polarity of the mobile phase as the retention is governed by the degree of hydrophobic interactions. Thus, especially affecting the analysis of basic analytes, poor peak symmetry combined with unexpected high retention can be observed depending on the utilized stationary phases and mobile phase conditions which can be affiliated to secondary interactions. Silanophilic interactions which are interactions of the analyte with surface silanol groups, are responsible for this observation [49-52]. There are many attempts to systematically characterize these additional interactions [53-56]. The strategies which aim to improve column lifetime (compare chapter 1.2.2) like the removal or the shielding of the attachment sites, generally also reduce silanophilic interactions. Furthermore, the implementation of polar groups has gained popularity. Surface-near polar-embedded groups or polar end capping provide additional interaction sites and additional selectivities for polar compounds [57-59]. Besides, mobile phase additives can also support to improve the peak shape. In this context, acids like formic acid (FA) and trifluoracetic acid (TFA) are often used to suppress the dissociation of the surface silanol groups [52]. Alternative mobile phase additives are amines [49, 60], phosphate and volatile buffers [61] and ionic liquids [62]. Overloading effects can be avoided when the concentrations of the additives are adjusted to a sufficient level [63]. The polarity range of the investigated analytes can be extended by the addition of hydrophobic acids or bases to the mobile phase and the sample solution. This is known as ion pair reversed phase (IP RP) chromatography. Thereby, ion pairing agents form ion pairs with the analyte which appear less hydrophobic. Moreover, the ion pairing agent interacts with the surface of the stationary phase and offers additional interaction possibilities [52].

As the investigated pH value significantly contributes to the charge state of the analyte and therefore to its physicochemical properties, it significantly influences the retention [52, 64].

The temperature during the chromatographic process plays a decisive role. In general, the higher the temperature, the lower is the retention leading to decreased analysis times [52].

1.3.2. Ion Chromatography

The chromatography addressing especially charged analytes was introduced in the 1970ies [65]. The stationary phases which are used in this chromatographic mode, possess charged groups at the surface interacting with analytes. Depending on the polarity, anion (AEX) and cation exchange (CEX) site can be distinguished serving for attractive and repulsive electrostatic interactions. Strong ion exchange ligands (IEX) are formed, for example, by sulfonic acids (strong cation exchange (SCX)) and quaternary amines (strong anion exchange (SAX)). These modifications usually bear a charge if the pH value is lower than 12 or higher than 2, respectively [66]. The surface charge state can be better influenced in case of weak ion exchange sites which are only charged over a constrained pH range. This includes weak cation exchange site (WCX) like carboxylic acids but also weak anion exchange sites like primary, secondary, and tertiary amines (weak anion exchange (WAX)). The combination of both, anion and cation exchange site in the same separation material was also reported leading to zwitterionic (ZWIX) materials [67].
Polymeric coated materials are popular as support materials due to the increased stability [68, 69]. Nevertheless, the chromatographic selectivity can be influenced by support matrices [68]. Exemplarily, the use of polydivinylbenzene coated stationary phases lead to long retention times accompanied by peak tailing of polarizable anions [68, 70].
The mobile phase usually consists of water. Faster elution can be achieved by the addition of an organic modifier portion [68] which prevents specific adsorption [71].
A constant pH value and a controlled change of the pH value, respectively, is ascertained by the use of buffers as it can significantly affect the ion exchange capacity of the stationary phase as well as the charge state of the sample. Compared to the ion exchange site oppositely charged analytes are retained due to attractive electrostatic interactions. The ion exchange process can be described stoichiometrically. The stoichiometric displacement model expects a competition of the analyte and the buffer molecules whereby it is assumed, that the logarithm of the buffer concentration linearly correlates with the logarithm of the retention factor [72]. The retention time decreases with increasing counterion concentration. A detailed description and application can be found in chapter 4.1.4.34.1.4.3, 4.1.7.6, 4.2.4.4, 4.3.4.2.3 and 4.4.4.4. Additionally, increasing valences of the molecules enhance the affinity of the analyte to the stationary phase. The same situation is observed for the buffer besides other properties of the buffer influencing retention.

If the charge of a compound has the same polarity as the surface, repulsive interactions are occurring. Usually, retention times smaller than the void time are observed since the analytes are excluded and repelled by the separation material. This is known as Ion exclusion chromatography (IEC). The acidity and basicity, respectively, of the separation material as well

as of the analyte significantly contributes to the degree of repulsion. This means, the dissociation increases the higher the acidity/basicity [73]. The degree of resulting electrostatic forces is influenced by the acidity of the sample, in case strong ion exchangers are used. Broad analyte bands are usually observed for weak acids/bases due to partial dissociation and comparatively weak interactions [73, 74]. The kind and concentration of the buffer affects the separation as well. Ion exclusion phenomena can hardly be explained by stoichiometric models. Alternative models like the double layer theory assume a gradient of ions (declining for counterions) from the surface to the bulk mobile phase resulting in an accumulation of counterions on the surface. Thereby the so-called Stern layer is formed located in close proximity to the surface of the particle consisting of ions oppositely charged to the surface. Thereafter, the diffuse layer is formed by loosely bond counter- and co-ions as shown in Fig. 2 [72].

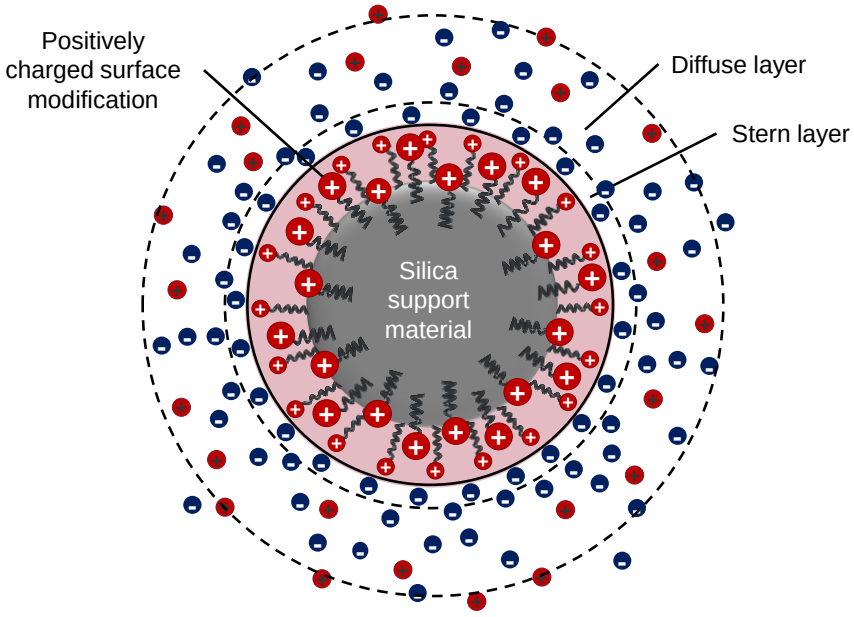

Fig. 2: Schematic illustration of the ion distribution of a modified silica particle in buffer solution according to the double layer theory [72]. (anions are shown in blue and cations in red).

Accordingly, the greater the distance from the surface the lower is the electrostatic potential. Increasing buffer concentrations lead to shielding effects of both, the charge of the ion exchange site as well as of the solute and consequently the retention enhances due to reduced repulsive forces [72, 75]. Besides electrostatic forces, additional interactions can occur due to, for example, hydrophobic molecule moieties contributing to the retention and selectivity. The degree of these interactions can be controlled by the use of organic modifiers [73].

1.3.3. Hydrophilic Interaction Chromatography (HILIC)

Analytes with dominant polar or acidic/basic physicochemical properties suffer from retention and/or selectivity in RPLC. Hydrophilic interaction chromatography (HILIC), the terminology was introduced by Alpert in 1990 [76], addresses these analytes. The utilized stationary phases possess polar and/or charged surface properties and can be classified into polar neutral stationary phases like amide [77], cyano [78] and diol modified silica [79], anionic stationary phases (polyaspartic [76, 80] or bare silica [78, 81], cationic stationary phases (amino [82], triazole [83]) and zwitterionic columns (sulfoalkylbetaine [84-86], phosphocholine [87], pyridinium based [88]).

Usually, mixtures of acetonitrile and water are used as mobile phase, whereby the acetonitrile content is very high (usually between 60 and 95%), including the use of additives like buffers and/or acids [89-92]. The polar surface combined with the aqueous acetonitrile rich mobile phases causes the formation of a water enriched layer on the surface of the stationary phase as depicted in Fig. 3 [90].

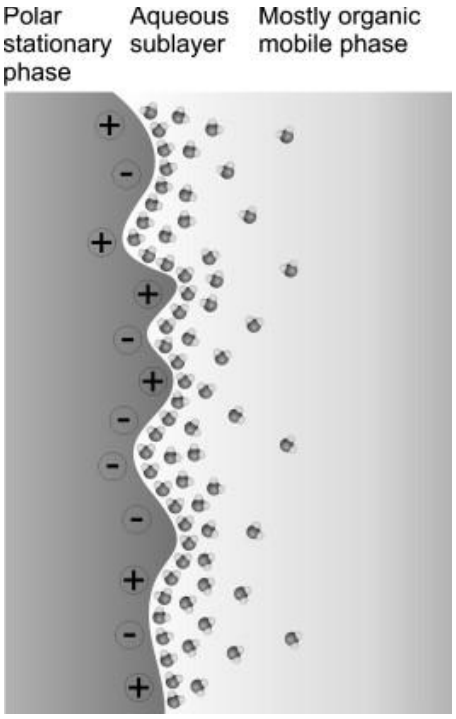

Fig. 3: Schematic accumulation of water at the surface of the stationary phase when using aqueous acetonitrile rich mobile phases, which leads to a water gradient towards the bulk mobile phase.
Reprinted from P. Jandera, Stationary and mobile phases in hydrophilic interaction chromatography: a review, Analytica Chimica Acta, 692 (2011) 1-25. (Ref. [90]) Copyright 2011 Elsevier B.V. with permission from Elsevier.

The extent of the water layer is affected by the polarity of the surface of the stationary phase and the composition of mobile phase [93-95]. Dynamic modelling studies of the water structure lead to the assumption of a gradient of the water density with decreased levels of coordination and order [96].

The retention mechanism is discussed as combined partitioning and adsorption process, also including contributions of electrostatic and polar interactions [89-92]. The retention of the analytes can be increased by enlarging the water content [90] up to a certain point when solvophobic interactions can occur. This dual mechanism leads to a rebound of the retention times resulting in the so-called U-shaped curves, when log k is plotted against the volume fraction of water (φ_{H2O}) [89-91, 97]. The affinity difference of the mobile phase components plays a crucial role in terms of the formation of the water layer [98]. While the selectivity is adversely influenced when acetonitrile is substituted by methanol [90, 92], other alcohols like ethanol or 2-propanol seem to compete less with water [90-92]. However, the elution strength can be controlled by the partial or complete replacement (non-aqueous HILIC or polar organic mode) of the protic modifier water with alcohols leading to alternative selectivities [91, 92, 99, 100].

Since the protonation of the eluite as well as the stationary phase can depend on the pH value [89-92], buffers are required in order to stabilize the chromatographic separation regarding the peak shape [90, 101]. Especially in case of weak acids and bases, the effect of a pH value change is more pronounced compared to strong analogues [92]. Besides others, ammonium acetate and ammonium formate are often used buffers. Since these buffers are volatile, they show good compatibility with detection methods like MS or CAD [89, 90]. While the retention times of non-ionizable compounds are weakly dependent on the investigated salt concentration, acidic, basic or zwitterionic analytes show a clear dependence, especially in combination with protic or charged stationary phases [102, 103]. The increase of the buffer concentration causes a decrease of retention times of compounds following an ion exchange process [89-92]. Analytes with the same polarity as the stationary phase surface are repelled. Thus, these analytes show a significant retention when high levels of organic modifier are used. This phenomenon is known as Electrostatic repulsion liquid chromatography (ERLIC) [104]. Depending on the solute-stationary phase combination, the temperature can be used as an additional parameter for optimizations [92].

Compared to RP LC, HILIC shows improved sensitivity with MS. On the one hand, this can be attributed to the high amount of acetonitrile which efficiently evaporates using Electrospray ionization (ESI). On the other hand, the dissociation of the analytes is altered beneficially influencing the MS sensitivity [105].

1.3.4. Mixed Mode Chromatography (MMC)

In traditional RP LC chromatography, secondary interactions like for example silanol effects were regarded as disadvantageous due to the possible deteriorated performance of the chromatographic separation [55]. Besides the numerous approaches to eliminate them [52], this supposed drawback is instrumentalized by Mixed-Mode Chromatography or Multi-Modal-Chromatography (MMC) and turned into an advantage whereby multiple different types of interactions sites are available for the separation of the analyte mixtures [106, 107]. In consequence, MMC stationary phases benefit from a flexible use of elution conditions [108] combined with an extended field of application [109, 110], complementarity to RP LC [106, 111].

1.3.4.1. Variety of the Design of the Stationary Phases

The idea of offering multiple interactions simultaneously in order to separate challenging samples was developed already in the 1960ies when proteins were purified with MMC mode materials [112]. The rediscovery of the potential of MMC stationary phases started at the beginning of this century [113]. Alongside the inline coupling of two columns [114] different types of MMC materials based on silica have been developed. Basically, the materials can be divided into bimodal and trimodal types which differ in the number of incorporated functional groups. The combination of unpolar interaction moieties and polar and/or ionic functional groups leads to RP/IEX, RP/HILIC, RP/HILIC/IEX and RP/AEX/CEX = RP/ZWIX materials, while polar and ionic functional groups from HILIC/AEX, HILIC/CEX and HILIC/AEX/CEX, also known as HILIC/ZWIX materials [106, 113]. The unpolar moieties are often formed by alkyl chains (e.g. C3 to C18) [115, 116] and aromatic groups [116]. The polar groups are hydroxyl [117], thioether [108], amide [118] and carbamate [118] groups besides others. The ion exchange sites can be divided into strong ion exchangers like sulfonic acids [119], phosphoric acids [120], quaternary nitrogens as a part of a heterocycle [116, 121] and weak ion exchangers like carboxylic acids [118] and primary, secondary and tertiary amines [108].

Furthermore, the design of the stationary phases can be distinguished in terms of the different locations of the interaction functionalities like illustrated in Fig. 4 [122]:

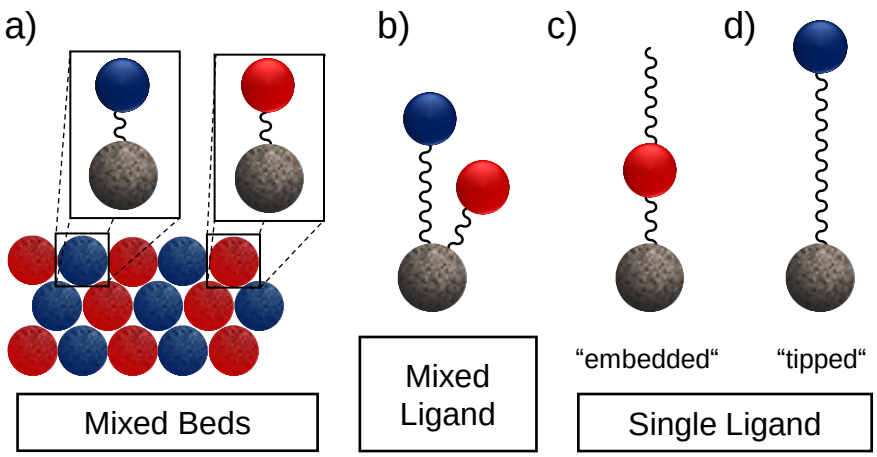

Fig. 4: Different design types of mixed mode stationary phases as classified in Ref. [122]: The multiple interaction sites can be implemented in the stationary phases by a) mixture of differently modified silica particles, b) modification of silica particles with different chromatographic ligands or single selectors with c) “embedded”, or d) “tipped” integrated interaction sites. Functionalities of different kinds are represented by the waved line, and the blue and red points.
For further information, the reader is referred to Ref. [122].

(i) Mixed beds: Two differently modified silica gel particles, e. g. SCX and AEX [114] or RP and IEX [123], are mixed and packed into one column. A disadvantage of this type is poor reproducibility [106].

(ii) Mixed ligands: Different chromatographic ligands are immobilized on the same chromatographic support like for example alkyl chains and diol groups (RP/HILIC) for bimodal materials [117] or RP/WAX ligands and CEX ligands for trimodal materials [41, 115, 119].

(iii) Single ligands: The chromatographic ligand integrates two or more functionalities available for solute-stationary phase interactions. Polar or ionizable groups can be located close to the silica surface (“embedded”) or at the end of the chromatographic ligand (“tipped”). An example for the “embedded” type was synthesized by Jiang et. al. combining benzimidazolium with an C8 alkyl chain [116]. A “tipped” ligand is represented by the combination of a hydrophobic carbon chain and 3-aminoquinuclidine as anion exchange site [124].

However, mixed mode stationary phases were developed showing a huge variety of surface modifications with manifold designs in the past years [113, 125].
A popular field of research is the use of ionic liquids derived from pyridine and imidazole, for example, [119, 126] combined with different functional moieties such as hydrophobic alkyl chains [116], polar groups [118], acids and bases [127] or even with two functionalities [119], for instance.
Examples for more complex ligands than the already mentioned ones, are calixarene derived stationary phases combined with polar groups [128] or ionic liquids [129] and the exploitation of the functional groups present in peptides immobilized on silica gels [130, 131].

Alongside brush-type stationary phases, the immobilization of a functional polymer coating gains rising importance as it combines the advantages of both materials. The physical, chemical and kinetic properties of silica are maintained and additionally enhanced by the diverse modification possibilities of polymers as well as the outstanding good chemical stability [113].

Homo polymeric chains with multiple functional groups [132] as well as the mixture of polymerization substrates in a random [133] as well as in a block copolymerization reaction [134] were reported. The latter two examples offer the possibility to adjust the physicochemical surface properties by the adjustment of the ratio of the substrates [133].

An alternative ligand design is represented by dendritic stationary phases [135], just to mention a few.

1.3.4.2. Multi Modal Applicability

The manifold designs of mixed mode stationary phases share the incomparable flexibility of the choice of the chromatographic mode. Hence, the selection of the elution conditions affects the dominant interactions responsible for the retention and separation of the analytes. An example is shown in Fig. 5. The same RP/WAX stationary phase shows successful separations of dipeptides under both, RP (a) (according to the lipophilicity) and (b) HILIC conditions (according to their hydrophilicity) [108] while single mode columns would usually lack of retention in one mode. Therefore, mixed mode stationary phases can be used under multiple chromatographic conditions offering promising, often complementary results [41, 106-108, 111, 113, 115, 120, 124, 125, 136]. Adjustable parameters for optimization approaches are the kind and concentration of the organic modifier and buffer as well as the adjusted pH value as well as the temperature [110, 124].

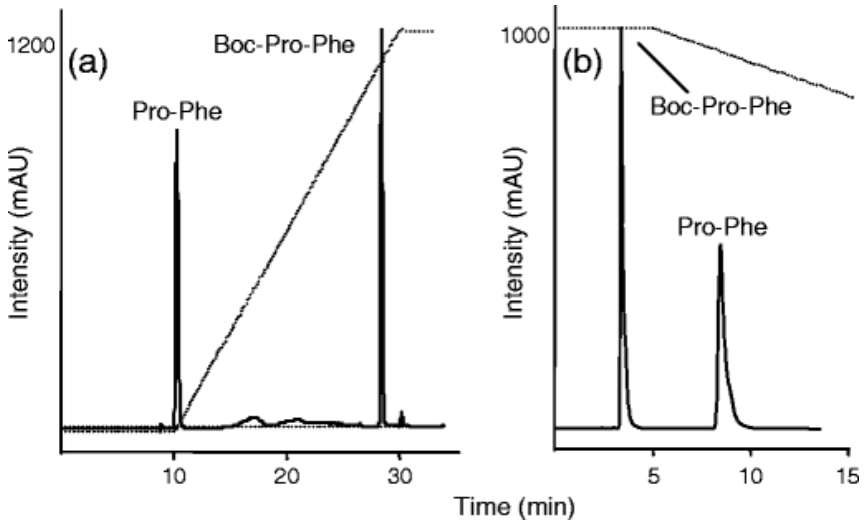

Fig. 5: Multi modal applicability of a RP/WAX mixed mode stationary phase: separation of Pro-Phe and Boc-Pro-Phe under a) RP conditions and b) under HILIC conditions with reversed elution order. Experimental conditions: a) mobile phase: A: H_2O, B: ACN, C: 100 mM H_3PO_4, triethylamine was used for pH adjustment (pH=3) gradient: C was constant at 10%C during the analysis time, 0% B 0–10 min, 0-90% B 10–30 min; 0.2 ml/min from 0–5 min, .0.2 to 1 ml/min from 5–10 min, 1 ml/min 10-30 min; 25 °C; 215 nm b) mobile phase: A: H_2O, B: ACN, C: 200 mM H_3PO_4, triethylamine was used for pH adjustment (pH=3); gradient: C was constant at 5%C during the analysis time, 90% B 0–5 min,90-50% B in 60 min; 1 ml/min; 25 °C; 215 nm Reprinted with permission from Springer Nature Customer Service Centre GmbH: Spinger Nature: M. Lämmerhofer, R. Nogueira, W. Lindner, Multi-modal applicability of a reversed-phase/weak-anion exchange material in reversed-phase, anion-exchange, ion-exclusion, hydrophilic interaction and hydrophobic interaction chromatography modes, Anal Bioanal Chem, 400 (2011) 2517-2530. (Ref. [108]), Copyright © 2011, Springer Nature

For the demonstration of the suitability of the separation material under a respective chromatographic mode, test mixtures containing selected compounds are often used. Polycyclic aromatic carbohydrates [137, 138] as well as alkylbenzenes with differing alkyl chain length [111, 139] are often used to show the RP suitability. The increase of the organic modifier portion leads usually to dropped retention times of hydrophobic molecules as it is the case in traditional RP LC [115, 120, 137]. Especially in case of RP/IEX, an ion exchange process can be additionally observed. In order to monitor the mixed mechanism, acids and bases with distinct degree of polarity are additionally investigated [111, 139].

The ion exchange process is often further demonstrated by the separation of inorganic ions [118, 137, 138]. A quantification of the ion exchange process was described by the application of the stoichiometric displacement model as the retention time increases with decreased buffer concentration [41, 108, 115, 120, 124, 136].

Mixed mode stationary phases benefit from the manifold interaction sites present at the surface. Thus, the HILIC suitability was often demonstrated by the analysis of polar analytes such as nucleosides [111, 115, 118-121, 129, 132-135, 138], vitamins [111, 115, 119, 120, 132, 135] and xanthins [111, 115, 120]. The study of the retention factor in dependency of the used amount of organic modifier leads also for many mixed mode stationary phases to U-shaped curves (dual retention mechanism) like it is observed for HILIC stationary phases [115, 117, 120, 131].

ERLIC conditions can also be exploited for analytes bearing the same charge like the stationary phase [104]. Since mixed mode chromatography columns offer additional interactions possibilities, the chromatographic process is influenced beneficially which was shown by the reversed phase/cation exclusion separation of the proteins [140].

Therefore, it is not surprising that mixed mode stationary phases cover a broad range of application fields from small to macro molecules. In pharmaceutical analysis, MMC can support beneficially the current chromatographic methods and reduce the effort [107]. Zhang et. al developed a method which analyzes simultaneously organic and inorganic anions and cations using a trimodal mixed mode stationary phase [141]. The analysis of drugs and related substances [142] as well as the analysis of excipients [143] were reported.
Another field is the analysis of drug levels in human plasma [144] and targeted metabolite studies [145, 146]. Additionally, the profiling of complex samples with a high degree of heterogeneity such as plant extracts [121, 133, 134] or metabolomic profiles [147] were described.
Furthermore, peptide separations under multiple chromatographic conditions were reported [108] as well as successful separations of unmodified peptides, phosphorylated peptides and sialylated glycopeptides [148]. Recombinant proteins can show impurities including misfolding and aggregates which could be easily separated by a combined salt/pH gradient using mixed mode stationary phases [149].
Moreover, oligonucleotides were successfully analyzed using mixed mode stationary phases [110, 150] showing better results compared to the respective single mode column AEX and RP columns [110].

Solid phase extraction materials which are important in the preanalytical treatment of many samples, can also benefit from the mixed mode modifications. The matrix can be removed easily, and substance of interest can be enriched [151, 152]. Additionally, the loading capacity is increased compared to RP materials.

1.4. Classification of Stationary Phases

The large number of available stationary phases offer many possibilities concerning the choice of the optimal chromatographic system. Hence, systematic comparative characterizations of stationary phases can facilitate the decision for suitable stationary phases. On the one hand, this includes similar stationary phases when surrogate columns for a specific application are needed. On the other hand, if a utilized stationary phase shows a lack of selectivity, complementary stationary phases will be of interest.

For RP columns numerous tests were developed. Tanka et. al. developed a test method which uses selected analytes and analytes pairs in order to describe distinct properties of the stationary phase such as hydrophobicity, hydrogen bonding, silanol activity/metal activity and steric selectivity for bulky or plane structures, for example [153]. This test was further developed through the statistical processing of the properties via cluster analysis and principal component analysis by Euerby [154] besides other development procedures. An alternative option, following the same principle is the Neue test [155] which allowed the grouping of polar embedded stationary phases by cluster analysis. Alongside another classification procedure, the United States Pharmacopeia (USP) offers a database based on the same principle using the SRM870 mixture provided by the National Institute of Standards and Technologies (NIST) comprising C18 and polar embedded C18 stationary phases [156].
Additionally, retention models like the linear solvation energy relationship (LSER) [157] and hydrophobic subtraction model (HSM) [158] which introduce descriptors in order to characterize the retention process, can be used for the classification of stationary phases. The latter is the basis for the test of the Product Quality Research Institute (PQRI), which is the second method offered by the USP for the elucidation of suitable columns [156]. The stationary phases can be compared by means of a comparison function which considers the evaluated stationary phase descriptors of two materials.

HILIC stationary phases were also compared with the help of similar strategies as used for the characterization of RP stationary phases. Selected analytes were used by Kawachi et. al. in order to characterize the retention behavior in terms of the hydrophilicity, methylene- and hydroxy- group selectivity, isomer and molecular shape selectivity, surface acidity and ion exchange properties [159]. Dinh et. al. characterized hydrophilic, electrostatic, dipol-dipol, hydrophobic and π-π interactions attributed to specific analytes and pairs of analytes [160]. Both models reflect the retention properties of analyte pairs in combination with principal component analysis while the former one additionally uses radar plots for individual illustration. In analogy to the HSM, the hydrophilic subtraction model was developed which considers hydrophilic partitioning, hydrogen bond acidity and basicity as well as cation and anion exchange [161]. Additionally, the LSER model was extended by two additional descriptors for

ionic interactions in order to consider the interactions present during a HILIC separation [162, 163]. This modification of the LSER model proved to be suitable for the characterization of a mixed mode stationary phase [164].

Another test for mixed mode stationary phases uses RP and HILIC conditions and a test set differing in the physicochemical properties. The retention data is processed via principal component analysis in order to elucidate similarities and dissimilarities [111].

1.5. Two-Dimensional Liquid Chromatography (2D-LC)

1.5.1. Principle, Instrumentation and Modes of Operation

The principle of two-dimensional separation techniques was discovered already a long time ago. Examples of the early attempts are paper chromatography [165] as well as thin layer chromatography [166]. Hereby, the ^{1}D separation was extended by a second dimension (^{2}D) by means of a mobile phase exchange and a 90° rotation after the separation in the first dimension (^{1}D). The benefit of the extension of the chromatographic space was also transferred to liquid chromatography [167]. In two-dimensional liquid chromatography (2D-LC), the (partially) collected ^{1}D eluent is subjected to a second chromatographic analysis using different conditions [15].

Basically, offline and online methods can be distinguished [1, 15]. Offline separations cover the collection of the ^{1}D eluent in suitable vessels during a selected time period. Afterwards, the eluent can be (partly) stored and/or used for other analytical methods comprising the second chromatographic dimension. Additionally, it is possible to concentrate the sample (reduced reconstitution volume after evaporation) and to exchange the solvent in order to prevent solvent mismatch problems in ^{2}D. The same standard HPLC system can be used for both dimensions. Consequently, the method length is not limited, and ultrafast separations are not necessary as the ^{1}D eluent is collected and intermediately stored. However, the degradation of the constituents during fraction collection, solvent evaporation, carry over and poor reproducibility are disadvantages of this methodology. Furthermore, many of these methods are time consuming [1].

Online separations use special 2D interfaces. This offers the possibility of an automatic direct transfer of the ^{1}D eluent into ^{2}D. Strong changes in the composition of the sampled ^{1}D eluent caused by decomposition or irreproducible changes of the concentration are less likely due to the timely and automated procedure leading to good reproducibilities. Due to the introduction of ^{2}D, the peak capacity is greatly enhanced which offers the possibility to approach complex samples [1, 15, 168, 169]. Furthermore, selected selectivities can be combined in order to address samples with closely related compounds such as isomers [15].

However, the benefits of 2D-LC is accompanied by some challenges like limited ^{2}D cycle times, insufficient sampling in ^{1}D (undersampling), solvent mismatch of ^{1}D and ^{2}D eluents and sensitivity loss due to the additional dilution in ^{2}D [1, 15, 168, 169]. In the following chapters, the theory, and approaches to overcome these issues are discussed.

1.5.1.1. Instrumentation and 2D-LC Modes

In principle, the hardware of a 2D-LC system comprises the one of two HPLC systems as shown in Fig. 6. Thereby, the autosampler of ^{2}D is replaced by the modulator, also called interface or 2D-LC valve. It injects the ^{1}D eluent into the ^{2}D for further analysis.

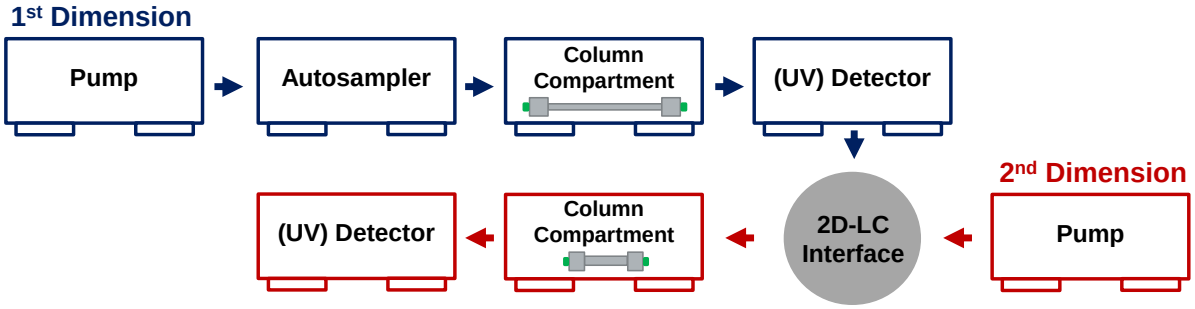

Fig. 6: Configuration of the required HPLC modules for online two-dimensional liquid chromatography separations.

In dependency of the intention of use, different variants of the interface are possible. If only a single ^{1}D fraction needs to be subjected to a ^{2}D analysis, a 2-position/6-port valve can be used as shown in Fig. 7 a) besides other possible configurations [1, 170]. If several ^{1}D peaks are planned to be analyzed in ^{2}D, two 6-port valves can be combined. Alternatively, one 2-position/8- (Fig. 7 b)) or 10- port valve can be utilized [1, 13, 169].

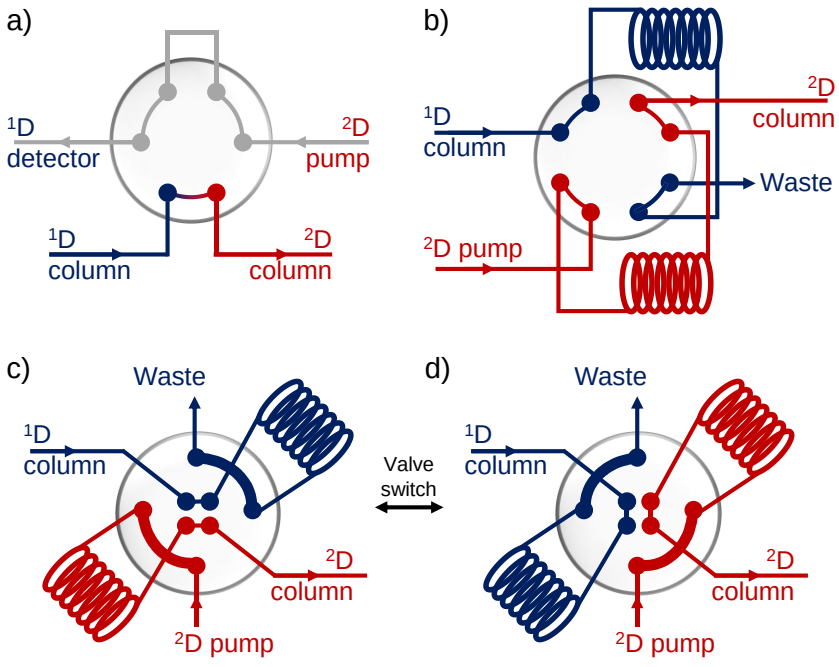

Fig. 7: A selection of possible 2D-LC interfaces: a) 6-port/2-position valve [1, 170], b) 8-port/2-position valve [1, 170] and c) 2-position/4-port duo valve [1, 169] d) including valve switch. For further information the reader is referred to the respective Ref.

The 2D-LC system Infinity II from Agilent Technologies (Waldbronn, Germany) which was used for the 2D-LC measurements in the presented studies, possess a 2-position/4-port duo valve (Fig. 7 c)) as 2D-LC interface. Thanks to the symmetrical construction, there are two identical

flow paths which are connected to a sample loop of adjustable size in each case. Thereby, one loop collects the ^{1}D eluent and the other one transfers ("injects") the ^{1}D eluent which was collected in the previous cycle with the help of the ^{2}D flow onto the ^{2}D column for further analysis. The ^{1}D and ^{2}D flow paths are changed by the valve switch and the corresponding other sample loop serves for sampling of the ^{1}D eluent and the content of the other loop is "injected" into ^{2}D (Fig. 7 d). Additional flexibility arises when the sample loops are replaced by two 6-positions/14-port valves.

Depending on the used set-up, three operation modes are possible which are illustrated in Fig. 8.: a) (multiple) Heartcutting 2D-LC ((m)LC-LC), b) selective comprehensive 2D-LC (sLC×LC), also known as High Resolution Sampling, and c) full comprehensive 2D-LC (LC×LC).

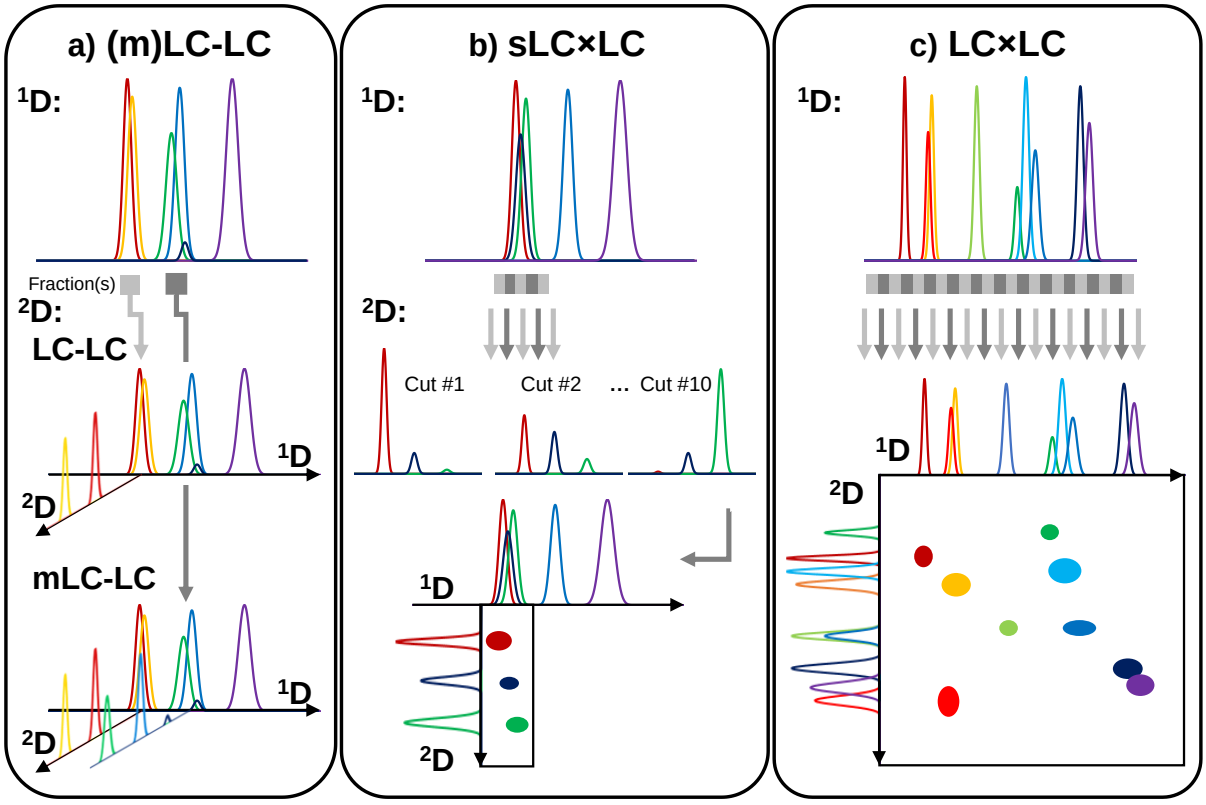

Fig. 8: Comparison of the possible 2D-LC modes: In Heartcutting 2D-LC (LC-LC) (a)) one (LC-LC) or multiple peaks (mLC-LC) are partly transferred into ^{2}D, while in full comprehensive 2D-LC (LC×LC) (c)) the ^{1}D eluent is completely analyzed in ^{2}D. In selective comprehensive 2D-LC (sLC×LC) (b)), the completely covering ^{2}D analysis is confined to a comparatively small area, for example a peak cluster.

In LC-LC (Fig. 8 a)), a selected part (here: maximum one loop fill) of the ^{1}D chromatogram is sampled in one sample loop of the 2D-LC valve. After the valve switch at the end of the selected ^{1}D section, it is analyzed in ^{2}D. This procedure can be repeated as soon as the analysis of the previous cut is completed (minus the time required for the loop fill). If there are more peaks of interest, the set-up can be extended by the replacement of the sample loops with Multiple Heartcutting (MHC) valves (6-position/14-port valves). Each of these valves possess six loops for intermediate eluent storage whereby one loop is always required for the

mobile phase flow either to waste (^{1}D) or to the column (^{2}D). Therethrough, the flexibility of the mLC-LC methods increases since the ^{1}D fractions can be collected while already sampled ones can be analyzed in ^{2}D [15, 171]. As long as the number of loops is sufficient, the ^{2}D analysis time is not constrained.

(m)LC-LC (Fig. 8 a)) is well suited for the analysis of seemingly simple samples with a moderate number of analytes that contain structurally very similar compounds such as enantiomers [172] or isomers [15]. The lack of enantioselectivity in ^{1}D, for example, can be overcome by the use of suitable ^{2}D conditions [172]. Furthermore, this mode can be used as a tool for improving MS compatibility [173, 174]. On the one hand, matrix constituents coeluting with the compound of interest and thus decreasing detection sensitivity in mass spectrometry can be removed by an additional separation in ^{2}D [175].

On the other hand, the ^{1}D separation can be performed using non-volatile buffers like phosphate buffer, for example. The polar buffer lacks of retentivity in a RP phase system which can be used in ^{2}D. Consequently, it elutes within the void volume of the utilized column. By the use of a diverter valve, this part of the chromatogram can be directed to the waste. Afterwards, the diverter valve can switch and direct the remaining part of the chromatogram to the mass spectrometer [173].

Furthermore, ion pairing agents were removed with the additional use of trapping cartridges [176]. Increased detection sensitivity of impurities of therapeutic oligonucleotides was reported by IPRP-HILIC and AEX-HILIC measurements being MS compatible [174]. The quantitation of compounds of interest in ^{2}D is possible in this mode. Thereby, it is recommended to transfer small volumes of the peak located close to its maximum but slightly changing retention time significantly affect the result. In order to overcome this problem, large volumes containing more than the target peak volume can be transferred in ^{2}D. Hence, this can lead to crowded chromatograms [15].

In sLC×LC (Fig. 8 b)), a comparatively small part of the ^{1}D chromatogram is sampled in consecutive cuts and analyzed in ^{2}D [177]. Closely related substances [12], elucidation of coelutions [12, 178] and improvement of MS compatibility and sensitivity [175] can be addressed with sLC×LC, for example. The MHC valves are necessarily required for this mode and serve for the short-term storage of the collected fractions of ^{1}D. This provides flexibility in terms of the analysis time in ^{2}D, but also limits the number of possible cuts according to the number of available loops (maximum ten). Valuable information which can be lost due to undersampling issues in other modes, is obtained because of the complete coverage across the selected time period. In consequence, it is possible to accurately quantify the sampled compounds [15, 171, 175]. In the context of absolute quantification, it should be noted, that

parabolic flow profiles can lead to sample loss. Therefore, a loop fill level of approximately 50% is recommended [168].

As contrasted with LC-LC and sLC×LC which only partly analyses the ^{1}D chromatogram in ^{2}D, full comprehensive 2D-LC (LC×LC) transfers comprehensively the ^{1}D eluent into ^{2}D. The highest degree of information about the eventually numerous analytes can be obtained by the use of this mode [15]. The principle is illustrated in Fig. 8 c). Instead of the MHC valves, loops of equal size are used. Thus, the sampling into one loop and the analysis of the previously sampled fraction in the other loop happens simultaneously. The valve switch changes responsibility of the loops (sampling from ^{1}D and analysis in ^{2}D). As a result, the ^{2}D cycle time which comprises gradient time and re-equilibration (also: modulation or sampling time), is constrained by the time required to fill the loop with ^{1}D eluent. Consequently, lower ^{1}D flowrates lead to longer ^{2}D cycle times. However, the choice of suitable column combinations is of utmost importance [168]. In some cases, however, time can be gained by partial equilibration [179, 180]. Anyway, ultrafast separations achieved by sub-2µm particles or superficially porous particles are required in ^{2}D significantly enhancing the separation power of the 2D-LC method compared to the 1D-LC method [18]. The enlarged separation power is especially suitable for very complex samples [15], for example biological samples in the field of Omics [181], dyes [182] and polymers [183]. The numerous analytes present in these samples can often be not separated by 1D-LC.

1.5.2. Peak Capacity and Undersampling

The peak capacity (n_C) is often mentioned and an important performance parameter in connection with 2D-LC. It characterizes the separation power of the chromatographic system as the number of peaks which can theoretically be observed as a maximum in a (1D) chromatogram [184]. It is assumed, that the peak width is constant under gradient elution conditions. Thus, the peak capacity can be described as follows [185]:

$$n_C = 1 + \frac{t_{R,n} - t_{R,1}}{W} \quad (2)$$

with $t_{R,1}$ and $t_{R,n}$ as the elution times of the first and the last eluting compound, respectively, and W as the average baseline peak width. 1D-LC is already quite powerful and attains already quite high peak capacities [15]. However, in case of very complex samples with thousands of ingredients, the separation space offered by 1D-LC is not sufficient which can be estimated with the help of the Statistical Theory of peak Overlap (STO) [186]. It was revealed that statistically a maximum of 37 % of the possible peak capacity is used with 18 % being single peaks. On the basis of this assumption, 1D-LC is not powerful enough in order to resolve the majority of the analytes in complex samples such as a tryptic digest of a cell extract, a lipidomic or metabolomic samples [186]. This can be overcome by the introduction of a second chromatographic dimension.

The theory of peak capacity can be extended to 2D-LC by multiplying the peak capacities of ^{1}D (^1n_C) and ^{2}D (^2n_C) [187]:

$$\mathrm{n_{C,2D}} = {}^1\mathrm{n_C} \cdot {}^2\mathrm{n_C} \quad (3)$$

The calculated values by means of Eq. (3) usually results in overestimated values compared to the experimentally observed peak capacity due to the assumption of ideal circumstances. Therefore, Eq. (3) was corrected by factors considering the sampling rate in ^{1}D (undersampling correction factor) and the coverage of the two-dimensional retention space.

Undersampling is a result of an insufficient number of collected fractions in ^{1}D. The in ^{1}D separated compounds are remixed during the transfer from ^{1}D into ^{2}D as the volume fraction is too big compared to the ^{1}D peak widths [188].

Fig. 9 illustrates this effect. The sampling rate is indicated within the grey box across the ^{1}D chromatogram and the reconstruction of the ^{1}D chromatogram from the ^{2}D signal below it. The lower the number of collected fractions in ^{1}D, the more pronounced is remixing in ^{2}D as shown in Fig. 9a) [188].

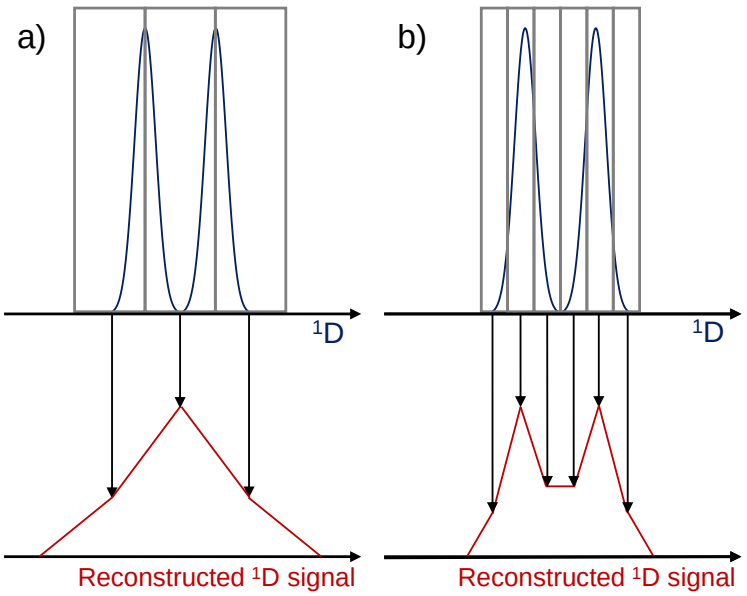

Fig. 9: Schematic depiction of the influence of different sampling rates in ^{1}D on the reconstructed ^{1}D chromatogram from the ^{2}D signal based on the study of Murphy, Schure and Foley [188]. The grey frames indicate the sampled fractions. a) Insufficient sampling rate causes re-mixing of the ^{1}D effluent containing the peaks which were separated in ^{1}D. b) Increasing sampling rates preserves ^{1}D separation in ^{2}D. For detailed information, the reader is referred to Ref. [188].

This effect was studied by a comprehensive investigation of Murphy, Schure and Foley [188]. In order to prevent it, at least three to four fractions across the ^{1}D 8σ peak width are recommended as result of this study [188]. Therefore, the average peak-broadening $\langle\beta\rangle$ was introduced with ^{1}W as the average ^{1}D peak width and t_s as ^{2}D cycle time [189]:

$$\langle\beta\rangle = \sqrt{1 + \kappa\left(\frac{t_s}{{}^{1}W}\right)^2} \;;\; \kappa = 0.21\overline{4} \pm 0.01\overline{0}\,, for\; 0.2 \leq \frac{t_s}{{}^{1}W} \leq 16 \qquad (4)$$

Additionally, the two-dimensional retention space which is used for the elution of compounds ($f_{coverage}$) is implemented into the following equation [190]:

$$n^{*}_{C,2D} = \frac{{}^{1}n_C \cdot {}^{2}n_C \cdot f_{coverage}}{\langle\beta\rangle} \qquad (5)$$

The introduction of the correction factors leads to realistic calculations and less overestimated values of the effective peak capacity $n^{*}_{C,2D}$ but simultaneously a strong dependency of the sample type is introduced [168].

1.5.3. Orthogonality

In order to benefit from the separation power of two-dimensional separations, a suitable combination of separation mechanisms is required. Strongly correlating separation mechanisms are not the most promising combinations in 2D-LC. The greater the degree of independence of the separation mechanisms, the better will be the usage of the separation space which is described by the orthogonality [191, 192].

However, this expects the use of samples which are suited for two dimensional separations by being multidimensional itself, meaning the compounds possess multiple factors which can contribute to the retention [193]. For example, a homologous series of alkylbenzenes with differing chain length is separated due to one relevant factor, the carbon chain length space [193, 194]. Therefore, this sample would be defined as one-dimensional and in consequence there is no benefit by extending the separation space [193, 194]. Another example is a complex sample like a protein digest or other biological samples which contain numerous heterogenous compounds. Such kind of sample will exhibit at least a second factor (net charge, hydrophilicity, molecular volume, besides others). Consequently, the introduction of a second dimension is senseful [194]. Thereby, the dimensionality of the separation system cannot exceed the sample dimensionality, additionally presuming that the decisive factors of the sample are considered during the chromatographic process [193, 194]. This shows that the orthogonality of a separation system is influenced by the chromatographic conditions as well as on the investigated sample and the quality of the interplay.

The correlation of two chromatographic methods can be illustrated by a diagram of the available space for retention, meaning ^{1}D versus the ^{2}D retention times. Therefore, the retention times can be normalized in advance. The retention data of a multi-dimensional sample measured with highly correlating chromatographic methods will cluster along the diagonal across the two-dimensional space as shown in Fig. 10 a). If chromatographic methods are completely uncorrelated, the elution pattern will be equally distributed and ideally ordered (Fig. 10 b)). In practice, the distribution will be more randomly like shown in Fig. 10 c). Additionally, due to a remaining degree of correlation, compound groups and classes, respectively, which elute together in close proximity, can be observed (Fig. 10 d) [168].

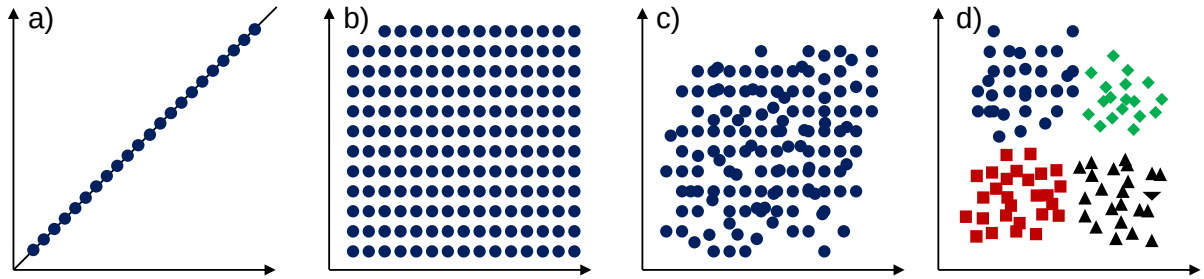

Fig. 10: Different degrees of usage of the 2D separation space with a) highly correlated, b) ideally uncorrelated and c)+d) realistic uncorrelated conditions, In c) a random distribution is shown, while in d) elution of compound group clusters are observed.
Adapted from B.W.J. Pirok, A.F.G. Gargano, P.J. Schoenmakers, Optimizing separations in online comprehensive two-dimensional liquid chromatography, Journal of Separation Science, 41 (2018) 68-98.(Ref. [168]), licensed under CC BY 4.0.

Numerous methods have been developed in order to quantify the orthogonality. Basically, discretizing and non-discretizing methods can be distinguished [192]. Discretizing methods use the division of the separation space into bins according the rules defined in the respective method [192]. This procedure helps to identify used and unused space [192]. Examples are the box-counting dimension D_{BC} [195], the fractional surface coverage SC_G [196] and its modification SC_S [197]. The non-discretizing methods include orthogonality metrics (OM) based on the convex hull method [198], different types of correlation coefficients [199], nearest neighbor distributions [200] and the asterisk method [201] besides others.

The box counting dimension D_{BC} divides the available retention space into different number of boxes due to the mathematical concept of fractals. In the double logarithmic depiction of scaling parameters of the boxes against the number of boxes occupied by eluting compounds, the fractal dimension D_{BC} can now be determined from the slope of least squares regression in the linear data range multiplied by -1 [195]. When two chromatographic dimensions are used, the maximum observed value is 2 representing the highest possible degree of orthogonality.

The bin counting method SC_G developed by Gilar pursues a simpler approach [196]. Thereby, the box size is constant and oriented on the number of sample components. The proportion of occupied bins in the normalized retention space are determined [196]. The modified SC_G method, the SC_S, also includes unoccupied bins that are located between occupied bins [197] leading in some cases to overestimated values [191]. The decision of the number of bins is crucial significantly contributing to orthogonality [191].

The convex hull method which counts to the non-discretizing methods, defines the used retention space by the area which is edged by the connection of the marginal peaks. Due to their similarity, the orthogonality estimation of the convex hull method and SC_S showed similar results in a comparative study [191].

Some correlation coefficients (Pearson, Spearman, Kendal) were tested in order to represent the orthogonality. In studies, the correlation coefficients were compared with other

orthogonality metrics like for example geometric approaches [199]. The Kendall correlation coefficient resulted as the most suitable one [199]. In general, these kinds of descriptors show their strength in the description of correlation [191].

Furthermore, the nearest neighbor distance uses different kinds of mean values of the distance between a compound and the closest one eluting to it [200]. The distances represent the compactness of the separation. The arithmetic mean describes the peak spreading and the harmonic mean the quality of the separation (clustering) [200]. The higher calculated values the higher are the orthogonalities [200].

The asterisk method measures the distribution of peaks in two-dimensional space by determining the standard deviation (SD) of the shortest distance to the introduced Z lines. These four lines cross the retention space. On the basis of SD, the Z values are calculated which serve as a measure of the distribution around the respective Z line. Finally, the orthogonality can be calculated by means of all Z values [201].

For many methods for the determination of the orthogonality, the underlying chromatographic attributes were found to be related. [192]. Furthermore, it was found that it can be differed between measures for near (local) and the far (global) peak distribution [192]. The creation of a combined orthogonality metric by multiplication of, for example the dimensionality as local and the convex hull method as global parameter, showed a benefit. However, other combinations of other descriptors are also conceivable [192].

In general, however, the quality of the determination of the orthogonality improves as the number of peaks increases [191, 192].

1.5.4. Detection Sensitivity and Solvent Incompatibility

Liquid chromatography is always accompanied by a dilution of the sample [202] due to the diffusion of the analyte in the column bed (band broadening effect) [15]. Hence, the additional chromatographic dimension which is introduced in 2D-LC amplifies this effect. The multiplication of both ^{1}D dilution factors leads to the dilution factor of both dimensions [168, 203, 204] considering corrections due to band broadening effects as well as possible focusing in ^{2}D prior to the ^{2}D analysis [168].

Generally, solvent mismatch effects are observed more frequently for weakly retained compounds and usually restrain their detection sensitivity [13, 204]. Especially, highly orthogonal combinations of separation conditions often lead to solvent incompatibilities. Basically, two scenarios are mainly responsible for detrimental effects on the peak shape and performance in ^{2}D.

(i) If there is a significant difference of the viscosities of the ^{1}D and the ^{2}D mobile phase, the eluent with low viscosity (^{1}D) is partially mixed with the high viscosity eluent (^{2}D) at the interface which results in finger profiles (viscous fingering) when it is further transported through the porous media [205]. Broad deformed peaks like shown in Fig. 11, and peak splitting result in the chromatogram [205].

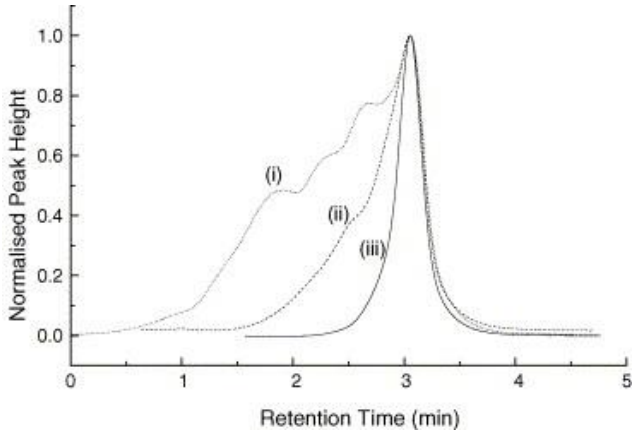

Fig. 11: Influence of the injection volume on the peak profile of p-cresol ((i) 200 µL, (ii) 100µL and (iii) 30 µL) on the peak shape.
Experimental conditions: sample solvent: 100 % ACN, mobile phase 40/60 (v/v) water/methanol [205].
Reprinted from K.J. Mayfield, R.A. Shalliker, H.J. Catchpoole, A.P. Sweeney, V. Wong, G. Guiochon, Viscous fingering induced flow instability in multidimensional liquid chromatography, Journal of Chromatography A, 1080 (2005) 124-131 (Ref. [205]), Copyright 2005 Elsevier B.V. with permission from Elsevier.

(ii) If the ^{1}D mobile phase, which serves as sample solvent in ^{2}D, has a higher elution strength than the ^{2}D mobile phase, the sample retention and performance will be affected adversely, meaning poor performance, deterioration and splitting of the peak up to break through phenomena are possible [13, 204, 206, 207]. Also, pH mismatches show these effects especially for protic analytes as the protonation states can differ [208]. However, very small injection volumes, as can be used in 1D-LC, can weaken or overcome this effect [209]. In

context of 2D-LC comparable high injection volumes are inevitable leading to overloading effects in form of deteriorated peak shape and detection sensitivity [13, 206, 207].

In order to overcome these problems, many strategies have been developed aiming to preserve the retention mechanism which was intended.

Considerations which do not afford additional hardware comprise the ^{2}D injection volumes and the column dimension combination as well as the chromatographic modes in ^{1}D and ^{2}D. The influence of large ^{2}D injection volumes can be relativized by the choice of the appropriate ratio of sample loop size and ^{2}D column volume [168, 174]. Consequently, the sampled ^{1}D volume should be 15 % or less of the ^{2}D column volume [168].

Furthermore, the peak shape and chromatographic performance is beneficially influenced if the ^{1}D mobile phase has a low elution strength in ^{2}D as it serves as sample solvent. This is often the case for RP×RP separations [210], for example. Alternatively, for polar analytes the combination of non-aqueous and aqueous HILIC conditions is suitable [211].

However, there are also alternative solutions required which modulate the solvent mismatch considering for example HILIC×RP separations. Additionally, the ^{1}D effluent can affect the ^{2}D column lifetime when it exceeds the operating limits concerning for example the pH value [169]. Basically, the followed strategies comprised the dilution or replacement of the ^{1}D eluent in order to overcome these issues. A simple approach is the so-called make-up or assistant flow. It dilutes the ^{1}D eluent by means of an additional pump after the ^{1}D detector as shown in Fig. 12 a) [1, 13]. The ratio of the ^{1}D and make-up flowrate determines the dilution. Though, the combination of flows leads to an overall flowrate increase. This arises either the need for increased sample loops or the ^{2}D cycle time need to be decreased in order to prevent the loss of ^{1}D eluent. Alternatively, the use of a flow splitter prior to dilution could prevent the increased sample volumes and additionally improved detection sensitivity [13].

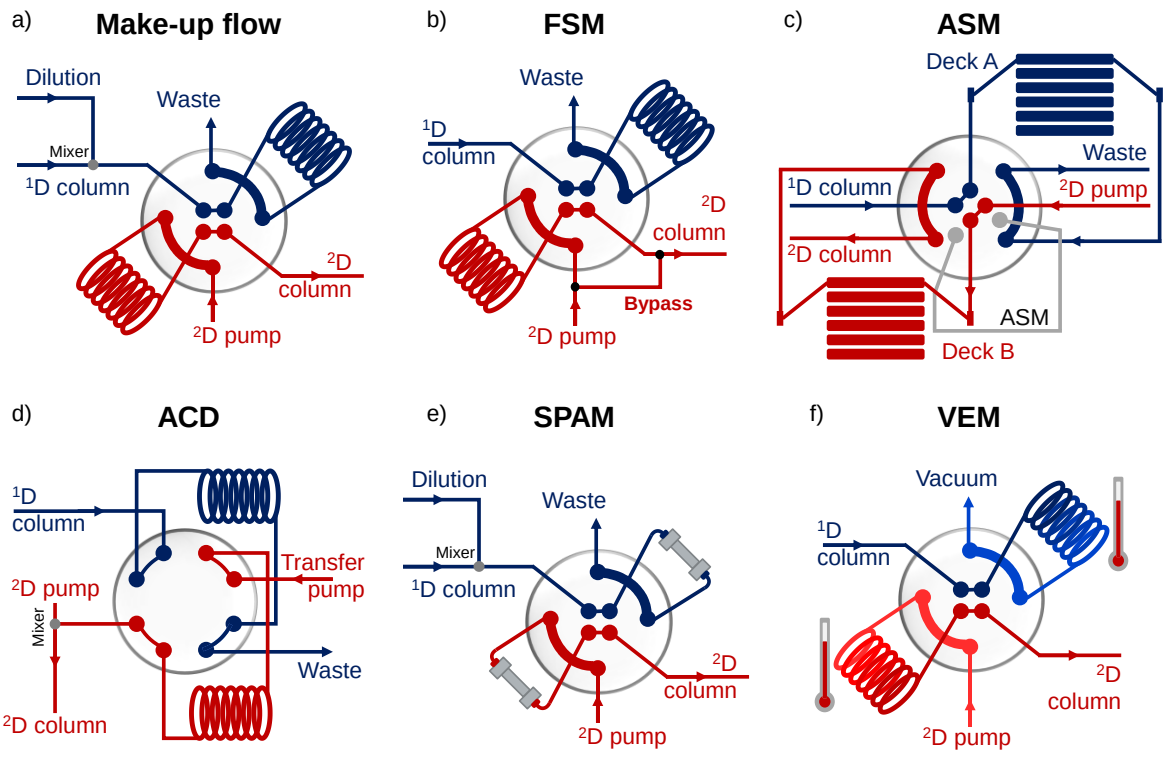

Fig. 12: Different solvent modulation set-ups in order to overcome solvent mismatch in 2D-LC: a) Make-up flow [1, 13], b) Fixed solvent modulation (FSM) [212], c) Active solvent modulation (ASM) with installed multiple heart cutting valves instead of loops [212], d) at column dilution (ACD) [213], e) Stationary phase assisted modulation (SPAM) [214] and f) vacuum evaporation modulation (VEM) [215].

Another approach, Fixed solvent modulation (FSM), aims at the dilution of the ^{1}D eluent with the ^{2}D mobile phase with the help of a bypass starting before the valve and reunites the flow before the ^{2}D column (Fig. 12 b) [212]. Appropriate conditions during the loop flush lead automatically to a dilution of the ^{1}D eluent. The loop content is transferred onto the ^{2}D column and previously diluted with ^{2}D mobile phase and shows consequently less frequently solvent mismatches. However, numerous baseline disturbances due to complex solvent profiles in gradient elution were reported [212]. The re-equilibration time is also influenced by the complex solvent profiles. Furthermore, it needs to be noted, that due to the flow split the loop flush time is prolonged which can significantly contribute to the ^{2}D cycle time [212].

Thus, this approach was further developed to the so-called Active Solvent Modulation (ASM) where the bypass ports are integrated into the 2D-LC valve (Fig. 12 c). Thereby, the valve position can be switched back to the normal loop flush position after the finished transfer stabilizing the solvent flow under gradient conditions. The dilution factor can be adjusted as the flow split is dependent on the flow restriction by the bypass capillary. This means the shorter the capillary the higher is the dilution factor of the ^{1}D eluent assuming the same inner diameter [212].

However, also in this variant of solvent modulation, the flow split causes increased transfer times from ^{1}D eluent into ^{2}D consequently increasing the ^{2}D cycle time. The lower the dilution

factor the less time is needed to flush the loop. Additionally, the doubled number of valve switches is required per ^{2}D cycle which might shorten the lifetime of the valve especially in LC×LC compared to the normal 2-position/4-port duo valve.
Another approach, depicted in Fig. 12 d), is the so-called At-Column Dilution (ACD) which requires an additional pump [213]. The sample is injected into ^{2}D by means of a transfer flow which is united with the ^{2}D gradient flow via a T-piece and a mixer module [213]. The dilution factor is controlled by the transfer time of collected ^{1}D fraction. This means if high flowrates are used which are suitable for LC × LC application, the dilution factor will be small. In contrary, low transfer flow rates lead to high dilution factors which are suitable for LC + LC applications in respect of the required time for transfer [213].

Moreover, trapping columns were installed into the sample loops. The combination with a make-up flow offers the possibility to trap compounds eluting from ^{1}D and transfer them afterwards onto the ^{2}D column with the help of the ^{2}D flow. This set-up is known as Stationary Phase Assisted Modulation (SPAM) (Fig. 12 e)) [182, 214, 216]. Due to the focusing effect on the trapping column, the observed peaks in ^{2}D are narrow and sharp. However, the choice of the kind of trapping column is important in order to retain as many compounds as possible during the complete sampling time. Additionally, the conditions of trapping cartridges crucially responsible for the same sampling conditions, for example, ageing effects [169].

Furthermore, the complete replacement of the ^{1}D mobile phase is realized by Vacuum-Evaporation Modulation (VEM) with the help of heated sample loops and the connection of a vacuum pump after the outlet port in the ^{1}D sampling position of the 2D-LC valve [215]. The set-up is shown in Fig. 12 f). During the sampling, the solvent is evaporated due to the increased temperature and the applied vacuum. After the valve switch, heat treatment helps to improve the dissolution rate in the ^{2}D mobile phase. This technique requires ^{1}D solvents which easily evaporate and non-volatile, easy to reconstitute sample components [169].

Most of these solvent modulation techniques cause a significant increase of the detection sensitivity as reported in the literature [13, 174, 182, 183, 213, 216]. However, this result is not surprising as the consequences of large injection volumes (with higher elution strength of the mobile phase) are attenuated. In some cases, this is additionally accompanied with focused chromatographic bands. The combination of both effects improves the peak shape and enhances the peak height, consequently influencing the detection sensitivity beneficially. The successful validation of 2D-LC techniques was reported offering the use in pharmaceutical quality control [217].

1.6. References

[1] M. Iguiniz, S. Heinisch, Two-dimensional liquid chromatography in pharmaceutical analysis. Instrumental aspects, trends and applications, Journal of Pharmaceutical and Biomedical Analysis, 145 (2017) 482-503.

[2] International Council for Harmonisation of Technical Requirements for Pharmaceuticals for Human Use (ICH), Impurities in New Drug Substances Q3A (R2), 2006.

[3] International Council for Harmonisation of Technical Requirements for Pharmaceuticals for Human Use (ICH), Impurities in New Drug Products Q3B (R2), 2006.

[4] R. Holm, D.P. Elder, Analytical advances in pharmaceutical impurity profiling, European Journal of Pharmaceutical Sciences, 87 (2016) 118-135.

[5] International Council for Harmonisation of Technical Requirements for Pharmaceuticals for Human Use (ICH), Validation of Analytical Procedures: Text and Methodology Q2(R1), (2005).

[6] R. Nageswara Rao, A. Narasa Raju, R. Narsimha, Isolation and characterization of process related impurities and degradation products of bicalutamide and development of RP-HPLC method for impurity profile study, Journal of Pharmaceutical and Biomedical Analysis, 46 (2008) 505-519.

[7] N. Rajana, D.R. Devi, D.N. Kumar Reddy, J.M. Babu, K. Basavaiah, K. Balakumaran, Characterization of Five Oxidative Degradation Impurities and One Process Impurity of Suvorexant Drug Substance by LC-MS/MS, HR-MS and 1D, 2D NMR: Validation of Suvorexant Drug Substance and Process Impurities by HPLC and UPLC, Journal of Chromatographic Science, 58 (2020) 433 - 444.

[8] S. Görög, Critical review of reports on impurity and degradation product profiling in the last decade, TrAC Trends in Analytical Chemistry, 101 (2018) 2-16.

[9] International Council for Harmonisation of Technical Requirements for Pharmaceuticals for Human Use (ICH), Stability Testing of New Drug Substances and Products Q1A(R2), (2003).

[10] K. Zhang, K.L. Kurita, C. Venkatramani, D. Russell, Seeking universal detectors for analytical characterizations, Journal of Pharmaceutical and Biomedical Analysis, 162 (2019) 192-204.

[11] R. Agrawal, S. Belemkar, C. Bonde, Orthogonal Separations in Reversed-Phase Chromatography, Chromatographia, 81 (2018) 565-573.

[12] K. Zhang, Y. Li, M. Tsang, N.P. Chetwyn, Analysis of pharmaceutical impurities using multi-heartcutting 2D LC coupled with UV-charged aerosol MS detection, Journal of Separation Science, 36 (2013) 2986-2992.

[13] D.R. Stoll, E.S. Talus, D.C. Harmes, K. Zhang, Evaluation of detection sensitivity in comprehensive two-dimensional liquid chromatography separations of an active pharmaceutical ingredient and its degradants, Analytical and Bioanalytical Chemistry, 407 (2015) 265-277.

[14] C.J. Pickens, I.A. Haidar Ahmad, A.A. Makarov, R. Bennett, B.F. Mann, E.L. Regalado, Comprehensive online multicolumn two-dimensional liquid chromatography-diode array detection-mass spectrometry workflow as a framework for chromatographic screening and analysis of new drug substances, Analytical and Bioanalytical Chemistry, 412 (2020) 2655–2663.

[15] D.R. Stoll, P.W. Carr, Two-Dimensional Liquid Chromatography: A State of the Art Tutorial, Anal Chem, 89 (2017) 519-531.

[16] H. Qiu, X. Liang, M. Sun, S. Jiang, Development of silica-based stationary phases for high-performance liquid chromatography, Analytical and Bioanalytical Chemistry, 399 (2011) 3307-3322.

[17] J.L. Dores-Sousa, J. De Vos, S. Eeltink, Resolving power in liquid chromatography: A trade-off between efficiency and analysis time, Journal of Separation Science, 42 (2019) 38-50.

[18] A.S. Kaplitz, G.A. Kresge, B. Selover, L. Horvat, E.G. Franklin, J.M. Godinho, K.M. Grinias, S.W. Foster, J.J. Davis, J.P. Grinias, High-Throughput and Ultrafast Liquid Chromatography, Analytical Chemistry, 92 (2020) 67-84.

[19] F. Gritti, G. Guiochon, Comparison of heat friction effects in narrow-bore columns packed with core–shell and totally porous particles, Chemical Engineering Science, 65 (2010) 6310-6319.

[20] C.G. Horvath, B.A. Preiss, S.R. Lipsky, Fast liquid chromatography. Investigation of operating parameters and the separation of nucleotides on pellicular ion exchangers, Analytical Chemistry, 39 (1967) 1422-1428.

[21] J.J. Kirkland, Controlled surface porosity supports for high-speed gas and liquid chromatography, Analytical Chemistry, 41 (1969) 218-220.

[22] V. González-Ruiz, A.I. Olives, M.A. Martín, Core-shell particles lead the way to renewing high-performance liquid chromatography, TrAC Trends in Analytical Chemistry, 64 (2015) 17-28.

[23] D. Cabooter, A. Fanigliulo, G. Bellazzi, B. Allieri, A. Rottigni, G. Desmet, Relationship between the particle size distribution of commercial fully porous and superficially porous high-performance liquid chromatography column packings and their chromatographic performance, Journal of Chromatography A, 1217 (2010) 7074-7081.

[24] D.V. McCalley, Some practical comparisons of the efficiency and overloading behaviour of sub-2μm porous and sub-3μm shell particles in reversed-phase liquid chromatography, Journal of Chromatography A, 1218 (2011) 2887-2897.

[25] E.M. Borges, D.A. Volmer, Silica, Hybrid Silica, Hydride Silica and Non-Silica Stationary Phases for Liquid Chromatography. Part II: Chemical and Thermal Stability, J Chromatogr Sci, 53 (2015) 1107-1122.

[26] H.A. Claessens, Trends and progress in the characterization of stationary phases for reversed-phase liquid chromatography, TrAC Trends in Analytical Chemistry, 20 (2001) 563-583.

[27] H.A. Claessens, M.A. van Straten, Review on the chemical and thermal stability of stationary phases for reversed-phase liquid chromatography, J Chromatogr A, 1060 (2004) 23-41.

[28] B. Schulze, T. Bader, W. Seitz, R. Winzenbacher, Column bleed in the analysis of highly polar substances: an overlooked aspect in HRMS, Analytical and Bioanalytical Chemistry, 412 (2020) 4837–4847.

[29] T. Teutenberg, J. Tuerk, M. Holzhauser, T.K. Kiffmeyer, Evaluation of column bleed by using an ultraviolet and a charged aerosol detector coupled to a high-temperature liquid chromatographic system, Journal of Chromatography A, 1119 (2006) 197-201.

[30] J.J. Kirkland, M.A. van Straten, H.A. Claessens, High pH mobile phase effects on silica-based reversed-phase high-performance liquid chromatographic columns, Journal of Chromatography A, 691 (1995) 3-19.

[31] L. Ma, P.W. Carr, Loss of Bonded Phase in Reversed-Phase Liquid Chromatography in Acidic Eluents and Practical Ways To Improve Column Stability, Analytical Chemistry, 79 (2007) 4681-4686.

[32] K.D. Wyndham, J.E. O'Gara, T.H. Walter, K.H. Glose, N.L. Lawrence, B.A. Alden, G.S. Izzo, C.J. Hudalla, P.C. Iraneta, Characterization and Evaluation of C18 HPLC Stationary Phases Based on Ethyl-Bridged Hybrid Organic/Inorganic Particles, Analytical Chemistry, 75 (2003) 6781-6788.

[33] J.J. Pesek, M.T. Matyska, Hydride-based silica stationary phases for HPLC: Fundamental properties and applications, Journal of Separation Science, 28 (2005) 1845-1854.

[34] J.J. Kirkland, J.L. Glajch, R.D. Farlee, Synthesis and characterization of highly stable bonded phases for high-performance liquid chromatography column packings, Anal Chem, 61 (1989) 2-11.

[35] A.B. Scholten, J.W. De Haan, H.A. Claessens, L.J.M. van de Ven, C.A. Cramers, 29-Silicon NMR evidence for the improved chromatographic siloxane bond stability of bulky alkylsilane ligands on a silica surface, J Chromatogr A, 688 (1994) 25-29.

[36] J.J. Kirkland, J.W. Henderson, J.J. DeStefano, M.A. van Straten, H.A. Claessens, Stability of silica-based, endcapped columns with pH 7 and 11 mobile phases for reversed-phase high-performance liquid chromatography, J Chromatogr A, 762 (1997) 97-112.

[37] J.J. Kirkland, J.B. Adams, M.A. van Straten, H.A. Claessens, Bidentate Silane Stationary Phases for Reversed-Phase High-Performance Liquid Chromatography, Anal Chem, 70 (1998) 4344-4352.

[38] J.M. Wirth, H.O. Fatunmbi, Horizontal polymerization of mixed trifunctional silanes on silica. 2. Application to chromatographic silica gel, Anal Chem, 65 (1993) 822-826.

[39] M.J.J. Hetem, J.W. De Haan, H.A. Claessens, C.A. Cramers, A. Deege, G. Schomburg, Characterization and stability of silanized and polymercoated octadecyl reversed phases, Journal of Chromatography A, 540 (1991) 53-76.

[40] A. Zimmermann, J. Horak, A. Sievers-Engler, C. Sanwald, W. Lindner, M. Kramer, M. Lämmerhofer, Surface-crosslinked poly(3-mercaptopropyl)methylsiloxane-coatings on silica as new platform for low-bleed mass spectrometry-compatible functionalized stationary phases synthesized via thiol-ene click reaction, Journal of Chromatography A, 1436 (2016) 73-83.

[41] S. Bäurer, A. Zimmermann, U. Woiwode, O.L. Sánchez-Muñoz, M. Kramer, J. Horak, W. Lindner, W. Bicker, M. Lämmerhofer, Stable-bond polymeric reversed-phase/weak anion-exchange mixed-mode stationary phases obtained by simultaneous functionalization and crosslinking of a poly(3-mercaptopropyl)methylsiloxane-film on vinyl silica via thiol-ene double click reaction, Journal of Chromatography A, 1593 (2019) 110-118.

[42] K. Qian, Z. Yang, F. Zhang, B. Yang, P.K. Dasgupta, Low-Bleed Silica-Based Stationary Phase for Hydrophilic Interaction Liquid Chromatography, Analytical Chemistry, 90 (2018) 8750-8755.

[43] N. Tanaka, K. Sakagami, M. Araki, Effect of alkyl chain length of the stationary phase on retention and selectivity in reversed-phase liquid chromatography: Participation of solvent molecules in the stationary phase, Journal of Chromatography A, 199 (1980) 327-337.

[44] K.D. Lork, K.K. Unger, Solute retention in reversed-phase chromatography as a function of stationary phase properties: Effect of n-alkyl chain length and ligand density, Chromatographia, 26 (1988) 115-119.

[45] N. Tanaka, Y. Tokuda, K. Iwaguchi, M. Araki, Effect of stationary phase structure on retention and selectivity in reversed-phase liquid chromatography, Journal of Chromatography A, 239 (1982) 761-772.

[46] H. Glatz, C. Blay, H. Engelhardt, W. Bannwarth, New Fluorous Reversed Phase Silica Gels for HPLC Separations of Perfluorinated Compounds, Chromatographia, 59 (2004) 567-570.

[47] R.M. Smith, S.L. Miller, Comparison of the selectivity of cyano-bonded silica stationary phases in reversed-phase liquid chromatography, Journal of Chromatography A, 464 (1991) 297-306.

[48] S.R. Bakalyar, R. McIlwrick, E. Roggendorf, Solvent selectivity in reversed-phase high-pressure liquid chromatography, Journal of Chromatography A, 142 (1977) 353-365.

[49] E. Bayer, A. Paulus, Silanophilic interactions in reversed-phase high-performance liquid chromatography, J Chromatogr, 400 (1987) 1-4.

[50] J. Nawrocki, The silanol group and its role in liquid chromatography, J Chromatogr A, 779 (1997) 29-71.

[51] J. Nawrocki, B. Buszewski, Influence of silica surface chemistry and structure on the properties, structure and coverage of alkyl-bonded phases for high-performance liquid chromatography, J Chromatogr, 449 (1988) 1-24.

[52] D.V. McCalley, The challenges of the analysis of basic compounds by high performance liquid chromatography: some possible approaches for improved separations, J Chromatogr A, 1217 (2010) 858-880.

[53] B. Buszewski, S. Bocian, G. Rychlicki, M. Matyska, J. Pesek, Determination of accessible silanols groups on silica gel surfaces using microcalorimetric measurements, J Chromatogr A, 1232 (2012) 43-46.

[54] A. Mendez, E. Bosch, M. Roses, U.D. Neue, Comparison of the acidity of residual silanol groups in several liquid chromatography columns, J Chromatogr A, 986 (2003) 33-44.

[55] K. Okusa, Y. Suita, Y. Otsuka, M. Tahara, T. Ikegami, N. Tanaka, M. Ohira, M. Takahashi, Test compounds for detecting the silanol effect on the elution of ionized amines in reversed-phase LC, J Sep Sci, 33 (2010) 348-358.

[56] S.D. Rogers, J.G. Dorsey, Chromatographic silanol activity test procedures: the quest for a universal test, J Chromatogr A, 892 (2000) 57-65.

[57] T.L. Ascah, B. Feibush, Novel, highly deactivated reversed-phase for basic compounds, J Chromatogr A, 506 (1990) 357-369.

[58] J. Layne, Characterization and comparison of the chromatographic performance of conventional, polar-embedded, and polar-endcapped reversed-phase liquid chromatography stationary phases, J Chromatogr A, 957 (2002) 149-164.

[59] L.-L. Jing, R. Jiang, P. Liu, P.-A. Wang, T.-Y. Shi, X.-L. Sun, Selectivity differences between alkyl and polar-modified alkyl phases in reversed phase high performance liquid chromatography, Journal of Separation Science, 32 (2009) 212-220.

[60] S. Calabuig-Hernandez, M.C. Garcia-Alvarez-Coque, M.J. Ruiz-Angel, Performance of amines as silanol suppressors in reversed-phase liquid chromatography, J Chromatogr A, 1465 (2016) 98-106.

[61] D.V. McCalley, Comparison of peak shapes obtained with volatile (mass spectrometry-compatible) buffers and conventional buffers in reversed-phase high-performance liquid chromatography of bases on particulate and monolithic columns, J Chromatogr A, 987 (2003) 17-28.

[62] J.J. Fernandez-Navarro, M.C. Garcia-Alvarez-Coque, M.J. Ruiz-Angel, The role of the dual nature of ionic liquids in the reversed-phase liquid chromatographic separation of basic drugs, J Chromatogr A, 1218 (2011) 398-407.

[63] D.V. McCalley, Rationalization of Retention and Overloading Behavior of Basic Compounds in Reversed-Phase HPLC Using Low Ionic Strength Buffers Suitable for Mass Spectrometric Detection, Analytical Chemistry, 75 (2003) 3404-3410.

[64] U.D. Neue, C.H. Phoebe, K. Tran, Y.-F. Cheng, Z. Lu, Dependence of reversed-phase retention of ionizable analytes on pH, concentration of organic solvent and silanol activity, Journal of Chromatography A, 925 (2001) 49-67.

[65] H. Small, T.S. Stevens, W.C. Bauman, Novel ion exchange chromatographic method using conductimetric detection, Analytical Chemistry, 47 (1975) 1801-1809.

[66] S. Fekete, A. Beck, J.-L. Veuthey, D. Guillarme, Ion-exchange chromatography for the characterization of biopharmaceuticals, Journal of Pharmaceutical and Biomedical Analysis, 113 (2015) 43-55.

[67] E.P. Nesterenko, P.N. Nesterenko, B. Paull, Zwitterionic ion-exchangers in ion chromatography: A review of recent developments, Analytica Chimica Acta, 652 (2009) 3-21.

[68] J.S. Fritz, Factors affecting selectivity in ion chromatography, Journal of Chromatography A, 1085 (2005) 8-17.

[69] A.V. Zatirakha, A.D. Smolenkov, O.A. Shpigun, Preparation and chromatographic performance of polymer-based anion exchangers for ion chromatography: A review, Analytica Chimica Acta, 904 (2016) 33-50.

[70] L.M. Nair, B.R. Kildew, R. Saari-Nordhaus, Enhancing the anion separations on a polydivinylbenzene-based anion stationary phase, Journal of Chromatography A, 739 (1996) 99-110.

[71] T. Okada, Nonaqueous anion-exchange chromatography I. Role of solvation in anion-exchange resin, Journal of Chromatography A, 758 (1997) 19-28.

[72] J. Ståhlberg, Retention models for ions in chromatography: The publication of this article was delayed at the request of the author, Journal of Chromatography A, 855 (1999) 3-55.

[73] J.S. Fritz, Principles and applications of ion-exclusion chromatography, Journal of Chromatography A, 546 (1991) 111-118.

[74] M. Novič, P.R. Haddad, Analyte-stationary phase interactions in ion-exclusion chromatography, Journal of Chromatography A, 1118 (2006) 19-28.

[75] J. O'Reilly, P. Doble, K. Tanaka, P.R. Haddad, Retention behaviour of strong acid anions in ion-exclusion chromatography on sulfonate and carboxylate stationary phases, Journal of Chromatography A, 884 (2000) 61-74.

[76] A.J. Alpert, Hydrophilic-interaction chromatography for the separation of peptides, nucleic acids and other polar compounds, J Chromatogr, 499 (1990) 177-196.

[77] G. Karlsson, S. Winge, H. Sandberg, Separation of monosaccharides by hydrophilic interaction chromatography with evaporative light scattering detection, J Chromatogr A, 1092 (2005) 246-249.

[78] M. Bagheri, M. Taheri, M. Farhadpour, H. Rezadoost, A. Ghassempour, H.Y. Aboul-Enein, Evaluation of hydrophilic interaction liquid chromatography stationary phases for analysis of opium alkaloids, J Chromatogr A, 1511 (2017) 77-84.

[79] H. Tanaka, X. Zhou, O. Masayoshi, Characterization of a novel diol column for high-performance liquid chromatography, Journal of Chromatography A, 987 (2003) 119-125.

[80] A.J. Alpert, Cation-exchange high-performance liquid chromatography of proteins on poly(aspartic acid)-silica, J Chromatogr, 266 (1983) 23-37.

[81] J.C. Heaton, D.V. McCalley, Comparison of the kinetic performance and retentivity of sub-2 mum core-shell, hybrid and conventional bare silica phases in hydrophilic interaction, J Chromatogr A, 1371 (2014) 106-116.

[82] B.A. Olsen, Hydrophilic interaction chromatography using amino and silica columns for the determination of polar pharmaceuticals and impurities, J Chromatogr A, 913 (2001) 113-122.

[83] X. Xiong, Y. Liu, Chromatographic behavior of 12 polar pteridines in hydrophilic interaction chromatography using five different HILIC columns coupled with tandem mass spectrometry, Talanta, 150 (2016) 493-502.

[84] Y. Guo, S. Gaiki, Retention behavior of small polar compounds on polar stationary phases in hydrophilic interaction chromatography, J Chromatogr A, 1074 (2005) 71-80.

[85] W. Jiang, K. Irgum, Covalently Bonded Polymeric Zwitterionic Stationary Phase for Simultaneous Separation of Inorganic Cations and Anions, Anal Chem, 71 (1999) 333-344.

[86] E. Wikberg, J.J. Verhage, C. Viklund, K. Irgum, Grafting of silica with sulfobetaine polymers via aqueous reversible addition fragmentation chain transfer polymerization and its use as a stationary phase in HILIC, J Sep Sci, 32 (2009) 2008-2016.

[87] W. Jiang, G. Fischer, Y. Girmay, K. Irgum, Zwitterionic stationary phase with covalently bonded phosphorylcholine type polymer grafts and its applicability to separation of peptides in the hydrophilic interaction liquid chromatography mode, J Chromatogr A, 1127 (2006) 82-91.

[88] M. Takafuji, M. Shahruzzaman, K. Sasahara, H. Ihara, Preparation and characterization of a novel hydrophilic interaction/ion exchange mixed-mode chromatographic stationary phase with pyridinium-based zwitterionic polymer-grafted porous silica, J Sep Sci, 41 (2018) 3957-3965.

[89] B. Buszewski, S. Noga, Hydrophilic interaction liquid chromatography (HILIC)—a powerful separation technique, Analytical and Bioanalytical Chemistry, 402 (2011) 231-247.

[90] P. Jandera, Stationary and mobile phases in hydrophilic interaction chromatography: a review, Analytica Chimica Acta, 692 (2011) 1-25.

[91] P. Jandera, T. Hajek, Mobile phase effects on the retention on polar columns with special attention to the dual hydrophilic interaction-reversed-phase liquid chromatography mechanism, a review, J Sep Sci, 41 (2018) 145-162.

[92] D.V. McCalley, Understanding and manipulating the separation in hydrophilic interaction liquid chromatography, Journal of Chromatography A, 1523 (2017) 49-71.

[93] N.P. Dinh, T. Jonsson, K. Irgum, Water uptake on polar stationary phases under conditions for hydrophilic interaction chromatography and its relation to solute retention, J Chromatogr A, 1320 (2013) 33-47.

[94] D.V. McCalley, U.D. Neue, Estimation of the extent of the water-rich layer associated with the silica surface in hydrophilic interaction chromatography, J Chromatogr A, 1192 (2008) 225-229.

[95] J. Soukup, P. Jandera, Adsorption of water from aqueous acetonitrile on silica-based stationary phases in aqueous normal-phase liquid chromatography, J Chromatogr A, 1374 (2014) 102-111.

[96] S.M. Melnikov, A. Höltzel, A. Seidel-Morgenstern, U. Tallarek, Composition, Structure, and Mobility of Water−Acetonitrile Mixtures in a Silica Nanopore Studied by Molecular Dynamics Simulations, Analytical Chemistry, 83 (2011) 2569-2575.

[97] P. Jandera, T. Hajek, Utilization of dual retention mechanism on columns with bonded PEG and diol stationary phases for adjusting the separation selectivity of phenolic and flavone natural antioxidants, J Sep Sci, 32 (2009) 3603-3619.

[98] S.M. Melnikov, A. Höltzel, A. Seidel-Morgenstern, U. Tallarek, Evaluation of Aqueous and Nonaqueous Binary Solvent Mixtures as Mobile Phase Alternatives to Water–Acetonitrile Mixtures for Hydrophilic Interaction Liquid Chromatography by Molecular Dynamics Simulations, The Journal of Physical Chemistry C, 119 (2015) 512-523.

[99] W. Bicker, J. Wu, M. Lammerhofer, W. Lindner, Hydrophilic interaction chromatography in nonaqueous elution mode for separation of hydrophilic analytes on silica-based packings with noncharged polar bondings, J Sep Sci, 31 (2008) 2971-2987.

[100] A. Kumar, J.C. Heaton, D.V. McCalley, Practical investigation of the factors that affect the selectivity in hydrophilic interaction chromatography, J Chromatogr A, 1276 (2013) 33-46.

[101] J.C. Heaton, J.J. Russell, T. Underwood, R. Boughtflower, D.V. McCalley, Comparison of peak shape in hydrophilic interaction chromatography using acidic salt buffers and simple acid solutions, J Chromatogr A, 1347 (2014) 39-48.

[102] D.V. McCalley, Study of the selectivity, retention mechanisms and performance of alternative silica-based stationary phases for separation of ionised solutes in hydrophilic interaction chromatography, Journal of Chromatography A, 1217 (2010) 3408-3417.

[103] C. West, E. Auroux, Deconvoluting the effects of buffer salt concentration in hydrophilic interaction chromatography on a zwitterionic stationary phase, Journal of Chromatography A, 1461 (2016) 92-97.

[104] A.J. Alpert, Electrostatic Repulsion Hydrophilic Interaction Chromatography for Isocratic Separation of Charged Solutes and Selective Isolation of Phosphopeptides, Analytical Chemistry, 80 (2008) 62-76.

[105] A. Periat, J. Boccard, J.-L. Veuthey, S. Rudaz, D. Guillarme, Systematic comparison of sensitivity between hydrophilic interaction liquid chromatography and reversed phase liquid chromatography coupled with mass spectrometry, Journal of Chromatography A, 1312 (2013) 49-57.

[106] L. Wang, W. Wei, Z. Xia, X. Jie, Z.Z. Xia, Recent advances in materials for stationary phases of mixed-mode high-performance liquid chromatography, TrAC Trends in Analytical Chemistry, 80 (2016) 495-506.

[107] K. Zhang, X. Liu, Mixed-mode chromatography in pharmaceutical and biopharmaceutical applications, Journal of Pharmaceutical and Biomedical Analysis, 128 (2016) 73-88.

[108] M. Lämmerhofer, R. Nogueira, W. Lindner, Multi-modal applicability of a reversed-phase/weak-anion exchange material in reversed-phase, anion-exchange, ion-exclusion, hydrophilic interaction and hydrophobic interaction chromatography modes, Anal Bioanal Chem, 400 (2011) 2517-2530.

[109] W. Bicker, M. Lämmerhofer, W. Lindner, Mixed-mode stationary phases as a complementary selectivity concept in liquid chromatography–tandem mass spectrometry-based bioanalytical assays, Analytical and Bioanalytical Chemistry, 390 (2008) 263-266.

[110] A. Zimmermann, R. Greco, I. Walker, J. Horak, A. Cavazzini, M. Lämmerhofer, Synthetic oligonucleotide separations by mixed-mode reversed-phase/weak anion-exchange liquid chromatography, Journal of Chromatography A, 1354 (2014) 43-55.

[111] M. Lämmerhofer, M. Richter, J. Wu, R. Nogueira, W. Bicker, W. Lindner, Mixed-mode ion-exchangers and their comparative chromatographic characterization in reversed-phase and hydrophilic interaction chromatography elution modes, Journal of Separation Science, 31 (2008) 2572-2588.

[112] L.A. Kennedy, W. Kopaciewicz, F.E. Regnier, Multimodal liquid chromatography columns for the separation of proteins in either the anion-exchange or hydrophobic-interaction mode, Journal of Chromatography A, 359 (1986) 73-84.

[113] D. Sýkora, P. Řezanka, K. Záruba, V. Král, Recent advances in mixed-mode chromatographic stationary phases, Journal of Separation Science, 42 (2019) 89-129.

[114] Z. El Rassi, C. Horváth, Tandem columns and mixed-bed columns in high-performance liquid chromatography of proteins, Journal of Chromatography A, 359 (1986) 255-264.

[115] A. Zimmermann, J. Horak, O.L. Sánchez-Muñoz, M. Lämmerhofer, Surface charge fine tuning of reversed-phase/weak anion-exchange type mixed-mode stationary phases for milder elution conditions, Journal of Chromatography A, 1409 (2015) 189-200.

[116] Q. Jiang, W. Zhao, H. Qiu, S. Zhang, Silica-Based Phenyl and Octyl Bifunctional Imidazolium as a New Mixed-Mode Stationary Phase for Reversed-Phase and Anion-Exchange Chromatography, Chromatographia, 79 (2016) 1437-1443.

[117] Q. Wang, M. Ye, L. Xu, Z.-g. Shi, A reversed-phase/hydrophilic interaction mixed-mode C18-Diol stationary phase for multiple applications, Analytica Chimica Acta, 888 (2015) 182-190.

[118] G. Shen, F. Zhang, B. Yang, C. Chu, X. Liang, A novel amide stationary phase for hydrophilic interaction liquid chromatography and ion chromatography, Talanta, 115 (2013) 129-132.

[119] X. Ren, K. Zhang, D. Gao, Q. Fu, J. Zeng, D. Zhou, L. Wang, Z. Xia, Mixed-mode liquid chromatography with a stationary phase co-functionalized with ionic liquid embedded C18 and an aryl sulfonate group, Journal of Chromatography A, 1564 (2018) 137-144.

[120] A.F.G. Gargano, T. Leek, W. Lindner, M. Lämmerhofer, Mixed-mode chromatography with zwitterionic phosphopeptidomimetic selectors from Ugi multicomponent reaction, Journal of Chromatography A, 1317 (2013) 12-21.

[121] L. Qiao, W. Lv, M. Chang, X. Shi, G. Xu, Surface-bonded amide-functionalized imidazolium ionic liquid as stationary phase for hydrophilic interaction liquid chromatography, Journal of Chromatography A, 1559 (2018) 141-148.

[122] X. Liu, C.A. Pohl, HILIC behavior of a reversed-phase/cation-exchange/anion-exchange trimode column, Journal of Separation Science, 33 (2010) 779-786.

[123] M. Walshe, M.T. Kelly, M.R. Smyth, H. Ritchie, Retention studies on mixed-mode columns in high-performance liquid chromatography, Journal of Chromatography A, 708 (1995) 31-40.

[124] R. Nogueira, M. Lämmerhofer, W. Lindner, Alternative high-performance liquid chromatographic peptide separation and purification concept using a new mixed-mode reversed-phase/weak anion-exchange type stationary phase, Journal of Chromatography A, 1089 (2005) 158-169.

[125] L. Zhang, Q. Dai, X. Qiao, C. Yu, X. Qin, H. Yan, Mixed-mode chromatographic stationary phases: Recent advancements and its applications for high-performance liquid chromatography, TrAC Trends in Analytical Chemistry, 82 (2016) 143-163.

[126] M. Zhang, A.K. Mallik, M. Takafuji, H. Ihara, H. Qiu, Versatile ligands for high-performance liquid chromatography: An overview of ionic liquid-functionalized stationary phases, Analytica Chimica Acta, 887 (2015) 1-16.

[127] Y.R. Lee, K.H. Row, Ionic liquid-modified mesoporous silica stationary phase for separation of polysaccharides with size exclusion chromatography, Separation and Purification Technology, 196 (2018) 183-190.

[128] K. Hu, Y. Zhang, J. Liu, K. Chen, W. Zhao, W. Zhu, Z. Song, B. Ye, S. Zhang, Development and application of a new 25,27-bis(l-phenylalaninemethylester-N-carbonylmethoxy)-26,28-dihydroxy-para-tert-butylcalix[4]arene stationary phase, Journal of Separation Science, 36 (2013) 445-453.

[129] K. Hu, W. Zhang, H. Yang, Y. Cui, J. Zhang, W. Zhao, A. Yu, S. Zhang, Calixarene ionic liquid modified silica gel: A novel stationary phase for mixed-mode chromatography, Talanta, 152 (2016) 392-400.

[130] S. Ray, M. Takafuji, H. Ihara, Chromatographic evaluation of a newly designed peptide-silica stationary phase in reverse phase liquid chromatography and hydrophilic interaction liquid chromatography: Mixed mode behavior, Journal of Chromatography A, 1266 (2012) 43-52.

[131] K. Ohyama, Y. Inoue, N. Kishikawa, N. Kuroda, Preparation and characterization of surfactin-modified silica stationary phase for reversed-phase and hydrophilic interaction liquid chromatography, Journal of Chromatography A, 1371 (2014) 257-260.

[132] H. Wang, L. Zhang, T. Ma, L. Zhang, X. Qiao, Imidazolium-embedded iodoacetamide-functionalized silica-based stationary phase for hydrophilic interaction/reversed-phase mixed-mode chromatography, Journal of Separation Science, 39 (2016) 3498-3504.

[133] C. Bo, X. Wang, C. Wang, Y. Wei, Preparation of hydrophilic interaction/ion-exchange mixed-mode chromatographic stationary phase with adjustable selectivity by controlling different ratios of the co-monomers, Journal of Chromatography A, 1487 (2017) 201-210.

[134] C. Bo, Y. Wei, Preparation and evaluation of surface-grafted block copolymers and random copolymers via surface-initiated atom transfer radical polymerization for hydrophilic/ion-exchange stationary phases, RSC Adv., 7 (2017) 46812-46822.

[135] Y. Li, J. Yang, J. Jin, X. Sun, L. Wang, J. Chen, New reversed-phase/anion-exchange/hydrophilic interaction mixed-mode stationary phase based on dendritic polymer-modified porous silica, Journal of Chromatography A, 1337 (2014) 133-139.

[136] S. Bäurer, S. Polnick, O.L. Sánchez-Muñoz, M. Kramer, M. Lämmerhofer, N-Propyl-N′-2-pyridylurea-modified silica as mixed-mode stationary phase with moderate weak anion exchange capacity and pH-dependent surface charge reversal, Journal of Chromatography A, 1560 (2018) 45-54.

[137] M. Sun, J. Feng, X. Wang, H. Duan, L. Li, C. Luo, Dicationic imidazolium ionic liquid modified silica as a novel reversed-phase/anion-exchange mixed-mode stationary phase for high-performance liquid chromatography, Journal of Separation Science, 37 (2014) 2153-2159.

[138] X. Wang, J. Peng, H. Peng, J. Chen, H. Xian, R. Ni, S. Li, D. Long, Z. Zhang, Preparation of two ionic liquid bonded stationary phases and comparative evaluation under mixed-mode of reversed phase/ hydrophilic interaction/ ion exchange chromatography, Journal of Chromatography A, 1605 (2019) 460372.

[139] J. Wei, Z. Guo, P. Zhang, F. Zhang, B. Yang, X. Liang, A new reversed-phase/strong anion-exchange mixed-mode stationary phase based on polar-copolymerized approach and its application in the enrichment of aristolochic acids, Journal of Chromatography A, 1246 (2012) 129-136.

[140] L. Ding, Z. Guo, Z. Hu, X. Liang, Mixed-mode reversed phase/positively charged repulsion chromatography for intact protein separation, Journal of Pharmaceutical and Biomedical Analysis, 138 (2017) 63-69.

[141] K. Zhang, L. Dai, N.P. Chetwyn, Simultaneous determination of positive and negative pharmaceutical counterions using mixed-mode chromatography coupled with charged aerosol detector, Journal of Chromatography A, 1217 (2010) 5776-5784.

[142] X.-K. Liu, J.B. Fang, N. Cauchon, P. Zhou, Direct stability-indicating method development and validation for analysis of etidronate disodium using a mixed-mode column and charged aerosol detector, Journal of Pharmaceutical and Biomedical Analysis, 46 (2008) 639-644.

[143] D. Hewitt, M. Alvarez, K. Robinson, J. Ji, Y.J. Wang, Y.-H. Kao, T. Zhang, Mixed-mode and reversed-phase liquid chromatography–tandem mass spectrometry methodologies to study composition and base hydrolysis of polysorbate 20 and 80, Journal of Chromatography A, 1218 (2011) 2138-2145.

[144] M. Walshe, M.T. Kelly, M.R. Smyth, Comparison of two extraction methods for determination of propranolol and furosemide in human plasma by mixed-mode chromatography, Journal of Pharmaceutical and Biomedical Analysis, 14 (1996) 475-481.

[145] W. Bicker, M. Lämmerhofer, T. Keller, R. Schuhmacher, R. Krska, W. Lindner, Validated Method for the Determination of the Ethanol Consumption Markers Ethyl Glucuronide, Ethyl Phosphate, and Ethyl Sulfate in Human Urine by Reversed-Phase/Weak Anion Exchange Liquid Chromatography−Tandem Mass Spectrometry, Analytical Chemistry, 78 (2006) 5884-5892.

[146] H. Hinterwirth, M. Lämmerhofer, B. Preinerstorfer, A. Gargano, R. Reischl, W. Bicker, O. Trapp, L. Brecker, W. Lindner, Selectivity issues in targeted metabolomics: Separation of phosphorylated carbohydrate isomers by mixed-mode hydrophilic interaction/weak anion exchange chromatography, Journal of Separation Science, 33 (2010) 3273-3282.

[147] A.A. Ammann, M.J.F. Suter, Multimode gradient high performance liquid chromatography mass spectrometry method applicable to metabolomics and environmental monitoring, Journal of Chromatography A, 1456 (2016) 145-151.

[148] M. Gilar, Y.-Q. Yu, J. Ahn, J. Fournier, J.C. Gebler, Mixed-mode chromatography for fractionation of peptides, phosphopeptides, and sialylated glycopeptides, Journal of Chromatography A, 1191 (2008) 162-170.

[149] T. Arakawa, S. Ponce, G. Young, Isoform separation of proteins by mixed-mode chromatography, Protein Expression and Purification, 116 (2015) 144-151.

[150] A. Goyon, P. Yehl, K. Zhang, Characterization of therapeutic oligonucleotides by liquid chromatography, Journal of Pharmaceutical and Biomedical Analysis, 182 (2020) 113105.

[151] L. Culleré, M. Bueno, J. Cacho, V. Ferreira, Selectivity and efficiency of different reversed-phase and mixed-mode sorbents to preconcentrate and isolate aroma molecules, Journal of Chromatography A, 1217 (2010) 1557-1566.

[152] D. Salas, F. Borrull, R.M. Marcé, N. Fontanals, Study of the retention of benzotriazoles, benzothiazoles and benzenesulfonamides in mixed-mode solid-phase extraction in environmental samples, Journal of Chromatography A, 1444 (2016) 21-31.

[153] K. Kimata, K. Iwaguchi, S. Onishi, K. Jinno, R. Eksteen, K. Hosoya, M. Araki, N. Tanaka, Chromatographic Characterization of Silica C18 Packing Materials. Correlation between a Preparation Method and Retention Behavior of Stationary Phase, Journal of Chromatographic Science, 27 (1989) 721-728.

[154] E. Cruz, M.R. Euerby, C.M. Johnson, C.A. Hackett, Chromatographic classification of commercially available reverse-phase HPLC columns, Chromatographia, 44 (1997) 151-161.

[155] U.D. Neue, B.A. Alden, T.H. Walter, Universal procedure for the assessment of the reproducibility and the classification of silica-based reversed-phase packings: II. Classification of reversed-phase packings, Journal of Chromatography A, 849 (1999) 101-116.

[156] B. Bidlingmeyer, C.C. Chan, P. Fastino, R. Henry, P. Koerner, A.T. Maule, M.R.C. Marques, U. Neue, L.N. Pappa, H. , L. Sander, C. Santasania, L. Snyder, T. Wozniak, HPLC Column Classification, Pharmacopeial Forum, 31 (2005) 637-645.

[157] Y. Ishihama, N. Asakawa, Characterization of lipophilicity scales using vectors from solvation energy descriptors, Journal of Pharmaceutical Sciences, 88 (1999) 1305-1312.

[158] L.R. Snyder, J.W. Dolan, P.W. Carr, The hydrophobic-subtraction model of reversed-phase column selectivity, Journal of Chromatography A, 1060 (2004) 77-116.

[159] Y. Kawachi, T. Ikegami, H. Takubo, Y. Ikegami, M. Miyamoto, N. Tanaka, Chromatographic characterization of hydrophilic interaction liquid chromatography stationary phases: Hydrophilicity, charge effects, structural selectivity, and separation efficiency, Journal of Chromatography A, 1218 (2011) 5903-5919.

[160] N.P. Dinh, T. Jonsson, K. Irgum, Probing the interaction mode in hydrophilic interaction chromatography, Journal of Chromatography A, 1218 (2011) 5880-5891.

[161] J. Wang, Z. Guo, A. Shen, L. Yu, Y. Xiao, X. Xue, X. Zhang, X. Liang, Hydrophilic-subtraction model for the characterization and comparison of hydrophilic interaction liquid chromatography columns, Journal of Chromatography A, 1398 (2015) 29-46.

[162] R.-I. Chirita, C. West, S. Zubrzycki, A.-L. Finaru, C. Elfakir, Investigations on the chromatographic behaviour of zwitterionic stationary phases used in hydrophilic interaction chromatography, Journal of Chromatography A, 1218 (2011) 5939-5963.

[163] G. Schuster, W. Lindner, Comparative characterization of hydrophilic interaction liquid chromatography columns by linear solvation energy relationships, Journal of Chromatography A, 1273 (2013) 73-94.

[164] E. Lemasson, Y. Richer, S. Bertin, P. Hennig, C. West, Characterization of Retention Mechanisms in Mixed-Mode HPLC with a Bimodal Reversed-Phase/Cation-Exchange Stationary Phase, Chromatographia, 81 (2018) 387-399.

[165] R. Consden, A.H. Gordon, A.J.P. Martin, Qualitative analysis of proteins: a partition chromatographic method using paper, Biochemical Journal, 38 (1944) 224-232.

[166] M. Zakaria, M.-F. Gonnord, G. Guiochon, Applications of two-dimensional thin-layer chromatography, Journal of Chromatography A, 271 (1983) 127-192.

[167] M.M. Bushey, J.W. Jorgenson, Automated instrumentation for comprehensive two-dimensional high-performance liquid chromatography of proteins, Analytical Chemistry, 62 (1990) 161-167.

[168] B.W.J. Pirok, A.F.G. Gargano, P.J. Schoenmakers, Optimizing separations in online comprehensive two-dimensional liquid chromatography, Journal of Separation Science, 41 (2018) 68-98.

[169] B.W.J. Pirok, D.R. Stoll, P.J. Schoenmakers, Recent Developments in Two-Dimensional Liquid Chromatography: Fundamental Improvements for Practical Applications, Analytical Chemistry, 91 (2019) 240-263.

[170] M.E. León-González, N. Rosales-Conrado, L.V. Pérez-Arribas, V. Guillén-Casla, Two-dimensional liquid chromatography for direct chiral separations: a review, Biomedical Chromatography, 28 (2014) 59-83.

[171] M. Pursch, S. Buckenmaier, Loop-Based Multiple Heart-Cutting Two-Dimensional Liquid Chromatography for Target Analysis in Complex Matrices, Analytical Chemistry, 87 (2015) 5310-5317.

[172] U. Woiwode, S. Neubauer, W. Lindner, S. Buckenmaier, M. Lämmerhofer, Enantioselective multiple heartcut two-dimensional ultra-high-performance liquid chromatography method with a Coreshell chiral stationary phase in the second dimension for analysis of all proteinogenic amino acids in a single run, Journal of Chromatography A, 1562 (2018) 69-77.

[173] H. Luo, W. Zhong, J. Yang, P. Zhuang, F. Meng, J. Caldwell, B. Mao, C.J. Welch, 2D-LC as an on-line desalting tool allowing peptide identification directly from MS unfriendly HPLC methods, Journal of Pharmaceutical and Biomedical Analysis, 137 (2017) 139-145.

[174] A. Goyon, K. Zhang, Characterization of Antisense Oligonucleotide Impurities by Ion-Pairing Reversed-Phase and Anion Exchange Chromatography Coupled to Hydrophilic Interaction Liquid Chromatography/Mass Spectrometry Using a Versatile Two-Dimensional Liquid Chromatography Setup, Analytical Chemistry, 92 (2020) 5944–5951.

[175] S.R. Groskreutz, M.M. Swenson, L.B. Secor, D.R. Stoll, Selective comprehensive multidimensional separation for resolution enhancement in high performance liquid chromatography. Part II: Applications, Journal of Chromatography A, 1228 (2012) 41-50.

[176] Z. Long, Z. Zhan, Z. Guo, Y. Li, J. Yao, F. Ji, C. Li, X. Zheng, B. Ren, T. Huang, A novel two-dimensional liquid chromatography - Mass spectrometry method for direct drug impurity identification from HPLC eluent containing ion-pairing reagent in mobile phases, Analytica Chimica Acta, 1049 (2019) 105-114.

[177] S.R. Groskreutz, M.M. Swenson, L.B. Secor, D.R. Stoll, Selective comprehensive multi-dimensional separation for resolution enhancement in high performance liquid chromatography. Part I: Principles and instrumentation, Journal of Chromatography A, 1228 (2012) 31-40.

[178] S. Bäurer, W. Guo, S. Polnick, M. Lämmerhofer, Simultaneous Separation of Water- and Fat-Soluble Vitamins by Selective Comprehensive HILIC × RPLC (High-Resolution Sampling) and Active Solvent Modulation, Chromatographia, 82 (2019) 167-180.

[179] D.V. McCalley, Managing the column equilibration time in hydrophilic interaction chromatography, J Chromatogr A, (2019) 460655.

[180] C. Seidl, D.S. Bell, D.R. Stoll, A study of the re-equilibration of hydrophilic interaction columns with a focus on viability for use in two-dimensional liquid chromatography, J Chromatogr A, 1604 (2019) 460484.

[181] W. Lv, X. Shi, S. Wang, G. Xu, Multidimensional liquid chromatography-mass spectrometry for metabolomic and lipidomic analyses, TrAC Trends in Analytical Chemistry, 120 (2019) 115302.

[182] B.W.J. Pirok, M.J. den Uijl, G. Moro, S.V.J. Berbers, C.J.M. Croes, M.R. van Bommel, P.J. Schoenmakers, Characterization of Dye Extracts from Historical Cultural-Heritage Objects Using State-of-the-Art Comprehensive Two-Dimensional Liquid Chromatography and Mass Spectrometry with Active Modulation and Optimized Shifting Gradients, Analytical Chemistry, 91 (2019) 3062-3069.

[183] M. Pursch, A. Wegener, S. Buckenmaier, Evaluation of active solvent modulation to enhance two-dimensional liquid chromatography for target analysis in polymeric matrices, Journal of Chromatography A, 1562 (2018) 78-86.

[184] J.C. Giddings, Maximum number of components resolvable by gel filtration and other elution chromatographic methods, Analytical Chemistry, 39 (1967) 1027-1028.

[185] J.W. Dolan, L.R. Snyder, N.M. Djordjevic, D.W. Hill, T.J. Waeghe, Reversed-phase liquid chromatographic separation of complex samples by optimizing temperature and gradient time: I. Peak capacity limitations, Journal of Chromatography A, 857 (1999) 1-20.

[186] J.M. Davis, J.C. Giddings, Statistical theory of component overlap in multicomponent chromatograms, Analytical Chemistry, 55 (1983) 418-424.

[187] J.C. Giddings, Two-dimensional separations: concept and promise, Analytical Chemistry, 56 (1984) 1258A-1270A.

[188] R.E. Murphy, M.R. Schure, J.P. Foley, Effect of Sampling Rate on Resolution in Comprehensive Two-Dimensional Liquid Chromatography, Analytical Chemistry, 70 (1998) 1585-1594.

[189] J.M. Davis, D.R. Stoll, P.W. Carr, Effect of first-dimension undersampling on effective peak capacity in comprehensive two-dimensional separations, Anal Chem, 80 (2008) 461-473.

[190] D.R. Stoll, X. Wang, P.W. Carr, Comparison of the practical resolving power of one- and two-dimensional high-performance liquid chromatography analysis of metabolomic samples, Anal Chem, 80 (2008) 268-278.

[191] M. Gilar, J. Fridrich, M.R. Schure, A. Jaworski, Comparison of orthogonality estimation methods for the two-dimensional separations of peptides, Anal Chem, 84 (2012) 8722-8732.

[192] M.R. Schure, J.M. Davis, Orthogonal separations: Comparison of orthogonality metrics by statistical analysis, Journal of Chromatography A, 1414 (2015) 60-76.

[193] J.C. Giddings, Sample dimensionality: A predictor of order-disorder in component peak distribution in multidimensional separation, Journal of Chromatography A, 703 (1995) 3-15.

[194] D.R. Stoll, X. Li, X. Wang, P.W. Carr, S.E.G. Porter, S.C. Rutan, Fast, comprehensive two-dimensional liquid chromatography, Journal of Chromatography A, 1168 (2007) 3-43.

[195] M.R. Schure, The dimensionality of chromatographic separations, Journal of Chromatography A, 1218 (2011) 293-302.

[196] M. Gilar, P. Olivova, A.E. Daly, J.C. Gebler, Orthogonality of separation in two-dimensional liquid chromatography, Anal Chem, 77 (2005) 6426-6434.

[197] J.M. Davis, D.R. Stoll, P.W. Carr, Dependence of effective peak capacity in comprehensive two-dimensional separations on the distribution of peak capacity between the two dimensions, Anal Chem, 80 (2008) 8122-8134.

[198] G. Semard, V. Peulon-Agasse, A. Bruchet, J.P. Bouillon, P. Cardinael, Convex hull: a new method to determine the separation space used and to optimize operating conditions for comprehensive two-dimensional gas chromatography, J Chromatogr A, 1217 (2010) 5449-5454.

[199] R. Al Bakain, I. Rivals, P. Sassiat, D. Thiébaut, M.-C. Hennion, G. Euvrard, J. Vial, Comparison of different statistical approaches to evaluate the orthogonality of chromatographic separations: Application to reverse phase systems, Journal of Chromatography A, 1218 (2011) 2963-2975.

[200] W. Nowik, M. Bonose, S. Héron, M. Nowik, A. Tchapla, Assessment of Two-Dimensional Separative Systems Using the Nearest Neighbor Distances Approach. Part 2: Separation Quality Aspects, Analytical Chemistry, 85 (2013) 9459-9468.

[201] M. Camenzuli, P.J. Schoenmakers, A new measure of orthogonality for multi-dimensional chromatography, Anal Chim Acta, 838 (2014) 93-101.

[202] B.L. Karger, M. Martin, G. Guiochon, Role of column parameters and injection volume on detection limits in liquid chromatography, Analytical Chemistry, 46 (1974) 1640-1647.

[203] M.R. Schure, Limit of Detection, Dilution Factors, and Technique Compatibility in Multidimensional Separations Utilizing Chromatography, Capillary Electrophoresis, and Field-Flow Fractionation, Analytical Chemistry, 71 (1999) 1645-1657.

[204] K. Horváth, J.N. Fairchild, G. Guiochon, Detection issues in two-dimensional on-line chromatography, Journal of Chromatography A, 1216 (2009) 7785-7792.

[205] K.J. Mayfield, R.A. Shalliker, H.J. Catchpoole, A.P. Sweeney, V. Wong, G. Guiochon, Viscous fingering induced flow instability in multidimensional liquid chromatography, Journal of Chromatography A, 1080 (2005) 124-131.

[206] X. Jiang, A. van der Horst, P.J. Schoenmakers, Breakthrough of polymers in interactive liquid chromatography, Journal of Chromatography A, 982 (2002) 55-68.

[207] L.N. Jeong, R. Sajulga, S.G. Forte, D.R. Stoll, S.C. Rutan, Simulation of elution profiles in liquid chromatography-I: Gradient elution conditions, and with mismatched injection and mobile phase solvents, Journal of Chromatography A, 1457 (2016) 41-49.

[208] D.R. Stoll, K. O'Neill, D.C. Harmes, Effects of pH mismatch between the two dimensions of reversed-phase×reversed-phase two-dimensional separations on second dimension separation quality for ionogenic compounds—I. Carboxylic acids, Journal of Chromatography A, 1383 (2015) 25-34.

[209] J.C. Heaton, D.V. McCalley, Some factors that can lead to poor peak shape in hydrophilic interaction chromatography, and possibilities for their remediation, Journal of Chromatography A, 1427 (2016) 37-44.

[210] F. Cacciola, D. Mangraviti, F. Rigano, P. Donato, P. Dugo, L. Mondello, H.J. Cortes, Novel comprehensive multidimensional liquid chromatography approach for elucidation of the microbosphere of shikimate-producing Escherichia coli SP1.1/pKD15.071 strain, Analytical and Bioanalytical Chemistry, 410 (2018) 3473-3482.

[211] S. Bäurer, M. Ferri, A. Carotti, S. Neubauer, R. Sardella, M. Lämmerhofer, Mixed-mode chromatography characteristics of chiralpak ZWIX(+) and ZWIX(−) and elucidation of their chromatographic orthogonality for LC × LC application, Analytica Chimica Acta, 1093 (2020) 168-179.

[212] D.R. Stoll, K. Shoykhet, P. Petersson, S. Buckenmaier, Active Solvent Modulation: A Valve-Based Approach To Improve Separation Compatibility in Two-Dimensional Liquid Chromatography, Anal Chem, 89 (2017) 9260-9267.

[213] Y. Chen, J. Li, O.J. Schmitz, Development of an At-Column Dilution Modulator for Flexible and Precise Control of Dilution Factors to Overcome Mobile Phase Incompatibility in Comprehensive Two-Dimensional Liquid Chromatography, Analytical Chemistry, 91 (2019) 10251-10257.

[214] R.J. Vonk, A.F.G. Gargano, E. Davydova, H.L. Dekker, S. Eeltink, L.J. de Koning, P.J. Schoenmakers, Comprehensive Two-Dimensional Liquid Chromatography with Stationary-Phase-Assisted Modulation Coupled to High-Resolution Mass Spectrometry Applied to Proteome Analysis of Saccharomyces cerevisiae, Analytical Chemistry, 87 (2015) 5387-5394.

[215] H. Tian, J. Xu, Y. Guan, Comprehensive two-dimensional liquid chromatography (NPLC×RPLC) with vacuum-evaporation interface, Journal of Separation Science, 31 (2008) 1677-1685.

[216] A.F.G. Gargano, M. Duffin, P. Navarro, P.J. Schoenmakers, Reducing Dilution and Analysis Time in Online Comprehensive Two-Dimensional Liquid Chromatography by Active Modulation, Analytical Chemistry, 88 (2016) 1785-1793.

[217] S.H. Yang, J. Wang, K. Zhang, Validation of a two-dimensional liquid chromatography method for quality control testing of pharmaceutical materials, Journal of Chromatography A, 1492 (2017) 89-97.

2. List of Figures

3. Objective of the Thesis

The present work aims to elucidate and demonstrate the potential of mixed mode chromatography (MMC) as beneficial, flexible tool for achieving complementary selectivities which are required for the characterization of drug substances and drug products as well as in 2D-LC. On the one hand, the new MMC separation materials were comprehensively characterized in order to show their chromatographic potential. On the other hand, the benefit of mixed mode chromatography was elucidated by the application for the analysis of challenging pharmaceutical samples via 1D-LC and 2D-LC.

Therefore, multiple in-house synthesized mixed mode stationary phases as well as chiral stationary phases with mixed-mode selectivity principles were comprehensively characterized. The application suitabilities were evaluated by means of particle-based characterizations such as ζ-potential determinations as well as chromatographic tests including RP, HILIC and IEX chromatography. Similarities and dissimilarities of the retention profiles of RP, HILIC and MMC stationary phases were evaluated by a column classification test via principal component analysis of the retention data of compounds with differing physicochemical properties.
Special attention was paid to achiral chromatography using the chiral ZWIX(+) and ZWIX(-) stationary phases with the help of a systematic study of silica gels modified with selectors which are structural fragments of ZWIX(+) and ZWIX(-). Chromatographic tests, ζ-potential and CE measurements were supported by molecular modelling studies.
Furthermore, as the pharmaceutical analysis often requires the identification of compounds via MS, strategies were followed in order to improve MS compatibility concerning the use of buffers as well as column bleeding. The sensitivity of the MS signal decreases as the utilized buffer concentration increases which can be necessarily due to strong electrostatic interaction between multiply charged compounds and the stationary phase. Therefore, the surface charge state was altered by the means of two different strategies. On the one hand, a stationary phase with modified surface charge by the introduction of attached counterions (POLY-RP/WAX/SCX) was tested. On the other hand, the influence of decreased basicity of the anion exchange site was evaluated.
Additionally, the attachment stability of the chromatographic ligands affects the MS sensitivity. Therefore, chromatographic stress tests were performed in order to evaluate the stability of a previously developed stable attachment chemistry.

Moreover, the stationary phases were used for the separation of pharmaceutical test mixtures. 1D-LC experiments comprised the separation of nucleotides and oligonucleotides. For heterogeneous samples like fat- and water-soluble vitamins two-dimensional chromatography with orthogonal separation mechanism were used. By means of selective comprehensive

HIILIC × RP separation all investigated vitamins were baseline separated. Thereby, solvent mismatch issues were overcome by the use of active solvent modulation.

In order to address impurity profiling screening approaches, a 2D-LC method was developed combined with a complementary detector hyphenation set-up comprising DAD, CAD and MS. The chromatographic method addressed hydrophilic analytes as a HILIC × HILIC separation was used. Solvent mismatch issues were overcome by weakening the elution strength of the first dimension by means of non-aqueous elution conditions. The detector set-up allowed the characterization via UV spectra which can help to elucidate the origin of an impurity, the identification via MS and a universal calibration by CAD.

4. Results and Discussion

4.1. Stable-bond Polymeric Reversed-Phase/Weak Anion-Exchange Mixed-Mode Stationary Phases Obtained by Simultaneous Functionalization and Crosslinking of a Poly(3-mercaptopropyl)methylsiloxane-Film on Vinyl Silica via Thiol-ene Double Click Reaction

*Stefanie Bäurer [a], Aleksandra Zimmermann [a], Ulrich Woiwode [a], Orlando L. Sánchez-Muñoz [b], Markus Kramer [c], Jeannie Horak [a], Wolfgang Lindner [d,e], Wolfgang Bicker [e], Michael Lämmerhofer [a] **

[a] Institute of Pharmaceutical Sciences, Pharmaceutical (Bio-)Analysis, University of Tübingen, Auf der Morgenstelle 8, 72076 Tübingen, Germany

[b] Biomembranes Group, Institute of Molecular Science, Universitat de València. C/Catedrático José Beltrán 2, 46980 Paterna, Valencia, Spain

[c] Institute of Organic Chemistry, University of Tübingen, Auf der Morgenstelle 18, 72076 Tübingen, Germany

[d] Lindner Consulting GmbH, Ziegelofengasse 37, 3400 Klosterneuburg, Austria

[e] Institute of Analytical Chemistry, University of Vienna, Waehringerstrasse 38, 1090 Vienna, Austria

Reprinted with permission from Journal of Chromatography A, Volume 1593 (2019) Pages 110-118, DOI: 10.1016/j.chroma.2019.01.078

4.1.1. Abstract

A polymeric reversed-phase/weak anion exchange (Poly-RP/WAX) mixed-mode stationary phase has been prepared by coating of a poly(3-mercaptopropyl)methylsiloxane film on vinyl-modified silica (100 Å, 5 µm) and simultaneous *in situ* functionalization with *N*-(10-undecenoyl)-3-aminoquinuclidine as well as crosslinking to the vinyl silica surface by solventless thiol-ene double click reaction. Such bonding chemistry showed greatly enhanced stability compared to brush-type analogs with bifunctional siloxane bonding to silica. Solid-state ^{29}Si-CP/MAS NMR confirmed the immobilization of the siloxane layer. pH-Dependent ζ-potential determinations revealed a high anion-exchange capacity over the entire pH range with a maximum around pH 5. Oxidation of residual thiols yielded a zwitterionic Poly-RP/WAX/SCX mixed-mode phase with sulfonic acid endcapping and shifted the still net positive surface charge to lower ζ-potentials. It allowed a faster elution of strongly retained anionic species in particular of multiply negatively charged analytes such as oligonucleotides. Chromatographic tests under RPLC and HILIC elution mode with various test substances documented the multimodal utility and complementarity in retention profiles compared to RP, HILIC and commercial mixed-mode phases.

4.1.2. Introduction

Mixed-mode chromatography (MMC) gained recently great popularity as an alternative chromatographic mode to reversed-phase liquid chromatography (RPLC) and hydrophilic interaction chromatography (HILIC) [1,2] being complementary to both of them [3-6]. Its complementary retention profiles make it an ideal choice for secondary impurity profiling methods, supporting RPLC [7] and along with its excellent mobile phase compatibility with both RPLC and HILIC enables its straightforward integration in 2D-LC concepts [8-10]. MMC combines multiple retention principles through an assembly of hydrophobic, hydrophilic and ionic domains in one stationary phase and column, respectively, which can to some extent be independently controlled by specific parameters of the elution conditions. This enables great flexibility for method development and optimization of chromatographic separations through the choice of the selected chromatographic conditions [3, 6, 11-17]. The distinct interaction moieties, thereby, may be either on distinct particles which are blended, be located on simple separate brush ligands or on the same ligand with embedded or tipped ion-exchange or polar moiety [18, 19]. In other works, more complex brush ligands with e.g. peptides [20-22], calixarenes [23], cyclophanes [24] or dendritic structures [25] bearing distinctive interaction moieties have been proposed. Furthermore, materials described in the literature as ionic-liquid stationary phases for LC can be actually also classified as mixed-mode phases [26]. Besides,

polymeric mixed-mode phases have been reported as well having as advantage a higher stability but often suffer from much lower column efficiencies [27-29]. In terms of surface chemistry, MMC in itself appears in a variety of different modalities comprising HILIC/RP [30], RP/AX [16], RP/CX [10], HILIC/AX [31], HILIC/CX [22] and trimodal RP/AX/CX [32], HILIC/AX/CX [33]. Very often, indeed, individual mixed-mode phases are applicable per se in a number of distinct chromatographic modes making them truly multi-model separation materials. For instance, peptide separations in RP, WAX, HILIC, ion-exclusion and hydrophobic interaction chromatography mode on a single RP/WAX column with immobilized *N*-(10-undecenoyl)-3-aminoquinuclidine immobilized through thiol-ene click chemistry on 3-mercaptopropylsilica have been achieved [14]. This brush-type RP/WAX phase exhibited interesting application profiles for peptides [14], oligonucleotides [17], metabolites [34], mycotoxins [35], and biomarkers [36]. Unfortunately, brush-type mixed-mode phases which are immobilized via siloxane bond, although being relatively stable, show some minor bleeding. It contributes to detrimental background noise in LC-MS. Hence, concepts for different more stable immobilization strategies were devised.

In general, over the years a number of concepts have been pursued to increase the stability of bonded silica phases. For example, type C silica gels employ immobilization of ligands via a silica hydride surface which is more stable [37, 38]. More stable phases can also be obtained when the chromatographic ligand is immobilized via bidentate siloxane bonding [39, 40] or by incorporation of a steric shielding of hydrolytically labile siloxane bonds through bulky side chains attached to monofunctionally bonded silanes [41] Other concepts pursue polymer coating [42], horizontally polymerized silica [43] or hyper-crosslinking immobilization strategies [44] to mention just a few.

In this work, we present new silica-based mixed-mode RP/WAX stationary phases, which unlike to prior brush-type RP/WAX congener with bifunctional siloxane bonded ligand that show a slight bleeding, have been prepared by a stable polymer coating strategy. The new surface chemistry involves a poly-3-mercaptopropylmethylsiloxane film as a reactive polymer layer for both immobilization of the RP/WAX ligand, herein *N*-(10-undecenoyl)-3-aminoquinuclidine, and covalent attachment to vinyl silica by multiple linkages through a single step solventless thiol-ene double click reaction. In a second version of polymeric RP/WAX phase residual thiols were oxidized to sulfonic acids which can act like surface anchored counterions and accelerate separations of (multiply) negatively charged analytes such as oligonucleotides. The new mixed-mode phases, Poly-RP/WAX and Poly-RP/WAX/SCX, have been characterized by solid-state ^{29}Si-CP/MAS NMR spectroscopy, pH-dependent ζ-potential measurements and chromatographic tests documenting their complementary retention profiles. The chemical stability was evaluated by stress tests of the polymeric RP/WAX in

comparison to brush-type analog and 3-aminopropylsilica. It was also an objective to examine whether and to what extent the mixed-mode character and selectivity is compromised by the new polymer bonding chemistry and by the sulfonic acid endcapping compared to brush-type RP/WAX.

4.1.3. Materials and Methods

4.1.3.1. Materials

Poly(3-mercaptopropyl)methylsiloxane (PMPMS), 3-mercaptopropyl dimethoxymethylsilane and vinyltrichlorosilane were supplied by ABCR (Karlsruhe, Germany). Spherical silica gel Kromasil with 100 Å pore size and 5 µm particle size, was supplied by Eka Chemicals (Bohus, Sweden). 2,2'-Azobis(2-methylpropionitrile) (AIBN), 4-(dimethylamino)pyridine (DMAP), and hydrogen peroxide solution (30%) were purchased from Merck (Sigma Aldrich) (Munich, Germany). Chemicals used for the preparation of mobile phases and chromatographic test substances were from Merck (Sigma Aldrich) except for *N*-acetyl-L-phenylalanine (Ac-Phe) and *N*-tert-butoxycarbonyl-prolyl-phenylalanine (Boc-Pro-Phe) which were purchased from Bachem (Bubendorf, Switzerland). *O*,*O*-Diethylthiophosphate (DETP) was synthesized from *O*,*O*-diethylthiochlorophosphate by hydrolysis in presence of triethylamine, which was also obtained from Merck (Sigma Aldrich). The oligonucleotides were synthesized by Sigma Genosys and the desalted raw products were directly used for chromatographic separation. Ultra-pure water was prepared by an ElgaPurLab Ultra Purification system (Celle, Germany).

4.1.3.2. Synthesis of Polymeric RP/WAX Mixed-Mode Stationary Phase (Poly-RP/WAX)

5.2 g vinyl silica gel (ligand coverage 1.48 mmol/g) (the synthesis is described elsewhere [45]) was suspended in 25 mL methanol. 879 µL PMPMS (corresponding to 1 mmol sulfur per gram vinyl silica), 200 mg of radical initiator AIBN, 1.9 g of *N*-(10-undecenoyl)-3-aminoquinuclidine ligand and additional 25 mL methanol were added. Afterwards methanol was evaporated under vacuum at 35 °C. The flask was rinsed with nitrogen, closed with an air-tight plug and the thiol-ene click reaction was initiated at 60 °C in a drying cabinet overnight. After washing the modified silica gel with hot toluene and hot methanol multiple times, it was dried at 60 °C under vacuum overnight. The results of the CHNS-elemental analysis (performed by Institute of Organic Chemistry, University of Tübingen, Germany) are shown in Table 1 and the surface structure in Fig. 1a).

Table 1: Elemental analysis results of the *N*-(10-undecenoyl)-3-aminoquinuclidine modified polymer coated silica gel particles before and after oxidation with performic acid.

Stationary phases	% C	% H	% N	% S	N [mmol/g]	S [mmol/g]	RP/WAX Ligand coverage [mmol/g]	[µmol/m²]
Vinyl silica gel	5.32	1.09	0.03	0.01	-	-	1.48[a]	4.63
Poly-RP/WAX	16.20±0.01	2.92±0.01	1.17±0.01	2.38±0.19	0.84±0.01	0.74±0.06	0.42±0.01[b]	1.31
Poly-RP/WAX/SCX	15.42±0.01	2.94±0.04	1.11±0.01	2.16±0.19	0.79±0.01	0.67±0.06	0.39±0.002[b]	1.22

[a] - Calculation based on the assumption that one methoxy-group remains on the surface in average (bifunctional bonding).

[b] - Calculation based on the nitrogen content, considering two nitrogen atoms per selector molecule.

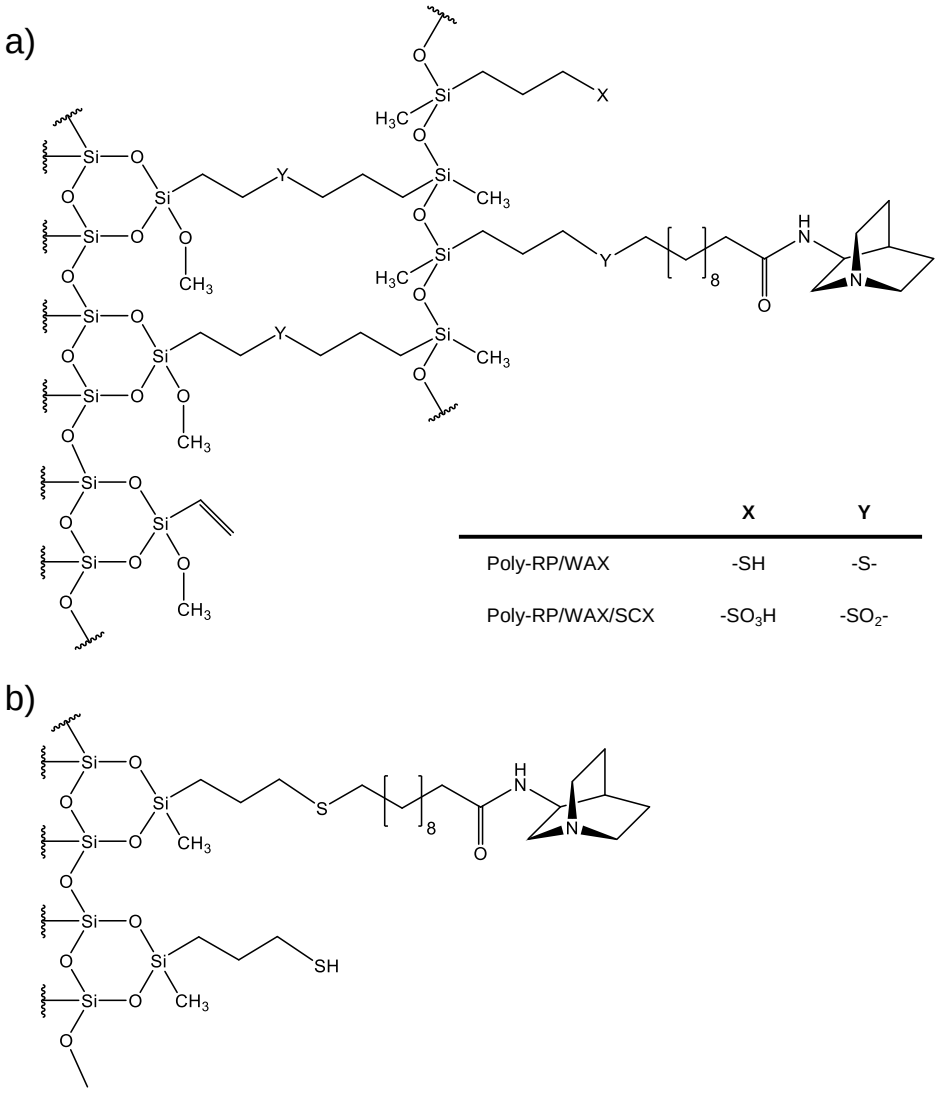

Fig. 1: Surface structure of a) the new coated RP/WAX (Poly-RP/WAX) stationary phase and its oxidized version (Poly-RP/WAX/SCX). b) Corresponding brush-type RP/WAX used for comparison.

4.1.3.3. Oxidation of Free Thiol Groups of Poly-RP/WAX (Synthesis of Poly-RP/WAX/SCX)

Poly-RP/WAX (2.5 g) with covalently bonded *N*-(10-undecenoyl)-3-aminoquinuclidine ligand was suspended in 25 mL methanol and 2.1 mL formic acid (99%). Under ice cooling and mechanical stirring 8.4 mL performic acid (prepared by adding 0.5 mL of 30% hydrogen peroxide to 9.5 mL of 99% formic acid and reaction at room temperature for 2 h) were dropwise added. After 4 additional hours of stirring at room temperature, the oxidized silica gel was washed with a mixture of water/methanol (50:50, v/v). When a neutral pH of the filtrate was obtained, multiple washing with hot methanol followed and the material was finally dried at 60 °C under vacuum. The surface structure is depicted in Fig. 1a and the elemental analysis results are summarized in Table 1.

4.1.3.4. Solid-State ^{29}Si Cross-Polarization Magic Angle Spinning (CP/MAS) NMR

The solid-state NMR spectra were measured on a Bruker Avance III HD XWB instrument (Bruker, Rheinstetten, Germany) operating at 300.13 MHz for ^{1}H and equipped with a 7 mm double resonance (^{1}H/X) probe. 10 kHz was used for the spinning rate of the 7 mm ZrO_2 rotor, 3.18 µs for the 90° proton pulse length, and 5 ms and 2 s contact and relaxation delay times, respectively.

4.1.3.5. Electrophoretic Mobility and ζ-potential Determinations

Poly-RP/WAX and Poly-RP/WAX/SCX, respectively, were dispersed in buffer solutions of different pH-values and electrophoretic mobilities were measured using a Zetasizer NanoZS particle analyzer equipped with a Universal Dip Cell (Malvern Instruments, Herrenberg, Germany). To obtain a constant ion strength, the slurries (0.2 mg/mL silica) contained 10 mM potassium chloride. To ensure constant pH values, the following buffers (pH 3.5 to 9.5, 1.0 mM) were included: formic acid/Na-formate, acetic acid/Na-acetate, histidine, tris/tris–HCl, boric acid/Na-borate [46]. Stable suspensions of the stationary phases were obtained by ultra-sonification. 1.0 mL sample aliquots were analyzed in triplicates at 25 ± 0.1 °C. The ζ-potentials were determined using the Von Smoluchowski approximation [46].

4.1.3.6. Liquid Chromatographic Experiments

The new separation materials were slurry packed (isopropanol/acetic acid, 10:1, v/v) into stainless steel columns (150 mm x 4 mm ID) using methanol as delivery solvent (80 MPa). RP and HILIC experiments were performed on an Agilent 1100 series LC system from Agilent Technologies (Waldbronn, Germany) equipped with an autosampler, degasser, quaternary pump, thermostated column compartment and diode array detector. The flow rate was 1.0 mL/min, column temperature 25°C and the injection volume 10 µL (sample concentration 1 mg/mL) unless otherwise stated. Physicochemical properties of analytes (log D, pK_a values) were calculated using Marvin Sketch. The principal component analysis (PCA) was done with the statistic software Umetrics SIMCA-P+ (level of significance: 95%, no weighting, autoscaled).

4.1.3.7. Stress Test

The new Poly-RP/WAX stationary phase (50 x 3 mm, slurry packed as previously described), a brush-type RP/WAX stationary phase (Fig. 1b) (100 x 4.0 mm, synthesized as described in [47]) and a representative commercial 3-aminopropyl modified silica stationary phase (100 x 4.0 mm) were continuously flushed (linear flow velocity: 1.33 mm/s) with highly aqueous mobile phase (ACN/H_2O/acetic acid, 30:70:0.1, v/v/v, mixture adjusted to pH 5 with ammonia) at elevated temperature of 60°C. After defined time periods (0, 7, 20, 50, 80, 110 and 137.5 h) the phases were characterized chromatographically.

4.1.4. Results and Discussion

4.1.4.1. Synthesis of Polymeric RP/WAX Stationary Phases

The chromatographic ligand of the new polymeric RP/WAX stationary phase was immobilized via polymer film. Thus, a reactive poly(3-mercaptopropyl)methylsiloxane was first coated onto the surface of vinyl silica in presence of the chromatographic mixed-mode ligand (*N*-10-undecenoyl-3-aminoquinuclidine). In a second step, immobilization of the mixed-mode ligand and crosslinking of the polythiol to vinyl silica occurred simultaneously by thiol-ene (double) click reaction yielding a surface chemistry as illustrated in Fig. 1a. Through multiple covalent attachments of the polythiol film on vinyl silica a more stable bonding compared to the brush-type RP/WAX phase [48] obtained by bi-functional bonding of trialkoxysilane (Fig. 1b) is expected. Both thiol content and selector coverage can be well controlled by addition of appropriate amounts of polythiol and RP/WAX selector. Based on experience with another chromatographic ligand (the chiral selector quinine carbamate [45]), the polythiol content in the reaction mixture was adjusted to 1 mmol sulfur/g vinyl silica to provide sufficient thiols for functionalization and immobilization, and 0.74 mmol sulfur/g were actually immobilized (Table 1) corresponding to a reaction yield of 74%. Furthermore, based on experience with quinine carbamate [45], the reaction mixture was charged with a 3-fold molar excess of the RP/WAX ligand with respect to the targeted coverage of 0.4 mmol/g (to closely match the one of the previous brush-type RP/WAX phase with 0.36 mmol/g used for comparison herein [47]). In good agreement with these considerations the reaction resulted in a ligand loading of 0.42 mmol/g (35% yield). The click reaction itself was carried out solventless. Solvent is just employed to homogenously coat the polysiloxane as a thin film to the surface. For this purpose, all constituents were dissolved in methanol, slurried in vinyl silica, and then the solvent evaporated to end up with a thin polymer film for solventless click reaction.

Elemental analysis showed that only a fraction of the reactive sulfhydryls of the polythiol film were used for immobilization of RP/WAX selector. It was further assumed that not all of the remaining sulfhydryls were utilized for crosslinking to vinyl silica. Thus, an aliquot of the poly-RP/WAX phase was further treated with performic acid oxidizing residual thiols to sulfonic acid groups and thioether functionalities to sulfonyl groups yielding a zwitterionic Poly-RP/WAX/SCX material (Fig. 1a). Polythiol, which is bound just via disulfide bridges to immobilized polymer layers on the silica surface, would be detached upon treatment with performic acid due to oxidative cleavage of disulfide bonds to sulfonic acid moieties. However, as can be seen from the elemental analysis results in Table 1 there is no significant change of the thiol coverage after performic acid oxidation.

The successful coating of the polysiloxane layer was also confirmed by ^{29}Si CP/MAS NMR spectra, which are depicted in Fig. 2.

The spectrum of vinyl silica is shown in Fig. 2a) and the one of Poly-RP/WAX in Fig. 2b) [45]. ^{29}Si resonance signals for unmodified residual silanol groups (-101 ppm) and for siloxane groups (-111 ppm) were observed in both modified silica gels (Fig. 2a) and b) [45, 49]. Additional signals can be seen at around 12 ppm (4) and -21 ppm (5) in the spectra of the coated Poly-RP/WAX (Fig. 2b) but not in the one of vinyl silica (Fig. 2a). These additional resonances can be assigned to the bonding of the polysiloxane layer. Thiol-ene click reaction was performed between the alkene residue of the vinyl silica and the thiol group of the poly(3-mercaptopropyl)methylsiloxane, resulting in signal 4 at 12 ppm. The polysiloxane coating with ligand attachment leads to signal 5 at -21 ppm. The remaining vinyl moieties on the silica surface lead to signal 1 of Poly-RP/WAX in Fig. 2b.

The ^{29}Si CP/MAS NMR spectra remain unchanged after performic acid oxidation. Neither, vinyl-silica (Fig. 2c) nor the mixed-mode phase oxidized to Poly-RP/WAX/SCX (Fig. 2d) show significantly altered ^{29}Si CP/MAS NMR spectra after performic acid treatment compared to the congeners before such treatment. Since the same resonances can be observed before and after performic acid oxidation both in the ^{29}Si NMR as well as in the ^{13}C NMR (see Suppl. Fig. S2), it can be concluded that no epoxide formation on residual vinyl groups occurs.

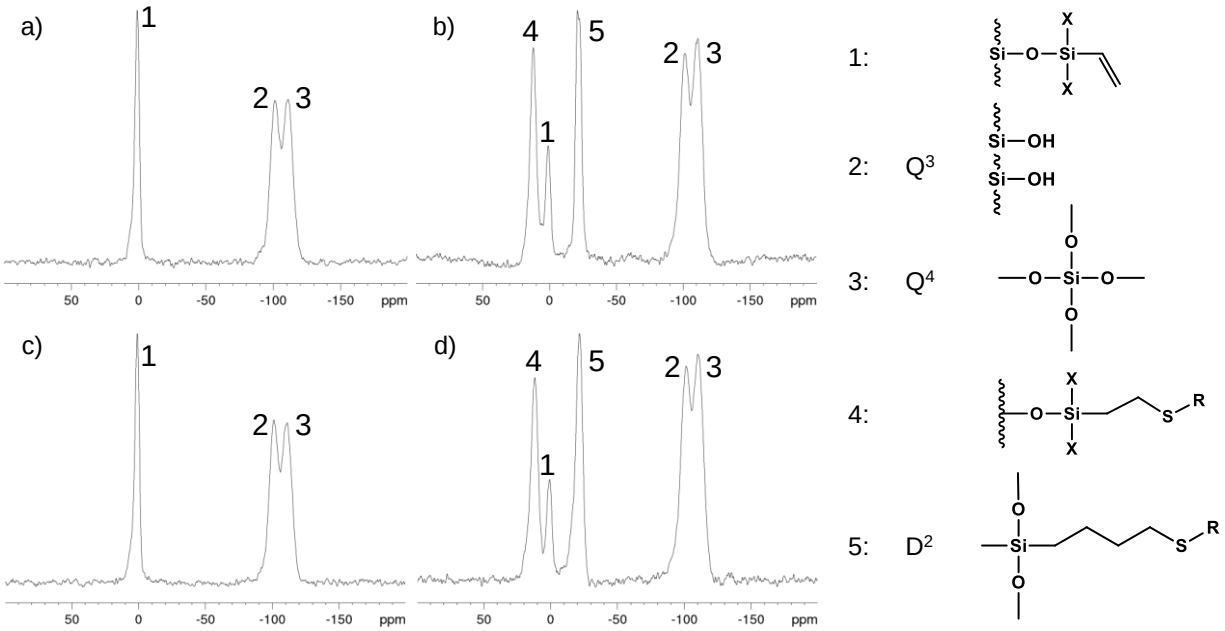

Fig. 2: ^{29} Si CP/MAS NMR spectra. a) Vinyl silica and b) polysiloxane-coated Poly-RP/WAX silica as well as corresponding phases after performic acid oxidation, c) oxidized vinyl silica and d) oxidized Poly-RP/WAX silica (i.e. Poly-RP/WAX/SCX).

4.1.4.2. ζ-Potential Determinations

Mixed-mode phases develop their peculiar separation characteristics through multiple interactions of solutes with various domains amongst others ion exchange sites. Since silica-based Poly-RP/WAX as well as the oxidized zwitterionic Poly-RP/WAX/SCX material feature distinct ionizable groups on the surface, characterization of their actual net charge state in dependence on the pH may be informative. In consequence, determination of their ζ-potentials in a pH dependent manner by electrophoretic light scattering (ELS) may be useful for understanding their retention characteristics of ionic analytes [12, 46, 50-52].

The surface concentration and dissociation status of residual silanol groups, of the immobilized RP/WAX selector and, in case of the oxidized Poly-RP/WAX/SCX silica gel, of the sulfonic acid residues actively contribute to the surface charge of the modified silica particles. In order to evaluate the pH dependency of the ζ-potentials of the modified silica gels, the determination was carried out for a pH range of 3.5 to 9.5, keeping the ionic strength constant at 10 mM KCl. The results are shown in Fig. 3. The immobilization of *N*-(10-undecenoyl)-3-aminoquinuclidine selector induces basic surface properties yielding positive ζ-potentials over the entire investigated pH range. Below pH 7.5, the dissociation of the WAX-ligand dominates the surface charge due to its pK_a of about 8.08 (calculated with Marvin Sketch) reaching full anion exchange capacity. At pH > 7.5 ζ-potentials and anion-exchange capacity drop due to increasing dissociation of residual silanols [46] and decreased ionization of the quinuclidine ring of the RP/WAX selector. Unlike to similar RP/WAX brush-phases [51], charge reversal (umpolung) to net negative surface charge at high pH was not observed for the poly-RP/WAX phase which indicates an efficient shielding of the residual silanols by the polysiloxane layer. The additional acidic sulfonic acid co-ligands of the Poly-RP/WAX/SCX phase lead to an offset i.e. an overall decrease of measured ζ-potentials compared to the Poly-RP/WAX phase (Fig 3). Furthermore, due to the influence of acidic co-ligands, the isoelectric point (pI) of the surface is shifted to slightly lower pH values and can be found at around pH 9. While the anion exchange capacity is maintained over a wide pH range (3.5 to 7.5) on Poly-RP/WAX/SCX, the acidic co-ligands impose a shift in the overall ζ-potentials, which might be of advantage for the separation of multiply charged acidic analytes.

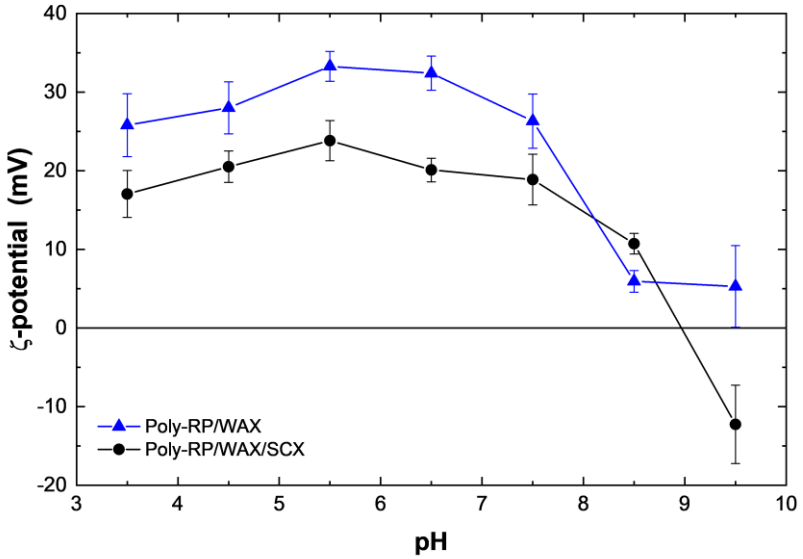

Fig. 3: Change of ζ-potential in dependency of the pH revealing the charge state of the new Poly-RP/WAX and Poly-RP/WAX/SCX stationary phases.

4.1.4.3. LC Characterization under RP, Weak Anion Exchange and HILIC Elution Modes

The polymeric RP/WAX phases were chromatographically tested under different elution conditions to demonstrate that their multimodal chromatographic characteristics was not compromised by the new immobilization chemistry. RP and HILIC conditions were utilized and the test chromatograms are shown in Fig. 4 in comparison to brush-type analogs. The neutral lipophilic test compounds butylbenzene (BuB) and pentylbenzene (PeB) were selected as probes to provide information on the methylene selectivity of the stationary phases. Their anion exchange character can be derived from the relative retention of the polar acids DETP and Boc-Pro-Phe of which the former is highly hydrophilic (but has a chromophore for UV detection) and the latter is more lipophilic, yet with polar groups embedded for the probing of the mixed-mode character. The chromatograms are shown in Fig. 4a and the chromatographic data in Supplementary Table S2. The methylene selectivity of the Poly-RP/WAX column (α_{CH2}=1.66) is slightly higher than for the brush type RP/WAX of Fig. 1b) (360 µmol/g) column (α_{CH2}=1.56 [47]) and the structurally closest commercially available RP/WAX phase (Acclaim Mixed Mode WAX-1; α_{CH2}=1.53 [47]) but slightly lower than the polar RP phase Synergi Fusion RP (α_{CH2}=1.79). The polysiloxane layer *per se* brings about some lipophilicity and slightly increases retention for hydrophobic compounds. On the contrary, the Poly-RP/WAX/SCX column shows significantly reduced methylene selectivity (α_{CH2}=1.44) due to hydrophilic sulfonyl and sulfonic acid moieties which make the surface more polar.

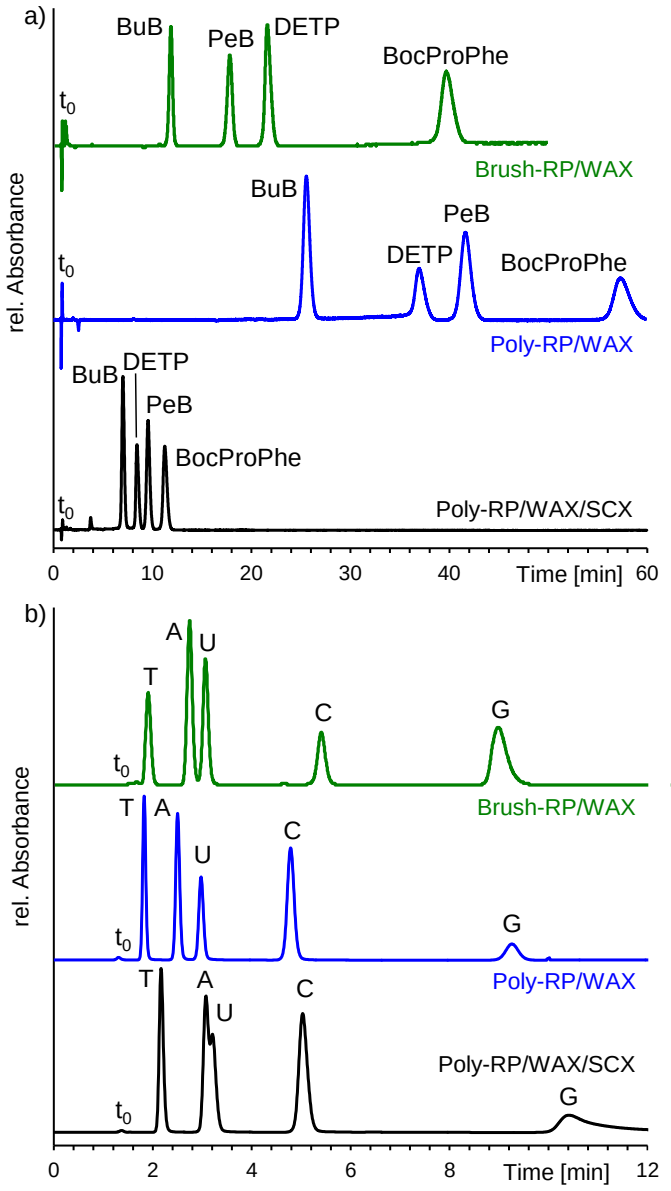

Fig.4: Multimodal applicability of the Brush-RP/WAX, Poly-RP/WAX and Poly-RP/WAX/SCX stationary phases illustrated by a) the separation of alkylbenzenes and organic acids under RP conditions, and b) the separation of nucleosides under HILIC conditions (for detailed conditions see Suppl. Material). Mobile phase: a) ACN/acetic acid (40:60, v/v) (C_{tot} = 50 mM), pH 6 adjusted with ammonia; butylbenzene (BuB); pentylbenzene (PeB), *O*,*O*-diethylthiophosphate (DETP); *N*-tert-butoxycarbonyl-prolyl-phenylalanine (Boc-Pro-Phe). b) ACN/ammonium acetate (90:10, v/v) (C_{tot} = 5 mM), apparent pH around 8; T, Thymidine; A, Adenosine; U, Uridine; C, Cytidine; G - Guanosine.

The hydrophilic acid DETP was not retained on RP phases such as Synergi Fusion RP under tested conditions [47]. In contrast, the Poly-RP/WAX mixed-mode phases sufficiently retained and resolved the two acids DETP and Boc-Pro-Phe due to their anion exchange character (see Suppl. Table S2). Selectivity got worse the higher the selector coverage. Amino phases like Luna Amino and Biobasic AX showed reversed elution order for these two test analytes. The Poly-RP/WAX/SCX column showed significantly smaller retention times also for the acidic test compounds. However, weak anion exchange mechanism still appears to be the dominating factor in spite of the presence of anionic co-ligands with repulsive electrostatic

interaction increments for these acids. It can be documented by the stoichiometric displacement model. This simple retention model assumes a direct proportional dependency of the logarithm of retention factors of oppositely charged compounds *k* and the logarithm of the concentration of counter ions *C* for a common ion-exchange process (see Suppl. Material for more details). For the Poly-RP/WAX/SCX this model needs to be modified to account for the immobilized surface anchored counterions (Eq. 1).

$$\log k = \log K_Z - Z \cdot \log[C]_m - X \cdot \log[C]_s \quad (1)$$

In this equation subscript m and s stand for counterions in the mobile (here acetate) and stationary phase (here sulfonate), respectively. Z and X are proportional to the effective charge numbers involved in the two processes (see Suppl. Material). This formalism clearly explains the shift to lower retention factors on the Poly-RP/WAX/SCX phase in comparison to Poly-RP/WAX, as exemplified in Fig. 5 for Ac-Phe. It is in agreement with the ζ-potential measurements in Fig. 3.

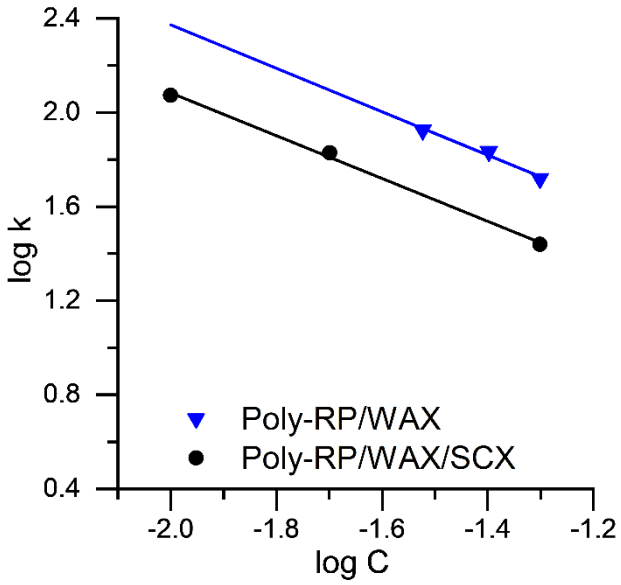

Fig. 5: Effect of retention factor of Ac-Phe on counterion concentration demonstrating that an anion-exchange retention principle dominates both on Poly-RP/WAX as well as Poly-RP/WAX/SCX stationary phases using the stoichiometric displacement model. Experimental conditions, mobile phase: ACN/H_2O (80:20, v/v), 10, 20, 50 and 30, 40, 50 mM acetic acid, pH 5 adjusted with ammonia.; flow rate,1.0 mL/min; injection volume, 10 µL; column temperature, 25 °C; Ac-Phe: 258 nm; sample concentration, 1 mg/mL; void volume marker, acetone.

With acetonitrile-rich eluents, hydrophobic interactions are set off and hydrophilic interactions become dominating leading to a HILIC elution mode for polar analytes such as nucleosides (Fig. 4b and Suppl. Table S2). All 5 nucleosides were well baseline resolved on the Poly-RP/WAX phase according to a HILIC mechanism. It clearly demonstrates the HILIC potential of this material. Surprisingly, the retention of the nucleobases only slightly increases on the oxidized Poly-RP/WAX/SCX phase. It seems that the HILIC performance is not further improved by the acidic co-ligands and the more polar surface.

In general, these tests clearly document the multimodal applicability of the new polymer bonded mixed-mode phases.

4.1.4.4. Stationary Phase Classification by Multivariate Data Analysis

Principal component analysis (PCA) is useful means for the elucidation of complementarities and similarities in generated chromatographic data sets [47, 53]. Herein, the retention factors obtained by the RPLC and HILIC tests on the two new polymeric mixed-mode phases (Poly-RP/WAX and Poly-RP/WAX/SCX), corresponding brush mixed-mode phase (RP/WAX-AQ360), some commercial mixed-mode phases (including Acclaim Mixed-mode WAX1), a chiral weak anion exchanger (Chiralpak QN-AX), some amino phases (Luna NH_2 and Biobasic AX), a number of HILIC columns and a polar RP phase (Synergi Fusion-RP) along with some synthesis intermediates of the polymeric RP/WAX phases were used as variables in PCA (structure of stationary phases, retention factors, and statistics are given in the Suppl. Material). The resultant score plot of the first two principal components, which represent latent variables on which stationary phases are ordered by increasing hydrophilicity on PC1 and from negative to positive surface charge on PC2, classifies the different columns in accordance to their similarity (Fig. 6). Stationary phases, which show similar retention behavior are clustered together, whereas stationary phases with distinct retention characteristics are distant from each other. PC1 explains around 55% of the variance in the data and PC2 around 25%; the two first PCs together about 80%.

Even though the predictive power of the PCA model is moderate (see Suppl. Material Table S6), the score plots are quite useful to illustrate the dominating retention characteristics of the examined stationary phases. The new Poly-RP/WAX phase is located in the score plot essentially equidistant from the RP column Synergi Fusion-RP and the HILIC columns (Fig. 6). Its positioning in the middle of PC1 between HILIC and RP may readily indicate its mixed-mode nature and applicability in both modes. Its chemical character and thus retention characteristics is resembling the Acclaim Mixed-mode WAX1 phase, but is significantly different to the other commercial mixed-mode phases. It is also evident in the score plot that the Poly-RP/WAX is shifted on PC1 scale to slightly higher lipophilicity as compared to the brush-type RP/WAX (RP/WAX-AQ360) and on PC2 to higher positive charge. This is indicative for a higher anion-exchange capacity due to slightly higher selector coverage but probably also due to more efficient shielding of silanols by the polysiloxane film. Upon introduction of the sulfonic acid moieties in the Poly-RP/WAX/SCX this stationary phase experiences a huge shift in direction to the HILIC phases due to a slight shift on PC1 to higher hydrophilicity and large shift on the charge scale of PC2.

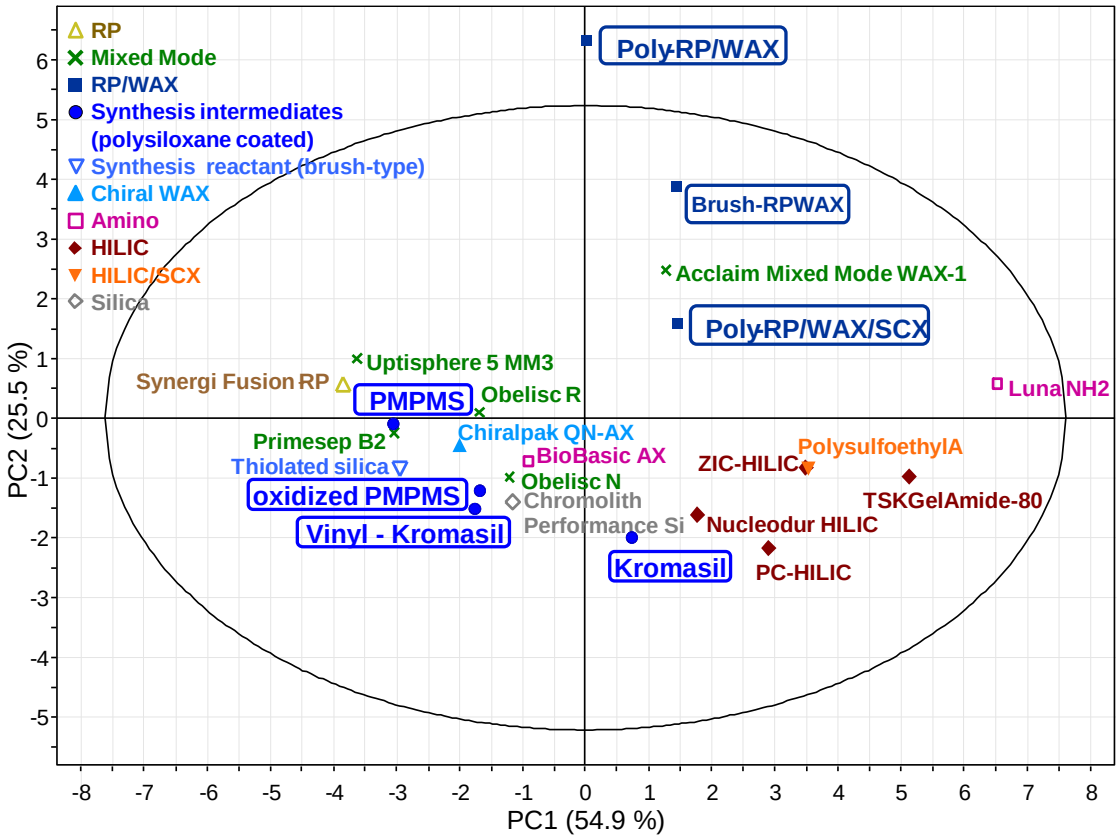

Fig. 6: Score plot of the principal component analysis of the retention data obtained by RP and HILIC tests revealing the classification of the polymer-bonded Poly-RP/WAX and Poly-RP/WAX/SCX stationary phases along with other chiral WAX, RP, HILIC and several commercial mixed-mode stationary phases.

The score plot also documents illustratively changes in the retention behavior in dependence of the surface modification in each step. Since bare silica possesses a highly polar surface and is hence well suited for the separation of polar analytes under HILIC conditions, it is not surprising that the raw material Kromasil is clustered together with HILIC phases (Fig. 6). The introduction of vinyl groups at the surface of the silica promotes hydrophobic interactions and as a result Vinyl-Kromasil is shifted towards more hydrophobic columns in the score plot. The coating of the silica particles with poly-3-mercaptopropylmethylsiloxane (PMPMS) and crosslinking to vinyl silica in absence of RP/WAX selector (further information can be found in the Suppl. Material) causes a further obvious increase of lipophilicity of the surface by increasing the carbon content on the stationary phase. Besides it is striking that this stationary phase is shifted on the PC 2 scale indicating a reduction of negative surface charge due to an additional shielding of residual surface silanol groups by the polymer coating. The oxidation of the polymer-coated silica (oxidized PMPMS, further information can be found in the Suppl. Material) introduces cation exchange groups on the surface, which is seen by a drift back towards Vinyl Kromasil. However, all these precursor and comparative phases are located in the score plot far distant from Poly-RP/WAX and Poly-RP/WAX/SCX which indicates the dominant influence of the RP/WAX ligand on the surface property and the resultant chromatographic retention characteristics.

4.1.4.5. Separation of Synthetic Oligonucleotides

Synthetic oligonucleotides are gaining increasing popularity as new therapeutics. The synthetic process for small scale production is based on the phosphoramidite chemistry, which yields besides the target sequence a large number of impurities with similar structure. For human use, further purification as well as analysis methods for quality control of these drugs are needed, in order to achieve and control pharmaceutical quality.

The applicability of the new stabilized separation materials for oligonucleotide separations was evaluated using a test mixture containing oligos with slight sequence alterations (see Fig. 7). It can be seen that the Poly-RP/WAX has remarkable selectivity for the separation of these structurally closely related oligonucleotides (for chromatographic data see Suppl. Table S7). Unfortunately, retention is strong on the Poly-RP/WAX due to the multiple negatively charged oligos and required application of a mixed triethylammonium phosphate (TEAP) buffer/pH gradient for their elution in reasonable time. The negatively charged immobilized sulfonic acid moieties of Poly-RP/WAX/SCX act like immobilized counterions and due to their long-range nature, they have the capability to reduce retention significantly. Selectivity, although slightly reduced, was still reasonable, yet the analytes now eluted within 20 min (Fig. 7). This documents the applicability of the two new polymeric mixed-mode phases for synthetic oligonucleotide separations and confirms that selectivity for this application was not compromised by the new polymer bonding chemistry compared to the brush-type RP/WAX analog [17]. More chromatograms of potential applications (xanthins, vitamins, and phosphorylated carbohydrates) are given in the supplementary information for interested readers.

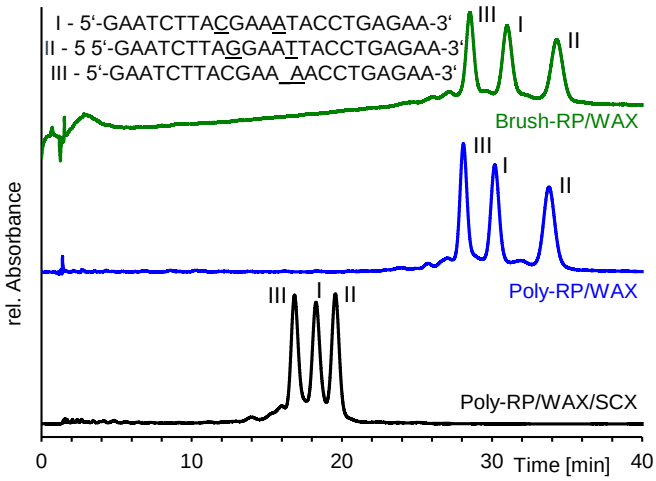

Fig. 7: Separation of synthetic oligonucleotides with minor sequence differences on brush-type (Brush-RP/WAX), polymer coated Poly-RP/WAX and oxidized coated Poly-RP/WAX/SCX stationary phases highlighting the repulsive character (surface-anchored counterion effect) obtained by additional acidic co-ligands allowing milder elution conditions. Experimental conditions: Poly-RP/WAX and Poly-RP/WAX/SCX: mobile Phase: A: 20 % ACN,50 mM phosphoric acid, pH 7 adjusted with triethylamine in the final mixture, B: 20 % ACN, 100 mM phosphoric acid, pH 8 adjusted with triethylamine; Brush-RP/WAX: mobile Phase: A: 20 % ACN, 100 mM phosphoric acid, pH 7 adjusted with triethylamine in the final mixture, B: 20 % ACN, 200 mM phosphoric acid, pH 8 adjusted with triethylamine in the final mixture, gradient: in 25 min 50 to 100 % B, hold 100 % B for 27 min, in 0.5 min 100 % to 0 % B, 8 min 0 % B; 40°C, 10 µL (8.0 µM each oligonucleotide), 254 nm, for further details about conditions see Suppl.

4.1.4.6. Column Stability Test

Polar stationary phases and in particular amino phases are known to suffer from ligand bleeding due to hydrolysis of the siloxane (Si-O-Si) bond by which the chromatographic ligand is attached to the silica surface. This effect is more pronounced under aqueous rich elution conditions. In the most severe form, this problem has been observed for 3-aminopropyl silica (APS) phases which have been synthesized by silanization reaction of silica with APTES (3-aminopropyltriethoxysilane), the classical amino phase on the market [54]. It has been reported that the aminopropyl ligand can bend back towards the silica surface and catalyze the hydrolytic cleavage of the siloxane bond leading to leaching of 3-aminopropylsilane. This makes this classical amino phase relatively unstable. In order to test the claimed improved stability of the polymer bonded Poly-RP/WAX, a stress test under highly aqueous conditions (ACN/H_2O/Acetic acid = 30/70/0.1, pH 5 adjusted with ammonia) and elevated temperature (60°C) was devised using a brush-type RP/WAX (selector coverage 360 µmol/g; Fig. 1b) and a commercial, classical APS phase for comparison. After certain time intervals of column stressing, the retention of hydrophobic (butylbenzene, pentylbenzene) and acidic test compounds (Boc-Pro-Phe and DETP) were monitored under RP conditions. Fig. 8 shows the percentage of retention remaining after a certain volume of stress solution was pumped through the column at 60°C. As can be seen retention dropped to about 60% for alkylbenzenes (Fig. 8a and 8b) and to about 25% of the initial value for acidic test analytes (Fig. 8c and 8d) after around 3000 column volumes (i.e. 3000 x V_0) of stress solution was pumped through the

brush-type RP/WAX column. The acidic compounds are more sensitive to minor losses of RP/WAX ligand because besides less attractive ionic interactions with the RP/WAX moiety, repulsive electrostatic interactions with newly generated silanols both reduce retention. The retention loss due to bleeding is significantly more pronounced for the 3-aminopropyl-silica phase for which only approximately 6% of the initial retention of the acids was observed after 3000 column volumes of stress solution (Fig. 8c and 8d). In sharp contrast, the Poly-RP/WAX column exhibited still about 95% of the initial retention for the alkylbenzenes (Fig. 8a and 8b) after 3000 column volumes and more than 85% of the initial retention for the acidic test solutes (Fig. 8c and 8d). Even after 16,000 column volumes a high percentage of retention could be preserved on the Poly-RP/WAX column indicating its significantly enhanced column stability through immobilization via the polymeric film with multiple covalent linkages to the silica surface.

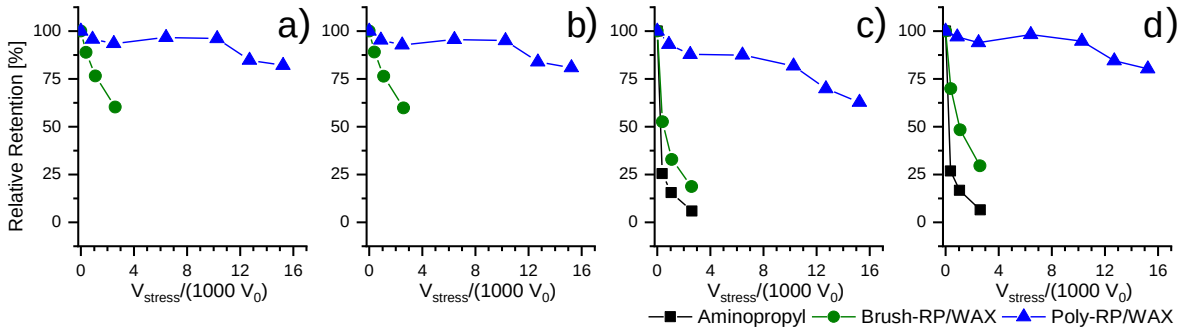

Fig. 8: Relative retention of butylbenzene (a), pentylbenzene (b),Boc-Pro-Phe (c) and DETP (d) after flushing several column volumes (V_0) of stress solution (ACN/H_2O/acetic acid, 30/70/0.1 (v/v/v), pH 5 adjusted with ammonia, 60°C) through the column. For chromatographic test conditions see Fig. 4.

4.1.5. Conclusions

In this study, two stable polymer-coated RP/WAX mixed-mode phases (Poly-RP/WAX and Poly-RP/WAX/SCX) were synthesized and characterized. The controlled synthesis by thiol-ene double click reaction comprising simultaneous ligand immobilization on a polythiol and its crosslinking to vinyl silica allowed to adjust a selector coverage (of *N*-undecenoyl-3-aminoquinuclidine) of 420 µmol/g (Poly-RP/WAX) closely matching the one of a brush-type RP/WAX analog which was used for comparison. Performic acid oxidation of residual thiols of Poly-RP/WAX introduced acidic co-ligands yielding a zwitterionic Poly-RP/WAX/SCX phase. Solid-state ^{29}Si CP/MAS NMR of the modified silica particles verified the attachment chemistry. The pH dependent ζ-potential determinations showed positive surface charge for Poly-RP/WAX over the entire pH range investigated with maxima at around pH 5 (corresponding to maximal anion-exchange capacity). The introduced sulfonic acid moieties upon oxidation caused a significant off-set to lower charge for the Poly-RP/WAX/SCX, as targeted by the design of the surface chemistry. The latter RP/WAX mixed-mode stationary phase with immobilized sulfonate counterions can be advantageously utilized for the analysis of multiply negatively charged analytes such as oligonucleotides which are too strongly adsorbed on RP/WAX without acidic co-ligands. While these acidic co-ligands reduced the retention, the selectivity was not much influenced indicating the still dominating role of the RP/WAX ligand of the Poly-RP/WAX/SCX mixed-mode phase. A PCA of retention data documented the complementarity of the retention profiles of the new polymeric RP/WAX phases compared to HILIC, commercial MMC and polar RP phases. Stress tests confirmed the greatly superior stability of the new polymer bonded RP/WAX phases compared to brush-type analogs. Due to their general mobile phase compatibility and orthogonal retention patterns in both elution modes these new stationary phases could be valuable alternatives in 2D-LC.

4.1.6. References

[1] P. Jandera, P. Janas, Recent advances in stationary phases and understanding of retention in hydrophilic interaction chromatography. A review, Anal Chim Acta, 967 (2017) 12-32.

[2] D.V. McCalley, Understanding and manipulating the separation in hydrophilic interaction liquid chromatography, J Chromatogr A, 1523 (2017) 49-71.

[3] E. Lemasson, S. Bertin, P. Hennig, E. Lesellier, C. West, Mixed Mode Chromatography - A Review, Suppl. to LCGC - Eur./LCGC North Am. , (2017) 22-33.

[4] L. Wang, W. Wei, Z. Xia, X. Jie, Z. Zilu Xia, Recent advances in materials for stationary phases of mixed-mode high-performance liquid chromatography, TrAC Trends in Analytical Chemistry, 80 (2016).

[5] K. Zhang, X. Liu, Mixed-mode chromatography in pharmaceutical and biopharmaceutical applications, J Pharm Biomed Anal, 128 (2016) 73-88.

[6] L. Zhang, Q. Dai, X. Qiao, C. Yu, X. Qin, H. Yan, Mixed-mode chromatographic stationary phases: Recent advancements and its applications for high-performance liquid chromatography, TrAC Trends in Analytical Chemistry, 82 (2016) 143-163.

[7] R. Kuhnreich, U. Holzgrabe, Impurity profiling of L-methionine by HPLC on a mixed mode column, J Pharm Biomed Anal, 122 (2016) 118-125.

[8] S. Bäurer, W. Gua, S. Polnick, M. Lämmerhofer, Simultaneous Separation of Water- and Fat-Soluble Vitamins by Selective Comprehensive HILIC × RPLC (High-Resolution Sampling) and Active Solvent Modulation, Chromatographia, (2018).

[9] C.J. Venkatramani, Y.-. Zelechonok, Two-dimensional liquid chromatography with mixed mode stationary phases, J. Chromatogr. A 1066 (2005) 47–53.

[10] X. Cai, Z. Guo, X. Xue, J. Xu, X. Zhang, X. Liang, Two-dimensional liquid chromatography separation of peptides using reversed-phase/weak cation-exchange mixed-mode column in first dimension, J Chromatogr A, 1228 (2012) 242-249.

[11] T. Aral, H. Aral, B. Ziyadanogullari, R. Ziyadanogullari, Synthesis of a mixed-model stationary phase derived from glutamine for HPLC separation of structurally different biologically active compounds: HILIC and reversed-phase applications, Talanta, 131 (2015) 64-73.

[12] S. Bäurer, S. Polnick, O.L. Sánchez Muñoz, M. Kramer, M. Lämmerhofer, N-Propyl-N'-2-pyridylurea-modified silica as mixed-mode stationary phase with moderate weak anion exchange capacity and pH-dependent surface charge reversal, J Chromatogr A, 1560 (2018) 45-54.

[13] J.L. Dores-Sousa, J. De Vos, W.T. Kok, S. Eeltink, Probing selectivity of mixed-mode reversed-phase/weak-anion-exchange liquid chromatography to advance method development, J Chromatogr A, 1570 (2018) 75-81.

[14] M. Lämmerhofer, R. Nogueira, W. Lindner, Multi-modal applicability of a reversed-phase/weak-anion exchange material in reversed-phase, anion-exchange, ion-exclusion, hydrophilic interaction and hydrophobic interaction chromatography modes, Anal Bioanal Chem, 400 (2011) 2517-2530.

[15] Y. Li, Y. Feng, T. Chen, H. Zhang, Imidazoline type stationary phase for hydrophilic interaction chromatography and reversed-phase liquid chromatography, J Chromatogr A, 1218 (2011) 5987-5994.

[16] R. Nogueira, M. Lämmerhofer, W. Lindner, Alternative high-performance liquid chromatographic peptide separation and purification concept using a new mixed-mode reversed-phase/weak anion-exchange type stationary phase, J Chromatogr A, 1089 (2005) 158–169.

[17] A. Zimmermann, R. Greco, I. Walker, J. Horak, A. Cavazzini, M. Lämmerhofer, Synthetic oligonucleotide separations by mixed-mode reversed-phase/weak anion-exchange liquid chromatography, J Chromatogr A, 1354 (2014) 43-55.

[18] X. Liu, C.A. Pohl, HILIC behavior of a reversed-phase/cation-exchange/anion-exchange trimode column, J Sep Sci, 33 (2010) 779-786.

[19] L. Wang, W. Wei, Z. Xia, X. Jie, Z. Zilu Xia, Recent advances in materials for stationary phases of mixed-mode high-performance liquid chromatography, Trends in Analytical Chemistry, 80 (2016) 495-506.

[20] Y. Li, Z. Xu, Y. Feng, X. Liu, T. Chen, H. Zhang, Preparation and Evaluation of Poly-L-Lysine Stationary Phase for Hydrophilic Interaction/Reversed-Phase Mixed-Mode Chromatography, 74 (2011) 523–530.

[21] S. Ray, M. Takafuji, H. Ihara, Chromatographic evaluation of a newly designed peptide-silica stationary phase in reverse phase liquid chromatography and hydrophilic interaction liquid chromatography: mixed mode behavior, J Chromatogr A, 1266 (2012) 43-52.

[22] A. Shen, X. Li, X. Dong, J. Wei, Z. Guo, X. Liang, Glutathione-based zwitterionic stationary phase for hydrophilic interaction/cation-exchange mixed-mode chromatography, J Chromatogr A, 1314 (2013) 63-69.

[23] W. Zhao, X. Lou, J. Guo, P. Sun, Y. Jia, L. Zheng, L. He, S. Zhang, Investigation of the chromatographic regulation properties of benzyl groups attached to bridging nitrogen atoms in a calixtriazine-bonded stationary phase, J Sep Sci, 41 (2018) 2110-2118.

[24] K. Hu, Z. Deng, B. Wang, Y. Cui, M. Miao, W. Liu, Q. Jiang, W. Zhao, Y. Huang, S. Zhang, Development of a decaaza-cyclophane stationary phase for high-performance liquid chromatography, J Sep Sci, 38 (2015) 60-66.

[25] D. Zhou, J. Zeng, Q. Fu, D. Gao, K. Zhang, X. Ren, K. Zhou, Z. Xia, L. Wang, Preparation and evaluation of a reversed-phase/hydrophilic interaction/ion-exchange mixed-mode chromatographic stationary phase functionalized with dopamine-based dendrimers, J Chromatogr A, 1571 (2018) 165-175.

[26] X. Shi, L. Qiao, G. Xu, Recent development of ionic liquid stationary phases for liquid chromatography, J Chromatogr A, 1420 (2015) 1-15.

[27] Z. Chu, L. Zhang, W. Zhang, Preparation and evaluation of maltose modified polymer-silica composite based on cross-linked poly glycidyl methacrylate as high performance liquid chromatography stationary phase, Anal Chim Acta, 1036 (2018) 179-186.

[28] M. Sun, H. Qiu, L. Wang, X. Liu, S. Jiang, Poly(1-allylimidazole)-grafted silica, a new specific stationary phase for reversed-phase and anion-exchange liquid chromatography, J Chromatogr A, 1216 (2009) 3904-3909.

[29] M. Takafuji, M. Shahruzzaman, K. Sasahara, H. Ihara, Preparation and characterization of a novel hydrophilic interaction/ion exchange mixed-mode chromatographic stationary phase with pyridinium-based zwitterionic polymer-grafted porous silica, J Sep Sci, 41 (2018) 3957-3965.

[30] Q. Wang, M. Ye, L. Xu, Z.G. Shi, A reversed-phase/hydrophilic interaction mixed-mode C18-Diol stationary phase for multiple applications, Anal Chim Acta, 888 (2015) 182-190.

[31] L. Qiao, S. Wang, H. Li, Y. Shan, A. Dou, X. Shi, G. Xu, A novel surface-confined glucaminium-based ionic liquid stationary phase for hydrophilic interaction/anion-exchange mixed-mode chromatography, J Chromatogr A, 1360 (2014) 240-247.

[32] X. Liu, C. Pohl, A. Woodruff, J. Chen, Chromatographic evaluation of reversed-phase/anion-exchange/cation-exchange trimodal stationary phases prepared by electrostatically driven self-assembly process, J Chromatogr A, 1218 (2011) 3407-3412.

[33] M.E. Ibrahim, C.A. Lucy, Mixed mode HILIC/anion exchange separations on latex coated silica monoliths, Talanta, 100 (2012) 313-319.

[34] H. Hinterwirth, M. Lämmerhofer, B. Preinerstorfer, A. Gargano, R. Reischl, W. Bicker, O. Trapp, L. Brecker, W. Lindner, Selectivity issues in targeted metabolomics: Separation of phosphorylated carbohydrate isomers by mixed-mode hydrophilic interaction/weak anion exchange chromatography, J Sep Sci, 33 (2010) 3273-3282.

[35] E. Apfelthaler, W. Bicker, M. Lämmerhofer, M. Sulyok, R. Krska, W. Lindner, R. Schuhmacher, Retention pattern profiling of fungal metabolites on mixed-mode reversed-phase/weak anion exchange stationary phases in comparison to reversed-phase and weak anion exchange separation materials by liquid chromatography-electrospray ionisation-tandem mass spectrometry, J Chromatogr A, 1191 (2008) 171-181.

[36] W. Bicker, M. Lämmerhofer, T. Keller, R. Schuhmacher, R. Krska, W. Lindner, Validated Method for the Determination of the Ethanol Consumption Markers Ethyl Glucuronide, Ethyl Phosphate, and Ethyl Sulfate in Human Urine by Reversed-Phase/Weak Anion Exchange Liquid Chromatography-Tandem Mass Spectrometry, Anal Chem, 78 (2006) 5884-5892.

[37] E.M. Borges, Silica, hybrid silica, hydride silica and non-silica stationary phases for liquid chromatography, J Chromatogr Sci, 53 (2015) 580-597.

[38] D.H. Marchand, L.R. Snyder, J.W. Dolan, Characterization and applications of reversed-phase column selectivity based on the hydrophobic-subtraction model, J Chromatogr A, 1191 (2008) 2-20.

[39] J.J. Kirkland, J.J.B. Adams, M.A. van Straten, H.A. Claessens, Bidentate Silane Stationary Phases for Reversed-Phase High-Performance Liquid Chromatography, Anal Chem, 70 (1998) 4344-4352.

[40] J.J. Kirkland, J.L. Glajch, R.D. Farlee, Synthesis and Characterization of Highly Stable Bonded Phases for High-Performance Liquid Chromatography Column Packings, Anal Chem, 61 (1989) 2-11.

[41] J.J. Kirkland, Development of some stationary phases for reversed-phase HPLC, Journal of Chromatography A, 1060 (2004) 9-21.

[42] M.J.J. Hetem, J.W. De Haan, H.A. Claessens, C.A. Cramers, A. Deege, G. Schomburg, Characterization and stability of silanized and polymercoated octadecyl reversed phases, Journal of Chromatography, 540 (1991) 53-76.

[43] M.J. Wirth, H.O. Fatunmbi, Horizontal Polymerization of Mixed Trifunctional Silanes on Silica: A Potential Chromatographic Stationary Phase, Anal Chem, 64 (1992) 2783-2786.

[44] Y. Zhang, P.W. Carr, Novel ultra stable silica-based stationary phases for reversed phase liquid chromatography--study of a hydrophobically assisted weak acid cation exchange phase, J Chromatogr A, 1218 (2011) 763-777.

[45] A. Zimmermann, J. Horak, A. Sievers-Engler, C. Sanwald, W. Lindner, M. Kramer, M. Lämmerhofer, Surface-crosslinked poly(3-mercaptopropyl)methylsiloxane-coatings on silica as new platform for low-bleed mass spectrometry-compatible functionalized stationary phases synthesized via thiol-ene click reaction, J Chromatogr A, 1436 (2016) 73-83.

[46] O.L. Sánchez Muñoz, E.P. Hernández, M. Lämmerhofer, W. Lindner, E. Kenndler, Estimation and comparison of zeta-potentials of silica-based anion-exchange type porous particles for capillary electrochromatography from electrophoretic and electroosmotic mobility, Electrophoresis, 24 (2003) 390–398.

[47] M. Lämmerhofer, M. Richter, J. Wu, R. Nogueira, W. Bicker, W. Lindner, Mixed-mode ion-exchangers and their comparative chromatographic characterization in reversed-phase and hydrophilic interaction chromatography elution modes, J Sep Sci, 31 (2008) 2572-2588.

[48] R. Nogueira, M. Lammerhofer, W. Lindner, Alternative high-performance liquid chromatographic peptide separation and purification concept using a new mixed-mode reversed-phase/weak anion-exchange type stationary phase, J Chromatogr A, 1089 (2005) 158-169.

[49] C. Hellriegel, U. Skogsberg, K. Albert, M. Lämmerhofer, N.M. Maier, W. Lindner, Characterization of a chiral stationary phase by HR/MAS NMR spectroscopy and investigation of enantioselective interaction with chiral ligates by transferred NOE, J Am Chem Soc, 126 (2004) 3809-3816.

[50] E.P. Nesterenko, P.N. Nesterenko, B. Paull, Zwitterionic ion-exchangers in ion chromatography: A review of recent developments, Anal Chim Acta, 652 (2009) 3-21.

[51] A. Zimmermann, J. Horak, O.L. Sánchez-Muñoz, M. Lämmerhofer, Surface charge fine tuning of reversed-phase/weak anion-exchange type mixed-mode stationary phases for milder elution conditions, J Chromatogr A, 1409 (2015) 189-200.

[52] U. Woiwode, A. Sievers-Engler, A. Zimmermann, W. Lindner, O.L. Sánchez Muñoz, M. Lämmerhofer, Surface-anchored counterions on weak chiral anion-exchangers accelerate separations and improve their compatibility for mass-spectrometry-hyphenation, J Chromatogr A, 1503 (2017) 21-31.

[53] M.R. Euerby, P. Petersson, Chromatographic classification and comparison of commercially available reversed-phase liquid chromatographic columns using principal component analysis, Journal of Chromatography A, 994 (2003) 13-36.

[54] M. Etienne, A. Walcarius, Analytical investigation of the chemical reactivity and stability of aminopropyl-grafted silica in aqueous medium, Talanta 59 (2003) 1173 / 1188.

4.1.7. Supplemental Material

4.1.7.1. Materials

Kromasil 100 Å, 5µm, was from Eka Chemicals (Bohus, Sweden). Acetic acid, 2-propanol, 4-(dimethylamino)-pyridine (DMAP), 2,2-azobis-(2-methylpropionitrile) (AIBN), hydrogen peroxide (30% v/v), methanol and toluene in HPLC grade quality were supplied from Sigma Aldrich (Steinheim, Germany). Poly(3-mercaptopropyl)methylsiloxane (PMPMS) and vinyltrimethoxysilane were purchased from ABCR (Karlsruhe, Germany).

Trifluoroacetic acid (spectroscopy grade) (TFA) was supplied by Panreac Applichem (Darmstadt, Germany). Acetonitrile HPLC grade (ACN) was purchased from J.T.Baker (Netherlands).

The phosphorylated carbohydrates dihydroxyacetone phosphate dilithium (DHAP), glyceraldehyde-3-phosphate solution 50 mg/mL (GAP), D-ribose-5-phosphate disodium salt hydrate (Rib5P), D-glucosamine-6-phosphate (GlcN6P), D-fructose-6-phosphate disodium salt hydrate (F6P), α-D-glucose-1-phosphate sodium salt hydrate (G1P), and α-D-galactose-1-phosphate dipotassium salt pentahydrate (Gal1P) were obtained from Merck (Sigma Aldrich) (Munich, Germany).

4.1.7.2. Instrumentation

An Agilent 1100 series LC system (autosampler, degasser, quaternary pump, thermostated column compartment and diode array detector) was used for the analysis under RP and HILIC conditions as well as for the evaluation of the anion exchange capacity. For the analysis of the phosphorylated carbohydrates, a similar system was used differing in the installed pump (binary pump) and the detector (variable wavelength detector). It was additionally coupled to a charged aerosol detector (CAD) from Thermo Fisher Scientific (Munich, Germany). The chromatographic data of the synthetic oligonucleotides were measured on an Agilent 1290 series UHPLC system equipped with an autosampler, binary pump, degasser, thermostated column compartment and diode array detector.

4.1.7.3. Synthesis of Vinyl-Kromasil, Polymercoated and Oxidized Polymercoated Silica

Experimental

4.1.7.3.1. Vinyl-Kromasil

15.0 g dried Kromasil (100 Å, 5 µm) (under vacuum at 60 °C, overnight) was suspended in 200 mL toluene. To remove the water, the toluene was distilled with a distillation bridge. After discarding the first distilled milliliters, 50 mL toluene was distilled off. While cooling down, the system was purged with nitrogen. The vinylization was done by the addition of 5.043 mL vinyltrimethoxysilane and 150.0 mL DMAP. The mixture was refluxed overnight flushing constantly with nitrogen. Afterwards the silica gel was flushed three times with hot toluene and three times with hot methanol. The silica gel was dried overnight at 60 °C. The results of the CHNS elemental analysis are shown in Table S1 and the surface structure is shown in Fig. S1a).

4.1.7.3.2. Poly(3-Mercaptopropyl)methylsiloxane-Coated Silica (PMPMS Silica)

A suspension of 8.0 g vinyl silica and 80.0 mL methanol in a round bottom flask was formed. After the addition of 200 mg AIBN and 1.27 mL PMPMS (corresponding to 1 mmol sulfur per g vinyl silica), the suspension was sonicated and then evaporated to dryness using a rotary evaporator (337 mbar, 40 °C). Thereafter, the flask was flushed with nitrogen for two hours and the radical addition reaction was performed at 50-60°C overnight. Afterwards, hot toluene and hot methanol was used for the washing of the modified silica gel. It was dried overnight at 60 °C. The results of the elemental analysis are shown in Tab S1 and the surface structure in Fig S1b).

4.1.7.3.3. Oxidized Poly(3-Mercaptopropyl)methylsiloxane-Coated Silica (ox. PMPMS Silica)

6.0 g of the PMPMS-coated silica gel was suspended in 80.0 mL methanol and 4.2 mL formic acid. A mixture of 19.0 mL formic acid and 1 mL hydrogen peroxide (30 %, v/v) was prepared, allowed to stand for 2h at ambient temperature, and was then added dropwise under ice cooling and stirring for four hours. Subsequently, the silica was three times washed with a hot mixture of water and methanol (1:1, v/v). Afterwards the silica gel was dried overnight under vacuum at 60 °C. The results of the elemental analysis are shown in Table S1 and the surface structure in Fig S1b).

Table S1: Elemental analysis and calculated sulfur surface coverage of the modified silica gels

Stationary phase	% C	% H	% N	% S	Surface coverage S [mmol/g]	Surface coverage S [µmol/m^2]
Silica (unmodified)	0.27	0.50	-	-	-	-
Vinyl-Silica	3.,28	0.67	-	-	-	-
PMPMS-coated silica	7.93	1.65	0.12	3.18	0.99	3.31
Ox. PMPMS-silica	6.74	1.48	0.13	2.60	0.81	2.70

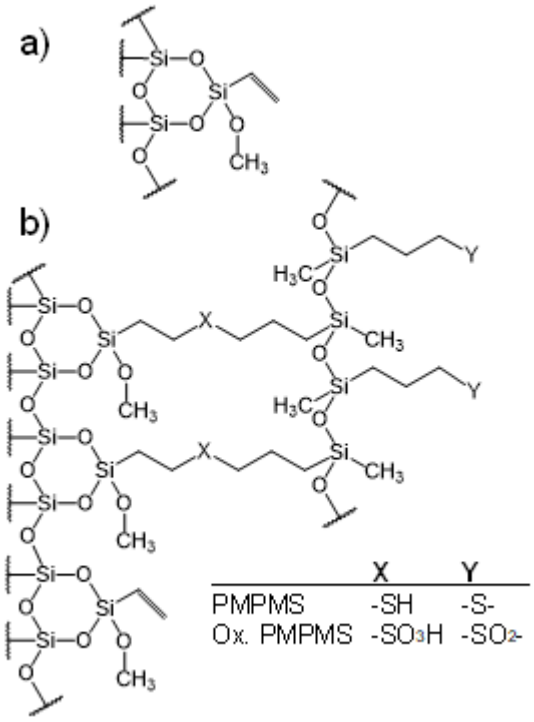

Fig. S1: Surface structure of the stationary phases used as reference materials for evaluation of the retention contributions by PCA

4.1.7.4. Solid-State ^{13}C Cross-Polarization Magic Angle Spinning (CP/MAS) NMR

The solid-state NMR spectra were measured on a Bruker Avance III HD XWB instrument (Bruker, Rheinstetten, Germany) operating at 300.13 MHz for ^{1}H and equipped with a 7 mm double resonance ($^{1}H/X$) probe. 10 kHZ was used for the spinning rate of the 7mm ZrO_2 rotor, 3.18 µs for the 90° proton pulse length and 5 ms and 2 s contact and relaxation delay times, respectively.

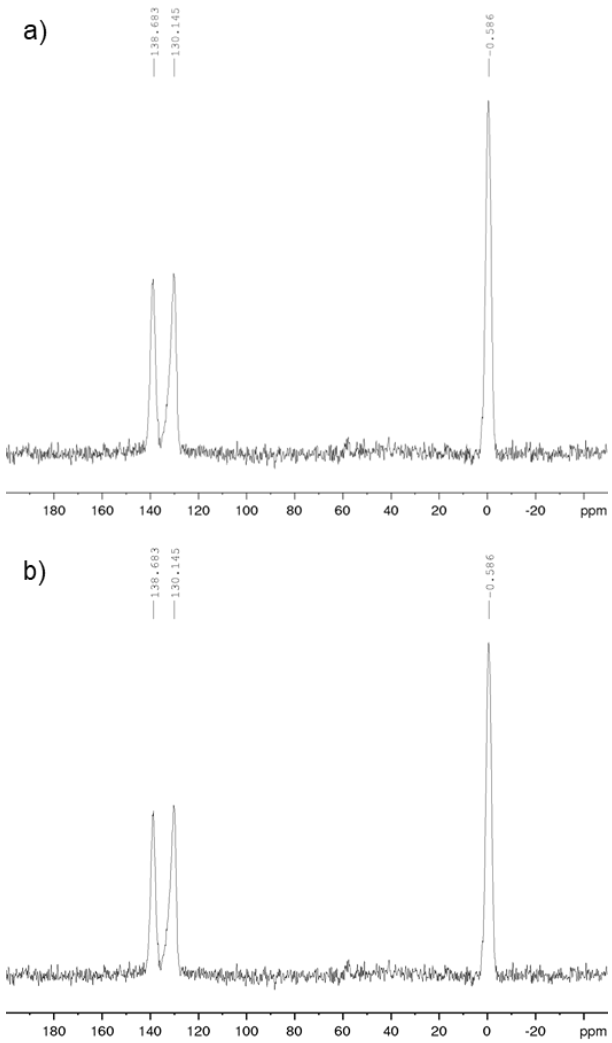

Fig S2: Solid-state ^{13}C CP/MAS NMR spectra of a) vinyl silica gel and b) vinyl silica gel after performic acid treatment.

Like the solid-state ^{29}Si CP/MAS NMR spectra (Fig 2), the ^{13}C CP/MAS NMR spectra showed no shifts of the vinyl signals which would indicate an oxidation of the vinyl group. The resonance signals did not change and it can be concluded that the vinyl group is not affected by the performic acid treatment.

4.1.7.5. Chromatographic Classification of the Stabilized Stationary Phases by Principal Component Analysis (PCA)

4.1.7.5.4. Classification under RP Conditions

The mobile phase was a mixture of ACN and water (40:60, v/v) containing 0.29 % acetic acid (C_{tot} = 50 mM). The pH value was adjusted to 6 with ammonia. The sample contained butylbenzene (BuB), pentylbenzene (PeB) and *N*-tert-butoxycarbonyl-propylphenylalanine (Boc-Pro-Phe) dissolved in the mobile phase; and *O*,*O*–diethylthiophosphate (DETP), which was prepared as follows. In the presence of an equimolar amount of triethylamine, *O*,*O*-diethylchlorothiophosphate was hydrolyzed to *O*,*O*-diethylthiophosphate in an acetonitrile/water (75:25; v/v) solution. The concentration of the analytes was 0.8 mg/mL. The injection volume was 10 µL. The linear flow velocity was 1.7 mm/s. The column was thermostated at 25 °C. The detection wavelength was 220 nm. The void volume was determined using uracil.

4.1.7.5.5. Classification under HILIC Conditions

Experimental

The mobile phases used for the xanthin mixture contained ACN/water (95:5, v/v) and for the vitamin and nucleoside a mixture of ACN/water (90:10, v/v), of which each was buffered with ammonium acetate to obtain a total concentration of 5 mM. The apparent pH was 8 (unadjusted). All samples were dissolved in the mobile phase to a concentration of 1.0 mg/mL from which 10 µL was injected. The linear flow velocity was 1.7 mm/s. The temperature of the columns was 25 °C. The samples were analyzed at a wavelength of 220 nm. The void volume was determined by toluene.

Results

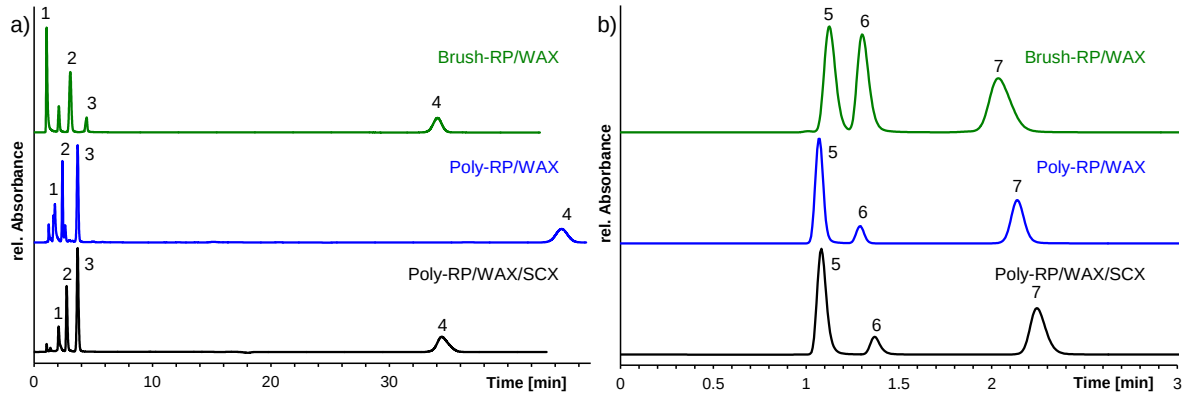

Fig S3: Separation of vitamins (a) and xanthines (b) under HILIC conditions using the new stationary phases. The investigated conditions were described above. 1. Thiamine, 2. Pyridoxine, 3. riboflavine, 4. nicotinic acid, 5. caffeine 6, Theobromine, 7. Theophylline.

4.1.7.5.6. Surface Structure of Investigated Stationary Phases

The RP and HILIC tests were done with the commercially available and in house synthetized stationary phases shown in Fig. S4. The obtained chromatographic data (Table S2 and S3) were used for the retention mapping by principal component analysis discussed in the main document

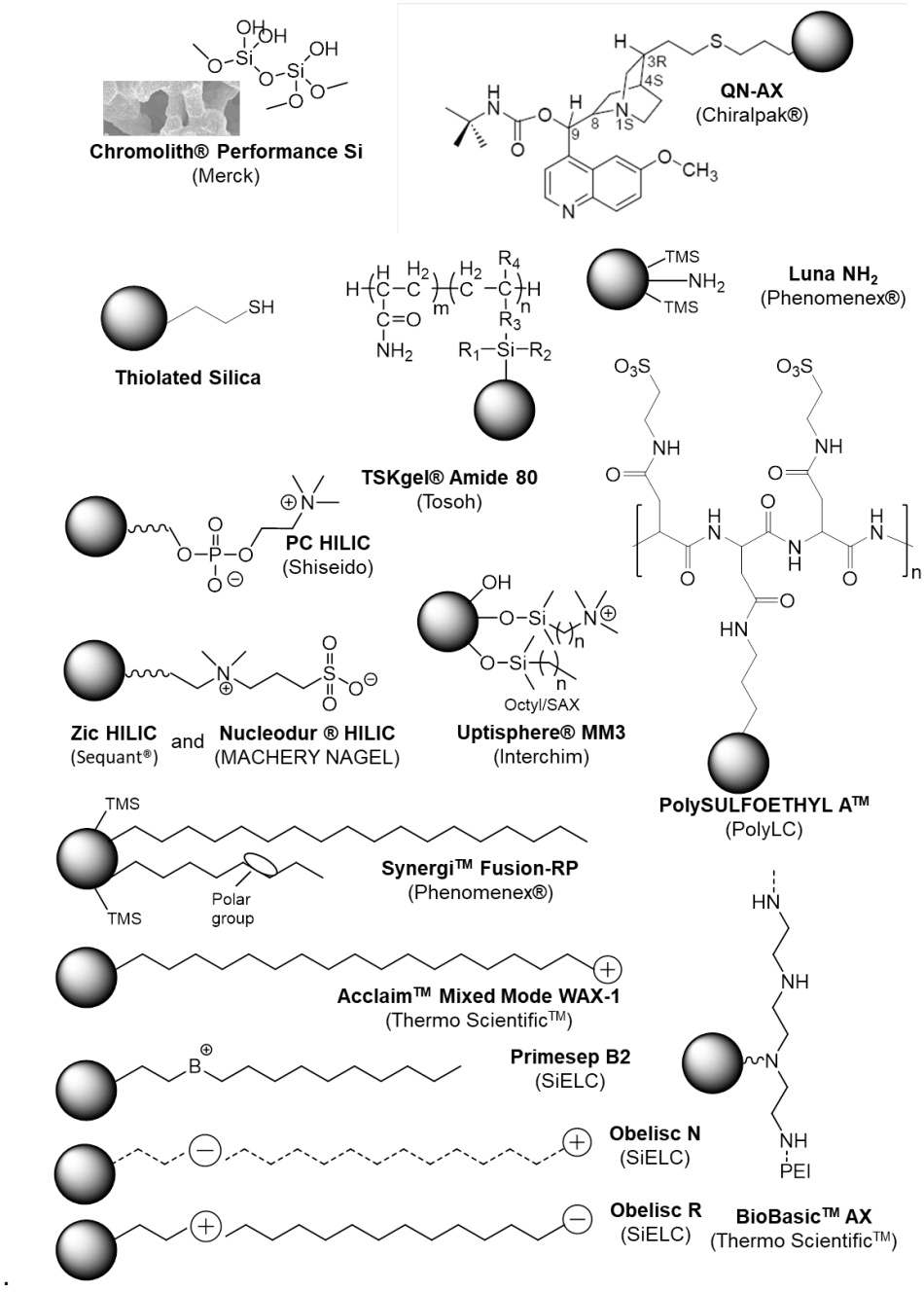

Fig. S4: Surface structure of the stationary phases which were used for the RP and HILIC tests to obtain a retention map.

Table S2: Retention factors and selectivities obtained by the separation of analytes of different polarity under RP and HILIC conditions

Column	Retention factor *k*					Selectivity α			
RP Conditions: [a]	BuB	PeB	DETP	BocProPhe		α(-DETP/BocProPhe)	α (-CH3-)		
Brush-RP/WAX	11.01	12.69	17.03	28.89		2.18	1.56		
Poly-RP/WAX	24.07	39.91	35.16	55.20		1.57	1.66		
Poly-RP/WAX/SCX	5.67	8.14	12.41	13.05		1.05	1.44		
HILIC Conditions: [b]	T	A	U	C	G	α (1,2)	α (2,3)	α (3,4)	α (4,5)
Brush-RP/WAX	0.79	1.59	1.89	4.12	7.52	2.01	1.19	2.18	1.83
Poly-RP/WAX	0.59	1.18	1.59	3.17	7.07	2.00	1.35	1.99	2.23
Poly-RP/WAX/SCX	0.99	1.82	1.94	3.61	8.55	1.84	1.07	1.86	2.37
	Thiamine	Pyridoxine	Riboflavine	Ascorbic acid	Nicotinic acid	α (1,2)	α (2,3)	α (3,4)	
Brush-RP/WAX	0.094	1.17	2.17	n.d.	34.37	12.45	1.85	15.84	
Poly-RP/WAX	0.77	1.39	2.56	n.d.	42.92	1.81	1.84	16.77	
Poly-RP/WAX/SCX	0.89	1.50	2.34	n.d.	30.28	1.69	1.56	12.94	
HILIC Conditions: [c]	Caffeine	Theobromine	Theophylline			α (1,2)	α (2,3)		
Brush-RP/WAX	0.17	0.35	1.11			2.06	3.17		
Poly-RP/WAX	0.00	0.14	0.89			n.a.	6.36		
Poly-RP/WAX/SCX	0.00	0.24	1.04			n.a.	4.33		

n.d. - not detected, n.a. – not available

[a] - Experimental conditions: ACN/H2O 40/60 (v/v), 50 mM acetic acid, pH 6 adjusted with ammonia, 1.7 mm/s, T=25°C, UV: 220 nm, 10 µL injected (0.8 mg/mL)

[b] - Experimental conditions: ACN/H2O 90/10 (v/v), 5 mM ammonium acetate, pH unadjusted, 1.7 mm/s, T=25°C, UV: 220 nm, 10 µL injected (1.0 mg/mL)

[c] - Experimental conditions: ACN/H2O 95/5 (v/v), 5 mM ammonium acetate, pH unadjusted, 1.7 mm/s, T=25°C, UV: 220 nm, 10 µL injected (1.0 mg/mL)

Table S3: Chromatographic efficiency under RP and HILIC conditions

Column	Plate Height H [10^{-6} m]				
RP Conditions: [a]	BuB	PeB	DETP	BocProPhe	
Brush-RP/WAX	19.57	18.47	15.23	20.70	
Poly-RP/WAX	21.17	20.59	22.90	25.03	
Poly-RP/WAX/SCX	33.33	34.16	33.17	36.85	
HILIC Conditions: [b]	T	A	U	C	G
Brush-RP/WAX	74.54	35.64	28.54	20.12	25.94
Poly-RP/WAX	42.85	35.66	33.22	28.40	25.95
Poly-RP/WAX/SCX	50.73	56.88	41.98	38.96	127.95
	Thiamine	Pyridoxine	Riboflavine	Ascorbic acid	Nicotinic acid
Brush-RP/WAX	204.21	71.12	80.33	n.d.	10.59
Poly-RP/WAX	108.11	31.74	35.01	n.d.	15.29
Poly-RP/WAX/SCX	96.15	51.37	47.99	n.d.	25.47
HILIC Conditions: [c]	Caffeine	Theobromine	Theophylline		
Brush-RP/WAX	75.87	56.83	74.87		
Poly-RP/WAX	60.07	42.25	37.25		
Poly-RP/WAX/SCX	74.61	52.01	47.60		

n.d. - not detected

[a] - Experimental conditions: ACN/H2O 40/60 (v/v), 50 mM acetic acid, pH 6 adjusted with ammonia, 1.7 mm/s, T=25°C, UV: 220 nm, 10 µL injected (0.8 mg/mL)

[b] - Experimental conditions: ACN/H2O 90/10 (v/v), 5 mM ammonium acetate, pH unadjusted, 1.7 mm/s, T=25°C, UV: 220 nm, 10 µL injected (1.0 mg/mL)

[c] - Experimental conditions: ACN/H2O 95/5 (v/v), 5 mM ammonium acetate, pH unadjusted, 1.7 mm/s, T=25°C, UV: 220 nm, 10 µL injected (1.0 mg/mL)

Table S4: Retention factors k obtained by the isocratic analysis of nucleosides (adenosine=A, cytidine=C, guanosine=G, thymidine=T, uridine=U), vitamins (riboflavine, ascorbic acid and nicotinic acid) and xanthines (caffeine, theobromine and theophylline) on several columns under HILIC conditions.

Column	T	A	U	C	G	Riboflavine	Ascorbic acid	Nicotinic acid	Caffeine	Theobromine	Theophylline
Brush-RP/WAX (AQ360)	0.79	1.59	1.89	4.12	7.52	2.17	n.d.	34.37	0.17	0.35	1.11
Thiolated silica	0	0.11	0	0.15	0.15	0.1	0	0	0	0	0
Acclaim Mixed Mode WAX-1	0.88	1.67	1.9	4.18	7.15	1.66	n.d.	31.14	0.1	0.26	0.84
Uptisphere 5 MM3	0	0.15	0.15	0.81	1.05	0.13	5.27	3.03	0	0	0
Primesep B2	0	0.1	0	0.22	0.22	0.04	0.04	0.73	0.02	0.02	0.11
Obelisc R	0.09	0.48	0.48	2.15	2.69	0.78	2.73	10.11	0.06	0.14	0.26
Obelisc N	0.23	0.59	0.48	2.75	1.61	1.15	1.15	0.66	0.15	0.22	0.22
Chiralpak QN-AX	0.15	0.15	0.15	0.29	0.29	0.32	n.d.	3.52	0.1	0.24	0.44
Luna NH2	1.21	3.8	3.8	11.99	19.18	3.1	28.74	24.9	0.31	0.67	3.19
BioBasic AX	0.35	0.84	0.75	2.18	3.42	0.89	n.d.	10.88	0.08	0.18	0.18
Synergi Fusion-RP	0	0.04	0	0.16	0.04	0	0	0.44	0	0	0
TSKGel Amide-80	1.27	3.12	3.45	10.2	12.8	4.77	20.7	5.49	0.4	0.76	1.16
PolysulfoethylA	0.77	2.08	3.14	15.02	16.69	3.1	n.d.	2.73	0.2	0.45	0.51
ZIC-HILIC	0.89	2.09	3.24	9.54	12.63	2.2	35.13	4.89	0.28	0.63	0.63
Nucleodur HILIC	0.91	1.64	2.08	5.05	6.53	1.78	6.26	1.78	0.36	0.67	0.67
Chromolith Performance Si	0.29	0.76	0.61	2.26	2.04	0.65	1.41	1.85	0.19	0.19	0.19
PC-HILIC	1	2.29	1.66	4.7	5.21	2.66	6.65	2.05	0.6	1.03	1.03
Kromasil	0.58	1.70	0.89	3.00	3.65	0.34	0.09	5.23	0.43	0.79	0.87
Vinyl-Kromasil	0.09	0.42	0.09	0.42	0.55	0.27	n.d.	1.28	0.25	0.30	0.30
PMPMS	0.02	0.17	0.02	0.17	0.17	0.11	0.11	0.47	0.21	0.21	0.21
oxidized PMPMS	0.19	0.46	0.24	0.76	0.91	0.58	n.d.	0.73	0.13	0.25	0.33

Table S5: Retention factors obtained by the isocratic analysis of hydrophobic alkylbenzenes (butylbenzene (BuB) and pentylbenzene (PeB)) and acidic compounds (diethylthiophosphate (DETP) and BocProPhe) on several columns under RP conditions.

Column	BuB	PeB	DETP	BocProPhe
Brush-RP/WAX (AQ360)	11.8	18.36	25.71	45.91
Thiolated silica	5.02	6.33	0	0
Acclaim Mixed Mode WAX-1	5.52	8.47	14.45	34.75
Uptisphere 5 MM3	27.73	48.89	0.19	0.28
Primesep B2	9.97	15.59	1.97	5.36
Obelisc R	6.22	9.47	3.59	10.97
Obelisc N	1	1.35	4	3.64
Chiralpak QN-AX	4.11	5.76	5.76	7.69
Luna NH2	0	0	4.39	1.76
BioBasic AX	0	0	1.05	0.53
Synergi Fusion-RP	24.17	43.28	0	0.06
TSKGel Amide-80	0	0	0	0
PolysulfoethylA	0	0	0	0
ZIC-HILIC	0	0	0.14	0
Nucleodur HILIC	0	0	0	0
Chromolith Performance Si	0	0	0	0
PC-HILIC	0	0	0.12	0.22
Kromasil	0.00	0.00	0.00	0.00
Vinyl-Kromasil	3.37	4.40	0.00	0.16
PMPMS	3.20	4.33	0.00	0.16
oxidized PMPMS	23.16	37.03	0.00	0.26

4.1.7.5.7. Statistical Results of the PCA

Table S6: Sum of squared residuals and predicted sum of squared errors of the principal component analysis using the investigated columns as objects and the calculated retention factors (Tab. S2, S4 and S5) as factors.

PC	R^2	Cumulative R^2	Q^2	Cumulative Q^2
1	0.549	0.549	0.453	0.453
2	0.255	0.803	0.35	0.644

4.1.7.6. Characterization of Anion Exchange Retention in a pH and Counterion Dependent Manner as well as Effect of Acidic Co-Ligands

The anion exchange capability of the new mixed-mode phases can be readily characterized by the stoichiometric displacement model [1-3]. This simple retention model assumes a direct proportional dependency of the logarithm of retention factors of charged compounds *k* and the logarithm of the concentration of counter ions *C* for a common ion-exchange process (Eq. 1).

$$\log k = \log K_Z - Z \cdot \log[C] \quad (1)$$

wherein *Z* is the slope and shows direct proportionality to the ratio of effective charge numbers of solute ($z_{eff,S}$) and counter-ion ($z_{eff,C}$). The intercept K_z, is a system specific constant, which is related to the equilibrium constant *K* (in L/mol). The dependency can be described as follows.

$$K_z = \frac{K \cdot S \cdot (q_x)^Z}{V_0} \quad (2)$$

whereby, *S* represents the surface area (in m^2/g stationary phase), q_x the number of ion exchange sites (available for adsorption) (in mol/m^2) and V_0 the volume of the mobile phase within the column (in L).

It can be seen that this simple linear model sufficiently well describes the effect of counterion concentration on retention factors and documents that for both Poly-RP/WAX and Poly-RP/WAX/SCX anion-exchange dominates the retention of *N*-Ac-Phe and *N*-Ac-Trp (Fig. S5). The highest actual anion-exchange capacity was observed at pH 5 which corroborates the results of ζ-potential determinations that showed a global maximum at this pH for both of the mixed-mode phases as well, and at which the acidic analytes are largely ionized.

It is striking that the trend lines of Poly-RP/WAX/SCX show a significant offset in retention compared to Poly-RP/WAX, just like the ζ-potential in Fig. 3. It means that Poly-RP/WAX/SCX shows significantly less retention for acidic solutes due to a lower positive net surface charge or due to an intramolecular counterion effect of the attached SCX moieties (which can be regarded as immobilized counterions). In view of this, the surface charge term q_x in Eq. 2 should be rewritten as Eq 3.

$$q_x = \sum_i^n z_i \cdot c_{s,i} \quad (3)$$

Wherein z_i and $c_{s,i}$ are the effective charge numbers and the concentrations of the distinct charged groups (here tertiary ammonium and SCX), respectively. Thus, it follows that

$$K_z = \frac{K \cdot S \cdot (\sum_i^n z_i \cdot c_{s,i})^Z}{V_0} = \frac{K \cdot S \cdot (z_{WAX} \cdot c_{WAX} + z_{SCX} \cdot c_{SCX})^Z}{V_0} \quad (4)$$

Since, z_{WAX} and z_{SCX} have opposite charge signs, a lower positive net charge is obtained with Poly-RP/WAX/SCX as compared to Poly-RP/WAX. This formalism can also be expressed in terms of surface anchored counterion effect by eq. 5.

$$\log k = \log K_Z - Z \cdot \log[C]_m - X \cdot \log[C]_s \quad (5)$$

In this equation subscript m and s stand for counterions in the mobile (acetate) and stationary phase (SCX), respectively. This formalism clearly explains the shift to lower retention factors on the Poly-RP/WAX/SCX phase in comparison to Poly-RP/WAX.

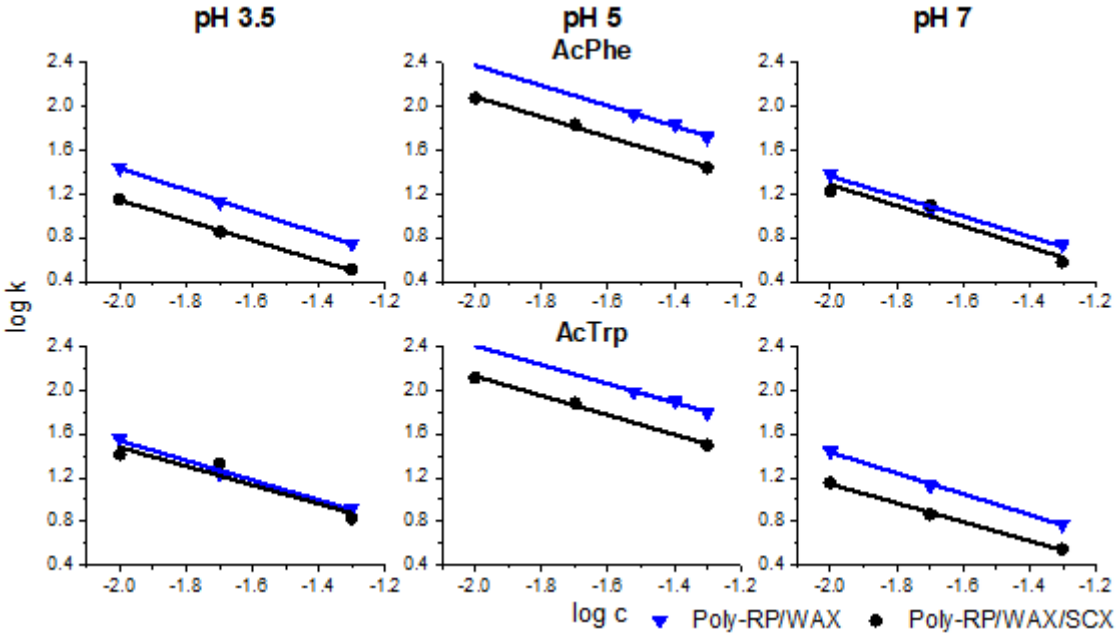

Fig. S5: Characterization of the anion exchange capacity of the Poly-RP/WAX and of the Poly-RP/WAX/SCX stationary phases in dependence of the pH using the stoichiometric displacement model. Analytes, *N*-acetylphenylalanine (AcPhe) and *N*-acetyltryptophan (AcTrp). Experimental conditions: mobile phase: ACN/H_2O (80:20, v/v), 10, 20 and 50 mM or 30, 40 and 50 mM acid (pH 3.5: formic acid, pH 5 and 7: acetic acid), pH 3.5, 5 or 7 adjusted with ammonia. Flow rate,1.0 mL/min; injection volume, 10 µL; column temperature, 25 °C; AcPhe: 258 nm, AcTrp: 280 nm; sample concentration, 1 mg/mL; void volume marker, acetone.

4.1.7.7. Application of the New Stationary Phases

4.1.7.7.8. Analysis of Synthetic Oligonucleotides by UHPLC-UV

Experimental

The mobile phases for the separation of the oligonucleotide mixture were a mixture of ACN and water (20:80, v/v). The ortho-phosphoric acid concentration in the mobile phases was 50 mM (A) and 100 mM (B) in the case of the polymer coated stationary phases and 100 mM (A) and 200 mM (B) in the case of the brush type stationary phase. The pH of the mobile phase A was adjusted to pH 7 with triethylamine (TEA) and mobile phase B to pH 8 in the final mixture. The investigated gradient started at 50 % mobile phase B and rised in 25 minutes to 100% B which was maintained for 27 minutes. In 2 minutes the amount of B was reduced to the initial percentage of 50 % B and was reequilibrated for 8 minutes.

The oligonucleotide test mixture had a concentration of 8.0 µM (each oligo). The injection volume was 10 µL, the flow rate was 1.0 mL/min. The column temperature was 40 °C and the detection wavelength was 254 nm.

Results

Table S7: Chromatographic data of the separation of synthetic oligo nucleotides with minor sequence differences, chromatographic conditions as described in Fig. 7

	Retention time [min]			**Peak width [min]**			**Resolution**	
	III[a]	**I[a]**	**II[a]**	**III[a]**	**I[a]**	**II[a]**	**$R_{III,I}$**	**$R_{I,II}$**
Brush-RP/WAX	28.53	31.00	34.3	0.43	0.51	0.63	3.11	3.43
Poly-RP/WAX	28.08	30.17	33.76	0.51	0.60	0.82	2.22	3.01
Poly-PR/WAX/SCX	13.94	15.33	16.55	0.50	0.51	0.53	1.63	1.38

[a] - Oligonucleotide sequence can be found in Fig. 7

4.1.7.7.9. Analysis of Phosphorylated Carbohydrates by LC-CAD

Experimental

The mobile phases of the isocratic experiments were a mixture of ACN/water (70:30, v/v) containing 0.1 % (v/v) TFA. The mobile phase A of the gradient elution of DHAP and GAP was an aqueous solution containing 0.1 % TFA, whereas the mobile phase B contained 0.1 % TFA in ACN. The gradient started at 80% of mobile phase B and decreased in 20 minutes to 20 % B. After 5 minutes holding 20 % B the amount of B returned to the starting conditions in 2 minutes followed by a reequilibration time of 5 min.

All samples were dissolved in water at a concentration of 0.05 mg/mL. The injection volume was 10 µL and the flow rate 1.0 mL/min. The column was thermostated at 25 °C. Analyte detection was performed with a charged aerosol detector.

Results and discussion

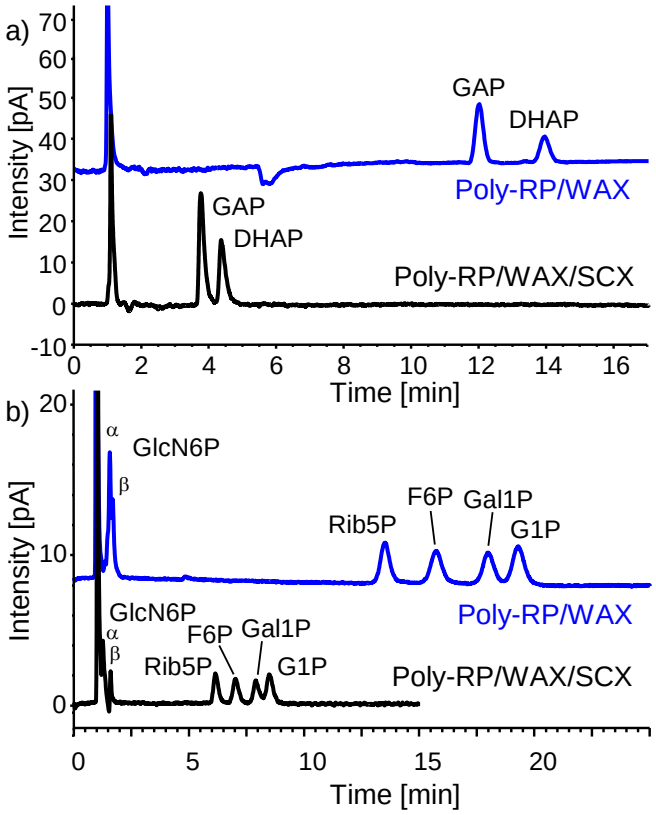

Fig S6: Separation of phosphorylated carbohydrates utilizing the Poly-RP/WAX and Poly-RP/WAX/SCX stationary phases. Separation of a) isomer GAP and DHAP, and b) of five phosphorylated C5/C6 carbohydrates. a) Mobile phase: A: 0.1 % TFA in H_2O, B: 0.1 % TFA in ACN; gradient: 20 min 80 to 20 % B, hold 20 % B for 5 min, reequilibration 80 % B for 5 min; b) Mobile phase: 0.1 % TFA in ACN/water (70/30, v/v). Abbreviations: GAP, glyceraldehyde-3-phosphate; DHAP, dihydroxyacetone phosphate; GlcN6P, glucosamine-6-phosphate; Rib5P, ribose-5-phosphate; F6P, fructose-6-phosphate; Gal1P, galactose-1-phoshpate; G1P, glucose-1-phosphate. For further details about conditions see experimental part above.

The separation of isomers of phosphorylated carbohydrates is a challenging yet highly relevant task in metabolomics [4]. A large number of constitutional isomers and diastereomers exist in this class of compounds which are difficult or impossible to distinguish by mass spectrometry. For example, special attention has to be paid in metabolic profiling studies to the isomeric structures of the glycolysis pathway such as the constitutional isomers DHAP and GAP, which are interconverted by the triose phosphate isomerase [4]. Both of the polymer-bonded RP/WAX phases of this study showed remarkable capability to chromatographically resolve these very hydrophilic isomeric compounds with a HILIC gradient under acidic conditions (0.1% TFA in mobile phase) (Fig. S6 a)). The resolution was 4.7 on the Poly-RP/WAX phase. In general, the Poly-RP/WAX stationary phase showed enhanced retention properties compared to the Poly-RP/WAX/SCX stationary phase. In spite of significantly reduced retention due to repulsive electrostatic interactions of SCX moieties on the Poly-RP/WAX/SCX, this MMC stationary phase still exhibited satisfactory isomer selectivity for the polar triose phosphates.

Additionally, a more complex mixture of phosphorylated C5/C6 carbohydrates was analyzed on the Poly-RP/WAX as well as on the Poly-RP/WAX/SCX stationary phase under similar but isocratic HILIC conditions (Fig. S6 b)). The epimers Gal1P and G1P were fully baseline separated on the Poly-RP/WAX column and the other phosphorylated sugar phosphates could be resolved as well. The additional repulsive electrostatic interactions caused by the SCX sites on the oxidized stationary phase had led to a decrease in retention, but only a small loss of selectivity. The faster elution on the Poly-RP/WAX/SCX is certainly of advantage as resolution is essentially maintained.

4.1.7.8. References

[1] A.F. Gargano, T. Leek, W. Lindner, M. Lämmerhofer, Mixed-mode chromatography with zwitterionic phosphopeptidomimetic selectors from Ugi multicomponent reaction, J Chromatogr A, 1317 (2013) 12-21.

[2] U. Woiwode, A. Sievers-Engler, A. Zimmermann, W. Lindner, O.L. Sánchez Muñoz, M. Lämmerhofer, Surface-anchored counterions on weak chiral anion-exchangers accelerate separations and improve their compatibility for mass-spectrometry-hyphenation, J Chromatogr A, 1503 (2017) 21-31.

[3] A. Zimmermann, J. Horak, O.L. Sánchez-Muñoz, M. Lämmerhofer, Surface charge fine tuning of reversed-phase/weak anion-exchange type mixed-mode stationary phases for milder elution conditions, J Chromatogr A, 1409 (2015) 189-200.

[4] H. Hinterwirth, M. Lämmerhofer, B. Preinerstorfer, A. Gargano, R. Reischl, W. Bicker, O. Trapp, L. Brecker, W. Lindner, Selectivity issues in targeted metabolomics: Separation of phosphorylated carbohydrate isomers by mixed-mode hydrophilic interaction/weak anion exchange chromatography, J Sep Sci, 33 (2010) 3273-3282.

4.2. *N* -Propyl- *N'* -2-Pyridylurea-Modified Silica as Mixed-Mode Stationary Phase with Moderate Weak Anion Exchange Capacity and pH-Dependent Surface Charge Reversal

*Stefanie Bäurer [a], Stefan Polnick [a], Orlando L. Sánchez-Muñoz [b], Markus Kramer [c], Michael Lämmerhofer [a] **

[a] Institute of Pharmaceutical Sciences, Pharmaceutical (Bio-)Analysis, University of Tübingen, Auf der Morgenstelle 8, 72076 Tübingen, Germany

[b] Biomembranes Group, Institute of Molecular Science, Universitat de València. C/ Catedrático José Beltrán 2, 46980 Paterna, Valencia, Spain

[c] Institute of Organic Chemistry, University of Tübingen, Auf der Morgenstelle 18, 72076 Tübingen, Germany

Reprinted with permission from Journal of Chromatography A, Volume 1560 (2018) Pages 45-54, DOI: 10.1016/j.chroma.2018.05.012

4.2.1. Abstract

Herein, we present a novel silica-based stationary phase modified with *N*-propyl-*N'*-2-pyridylurea selector. Due to the weakly basic properties of the pyridine selector and the presence of residual silanols after selector immobilization, a zwitterionic surface with a pI observed at approximately pH 5.5 was measured by electrophoretic light scattering in pH-dependent ζ-potential determinations. The capability of the new *N*-propyl-*N'*-2-pyridylurea-modified silica to serve as mixed-mode stationary phase was investigated. For this purpose, it was characterized under RP and HILIC conditions using test mixtures. Subsequent classification of this stationary phase in comparison to in-house and commercial benchmarks was carried by principal component analysis of resultant retention factors from chromatographic tests. The results show a relatively unique mixed-mode character amongst the tested stationary phases. The chromatographic retention characteristics of acidic compounds matched well the ζ-potential determinations. The application of anion-exchange at low pH values (e.g. pH 5) and ion exclusion chromatography at pH 7 for the separation of uridine 5'-mono-, di- and triphosphate demonstrated a pH-dependent umpolung of the stationary phase surface. The combination of these separation principles in a pH gradient from 5 to 7 gave rise to weak anion-exchange selectivity with a charge-inducted elution due to repulsive interactions at higher pH and resulted in a significant faster separation with improved peak shape under mild elution conditions.

4.2.2. Introduction

Mixed-mode chromatography (MMC) offers the possibility to exploit two or more kinds of interactions in one chromatographic column in order to separate complex analyte mixtures or develop unique selectivity profiles [1-3]. The advantage of this chromatographic mode is the application of different elution conditions when using the same stationary phase with complementary selectivity. Great flexibility in method development results from this multimodal applicability. Due to the combination of a weak anion exchanger and a hydrophobic side chain connected by polar embedded groups [4], it was possible to successfully use this RP/WAX silica gel for the separation of complex analyte mixtures such as peptides [5-7], metabolites [8-10] and oligonucleotides [11] in different chromatographic modes. A disadvantage of this adsorbent was that relatively high buffer concentrations were necessary to elute charged analytes, in particular multiply charged ones such as oligonucleotides [11], so that detection and identification by mass spectrometry was not possible. However, silica-based anion-exchange materials may change their electrostatic surface potential from positive at low pH to negative at high pH due to residual silanols which may allow efficient elution of acidic analytes

at pH of the mobile phase above the pI of the stationary phase. Unfortunately, on conventional silica-based anion-exchangers this pI is typically observed at high pH at which silica-based materials may be hydrolytically instable. The aim was therefore to tailor the surface in such a way that the pI of the silica-based mixed-mode phase can be observed at around neutral pH. Efficient retention of acidic analytes below the pI and efficient elution above the pI of the stationary phase could be easily adjusted by a pH switch. For this reason, *N*-propyl-*N'*-2-pyridylurea was chosen as the anion exchanger site in this study.

Pyridine based stationary phases are well known for their good suitability and alternative selectivities to diol-, cyanopropyl modified and bare silica in supercritical fluid chromatography (SFC) [12]. 2-Ethylpyridine and vinylpyridine modified stationary phases are very popular commercially available columns from several manufacturers and various applications [13-18]. Additional polar embedded groups (amide, urea) in the linker of the pyridine selector molecule brought about complementary selectivities [19-21]. Pyridine functionalities have been also part of so called ionic liquid based stationary phases with linkage via pyridine nitrogen yielding a quaternary pyridinium ion [22-25].

Pyridine phases are also used for biopharmaceuticals chromatography, on the one hand for plasmid DNA separations [26-28], on the other hand for purification of monoclonal antibodies. The latter type of chromatography was termed as hydrophobic charge induction chromatography based on 4-mercaptoethylpyridine (MEP) modified stationary phases on which proteins are eluted by a pH shift to acidic conditions after their adsorption under neutral conditions by hydrophobic interactions [29-32].

In this study, a novel pyridine-based stationary phase (Fig. 1a) was synthesized and characterized in comparison to a recently proposed reversed-phase/weak anion-exchange (RP/WAX) type mixed-mode phase (Fig. 1b). This stationary phase shows as a new structural feature a urea group adjacent to the pyridyl residue yielding a specific alignment of directed H-donor/acceptor systems. Carboxylic acids (and possibly other acids as well) can interact at the pyridine by simultaneous hydrogen bonding superimposed upon ionic interactions (Fig. 1c) which combined with hydrophobic interactions at the aromatic ring gives rise to mixed-mode separations. The stationary phase was characterized by elemental analysis, solid state ^{13}C and ^{29}Si cross-polarization/magic angle spinning (CP/MAS) NMR spectroscopy, electrophoretic light scattering measurements for pH-dependent ζ-potential determinations and various chromatographic tests to illustrate the peculiarities of this material.

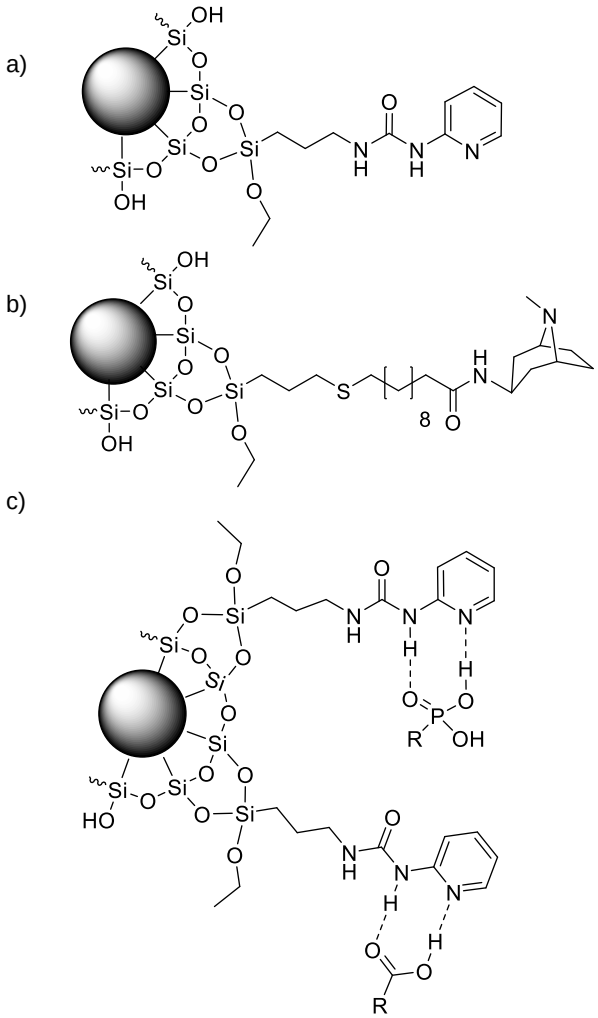

Fig. 1: Surface structure of the *N*-propyl-*N'*-2-pyridylurea (a) and *N*- (10-undecenoyl)-3-α-aminotropane (b) modified silica and the tentative molecular recognition mechanism for carboxylic and phosphonic (phosphoric) acids (c).

4.2.3. Materials and methods

4.2.3.1. Materials

3-Isocyanatopropyltriethoxysilane, dibutyl tin dilaurate, and 4-dimethylaminopyridine (DMAP) were supplied by ABCR (Karlsruhe, Germany). 2-Aminopyridine was purchased from Sigma Aldrich (Munich, Germany). Solvents for synthesis (toluene, methanol) were analytical grade and obtained from Sigma Aldrich. Kromasil 100 Å, 5 µm (Eka Chemicals, Bohus, Sweden) with a specific surface area of 320 m^2/g was used as supporting particles for the synthesis of the *N*-propyl-*N'*-2-pyridylurea -modified silica gel.

The compounds for characterization and classification of the synthesized stationary phase (butylbenzene (BuB), *O*,*O*-diethylchlorothiophosphate (DECTP), pentylbenzene (PeB), adenosine, guanosine, cytidine, thymidine, uridine, ascorbic acid, nicotinic acid, pyridoxine hydrochloride, riboflavin, thiamine hydrochloride, caffeine, theobromine, theophylline, L-phenylalanine (Phe), *N*-acetyl-L-phenylalanine (AcPhe), L-phenylalanine methyl ester (PheOMe), L-tryptophan (Trp), *N*-acetyl-L-tryptophan (AcTrp) and L-tryptophan-amide hydrochloride (Trp-amide) were supplied by Sigma Aldrich. *N*-*tert*-butoxycarbonyl-prolyl-phenylalanine (BocProPhe) and *N*-acetyl phenylalanine ethyl ester (AcPheOEt) were purchased from Bachem (Buchs, Switzerland). DETCP was hydrolysed to *O*,*O*-diethyl-thiophosphate (DETP) in the presence of an equimolar amount of triethylamine dissolved in acetonitrile/water (3:1; v/v). Uridine 5′-triphosphate trisodium salt hydrate (from yeast, type III, ≥96%) (UTP), Uridine 5′-(trihydrogen diphosphate) sodium salt (from *Saccharomyces cerevisiae*; 95-100%) (UDP) and Uridine 5′-monophosphate disodium salt (≥99%) (UMP) were supplied by Sigma Aldrich.

HPLC grade acetonitrile was from J.T. Baker (Netherlands). MilliQ water was prepared by purification of deionized water using Elga PurLab Ultra Purification system (Celle, Germany). The additives ammonium acetate, formic acid, acetic acid, phosphoric acid and ammonia were purchased from Sigma Aldrich in HPLC grade quality.

4.2.3.2. Synthesis of *N*-Propyl-*N*'-2-Pyridylurea -Bonded Stationary Phase

4.2.3.2.1. Synthesis of the Chromatographic Ligand

2.49 g (27.75 mmol) 2-aminopyridine was suspended in 80 mL of toluene and then dissolved under heat treatment. The remaining water in the mixture was removed by heating for 60 min to the boiling point under reflux followed by distillation of 30 mL toluene using a Liebig condenser and a measuring cylinder. The following steps were carried out under inert gas atmosphere (nitrogen). After cooling the solution, 3-isocyanatopropyltriethoxysilane (6.4 mL,

26.43 mmol) and the catalyst dibutyl tin dilaurate (15 µL) were added. After additional four hours of heating up to the boiling point, the solution was cooled down and the reaction product was characterized by FT-IR (ATR-technique) and NMR (see Suppl. material).

FT-IR (cm^{-1}): 3218, 2980, 2926, 2889, 1665, 1586, 1557, 1478, 1415, 1299, 1062, 954, 766, 687.

^{1}H-NMR ($CDCl_3$, 200MHz): δ in ppm, δ 9.38 (s, 1H), 8.15 (d, 1H), 7.75-7.48 (m, 2H), 6.92-6.80 (m, 2H), 3.94-3.72 (m, 9H), 3.48-3.30 (m, 2H), 1.86-1.60 (m, 2H), 1.16 (t, 9H), 0.81-0.53 (m, 2H).

^{13}C-NMR ($CDCl_3$, 200MHz): δ in ppm, δ 156.3, 153.5, 145.8, 138.4, 116.6, 112.1, 58.5, 42.5, 23.9, 18.3, 7.8.

4.2.3.2.2. Immobilization of the Chromatographic Ligand on Silica Gel

A suspension of 7.565 g silica gel (Kromasil 100 Å, 5 µm) and 80 mL toluene was heated for 60 min under reflux and then 40 mL of toluene were distilled off to remove water. Subsequently, 40 mL of the selector solution described in Chapter 4.2.3.2.1 as well as DMAP (0.05 mmol / g silica) were added and heated overnight under reflux and rinsing with nitrogen. The modified silica gel was washed 5 times with hot toluene and methanol each and then dried overnight at 60 °C in a vacuum drying oven. Afterwards, a sample was analyzed by elemental analysis (6.79% C, 1.18% H and 1.91% N), and solid-state ^{13}C and ^{29}Si cross-polarization magic angle spinning (CP/MAS) NMR (Fig. 2).

4.2.3.3. Column Packing

The *N*-propyl-*N'*-2-pyridylurea -modified silica was slurry packed into a stainless-steel column (150x4.6 mm ID) utilizing 800 bar and methanol as delivery solvent.

4.2.3.4. Structure Elucidation by Solid State ^{13}C and ^{29}Si Cross-Polarization Magic Angle Spinning NMR

Bruker ASX 300 spectrometer (Bruker, Rheinstetten, Germany) was used for the acquisition of ^{13}C and ^{29}Si CP/MAS NMR spectra. The modified silica (about 250 mg) was filled into a 7 mm double bearing ZrO_2 rotor and measured using a spinning rate of 10 kHz. For the ^{29}Si spectra the 90° proton pulse length was 3.2 µs, the contact time was 5 ms and the relaxation delay time was 2 s. Trimethylsilyl ester of octameric silica (Q_8M_8) was used for external reference of all chemical shifts. In order to acquire the ^{13}C NMR, the 90° puls length was 3.8 µs, the contact time 2 ms and the relaxation delay time was 4 s.

4.2.3.5. Electrophoretic Light Scattering Measurements and ζ–Potential Determinations

A Zetasizer NanoZS (Malvern Instruments, Herrenberg, Germany) particle analyzer with a Universal Dip Cell was used for measurement of the electrophoretic mobilities of the modified silica particles. For the calculation of the ζ-potentials, the Smoluchowski approximation was used. 0.2 mg/mL modified silica were suspended in 1 mM buffers. For evaluation of the pH dependency of the ζ-potentials in the pH range from 3.5 to 9.5 the following buffers were used: formic acid/Na-formate, acetic acid/Na-acetate, histidine, tris/tris-HCl, boric acid/Na-borate [33]. The ionic strength was fixed to 10 mM KCl. After sonification the suspension was measured three times at 25 ± 0.1°C for calculation of average values. Each measurement was the mean of 10 sub-runs.

4.2.3.6. Liquid Chromatographic Experiments

4.2.3.6.1. Instrumentation and Utilized Software

The measurements were carried out on an Agilent 1100 series LC system from Agilent Technologies (Waldbronn, Germany) equipped with a degasser, quaternary pump, autosampler, thermostated column compartment and diode array detector. Unless otherwise stated, the sample concentration was 1 mg/mL in mobile phase, the injection volume was 10 µL, the column temperature 25°C and the detection wavelength 220 nm. The pK_a values were calculated using MarvinSketch (ChemAxon). Principal component analysis was done with the statistic software JMP13.0.0 (SAS Institute).

4.2.3.6.2. Stationary Phase Characterization under RP Conditions

The evaluation of the chromatographic performance in RP mode was carried out using a mixture of ACN and water (40:60, v/v) as mobile phase. The total concentration of acetic acid was 50 mM. The pH was adjusted to 6 with ammonia. The linear velocity was adjusted to 1.7 mm/s. The void volume marker was uracil.

4.2.3.6.3. Stationary Phase Characterization under HILIC Conditions

The mobile phase for HILIC test conditions consisted of ACN and water mixtures. The mixing ratio was 95:5 (v/v) for the xanthines and 90:10 (v/v) for the vitamins and nucleosides. Both mobile phases contained 5 mM ammonia acetate and showed an unadjusted apparent pH of 8. The flow rate was calculated to the corresponding linear velocity of 1.7 mm/s. The void volume was determined by toluene.

4.2.3.6.4. Study of Anion Exchange Retention Mechanism in Dependence on pH

The mobile phases were a mixture of ACN/water (80:20, v/v) containing 10, 20 and 50 mM of the corresponding acid (formic acid: pH 3.5; acetic acid: pH 5 and 7), respectively. The pH was adjusted with ammonia. The flow rate was 1.0 mL/min. The detection of the phenylalanine derivatives was carried out at 258 nm and tryptophan derivatives at 280 nm. The void volume marker was uracil.

4.2.3.6.5. Separation of Nucleotides

The mobile phases for the isocratic experiments were a mixture of acetonitrile and water (1:4, v/v). The total ion strength was 1.25, 2.5 and 5 mM phosphoric acid and the pH was adjusted to 5 and 7, respectively, with ammonia. The following flow rates were investigated: 1.0 mL/min (isocratic and gradient experiments), 0.5 mL/min and 0.2 mL/min (isocratic experiments). The detection wavelength was 254 nm. The sample was a mixture of uridine mono-, di- and triphosphate (0.1 mg/mL) dissolved in mobile phase. The injection volume was 2 µL. The investigated gradient profiles are specified in the figure captions.

4.2.4. Results and Discussion

4.2.4.1. Synthesis of Mixed Mode Ligand and Immobilization on Silica Gel

The new mixed mode ligand was synthesized by reaction of 2-aminopyridine with the bifunctional linker 3-isocyanatopropyltriethoxysilane, which allowed the attachment to silica by a silanization reaction, in a stoichiometric ratio of 1:1 under water exclusion. In spite of the reactive trialkoxysilane group the synthesis product was sufficiently stable to allow its characterization by ATR-FT-IR spectroscopy, ^{1}H and ^{13}C NMR spectroscopy (Suppl. Material). Compared to the IR spectrum of the educt 2-aminopyridine, the IR spectrum of the product did not show an amine band at 3438 cm^{-1}. However, additional bands appeared at a wavenumber of 1665 cm^{-1} as well as in the range of 2980-2880 cm^{-1}. The former can be assigned to the urea group and the latter to the ethoxy functionalities and the propyl group of the linker. Also the chemical shifts of the ^{1}H and ^{13}C NMR indicated a successful synthesis of the ligand.

This pyridine derivative was immobilized on silica (100 Å, 5 µm) by a silanization reaction. In order to confirm the surface structure shown in Fig. 1a) solid state cross-polarization/magic angle spinning (ss CP/MAS) ^{13}C and ^{29}Si NMR spectra were measured (Fig. 2). The signals of the aliphatic carbon atoms stemming from the propyl-linker and remaining silyl ethoxy group can be found in the most shielded region of the ^{13}C NMR spectrum (0-60 ppm) (Fig. 2a). The aromatic carbon atoms and the carbonyl carbon of the urea are significantly shifted downfield (100–170 ppm). Since all expected ^{13}C signals could be observed, it was concluded that the immobilization reaction was successful.

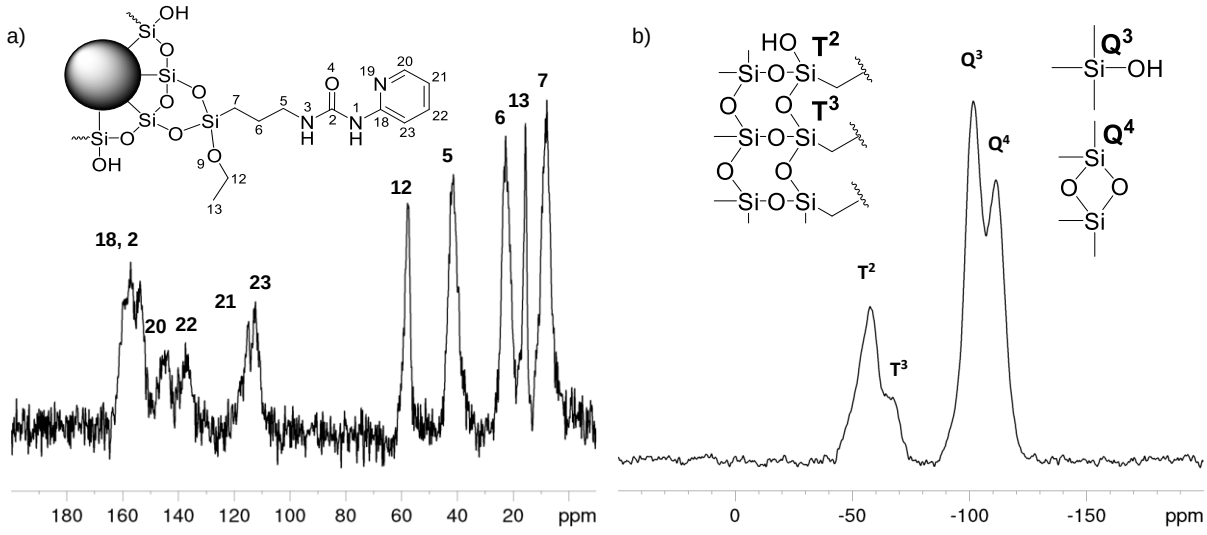

Fig. 2: Elucidation of the surface structure of the *N*-propyl-*N'*-2-pyridylurea silica gel by a) solid-state ^{13}C CP/MAS NMR, and b) solid state ^{29}Si CP/MAS NMR.

Siloxane bondings are generally sensitive to hydrolysis and are therefore of crucial importance when considering the lifetime of a stationary phase. The stability increases with the number of bonds per ligand (mono-, di- or trifunctional linkage). To investigate the siloxane bonding chemistry, a ss ^{29}Si CP/MAS NMR spectrum was acquired, which provides valuable information regarding the linkage type [24, 34–38]. In Fig. 2b) there are two groups of signals. The signals marked with Q are silicon atoms, which have only covalent bonds with oxygen atoms and are therefore located in the more unshielded chemical shift regions. In this case, the signals are related to siloxane groups (Q^4: -111 ppm) and free silanol groups (Q^3: -101 ppm). It becomes evident that there is a significant portion of free silanols which may have implications for the chromatographic behavior of the stationary phase (*vide infra*). The second signal set in the more shielded region provides information about the selector linkage chemistry which is of special interest from the chromatographic point of view (i.e. stability of the linkage; *vide supra*). Monofunctional siloxane bonds (T^1: -48 ppm), which are most sensitive to hydrolysis, are hardly present in the NMR spectrum. Based on the relative signal intensities of the di- (T^2: -58 ppm) and trifunctional (T^3: -64 ppm) siloxane bonds, it can be concluded that the majority of the ligands are bound by a difunctional siloxane bond and a smaller number by a trifunctional siloxane bond, which both give the surface bonding a higher stability and longevity [39].

Direct information on the surface concentration of the chromatographic ligand cannot be derived from these spectra. However, this information can be readily obtained from elemental analysis (6.79% C, 1.18% H and 1.91% N). Based on the nitrogen content, a ligand coverage of 455 µmol/g (which corresponds to about 1.4 µmol/m^2) was calculated. Since the silanol group surface coverage of unmodified silica is known to be 8.0±1.0 µmol/m^2 [39], the investigated conditions led to a reaction with about 35% of the available silanol groups under the assumption of an average bifunctional linkage of the ligand to the silica surface. The remaining free silanol groups can be calculated to be around 5.2 µmol/m^2.

4.2.4.2. Surface Charge Characterization

A key factor in ion exchange and mixed-mode chromatography is the surface charge of the resultant chromatographic particles. This valuable information about the charge state of the stationary phase can be readily obtained by determining ζ-potentials in a pH-dependent manner [4, 33, 40]. If charged particles are in a buffer solution, an electrical double layer is formed on the surface, the dimension of which depends on the effective charge of the particles. When an electric field is applied, the particles begin to migrate in the field according to their net charge which can be characterized by the ζ-potential. The ζ-potential is defined as the potential of the shear distance from the surface and can be calculated from mobilities

measured by ELS using the Smoluchowski equation. The variation of the pH value of the mobile phase is a valuable tool in chromatography for tuning the charge state of the surface of the stationary phase as well as controlling the ionization of the analytes. For this reason, the ζ-potentials determined over the chromatographically useful pH range offers valuable information for the decision of the best suitable pH value for a given separation. Thus, the measurements were carried out covering a pH range from 3.5 to 9.5 with a constant ionic strength of 10 mM KCl. The results are depicted in Fig. 3.

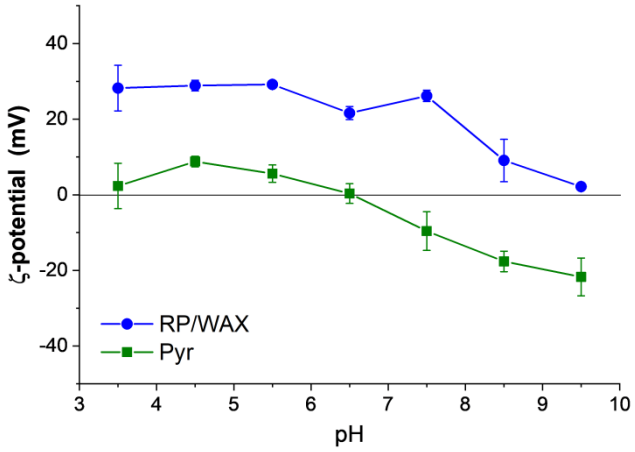

Fig. 3: Surface charge of the *N*-propyl-*N'*-2-pyridylurea modified silica illustrated by the determination of the ζ-potentials in dependency of the pH value.

At lower pH values (3.5 – 6) the ζ-potentials of the *N*-propyl-*N'*-2-pyridylurea modified silica showed positive sign in spite of an excess of residual silanols (5.2 µmol/m^2) over chromatographic ligand moieties (1.4 µmol/m^2) (Fig. 3, green curve). It indicates that the dissociation of the immobilized selector (pK_a = 3.88 as calculated by Marvin Sketch) dominated the surface charge. Further increase of the pH value of the suspension caused a decrease and then loss of the surface charge. At pH values above 6.5 it finally resulted in an umpolung i.e. negative surface charge. This phenomenon can be explained by the increasing dissociation of residual silanol groups (pK_a = 4 – 6) on the surface of the modified silica. The isoelectric point (pI) of the surface was observed at pH 6.5. The further negative values were mainly contributed by the dissociated silanol groups which was already observed with other chromatographic ligands [4, 33, 40].

For comparison Fig. 3 (blue curve) shows also the corresponding ζ-potentials of a previously described 3-aminotropane-based RP/WAX stationary phase [4] (for structure see Fig. 1b). It can be seen that the ζ-potentials of the pyridine-modified stationary phase are set off by around 20 mV as compared to the RP/WAX phase although showing a slightly higher selector coverage (RP/WAX: 0.38 mmol/g [4], *N*-propyl-*N'*-2-pyridylurea: 0.46 mmol/g). It can be

explained by the pK_a values of the two ligands: The calculated pK_a of the new *N*-propyl-*N'*-2-pyridylurea ligand is 3.88 while it is 10.45 for the mixed-mode ligand of the RP/WAX particles. It is evident that only a fraction of the immobilized pyridine ligands is protonated in the pH range between 3.5 and 5.5 explaining the much lower positive surface charge of the *N*-propyl-*N'*-2-pyridylurea -modified silica compared to the RP/WAX particles in this pH range. This offers the possibility to use milder elution conditions what the counterion concentration in the mobile phase is concerned. Furthermore, the pI of the pyridine-modified particles (pI ~ 6.5) is significantly shifted as compared to the RP/WAX particles which showed a positive surface charge over almost the entire measured pH range (pI ~ 9.5). This shift of the pI to lower pH value of around 6.5 should enable mild elution of strongly retained multiply negatively charged analytes by simple pH-gradient elution, e.g. from pH 5 - 7. Good recovery of multiply negatively charged species, e.g. oligonucleotides, can be expected due to a repulsive charge-inducted elution.

4.2.4.3. Chromatographic Characterization under RP and HILIC Conditions and Stationary Phase Classification by PCA

The new stationary phase offers multiple interaction possibilities. For example, under aqueous mobile phase conditions hydrophobic interactions with the propyl residue and the aromatic ring are possible. The urea group offers the possibility of interaction with electron donors and electron acceptors. The aromatic system of the pyridine ring is capable for π-π interactions and by protonation of the nitrogen an anion exchange site is present. This large variety of functional groups leads to a flexibility of the usable chromatographic modes. In order to evaluate the suitability of the new stationary phase under RP conditions, a simple test set was utilized composed of two lipophilic alkylbenzene derivatives which differ in a methylene unit (BuB and PeB thus probing for methylene selectivity of the phase) as well as two acids (DETP and BocProPhe) which differ in their acidity and lipophilic properties. The properties of the stationary phases and of the analytes, and the chromatographic data are summarized in Table 1 (The chromatogram is shown in Supplementary Fig. S5 a)).

Table 1: Comparison of the properties of the new *N*-propyl-*N'*-2-pyridylurea modified stationary phase and the well established RP/WAX stationary phase, the properties of the test compounds and comparison of the retention factors and selectivities of hydrophobic and acidic compounds under RP conditions

	% N[a]	Ligand- coverage [mmol/g] [b]	pKa [c]	RP Test									
				Log P (pH 6)		Log D (pH 6)		retention factor k				selectivity α	
				BuB	PeB	DETP	BocProPhe	BuB	PeB	DETP	BocProPhe	$\alpha_{\text{-CH2-}}$	$\alpha_{\text{DETP/BocProPhe}}$
Pyridylpropyl-urea	1.9	0.46	3.88	4.27	4.8	-2.8	-0.6	0.95	1.12	0.19	0.56	1.18	3.11
RP/WAX	1.3[d]	0.38	10.5					4.1	5.69	14.41	27.72	1.39 [d]	1.92 [d]

[a] determined by elemental analysis.

[b] Calculation based on the nitrogen content determined by elemental analysis.

[c] pK_a of the selector, calculated with Marvin Sketch.

[d] adopted from [4].

Compared to the already characterized RP/WAX phase [4], the new *N*-propyl-*N'*-2-pyridylurea stationary phase showed a significantly weaker retention of the analytes, both for the neutral lipophilic as well as acidic compounds (see retention factors in Table 1). Due to the lower carbon content (6.8% for the *N*-propyl-*N'*-2-pyridylurea phase vs 11.9% for the RP/WAX [4]) the significantly lower retention of the alkylbenzenes and the significantly lower methylene selectivity (separation factor for the two alkylbenzenes of 1.18 vs 1.39 for the RP/WAX phase [4]) was not surprising. Since acetonitrile was used as an organic modifier, it can be assumed that π-π interactions did not occur. The lower retention of the acidic compounds was a result of the very weakly protonated pyridine nitrogen at the selected pH (pH 6.0) and even eluted before the alkylbenzenes (i.e. reversed elution order of acids and alkylbenzenes compared to RP/WAX). Yet, it is remarkable that the selectivity for the two acids was maintained on the new stationary phase which provided a selectivity of 3.11 for BocProPhe and DETP, while the RP/WAX stationary phase showed a selectivity of 1.92. Considering the increased polarity, the *N*-propyl-*N'*-2-pyridylurea phase was also evaluated under HILIC conditions using vitamins, nucleosides and xanthines as test mixtures. In general, the newly synthesized phase also showed relatively low retention in HILIC mode under given conditions, although there is a good selectivity for the tested analytes (for chromatograms see Supplementary Fig. S5b-5d).

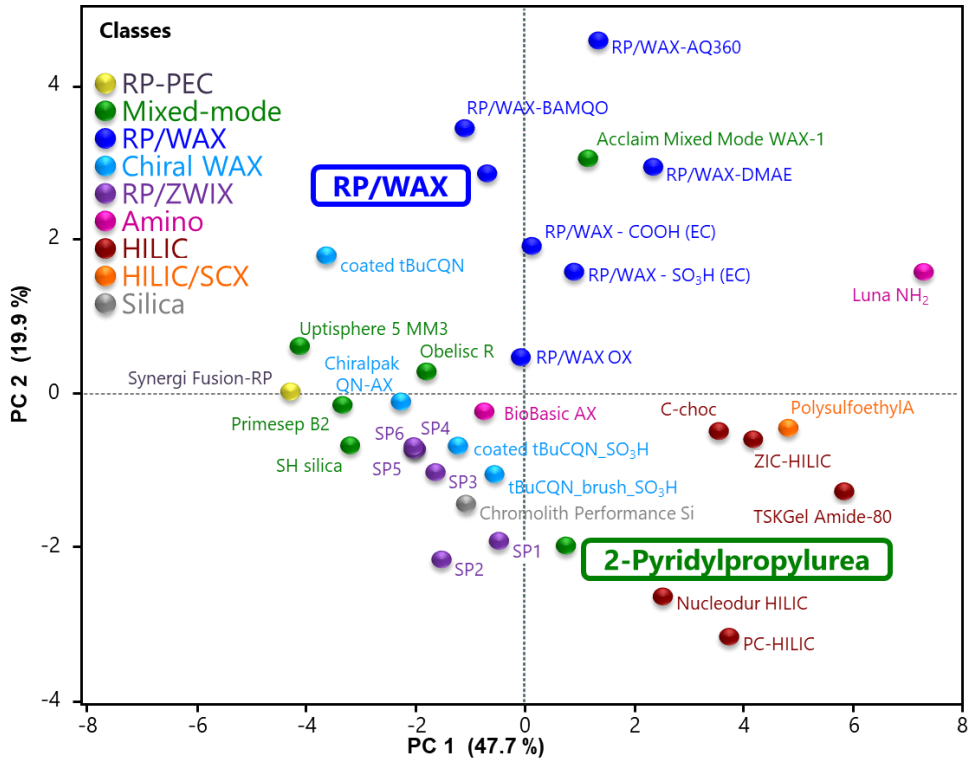

Fig. 4: Classification of the chromatographic properties of the *N*-propyl-*N'*-2-pyridylurea modified silica gel by principal component analysis. A detailed description of the columns included in the data set can be found in Ref. [4, 40–42]

In the past, we have already successfully used principal component analysis to classify new stationary phases [4, 40–42]. In this statistical procedure, the retention factors of different analytes as factors are used to mathematically show differences and similarities of the new and already characterized stationary phases [4, 40–42] as objects (for structures of stationary phases see Suppl. Fig. S6-7). The resulting score plot of the components PC1 and PC2 (Fig. 4) thus shows stationary phases with similar retention characteristics in close proximity to each other. The more different the retention behavior, the greater is the distance. Overall, approximately 68% of the variance in retention factors can be explained by the first two components. Along the PC1 axis, lipophilic separation materials such as the classical RP-phase Synergi Fusion RP are found at low values, while very hydrophilic (Luna NH_2, TSK Gel Amide-80, Polysulfoethyl A) are found at high values. The PC2 axis represents a degree of surface charge of the stationary phase. In the negative range there are stationary phases the surface charge of which is net negative (e.g. Nucleodur HILIC, Chromolith Performance Si) under the given conditions and in the case of high values columns with net positive surface charge (e.g Acclaim Mixed Mode WAX-1). The already described α-aminotropane-based RP/WAX phase [4, 42] is therefore found in the upper half of the PC2 axis. According to their lipophilicity, they are distributed in the midfield of PC1, whereas the HILIC phases are more likely to be found in higher PC2 values, depending on their suitability for polar analytes. The *N*-propyl-*N'*-2-pyridylurea phase is located near the silica gel column Chromolith Performance Si. Taking into account the pH values used (apparent pH for RP test 6 and approx. 8 for HILIC tests), this result is not surprising. The dissociation of the selector is low at these pH values. The polar embedded groups are available for additional hydrophilic interactions and the dissociation of the superficial silanol groups seem to be dominant. These chromatographic results and the stationary phase comparison give a useful indication of the characteristics and the multimodal applicability of the new *N*-propyl-*N'*-2-pyridylurea -modified stationary phase.

4.2.4.4. Anion Exchange Mechanism in Dependence on pH

For more detailed characterization of the effect of surface charge under chromatographic conditions, a series of test runs were carried out in which the pH value (pH 3.5, formic acid; 5 and 7, acetic acid) and ionic strength (10, 20 and 50 mM acid adjusted with ammonia to the respective pH) of the mobile phase were varied. For example, phenylalanine and tryptophan derivatives were selected as analytes, which show acidic (AcPhe, pK_a = 4.02; AcTrp, pK_a = 4.12), neutral (AcPheOEt), zwitterionic (Phe, pK_{a1} = 2.47 and pK_{a2} = 9.45; Trp, pK_{a1} = 2.54 and pK_{a2} = 9.40) and basic (PheOMe, pK_a = 6.97; TrpAmide, pK_a = 7.97) properties. Fig. 5a) depicts the chromatograms of the phenylalanine derivatives.

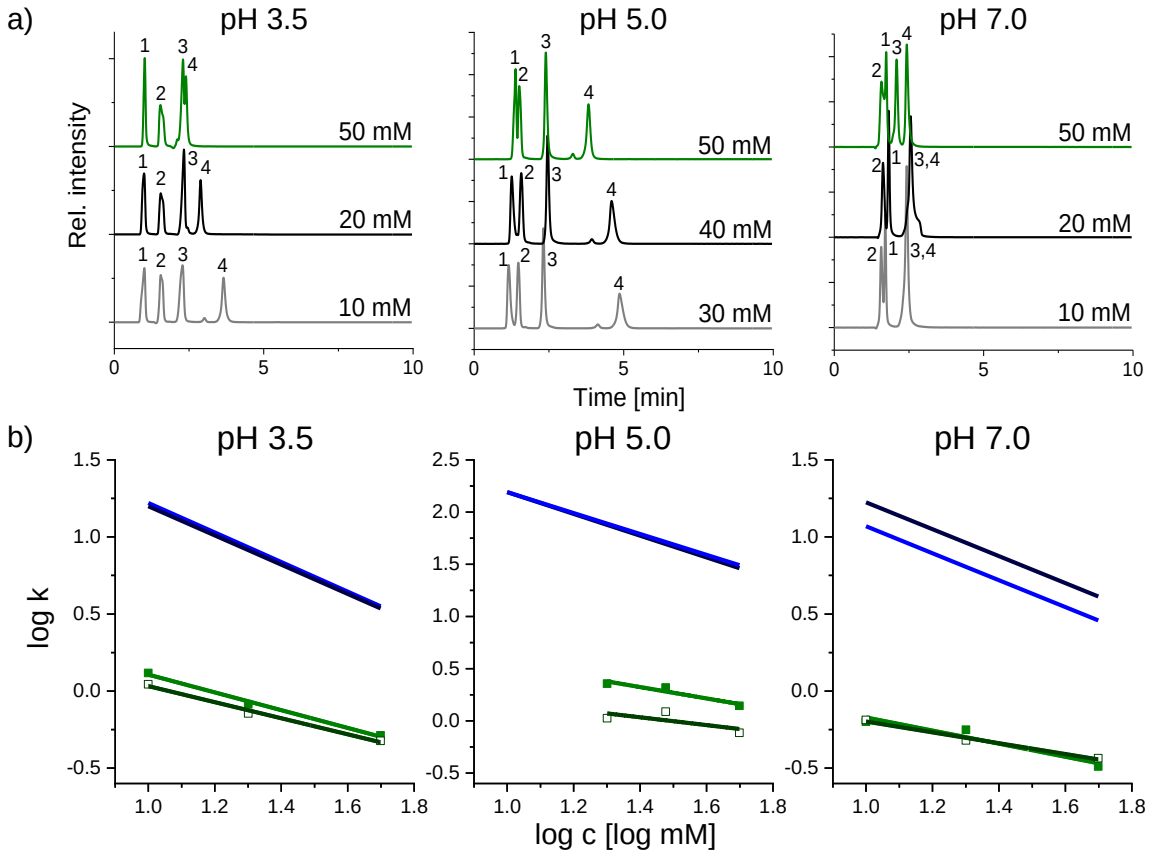

Fig. 5: a) Chromatographic characterization of the anion exchange retention behaviour depending on the pH value (1: PheOMe 2: Phe 3: AcPheOEt 4: AcPhe) and b) the applicability of the stoichiometric displacement model to the retention data obtained:
N-propyl-*N'*-2-pyridylurea -■- AcPhe -□- AcTrp; RP /WAX: -●- AcPhe -❍- AcTrp: -
Experimental conditions: ACN/H_2O (80:20, v/v) containing 10, 20, and 50 mM formic acid (pH 3.5) and acetic acid (pH 5 and 7), adjusted with ammonia; sample conc.: 1 mg/mL, dissolved in mobile phase, inj.vol. 10 µL, flow rate: 1.0 mL/min, detection: 258 nm.

The elution order for pH 3.5 and 5 was as follows: PheOMe < AcPheOEt < Phe < AcPhe. In contrast to this, the elution order changed for pH 7 and PheOMe is slightly retained due to a reversed polarity of the surface of the stationary phase. This already indicates that the effective charge of the analytes may be decisive for the retention behaviour, like the surface charge of the 2-pyridyl-modified silica phase. On the other hand, it turns out that the ionic strength has a significant effect (pH 3.5 and 5) solely for the acidic solute (Ac-Phe). The stochiometric displacement model (Eq. (1)) can be invoked to prove the prevalence of an anion exchange process [4, 10, 40, 43, 44].

$$log\ k = log\ K_z - Z \cdot log\ [C] \qquad (1)$$

$$K_z = \frac{K \cdot S \cdot (q_x)^Z}{V_0} \qquad (2)$$

The slope *Z* represents the effective involved charge ratio of analyte and counterions. K_Z, the intercept, describes the investigated ion exchange system taking account of the ion exchange equilibrium constant *K* [L/mol], the concentration of available ion exchange sites at the surface q_x [mol/m^2] correlated to the surface area of the particles *S* [m^2/g] and void volume of the column V_0 [L] (Eq. (2)).

Of particular interest as a factor of charge density on the surface of the stationary phase are the calculated y-axis intercepts of linear regression. In case of the *N*-propyl-*N'*-2-pyridylurea stationary phase, these show the highest values for pH 5 (AcPhe: 1.09; AcTrp: 0.56), followed by pH 3.5 (AcPhe: 0.68; AcTrp: 0.55) and pH 7 (AcPhe: 0.25; AcTrp: 0.15). This correlates very well with the trend of the ζ-potentials described above. In the neutral pH range, the protonation of the pyridine nitrogen is relatively low while dissociation of residual silanol groups gains importance, which reduces the number of positive charges available for anion exchange. This is reflected in the decrease of the y-axis intercepts for the 2-pyridiylurea phase as compared to the RP/WAX phase (Fig. 5b). Milder elution conditions (lower counterion/buffer concentrations) can be used, which may be also advantageous for ESI-MS detection, as less ion suppression, higher ionization yield and thus better sensitivity can be achieved.

4.2.4.5. Separation of Nucleoside Mono-, Di- and Triphosphates

Classical anion-exchange chromatography and also mixed-mode anion-exchange chromatography may be problematic if multiply charged analytes need to be investigated. The elution strength with commonly employed mobile phase conditions may not be enough which can lead to excessive retention times or trapping of these analytes (e.g. oligonucleotides). It is expected that the current *N*-propyl-*N'*-2-pyridylurea -based mixed-mode phase can better cope with such multiply charged species. To document this, uridine 5'-mono-, di- and triphosphates (UMP, UDP and UTP) were used as model analytes [7, 45, 46]and the separation investigated at pH 5 (anion-exchange under positive surface charge) and at pH 7 (ion-exclusion effects at negative surface). Furthermore, buffer concentration (1.25, 2.5 and 5 mM ammonium phosphate) and flow rate (0.2, 0.5 and 1.0 mL/min) dependencies were investigated. Resultant isocratic separations at pH 5 are shown in Fig. 6a-c) and at pH 7 in Fig. 6d-f). The corresponding plots following the stoichiometric displacement model are given in Fig.7.

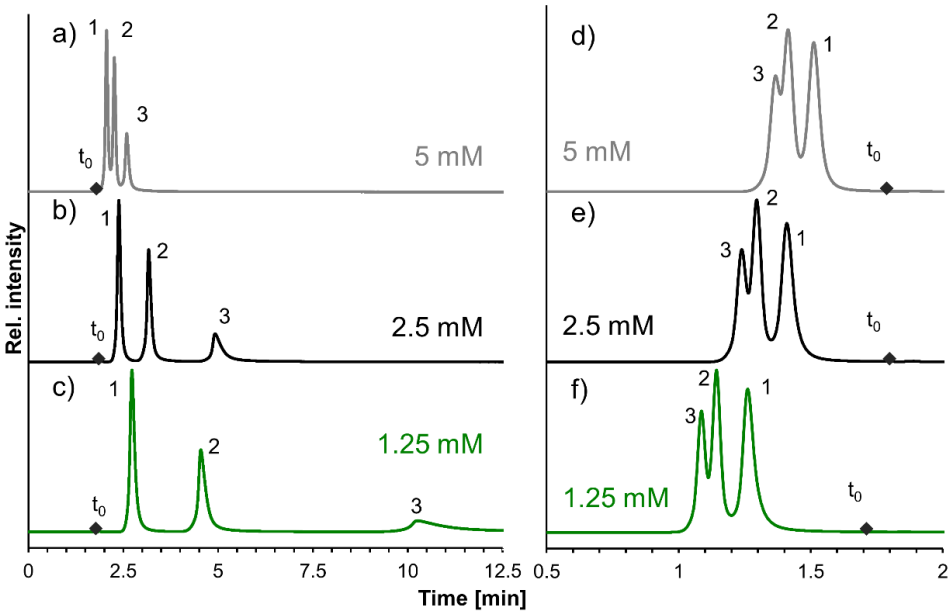

Fig. 6: Separation of UMP (1), UDP (2), and UTP (3) on *N*-propyl-*N'*-2-pyridylurea modified silica. Mobile phase: ACN/H_2O (1:4, v/v), a) 5.0 mM, b) 2.5 mM, c) 1.25 mM phosphoric acid, pH 5, adjusted with ammonia, d-f) ACN/H_2O (1:4, v/v), d) 5mM, e) 2.5 mM, f) 1.25 mM phosphoric acid, pH 7, adjusted with ammonia, flow rate: 1.0 mL/min, T=25°C, inj.vol. 2 µL, λ=254 nm, ♦=t_0.

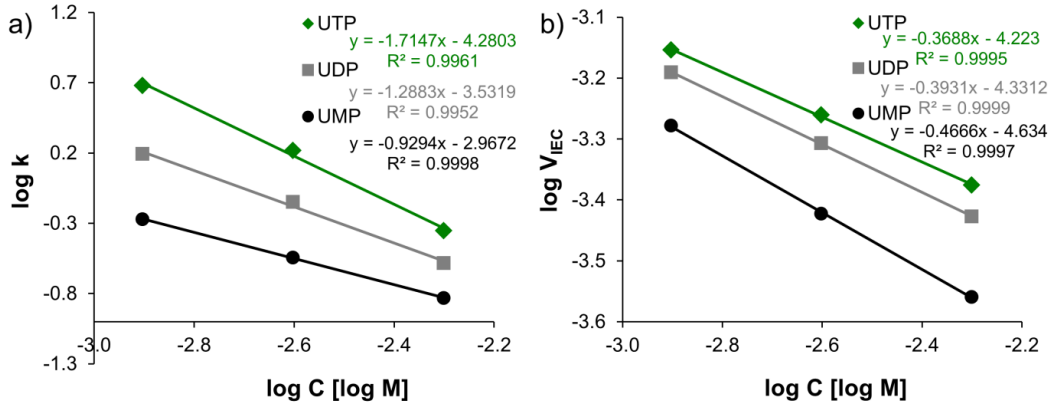

Fig. 7: Stoichiometric displacement model for the analysis of the nucleotides on pH 5 (a) and pH 7 (b).

It can be seen that at pH 5 (positive surface charge) retention decreases with the counterion concentration in accordance to an anion-exchange process. On the other hand, the retention of the negatively charged nucleoside mono-, di- and triphosphates increases in accordance to their net charge (Table 2), following the order: UMP<UDP<UTP. Slopes and intercepts (derived from stoichiometric displacement model) correlate well with the net charge, as expected for an anion-exchange process (Table 2).

Table 2: Acidic properties of the investigated nucleotides and the calculated parameters of the stoichiometric displacement model for *N*-propyl-*N*'-2-pyridylurea modified stationary phase.

Compound	pK_a [a, b]	net charge[a]		slope (Z) [c]		Intercept (K_Z) [c]	
		pH 5	pH 7	pH 5	pH 7	pH 5	pH 7
UMP	1.23 (P), 6.25 (P), 8.70 (U)	-1.1	-1.94	-0.929	-0.467	-2.967	-4.634
UDP	1.77 (P), 3.21 (P), 7.40 (P), 8.72 (U)	-2	-2.46	-1.288	-0.393	-3.532	-4.331
UTP	0.90 (P), 2.53 (P), 3.30 (P), 7.40 (P), 8.72 (U)	-3	-3.46	-1.715	-0.369	-4.28	-4.223

[a] calculated with Marvin Sketch

[b] *P*: phosphate residue, *U*: nitrogen atom in uridine

[c] investigated flowrate: 1.0 mL/min

At pH 7, the situation is completely different. Since the predominant interactions are of repulsive nature because of the negative charge of stationary phase and solutes, elution of the nucleotides occurred before the void volume V_0. Still, the separation mechanism was dominated by their charge. However, UTP eluted first i.e. with the lowest ion exclusion volume ΔV_{IEC} ($\Delta V_{IEC}=V_0-V_A$, wherein V_A is the elution volume of the anion), followed by UDP and UMP (reversed elution order compared to pH 5). Although a good linear regression can be achieved by the fit to the stoichiometric displacement model (Fig. 7b), the underlying explanation is more rational on the basis of the double layer theory [45]. As the ionic strength in the mobile phase decreases, the double layer thickness of the charged particle increases. In consequence the shielding of the charges (analyte and stationary phase) is less effective. In the case of ion exclusion chromatography, this leads to increased repulsive interactions and the elution volume is reduced i.e. the analyte elutes earlier. The effect is more pronounced for analytes with higher effective charges which therefore elute earlier than their congeners with lower charge. This explains the reversal of the elution order.

4.2.4.6. pH-Gradient with Stationary Phase Umpolung and Repulsive Charge-Supported Elution

The above isocratic experiments as well as the determination of the zeta potentials confirmed the umpolung of the surface charge between pH 5 and 7. The combination of these chromatographic modes (anion-exchange at pH 5 and ion-exclusion at pH 7) in the form of pH-gradient elution should lead to milder elution conditions. While this is less of relevance for the current model nucleotides, it may be necessary to elute highly charged species such as oligonucleotides under milder conditions [11].

Fig. 8 shows the chromatograms for the mixture of UMP, UDP and UTP under pH-gradient elution with constant ionic strength (1.25 mM) (Fig.8a) and with a mixed pH/counterion (buffer)

gradient (Fig. 8b). For comparison, a comparable pH-gradient separation of the same mixture at 5 mM constant ionic strength on the RP/WAX phase is shown in Fig. 8c. It is evident from a comparison with Fig. 6c that the pH-gradient on the pyridine phase at 1.25 mM ionic strength allows faster elution in particular of the strongly retained multiply charged UTP. Using a mixed pH/counterion gradient, retention times could be further shortened while essentially maintaining the selectivity (*cf.* Fig 8a and 8b).

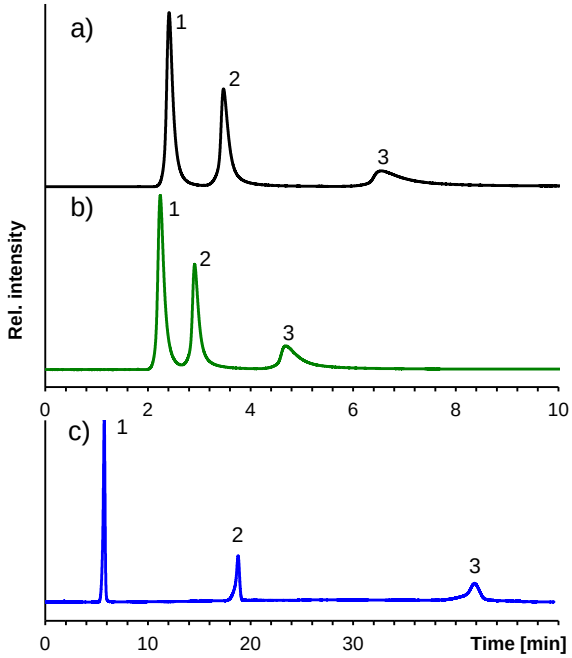

Fig. 8: pH-Gradient elution of UMP (1), UDP (2), and UTP (3) on *N*-propyl-*N'*-2-pyridylurea (a+b) and RPWAX phases (c). a) pH-gradient from 5 to 7 at constant ionic strength of 1.25 mM, b) mixed pH/counterion gradient (pH 5 – 7 and counterion concentration from 1.25 to 2.5 mM), and c) pH - gradient separation on RP/WAX modified silica.
Mobile phase: (a, b) ACN/H_2O (1:4, v/v), a) 1.25 mM and b) A: 1.25 mM and B 2.5 mM phosphoric acid, A: pH 5 and B: pH 7, adjusted with ammonia, gradient profile: 0 to 100 % B in 1.00-15.00 min, 100% B 15.00-20.00 min, 100 to 0% B 20.00-20.01, 0% B for 20.01-30.00min. (c) ACN/H_2O (1:4, v/v), 5.0 mM phosphoric acid, A: pH 5 and B: pH 7, adjusted with ammonia, gradient profile: 0 to 100 % B in 1.00-15.00 min, 100% B 15.01-40.00 min, 100 – 0% B 40.00-40.01, 0% B for 40.01-50.00min, flow rate: 1.0 mL/min, T = 25°C, inj. vol. 2 µL, λ=254 nm.

The favorable effect of the pH gradient and moderate surface charge of the 2-pyridyl phase for the separation of multiply charged analytes becomes striking from the comparison with the RP/WAX phase which still has positive charge at pH 7 and umpolung occurs only in the chromatographically inaccessible pH-range above pH 9 (stability problem of silica based stationary phases). Due to the still prevailing positive surface charge at pH 7, the anion exchange process is dominating the separation throughout, which required a subsequent hold phase of 25 minutes at pH 7 to enforce the elution of UTP. The analysis time could be reduced by using higher pH values, which also significantly restrict the dissociation of the RP/WAX selector. However, this is disadvantageous in relation to the lifetime of the column due to hydrolysis of siloxane bonds. It is clearly evident that the new *N*-propyl-*N'*-2-pyridylurea based stationary phase exhibits favorable chromatographic behavior for multiply charged anionic

species over classical anion-exchangers and mixed-mode anion-exchangers such as RP/WAX as it allows the separation of (multiply) charged analytes by pH-gradients with stationary phase umpolung around neutral pH and repulsive charge-supported elution in a short analysis time using mild elution conditions.

4.2.5. Conclusions

The surface structure of the *N*-propyl-*N'*-2-pyridylurea stationary phase was successfully elucidated by elemental analysis and solid-state ^{13}C and ^{29}Si NMR after the synthesis of the ligand and its immobilization by silanization. Compared to a previously characterized RP/WAX stationary phase, the *N*-propyl-*N'*-2-pyridylurea stationary phase showed a significantly lower pK_a value. This was reflected in the lowered ζ-potentials and a shift in the pI of the silica-based pyridine phase to lower values compared to RP/WAX. As a consequence, significantly reduced retentivity of this stationary phase for acidic analytes was observed while still working by an anion-exchange mechanism at pH 5. This requires significantly reduced counterion concentrations for the elution of anions. The umpolung of the surface of the stationary phase at pH 7 was verified by the analysis of nucleotides in ion exclusion chromatography mode. The combination of anion exchange and ion exclusion chromatography modes one separation realized by a pH gradient allowed the analysis of nucleotides with mild elution conditions.

4.2.6. References

[1] L. Zhang, Q. Dai, X. Qiao, C. Yu, X. Qin, H. Yan, Mixed-mode chromatographic stationary phases: Recent advancements and its applications for high-performance liquid chromatography, TrAC - Trends Anal. Chem. 82 (2016) 143–163. doi:10.1016/j.trac.2016.05.011.

[2] K. Zhang, X. Liu, Mixed-mode chromatography in pharmaceutical and biopharmaceutical applications, J. Pharm. Biomed. Anal. 128 (2016) 73–88. doi:10.1016/j.jpba.2016.05.007.

[3] E. Lemasson, S. Bertin, P. Henning, E. Lesellier, C. West, Mixed-Mode Chromatography - A Review, Suppl. to LCGC Eur. / LCGC North Am. (2017) 22–33.

[4] A. Zimmermann, J. Horak, O.L. Sánchez-Muñoz, M. Lämmerhofer, Surface charge fine tuning of reversed-phase/weak anion-exchange type mixed-mode stationary phases for milder elution conditions, J. Chromatogr. A. 1409 (2015) 189–200. doi:10.1016/j.chroma.2015.07.036.

[5] R. Nogueira, M. Lämmerhofer, W. Lindner, Alternative high-performance liquid chromatographic peptide separation and purification concept using a new mixed-mode reversed-phase/weak anion-exchange type stationary phase, J. Chromatogr. A. 1089 (2005) 158–169. doi:10.1016/j.chroma.2005.06.093.

[6] R. Noguiera, D. Lubda, A. Leitner, W. Bicker, N.M. Maier, M. Lämmerhofer, W. Lindner, Silica-based monolithic columns with mixed-mode reversed-phase/weak anion-exchange selectivity principle for high-performance liquid chromatography, J Sep.Sci. 29 (2006) 966–978. doi:10.1002/jssc.200500395.

[7] M. Lämmerhofer, R. Nogueira, W. Lindner, Multi-modal applicability of a reversed-phase/weak-anion exchange material in reversed-phase, anion-exchange, ion-exclusion, hydrophilic interaction and hydrophobic interaction chromatography modes, Anal. Bioanal. Chem. 400 (2011) 2517–2530. doi:10.1007/s00216-011-4755-3.

[8] E. Apfelthaler, W. Bicker, M. Lämmerhofer, M. Sulyok, R. Krska, W. Lindner, R. Schuhmacher, Retention pattern profiling of fungal metabolites on mixed-mode reversed-phase/weak anion exchange stationary phases in comparison to reversed-phase and weak anion exchange separation materials by liquid chromatography-electrospray ionisation-tandem mass , J. Chromatogr. A. 1191 (2008) 171–181. doi:10.1016/j.chroma.2007.12.067.

[9] W. Bicker, M. Lämmerhofer, W. Lindner, Determination of chlorpyrifos metabolites in human urine by reversed-phase/weak anion exchange liquid chromatography-electrospray ionisation-tandem mass spectrometry, J. Chromatogr. B Anal. Technol. Biomed. Life Sci. 822 (2005) 160–169. doi:10.1016/j.jchromb.2005.06.003.

[10] H. Hinterwirth, M. Lämmerhofer, B. Preinerstorfer, A. Gargano, R. Reischl, W. Bicker, O. Trapp, L. Brecker, W. Lindner, Selectivity issues in targeted metabolomics: Separation of phosphorylated carbohydrate isomers by mixed-mode hydrophilic interaction/weak anion exchange chromatography, J. Sep. Sci. 33 (2010) 3273–3282. doi:10.1002/jssc.201000412.

[11] A. Zimmermann, R. Greco, I. Walker, J. Horak, A. Cavazzini, M. Lämmerhofer, Synthetic oligonucleotide separations by mixed-mode reversed-phase/weak anion-exchange liquid chromatography., J. Chromatogr. A. 1354 (2014) 43–55. doi:10.1016/j.chroma.2014.05.048.

[12] C. Galea, D. Mangelings, Y. Vander Heyden, Characterization and classification of stationary phases in HPLC and SFC - a review, Anal. Chim. Acta. 886 (2015) 1–15. doi:10.1016/j.aca.2015.04.009.

[13] M. Dunkle, C. West, A. Pereira, S. Van Der Plas, E. Lesellier, Synthesis of stationary phases containing pyridine , phenol , aniline and morpholine via click chemistry and their characterization and evaluation in supercritical fluid chromatography, Sci. Chromatogr. 6 (2014) 85–103. doi:10.4322/sc.2014.023.

[14] B. Andri, A. Dispas, R.D. Marini, P. Hubert, P. Sassiat, R. Al Bakain, D. Thiébaut, J. Vial, Combination of partial least squares regression and design of experiments to model the retention of pharmaceutical compounds in supercritical fluid chromatography, J. Chromatogr. A. 1491 (2017) 182–194. doi:10.1016/j.chroma.2017.02.030.

[15] C. Foulon, P. Di Giulio, M. Lecoeur, Simultaneous determination of inorganic anions and cations by supercritical fluid chromatography using evaporative light scattering detection, J. Chromatogr. A. (2017). doi:10.1016/j.chroma.2017.12.047.

[16] J. Lundgren, J. Salomonsson, O. Gyllenhaal, E. Johansson, Supercritical fluid chromatography of metoprolol and analogues on aminopropyl and ethylpyridine silica without any additives, J. Chromatogr. A. 1154 (2007) 360–367. doi:10.1016/j.chroma.2007.02.028.

[17] A.J. Alexander, T.F. Hooker, F.P. Tomasella, Evaluation of mobile phase gradient supercritical fluid chromatography for impurity profiling of pharmaceutical compounds, J. Pharm. Biomed. Anal. 70 (2012) 77–86. doi:10.1016/j.jpba.2012.05.025.

[18] T. Takeuchi, K. Tokunaga, L.W. Lim, Separation of Inorganic Anions on a Pyridine Stationary phase in Ion Chromatography., Anal. Sci. 26 (2010) 511–514. doi:https://doi.org/10.2116/analsci.26.511.

[19] R. McClain, M.H. Hyun, Y. Li, C.J. Welch, Design, synthesis and evaluation of stationary phases for improved achiral supercritical fluid chromatography separations, J. Chromatogr. A. 1302 (2013) 163–173. doi:10.1016/j.chroma.2013.06.038.

[20] V. Desfontaine, J.L. Veuthey, D. Guillarme, Evaluation of innovative stationary phase ligand chemistries and analytical conditions for the analysis of basic drugs by supercritical fluid chromatography, J. Chromatogr. A. 1438 (2016) 244–253. doi:10.1016/j.chroma.2016.02.029.

[21] F. Jumaah, R. Jeȉdrkiewicz, J. Gromadzka, J. Namieśnik, S. Essén, C. Turner, M. Sandahl, Rapid and Green Separation of Mono- and Diesters of Monochloropropanediols by Ultrahigh Performance Supercritical Fluid Chromatography-Mass Spectrometry Using Neat Carbon Dioxide as a Mobile Phase, J. Agric. Food Chem. 65 (2017) 8220–8228. doi:10.1021/acs.jafc.7b02857.

[22] M. Zhang, A.K. Mallik, M. Takafuji, H. Ihara, H. Qiu, Analytica Chimica Acta Versatile ligands for high-performance liquid chromatography : An overview of ionic liquid-functionalized stationary phases, Anal. Chim. Acta. 887 (2015) 1–16. doi:10.1016/j.aca.2015.04.022.

[23] D.S. Van Meter, O.D. Stuart, A.B. Carle, A.M. Stalcup, Characterization of a novel pyridinium bromide surface confined ionic liquid stationary phase for high-performance liquid chromatography under normal phase conditions via linear solvation energy relationships, J. Chromatogr. A. 1191 (2008) 67–71. doi:10.1016/j.chroma.2008.02.048.

[24] L.M.L.A. Auler, C.R. Silva, K.E. Collins, C.H. Collins, New stationary phase for anion-exchange chromatography, J. Chromatogr. A. 1073 (2005) 147–153. doi:10.1016/j.chroma.2004.10.012.

[25] L.M.L.A. Auler, C.R. Silva, C.B.G. Bottoli, C.H. Collins, Anion separations for liquid chromatography using propylpyridinium silica as the stationary phase, Talanta. 84 (2011) 1174–1179. doi:10.1016/j.talanta.2011.03.026.

[26] J. Stadler, R. Lemmens, T. Nyhammar, Plasmid DNA purification, J Gene Med. 6 Suppl 1 (2004) S54-66. doi:10.1002/jgm.512.

[27] L.M. Sandberg, Å. Bjurling, P. Busson, J. Vasi, R. Lemmens, Thiophilic interaction chromatography for supercoiled plasmid DNA purification, J. Biotechnol. 109 (2004) 193–199. doi:10.1016/j.jbiotec.2003.10.036.

[28] R. Lemmens, U. Olsson, T. Nyhammar, J. Stadler, Supercoiled plasmid DNA: Selective purification by thiophilic/aromatic adsorption, J. Chromatogr. B Anal. Technol. Biomed. Life Sci. 784 (2003) 291–300. doi:10.1016/S1570-0232(02)00805-X.

[29] S.C. Burton, D.R.K. Harding, Hydrophobic charge induction chromatography: Salt independent protein adsorption and facile elution with aqueous buffers, J. Chromatogr. A. 814 (1998) 71–81. doi:10.1016/S0021-9673(98)00436-1.

[30] E. Boschetti, Antibody separation by hydrophobic charge induction chromatography, Trends Biotechnol. 20 (2002) 333–337. doi:10.1016/S0167-7799(02)01980-7.

[31] H.F. Tong, D.Q. Lin, X.M. Yuan, S.J. Yao, Enhancing IgG purification from serum albumin containing feedstock with hydrophobic charge-induction chromatography, J. Chromatogr. A. 1244 (2012) 116–122. doi:10.1016/j.chroma.2012.04.073.

[32] M. Wu, F. Zhang, Y. Liang, R. Wang, Z. Chen, J. Lin, L. Yang, Isolation and purification of immunoglobulin G from bovine colostrums by hydrophobic charge-induction chromatography, J. Dairy Sci. 98 (2015) 2973–2981. doi:10.3168/jds.2014-9142.

[33] O.L. Sánchez Muñoz, E. Pérez Hernández, M. Lämmerhofer, W. Lindner, E. Kenndler, Estimation and comparison of ζ-potentials of silica-based anion-exchange type porous particles for capillary electrochromatography from electrophoretic and electroosmotic mobility, Electrophoresis. 24 (2003) 390–398. doi:10.1002/elps.200390049.

[34] E. Bayer, K. Albert, J. Reiners, M. Nieder, D. Müller, Characterization of chemically modified silica gels by 29Si and 13C cross-polarization and magic angle spinning nuclear magnetic resonance, J. Chromatogr. A. 264 (1983) 197–213. doi:10.1016/S0021-9673(01)95023-X.

[35] K. Albert, E. Bayer, Characterization of bonded phases by solid-state NMR spectroscopy, J. Chromatogr. A. 544 (1991) 345–370. doi:10.1016/S0021-9673(01)83995-9.

[36] J.J. Kirkland, J.L. Glajch, R.D. Farlee, Synthesis and Characterization of Highly Stable Bonded Phases for High-Performance Liquid Chromatography Column Packings, Anal. Chem. 61 (1989) 2–11. doi:10.1021/ac00176a003.

[37] C. Hellriegel, U. Skogsberg, K. Albert, M. Lämmerhofer, N.M. Maier, W. Lindner, Characterization of a Chiral Stationary Phase by HR/MAS NMR Spectroscopy and Investigation of Enantioselective Interaction with Chiral Ligates by Transferred NOE, J. Am. Chem. Soc. 126 (2004) 3809–3816. doi:10.1021/ja0306359.

[38] A. Zimmermann, J. Horak, A. Sievers-Engler, C. Sanwald, W. Lindner, M. Kramer, M. Lämmerhofer, Surface-crosslinked poly(3-mercaptopropyl)methylsiloxane-coatings on silica as new platform for low-bleed mass spectrometry-compatible functionalized stationary phases synthesized via thiol-ene click reaction., J. Chromatogr. A. (2016). doi:10.1016/j.chroma.2016.01.058.

[39] J. Nawrocki, The silanol group and its role in liquid chromatography, J. Chromatogr. A. 779 (1997) 29–71. doi:10.1016/S0021-9673(97)00479-2.

[40] U. Woiwode, A. Sievers-Engler, A. Zimmermann, W. Lindner, O.L. Sánchez-Muñoz, M. Lämmerhofer, Surface-anchored counterions on weak chiral anion-exchangers accelerate separations and improve their compatibility for mass-spectrometry-hyphenation, J. Chromatogr. A. 1503 (2017) 21–31. doi:10.1016/j.chroma.2017.04.054.

[41] A.F.G. Gargano, T. Leek, W. Lindner, M. Lämmerhofer, Mixed-mode chromatography with zwitterionic phosphopeptidomimetic selectors from Ugi multicomponent reaction, J. Chromatogr. A. 1317 (2013) 12–21. doi:10.1016/j.chroma.2013.07.095.

[42] M. Lämmerhofer, M. Richter, J. Wu, R. Nogueira, W. Bicker, W. Lindner, Mixed-mode ion-exchangers and their comparative chromatographic characterization in reversed-phase and hydrophilic interaction chromatography elution modes, J. Sep. Sci. 31 (2008) 2572–2588. doi:10.1002/jssc.200800178.

[43] W. Kopaciewicz, M.A. Rounds, J. Fausnaugh, F.E. Regnier, Retention model for high-performance ion-exchange chromatography, J. Chromatogr. A. 266 (1983) 3–21. doi:10.1016/S0021-9673(01)90875-1.

[44] J. Ståhlberg, Retention models for ions in chromatography, J. Chromatogr. A. 855 (1999) 3–55. doi:10.1016/S0021-9673(99)00176-4.

[45] A.J. Alpert, Electrostatic repulsion hydrophilic interaction chromatography for isocratic separation of charged solutes and selective isolation of phosphopeptides, Anal. Chem. 80 (2008) 62–76. doi:10.1021/ac070997p.

[46] J. Domínguez-Álvarez, M. Mateos-Vivas, E. Rodríguez-Gonzalo, D. García-Gómez, M. Bustamante-Rangel, M.M. Delgado Zamarreño, R. Carabias-Martínez, Determination of nucleosides and nucleotides in food samples by using liquid chromatography and capillary electrophoresis, TrAC - Trends Anal. Chem. 92 (2017) 12–31. doi:10.1016/j.trac.2017.04.005.

4.2.7. Supplementary Material

4.2.7.1. Elucidation of the Structure of the Newly Synthesized Ligand and the Modified Silica Gel

4.2.7.1.1. Characterization of the Mixed-Mode Selector

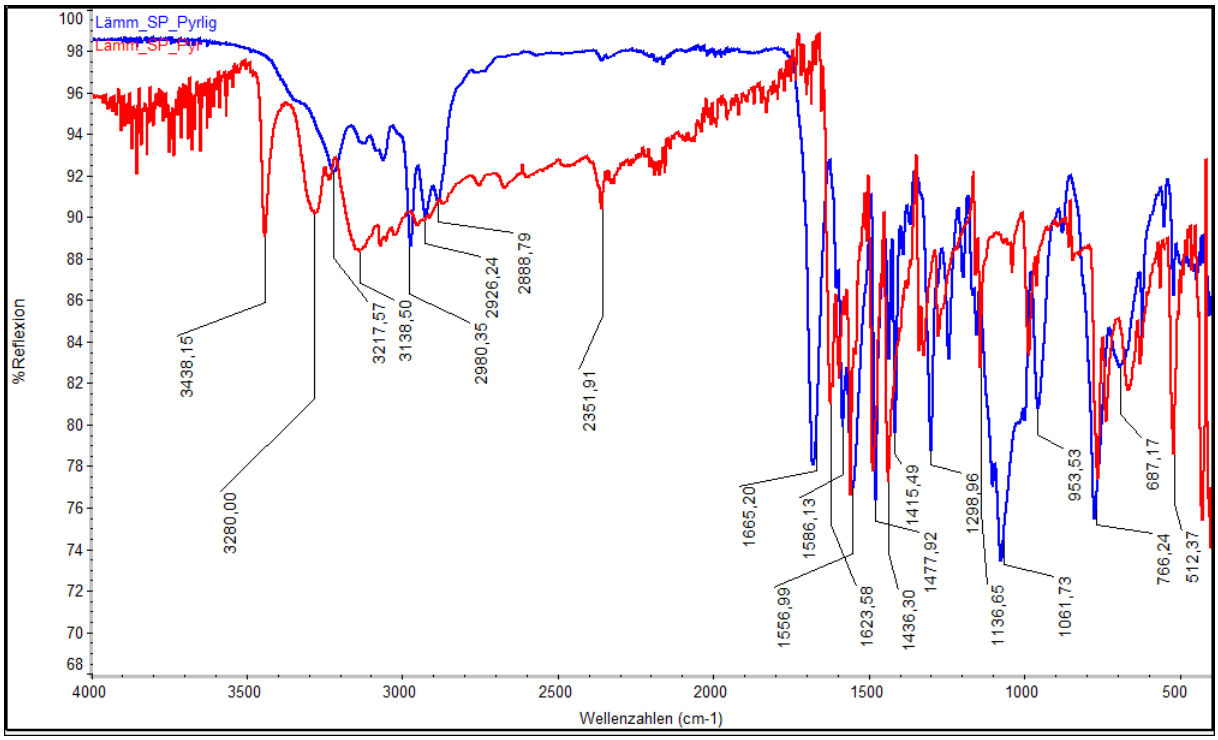

Fig. S 1: Comparison of the IR Spectra of the educt (2-amino pyridine) (red) and of the chromatographic ligand *N*-2-pyridyl-*N'*-3-triethoxysilylpropylurea (blue).

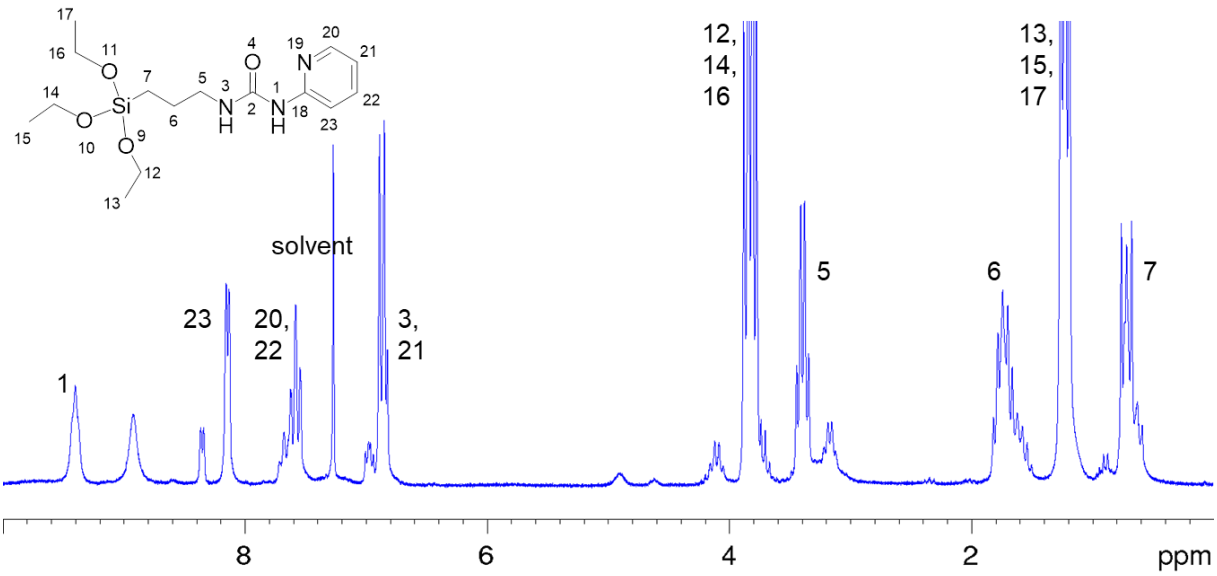

Fig. S 2: ^{1}H NMR spectrum of the chromatographic ligand *N*-2-pyridyl-*N'*-3-triethoxysilylpropylurea (product) (200 MHz, $CDCl_3$).

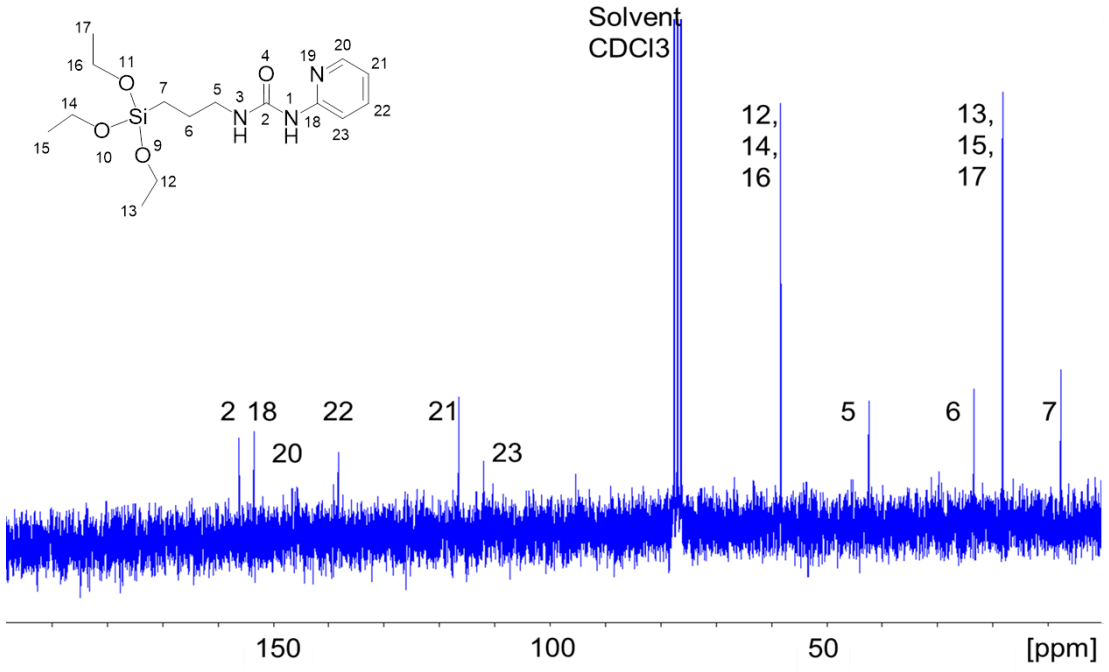

Fig. S 3: ^{13}C NMR spectrum of the chromatographic ligand N-2-pyridyl-N'-3-triethoxysilylpropylurea (product) (200 MHz, $CDCl_3$).

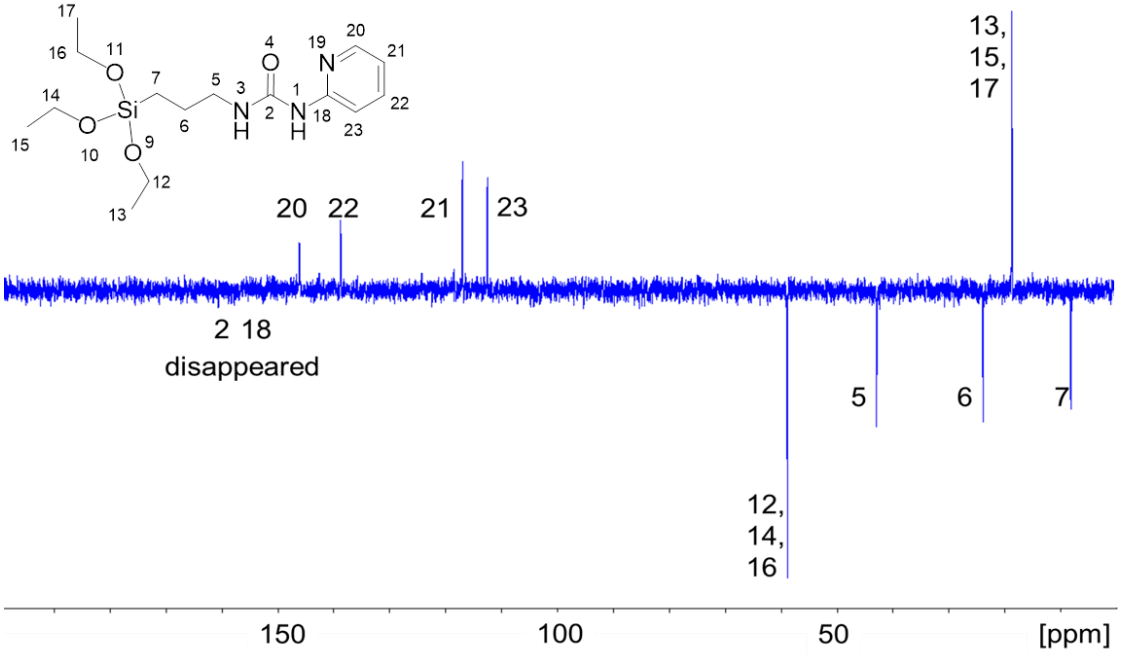

Fig. S 4: ^{13}C-DEPT NMR spectrum of the chromatographic ligand N-2-pyridyl-N'-3-triethoxysilylpropylurea (product) (200 MHz, $CDCl_3$).

4.2.7.2. Chromatographic Characterization

4.2.7.2.1. Retention Behavior of Acidic, Basic and Neutral Compounds under RP and HILIC Conditions

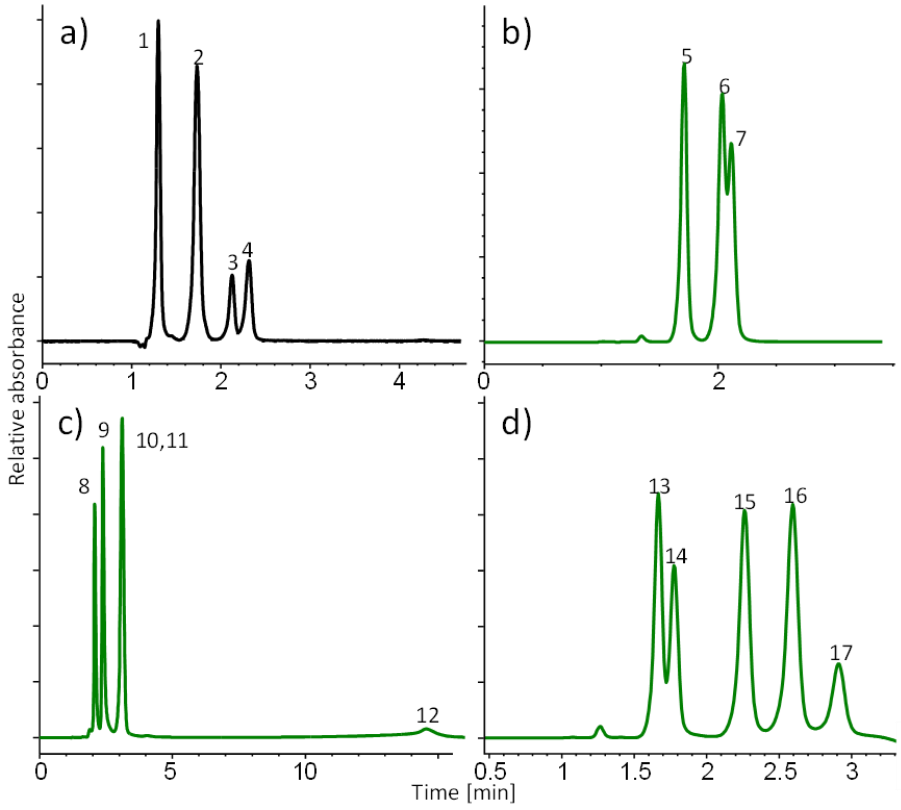

Fig. S 5: Separation of a) alkylbenzene derivatives and acids under RP conditions and b) xanthines, c) vitamins and d) nucleosides under HILIC conditions on the pyridine-modified stationary phase:
1 – DETP, 2 – BocProPhe, 3 – BuB , 4 – PeB, 5 – caffeine, 6 – theobromine, 7 – theophylline , 8 – pyridoxine HCl, 9 – ascorbic acid, 10 – nicotinic acid, 11 – riboflavin, 12 – thiamine, 13 – thymidine, 14 – uridine, 15 –adenosine, 16 – cytidine, 17 - guanosine
RP conditions a): 40 % (v/v) ACN, 50 mM, pH 6 adjusted with ammonia; sample: 0.8 mg/mL; flow vel.: 1.7 mm/s; column temperature: 25 °C; λ = 220 nm
HILIC conditions: ACN/ammonium acetate (b) C_{tot} = 5 mM (xanthines) and c-d) 10 mM (vitamins and nucleosides) (90:10, v/v), apparent pH around 8
sample conc.: 0.8 mg/mL; injection volume: 10 µL; flow vel.: 1.7 mm/s; column temperature: 25 °C; detection wavelength: 220 nm

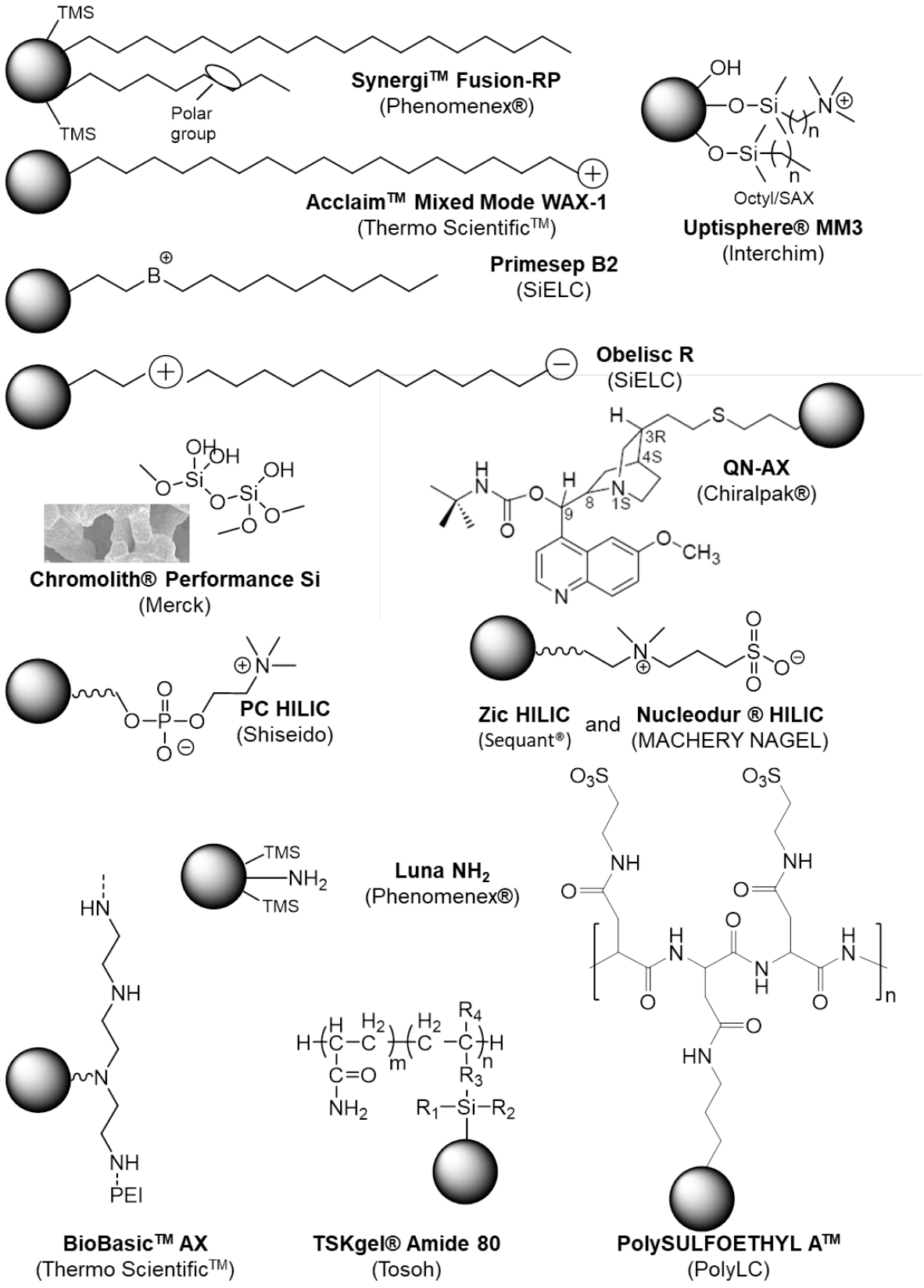

Fig. S 6: Surface Structure of commercially available RP, HILIC and Mixed mode columns which served for creating the retention map for principal component analysis shown in Fig. 4 of the main document

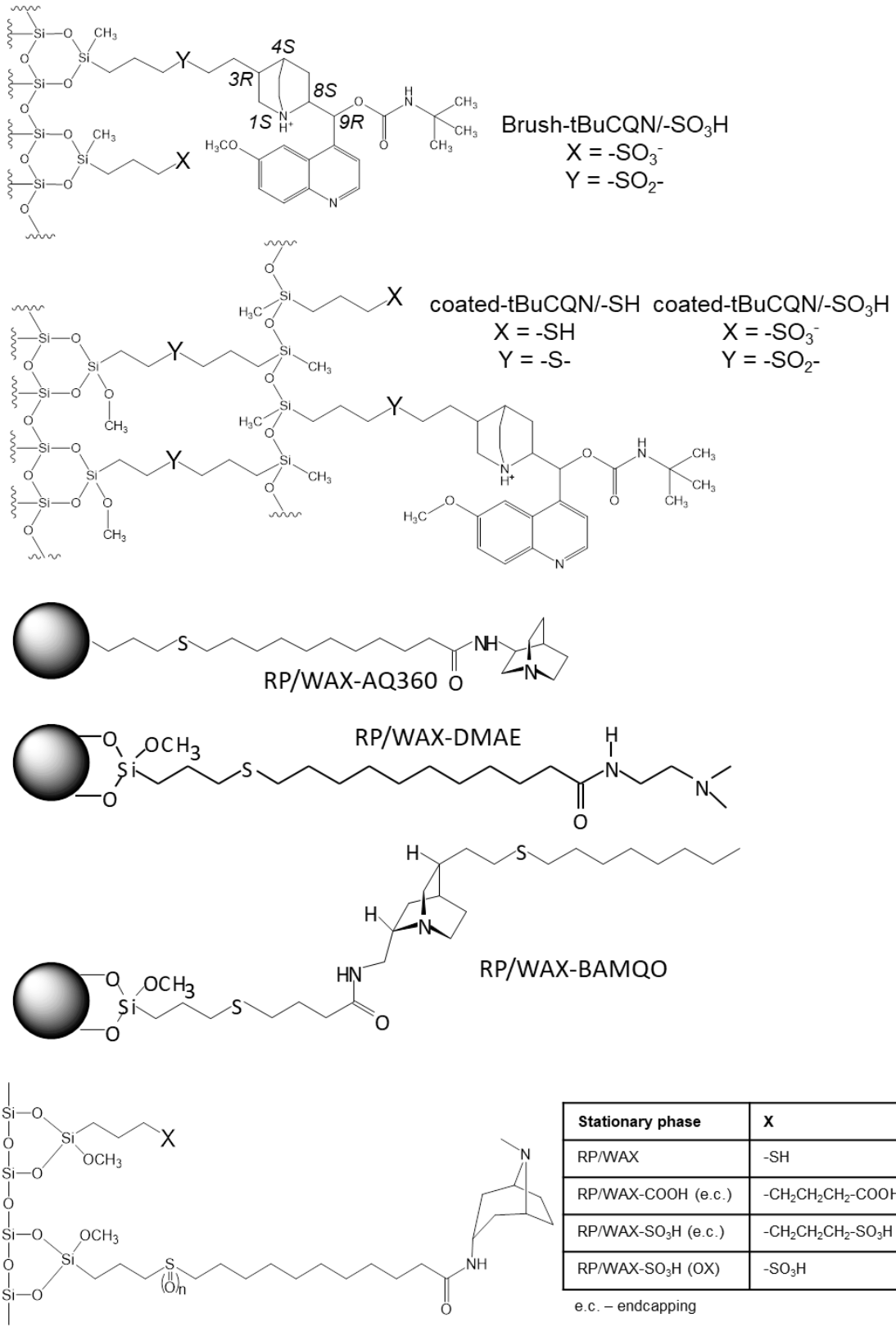

Stationary phase	X	n
RP/WAX	-SH	0
RP/WAX-COOH (e.c.)	$-CH_2CH_2CH_2-COOH$	0
RP/WAX-SO_3H (e.c.)	$-CH_2CH_2CH_2-SO_3H$	0
RP/WAX-SO_3H (OX)	$-SO_3H$	2

e.c. – endcapping

Fig. S 7: Surface structure of in house developed separation media which were also included in the retention map and classified by principal component analysis

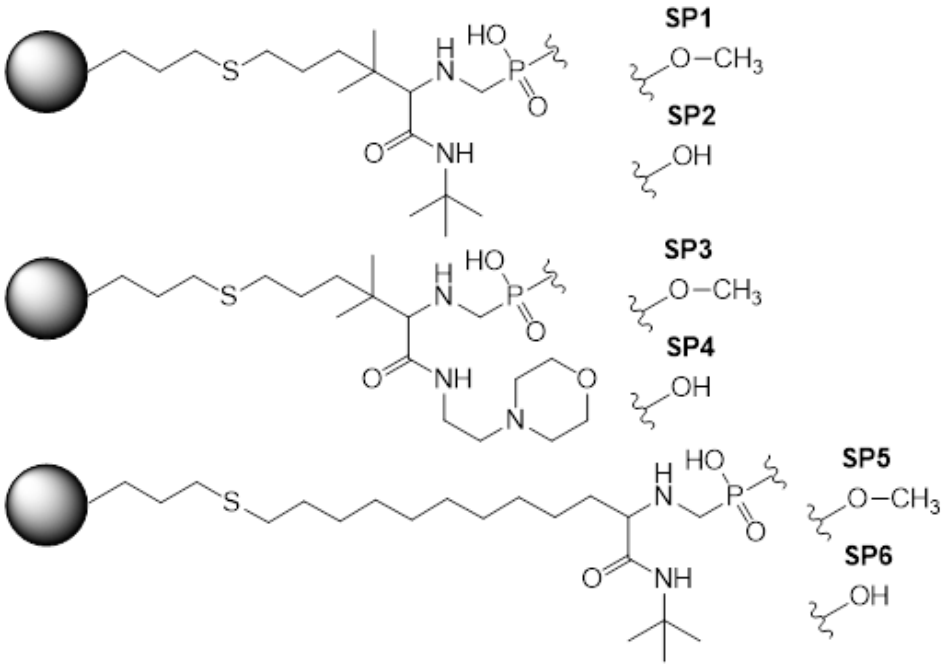

Fig. S 7: continued: Surface structure of in house developed columns which were included in the retention map and classified by principal component analysis

4.2.7.3. Milder Elution Conditions for Charged Analytes

4.2.7.3.1. Separation of Nucleotides using Ammonium Acetate as Buffer

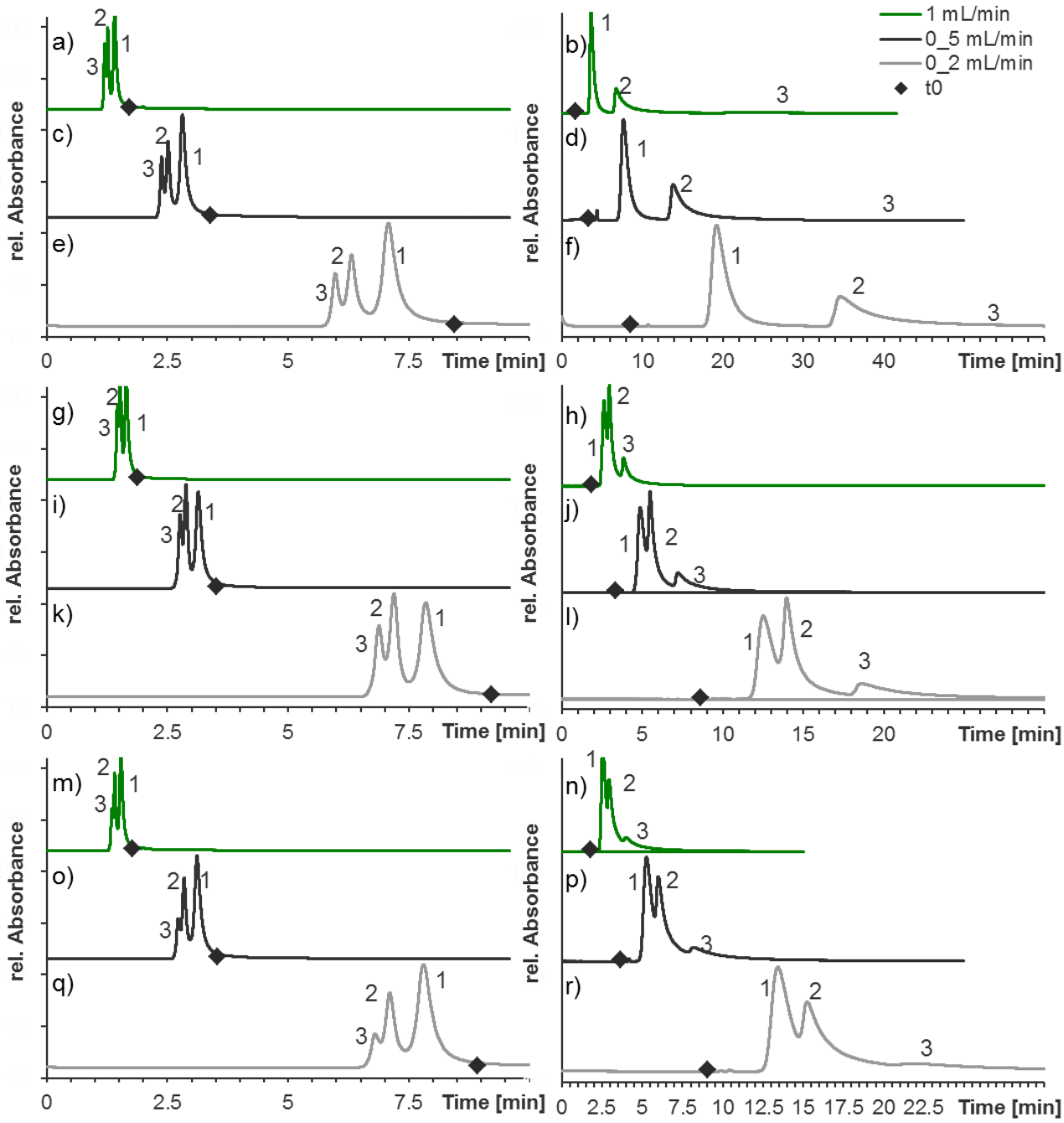

Fig. S 8: Separation of the Uridine mono-, di- and triphosphate on the pyridine modified silica using ammonium acetate buffer
Experimental conditions: isocratic separation:
ACN/H2O (1:4, v/v), a)-f) 12.5 mM, g)-l) 25 mM, m)-r) 50 mM ammonium acetate, pH 5: a), c), e), g), i), k), m), o) and q); pH 7: b), d), f), h), j) l), n), p) and r) with acetic acid, flowrate: 1.0 mL/min: a-b), g-h), m-n), 0.5 mL/min: c-d), i-j), o-p), 0.2 mL/min: e-f), k-l), q-r) The temperature was set to 25 °C, the detection wavelength was 254 , sample conc. mixture of uridine mono-(1), di-(2) and triphosphate (3) (0.1 mg/mL) dissolved in mobile phase. The injection volume was 2 µL.♦=t_0

Table S1: Retention times and the obtained resolution of nucleotide mono-, di- and triphosphates investigating different flow rates and ammonium acetate buffer concentrations under isocratic RP conditions

Flowrate [mL/min]	Buffer [mM]	pH 5					pH 7				
		Retention time [min]			Resolution		Retention time [min]			Resolution	
		UMP	UDP	UTP	UMP, UDP	UDP,UTP	UMP	UDP	UTP	UMP, UDP	UDP,UTP
1.0	50	2.55	2.94	3.97	0.70	1.05	1.54	1.41	1.57	1.19	0.69
0.5	50	5.26	5.99	8.20	0.71	1.11	3.11	2.85	2.72	1.35	0.75
0.2	50	13.42	15.25	21.74	0.77	1.05	7.80	7.10	6.80	1.47	0.80
1.0	25	2.61	2.95	3.83	0.71	1.66	1.65	1.52	1.46	1.07	0.64
0.5	25	4.87	5.48	7.21	0.77	1.52	3.14	2.88	2.76	1.31	0.74
0.2	25	12.52	13.97	18.64	0.89	1.67	7.85	7.19	6.88	1.52	0.85
0.1	25	24.76	27.57	37.02	1.02	1.91	15.46	14.13	13.51	1.59	0.90
1.0	15	4.81	6.75	22.87	2.49	2.02	1.41	1.26	1.20	1.46	0.81
0.5	15	7.65	13.83	42.35	3.07	2.80	2.81	2.51	2.38	1.63	0.97
0.2	15	19.23	34.62	n.d.	3.20	-	7.08	6.31	5.98	1.78	1.06

4.2.7.3.2. Isocratic Separation of Nucleotides using Ammonium Phosphate as Buffer

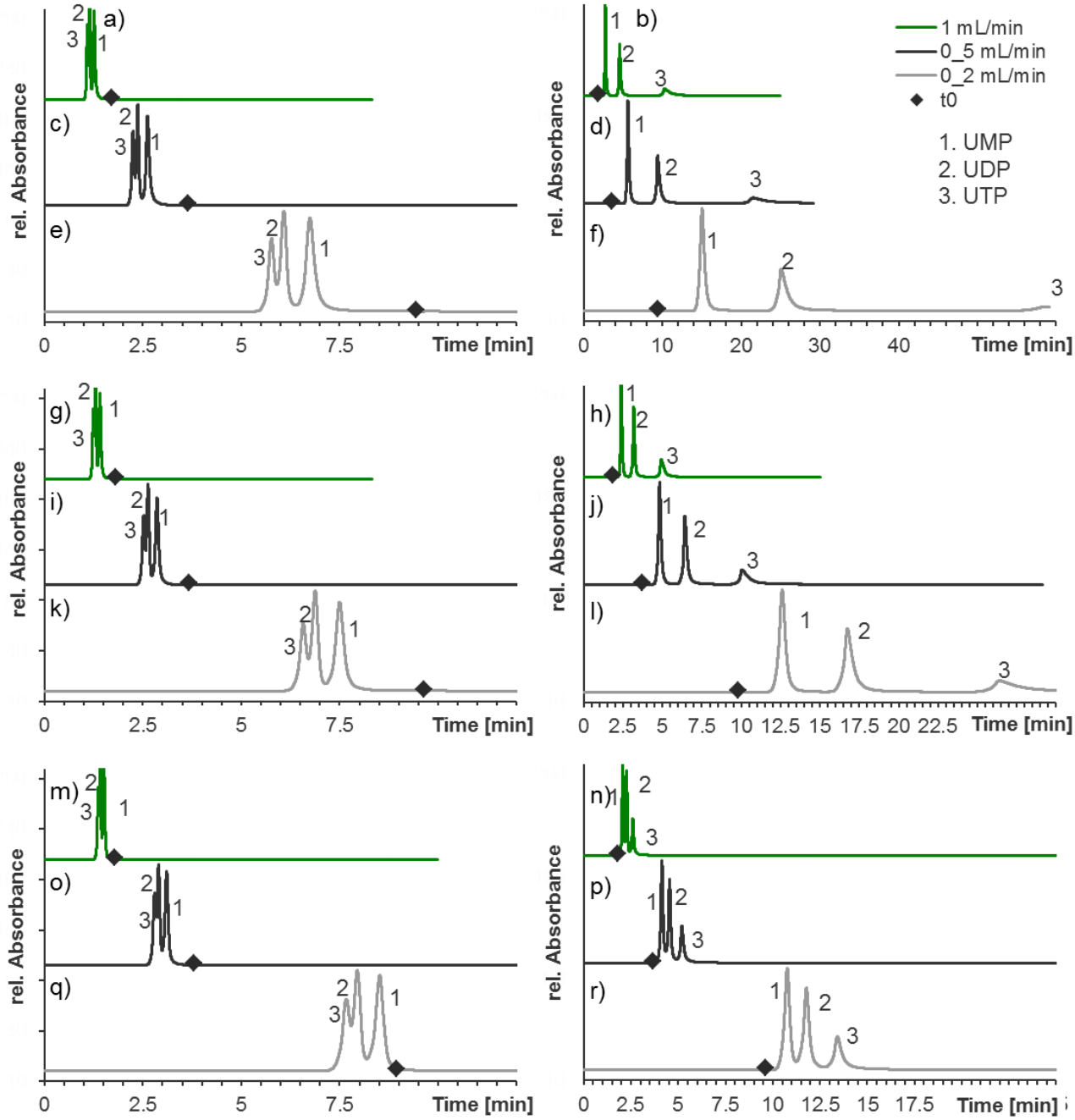

Fig. S 9: Separation of the Uridine mono-, di- and triphosphate on N-propyl-N'-2-pyridylurea modified silica using ammonium phosphate buffer
Experimental conditions: isocratic separation:
ACN/H2O (1:4, v/v), a)-f) 1.25 mM, g)-l) 2.5 mM, m)-r) 5.0 mM ammonium phosphate, pH 5: a), c), e), g), i), k), m), o) and q); pH 7: b), d), f), h), j) l), n), p) and r) with ammonia,
flowrate: 1.0 mL/min: a-b), g-h), m-n), 0.5 mL/min: c-d), i-j), o-p), 0.2 mL/min: e-f), k-l), q-r) The temperature was set to 25 °C, the detection wavelength was 254nm , sample: mixture of uridine 5'-mono- (1), di- (2) and triphosphate (3) (0.1 mg/mL) dissolved in mobile phase. The injection volume was 2 µL.♦=t_0

Table S 2: Retention times and the obtained resolution of nucleotide mono-, di- and triphosphates investigating different flow rates and ammonium phosphate buffer concentrations under isocratic RP conditions

Flowrate [mL/min]	Buffer [mM]	pH 5					pH 7				
		Retention time [min]			Resolution		Retention time [min]			Resolution	
		UMP	UDP	UTP	UMP, UDP	UDP,UTP	UMP	UDP	UTP	UMP, UDP	UDP,UTP
1.0 mL/min	1.25	2.73	4.55	10.26	6.40	6.27	1.26	1.14	1.26	1.64	0.90
0.5 mL/min	1.25	5.61	9.38	21.50	7.04	6.05	2.62	2.37	2.25	1.85	1.04
0.2 mL/min	1.25	15.02	25.08	58.85	7.18	10.88	6.75	6.08	5.77	1.97	1.09
1.0 mL/min	2.5	2.38	3.17	4.92	4.35	5.63	1.41	1.30	1.24	1.45	0.74
0.5 mL/min	2.5	4.82	6.42	10.05	4.93	5.86	2.86	2.63	2.52	1.65	0.83
0.2 mL/min	2.5	12.60	16.74	26.39	5.10	5.37	7.50	6.88	6.57	1.78	0.94
1.0 mL/min	5	2.06	2.27	2.59	1.64	2.17	1.51	1.41	1.37	1.16	0.60
0.5 mL/min	5	4.14	4.54	5.19	1.86	2.59	3.10	2.90	2.80	1.39	0.68
0.2 mL/min	5	10.77	11.79	13.42	1.93	2.61	8.52	7.95	7.67	1.53	0.74

4.2.7.3.3. Gradient Separation of Nucleotides using Ammonium Phosphate as Buffer

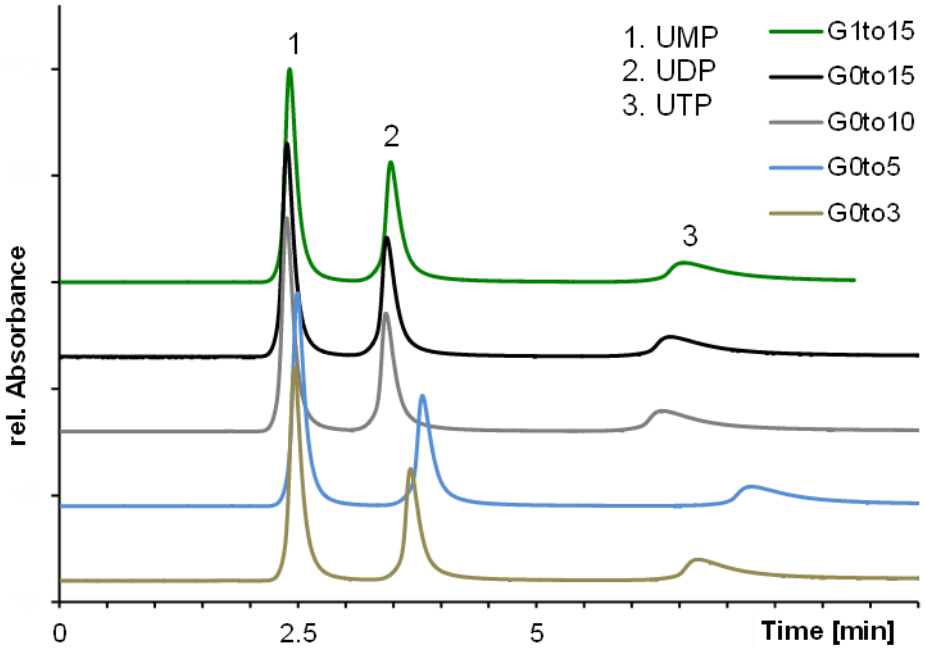

Fig. S 10: Separation of UXP's investigating pH gradients with different gradient profiles on N-propyl-N'-2-pyridylurea stationary phase:
G1to15: 0 to 100 % B in 1.00-15.00 min, 100% B 15.00-20.00 min, 100 to 0% B 20.00-20.01, 0% B for 20.01-30.00min
G0to15: 0 to 100 % B in 0.00-15.00 min, 100% B 15.00-20.00 min, 100 to 0% B 20.00-20.01, 0% B for 20.01-30.00min
G0to10: 0 to 100 % B in 0.00-10.00 min, 100% B 10.00-12.00 min, 100 to 0% B 12.00-12.01, 0% B for 12.01-30.00min
G0to5: 0 to 100 % B in 0.00-5.00 min, 100% B 5.00-7.00 min, 100 to 0% B 7.00-7.01, 0% B for 7.01-22.00min
G0to3: 0 to 100 % B in 0.00-3.00 min, 100% B 3.00-8.00 min, 100 to 0% B 8.00-8.01, 0% B for 8.01-19.00min
ACN/H2O (1:4, v/v), 1.25 mM H_3PO_4, A: pH 5 and B: pH 7, adjusted with ammonia, 1.0 mL/min, T=25 °C, λ=254nm , sample: mixture of uridine 5'-mono- (1), di- (2) and triphosphate (3) (0.1 mg/mL) dissolved in mobile phase. The injection volume was 2 µL.

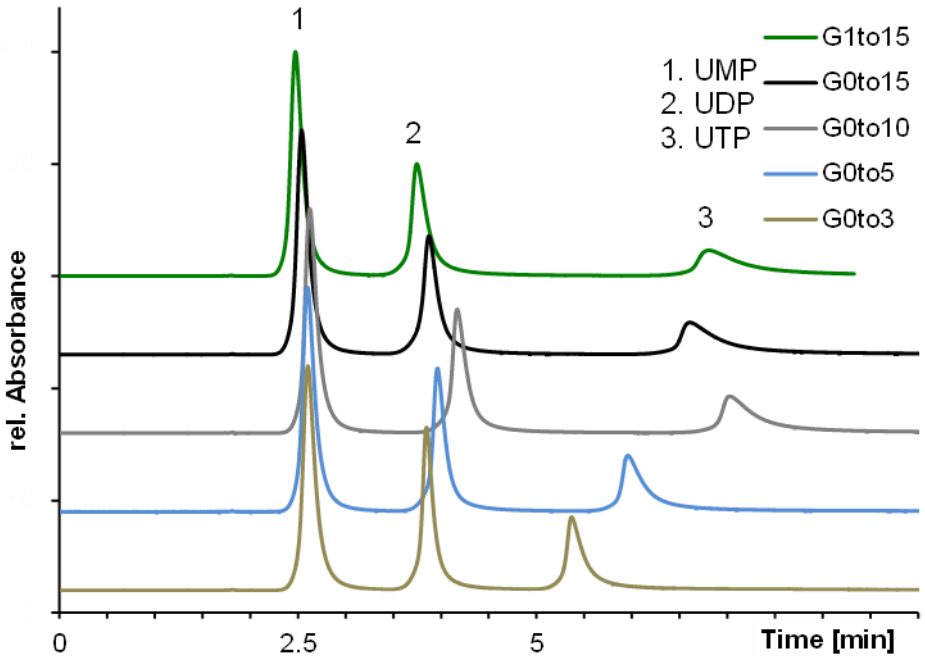

Fig. S 11: Separation of UXP's investigating salt gradients with different gradient profiles using on N-propyl-N'-2-pyridylurea modified column:
G1to15: 0 to 100 % B in 1.00-15.00 min, 100% B 15.00-20.00 min, 100 to 0% B 20.00-20.01, 0% B for 20.01-30.00min
G0to15: 0 to 100 % B in 0.00-15.00 min, 100% B 15.00-20.00 min, 100 to 0% B 20.00-20.01, 0% B for 20.01-30.00min
G0to10: 0 to 100 % B in 0.00-10.00 min, 100% B 10.00-12.00 min, 100 to 0% B 12.00-12.01, 0% B for 12.01-30.00min
G0to5: 0 to 100 % B in 0.00-5.00 min, 100% B 5.00-7.00 min, 100 to 0% B 7.00-7.01, 0% B for 7.01-22.00min
G0to3: 0 to 100 % B in 0.00-3.00 min, 100% B 3.00-8.00 min, 100 to 0% B 8.00-8.01, 0% B for 8.01-19.00min
ACN/H2O (1:4, v/v), A: 1.25 mM H_3PO_4, B: 2.5 mM H_3PO_4; pH 5, adjusted with ammonia, 1.0 mL/min, T=25 °C, λ=254nm , sample: mixture of uridine 5'-mono- (1), di- (2) and triphosphate (3) (0.1 mg/mL) dissolved in mobile phase. The injection volume was 2 µL.

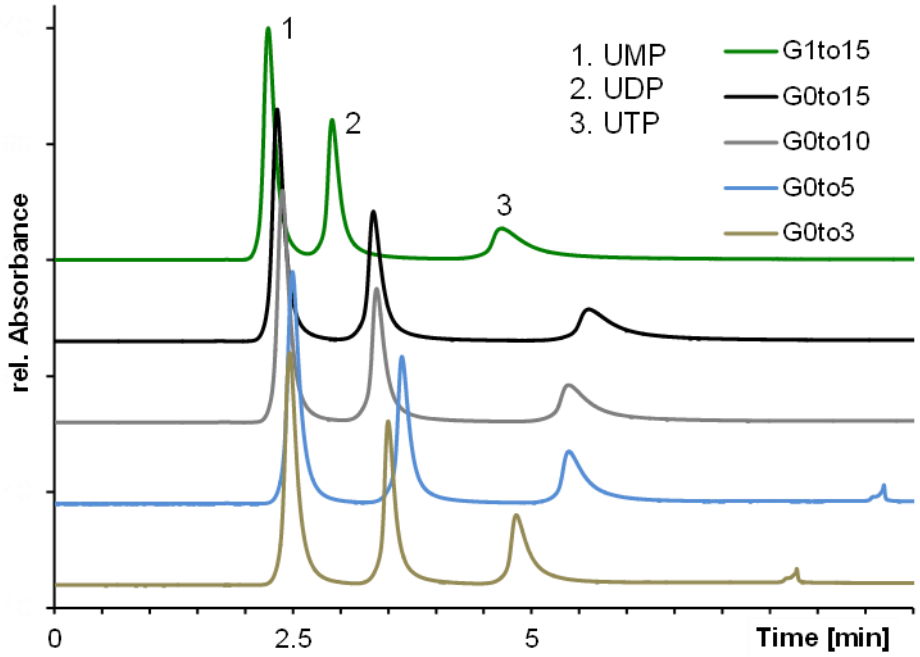

Fig S 12: Separation of UXP's investigating combined pH and salt gradients with different gradient profiles on N-propyl-N'-2-pyridylurea stationary phase:
G1to15: 0 to 100 % B in 1.00-15.00 min, 100% B 15.00-20.00 min, 100 to 0% B 20.00-20.01, 0% B for 20.01-30.00min
G0to15: 0 to 100 % B in 0.00-15.00 min, 100% B 15.00-20.00 min, 100 to 0% B 20.00-20.01, 0% B for 20.01-30.00min
G0to10: 0 to 100 % B in 0.00-10.00 min, 100% B 10.00-12.00 min, 100 to 0% B 12.00-12.01, 0% B for 12.01-30.00min
G0to5: 0 to 100 % B in 0.00-5.00 min, 100% B 5.00-7.00 min, 100 to 0% B 7.00-7.01, 0% B for 7.01-22.00min
G0to3: 0 to 100 % B in 0.00-3.00 min, 100% B 3.00-8.00 min, 100 to 0% B 8.00-8.01, 0% B for 8.01-19.00min
ACN/H2O (1:4, v/v), A: 1.25 mM H_3PO_4, B: 2.5 mM H_3PO_4 A: pH 5 and B: pH 7, adjusted with ammonia, 1.0 mL/min, T=25 °C, λ=254nm, sample: mixture of uridine 5'-mono- (1), di- (2) and triphosphate (3) (0.1 mg/mL) dissolved in mobile phase. The injection volume was 2 µL.

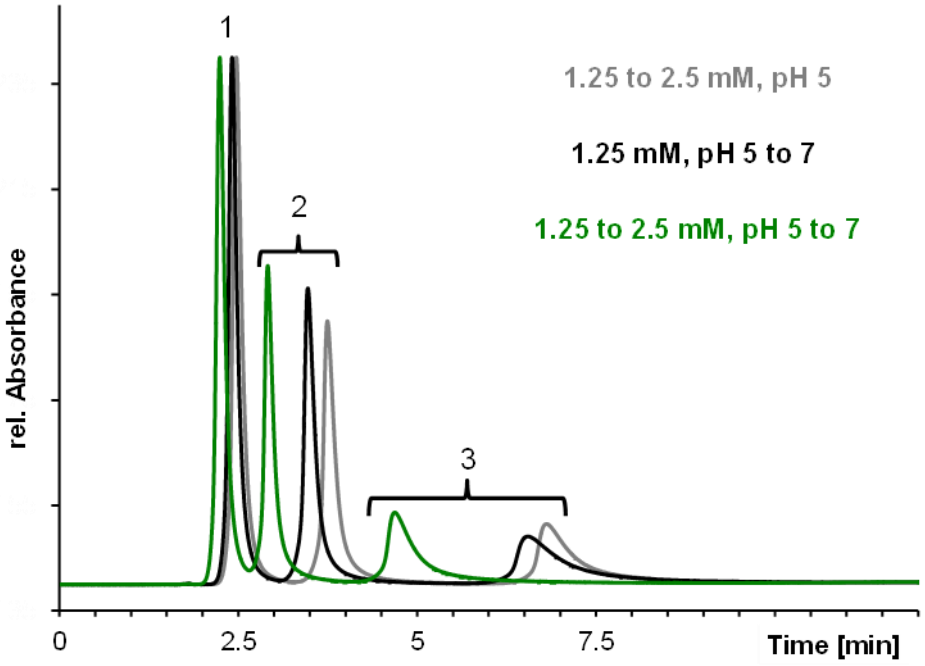

Fig. S 13: Comparison of the elution of the nucleotides (1. UMP, 2. UDP, 3. UTP) investigating primary and binary gradients on N-propyl-N'-2-pyridylurea modified silica
grey: salt gradient: ACN/H2O (1:4, v/v), A: 1.25 mM H_3PO_4, B: 2.5 mM H_3PO_4, pH 5 adjusted with ammonia
black: pH gradient: ACN/H2O (1:4, v/v), 1.25 mM H_3PO_4, A: pH 5 and B: pH 7, adjusted with ammonia
green: salt and pH gradient: ACN/H2O (1:4, v/v), A: 1.25 mM H_3PO_4, B: 2.5 mM H_3PO_4, A: pH 5 and B: pH 7, adjusted with ammonia, gradient profile: 0 to 100 % B in 1.00-15.00 min, 100% B 15.00-20.00 min, 100 to 0% B 20.00-20.01, 0% B for 20.01-30.00min, 1.0 mL/min, T=25 °C, λ=254nm , sample: mixture of uridine 5'-mono- (1), di- (2) and triphosphate (3) (0.1 mg/mL) dissolved in mobile phase. The injection volume was 2 µL.

4.2.7.3.4. Separation of Single- (ss) and Double Stranded (ds) Oligonucleotides

Single and double stranded oligonucleotides were analyzed as model compounds for multiple charged analytes. For the separation of ss and ds oligonucleotides mobile phase A consisted of 100 mM ammonium acetate dissolved in water (pH 7) whereas mobile phase B was a mixture of acetonitrile/water (1:1, v/v). A two-step gradient was performed with the following gradient profile: 0-2 min: 0%B, 2-17 min 10-20% B, 17-22 min: 20-100% B, hold 100% B for 2 min, 24-30 min: 100-0% B, 5 min equilibration at 0% B. The self-complementary oligonucleotide dodecamer (5'- CGCAAATTTGCG - 3' was dissolved in water (1 mg/mL). An aliquot was heated to 95 °C und gently cooled down to room temperature. None heated and previously heated solution was mixed in the ratio 1:1 (v,v). The injection volume was 2.86 µL. The flowrate was 0.378 mL/min. The column was thermostated at 25 °C and the oligonucleotides were detected at 258 nm.

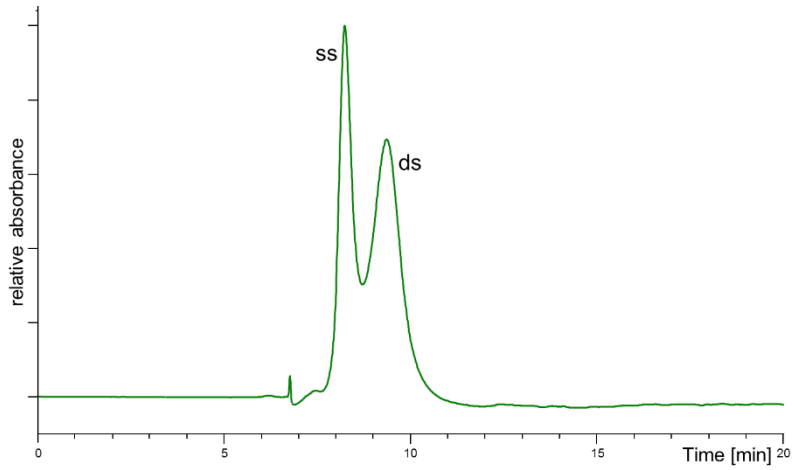

Fig. S 14: Separation of single and double stranded oligonucleotides (5'- CGCAAATTTGCG - 3') on N-propyl-N'-2-pyridylurea stationary phase
Experimental conditions: mobile phase A: 100 mM NH_4Ac, B: ACN/H_2O (50/50, v/v); gradient: 0-2 min: 0 %B, 2-17 min 10-20 % B, 17-22 min: 20-100 % B, hold 100 % B for 2 min, 24-30 min: 100-0 % B, 5 min equilibration at 0 % B; flow: 0.378 mL/min; T=25°C; 1mg; λ = 258 nm

An increased salt concentration was used, but the pH was kept constant in the neutral range. Under these conditions a close to baseline separation of single and double stranded oligonucleotides was observed. Further method optimization could lead to baseline separation but was not the subject of the present study.

4.3. Simultaneous Separation of Water- and Fat-Soluble Vitamins by Selective Comprehensive HILIC × RPLC (High-Resolution Sampling) and Active Solvent Modulation

*Stefanie Bäurer [1], Wenkai Guo [1], Stefan Polnick[1], Michael Lämmerhofer [1] **

[1] Institute of Pharmaceutical Sciences, Pharmaceutical (Bio-)Analysis, University of Tübingen, Auf der Morgenstelle 8, 72076 Tübingen, Germany

Reprinted by permission from Springer Nature Customer Service Centre GmbH:
Springer Nature, Journal: Chromatographia:
Simultaneous Separation of Water- and Fat-Soluble Vitamins by Selective Comprehensive HILIC × RPLC (High-Resolution Sampling) and Active Solvent Modulation, S. Bäurer, W. Guo, S. Polnick, M. Lämmerhofer, Volume 82 (2019) Pages 167-180,
DOI: 10.1007/s10337-018-3615-0

4.3.1. Abstract

The simultaneous liquid chromatographic analysis of water- and fat-soluble vitamins is challenging because of their wide polarity range. Typically, water-soluble vitamins are separated and analyzed by hydrophilic interaction chromatography (HILIC) while fat-soluble vitamins are analyzed by reversed-phase liquid chromatography (RPLC). The combination of these two retention principles in a column coupling or multidimensional liquid chromatography approach seems to be a logical consequence to solve the problem. In this work, a selective comprehensive HILIC × RPLC 2D-LC approach is investigated. In this method, the polar water-soluble vitamins are resolved in the first dimension (^{1}D) on a 2-pyridylurea mixed-mode phase operated by a HILIC gradient and the coeluted fat-soluble vitamins in the early part of the chromatogram are comprehensively transferred in ten 40-µL fractions into a second dimension (^{2}D) separation by RPLC on a C8 core–shell column. This mode of separation is also known as high-resolution sampling. The separations in ^{1}D and ^{2}D were optimized systematically and the retention mechanism on the mixed-mode column interpreted by support of these chromatographic data. The solvent incompatibility of ^{1}D HILIC and ^{2}D RPLC conditions due to sampling of acetonitrile-rich fractions from ^{1}D into ^{2}D RPLC led to severe peak broadening when a direct fraction transfer was carried out. An isocratic refocusing step could partly improve the situation for the stronger retained fat-soluble vitamins. Active solvent modulation with a specifically designed valve which allows a bypass of the weak eluent from the ^{2}D pump to the column head and dilution of the fractionated sample from the sampling loop completely solved the problem and provided perfect peak shapes and chromatographic efficiencies.

4.3.2. Introduction

Multivitamin formulations for nutritional supplementation are recommended under certain situations of malnutrition, some diseases, strong alcohol abuse, and heavy smoking. For pharmaceutical multivitamin products, adequate quality control is mandatory. Yet, the simultaneous analysis of fat- and water-soluble vitamins in one analytical procedure or method is not a trivial task because of the wide physicochemical properties of these vitamins.

Quite often, two distinct methods are adopted for the analysis of fat- and water-soluble vitamins [1,2,3,4,5], while their simultaneous analysis, e.g., by a single chromatographic method is rare. Separation of water- and fat-soluble vitamins into separate samples by solid-phase extraction and subsequent analysis on RP columns with methanol-buffer (aqueous RPLC) for water-soluble vitamins and methanol–acetonitrile (nonaqueous RPLC) for fat-soluble vitamins was one reported approach [1, 2]. Buszewski and Zbanyszek performed the analysis on two distinct C18 columns varying in the ligand density and combined those separations via a column-

switching technology [3, 4]. In another work, two distinct LC–MS methods based on two distinct C18 columns were developed for both fat- and water-soluble vitamins and applied to the measurement of NIST vitamin standard reference materials [5].

Single-column analysis approaches are reported as well. For example, Li and Chen [6] employed multi-step gradients consisting of methanol (A), potassium phosphate (B) and water (C) to accomplish separation of 12 fat- and water-soluble vitamins on a C18 column. Klejdus et al. [7] suggested to cope with this problem by applying in a single run a combination of isocratic and linear gradient elution to separate both classes of vitamins. Dabre et al. [8] solved the problem of separating both classes of vitamins by mixed-mode chromatography.

A general review of the state of art in analysis of vitamins by liquid chromatography is given in Ref. [9]. The determination of water- and fat-soluble vitamins in biological fluids has been recently reviewed [10]. The state of art in fat-soluble vitamin analysis was reviewed by Fanali et al. [11].

More recent work focused on a sequential extraction and subsequent analysis of both classes of vitamins by coupling the extraction steps to LC–MS/MS and LC-DAD in order to quantify the free vitamin content [12]. Similarly, sequential analysis of water- and fat-soluble vitamins on the same column, a core–shell C18 particle column, and same UHPLC instrument with different gradient elution conditions for the two distinct vitamin classes was suggested by Tayade et al. [13]. Very recently, fat-soluble and water-soluble vitamins were separated by a unified supercritical fluid chromatography–liquid chromatography approach with MS/MS detection in which the mobile phases state was changing continuously during the elution from supercritical (at 100% CO_2), to subcritical (increasing percentage of methanol as additive), to finally liquid (at 100% methanol) [14]. In another approach, electrokinetic chromatography (EKC) with polymeric micelles was utilized to separate and analyze 11 kinds of water- and fat-soluble vitamins [15].

Besides these works, there are numerous publications describing the separation of water-soluble vitamins by hydrophilic interaction chromatography (HILIC). Fat-soluble vitamins elute close to the void in such methods. Therefore, HILIC has not been widely adopted in concepts of simultaneous analysis of water- and fat-soluble vitamins.

In this work, we evaluate the simultaneous liquid chromatographic separation of water- and fat-soluble vitamins by selective comprehensive HILIC × RPLC (also known as high-resolution sampling) [16]. A new mixed-mode chromatography stationary phase based on an *N*-propyl-*N'*-2-pyridylurea ligand linked to silica (Fig. 1) is utilized and employed under HILIC conditions for the separation of the water-soluble vitamins. The apolar fat-soluble vitamins, eluting close to the void volume of the column, are comprehensively sampled into a second dimension (^{2}D)

separation. Since HILIC is not very well compatible with the RP conditions of the ^{2}D separation and leads to extra band broadening [17], active solvent modulation (ASM) [18,19,20] was adopted to refocus the analyte zones on the ^{2}D-RPLC column [20]. This work should document the potential of active solvent modulation to hyphenate HILIC and RPLC in online two-dimensional LC approaches and give some insight into the potential of mixed-mode columns [21] for generating complementary selectivity.

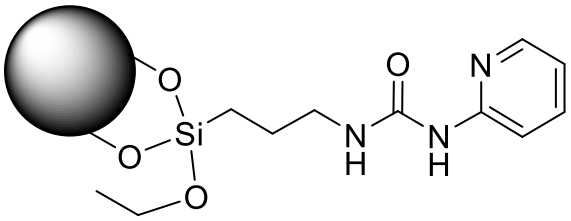

Fig. 1: Surface structure of the investigated stationary phase (*N*-propyl-*N*′-2-pyridylurea-modified silica particles).

4.3.3. Material and Methods

4.3.3.1. Materials

Vitamins A-palmitate (hereafter short vitamin A), B_1, B_2, B_3, B_6, B_9, B_{12}, C, D, E and K (Fig. 2) were a generous gift by Fresenius Kabi (Bad Homburg, Germany). Ammonium acetate, acetic acid and formic acid were purchased from Sigma Aldrich (Munich, Germany). Acetonitrile HPLC grade was supplied by J.T. Baker (Netherlands). MilliQWater was prepared by further deionization of demineralized water using Elga PurLab Ultra Purification system (Celle, Germany).

N-Propyl-*N'*-2-pyridylurea-modified silica stationary phase (150 × 4.6 mm, 5 µm, 100 Å) (Fig. 1) was in-house synthesized and previously characterized in detail as described elsewhere [22]. For the second dimension (^{2}D) separation a Kinetex C8 column (50 × 2.1 mm, 2.6 µm, 100 Å) from Phenomenex (Torrance, CA, USA) was used.

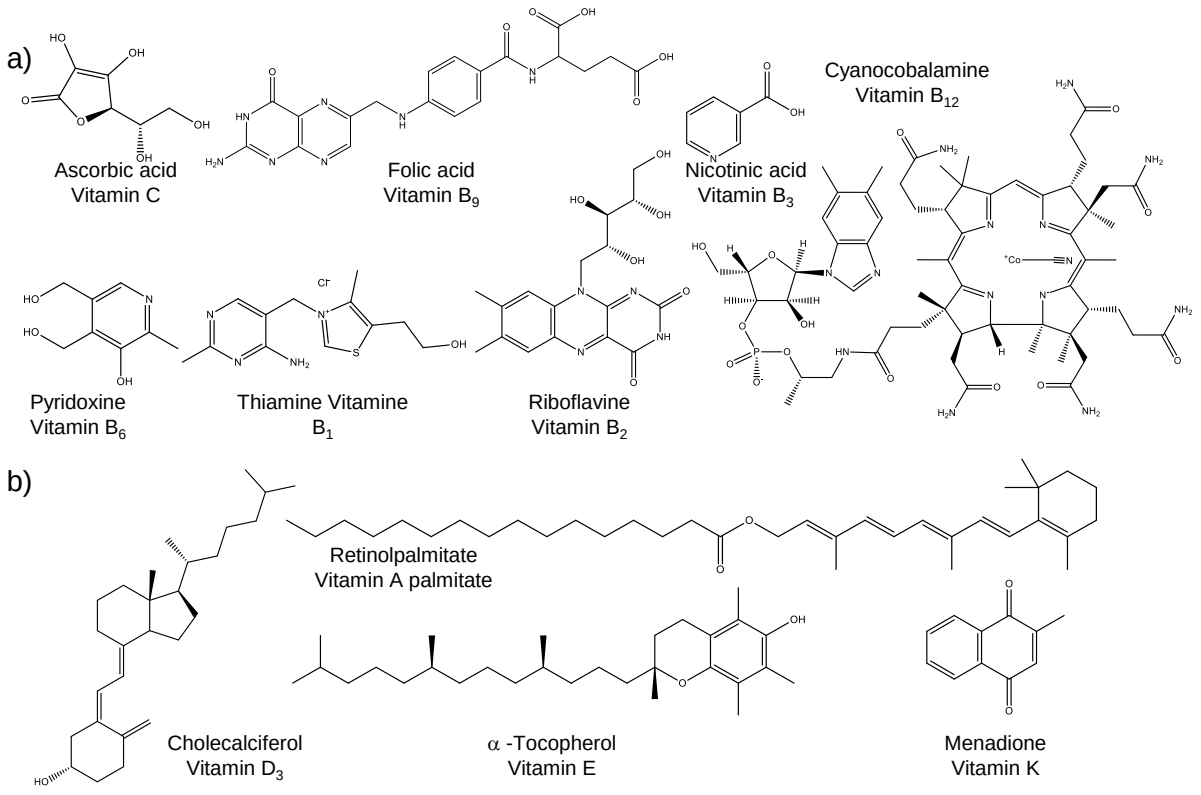

Fig. 2: Structure of the investigated **a** water-soluble and **b** fat-soluble vitamins.

4.3.3.2. Instrumentation and Software

The screening for general elution conditions (RPLC vs HILIC) was performed using an Agilent 1100 series LC system from Agilent Technologies (Waldbronn, Germany) equipped with an autosampler, degasser, binary pump, thermostated column compartment, and variable wavelength detector (VWD). The system was controlled by OpenLab CDS ChemStation—Edition for LC & LC/MS System (Rev.C.01.07 SR3 [465]). Data were analyzed using ChemStation software (Rev. B.04.03.16). The physicochemical data were calculated with Marvin Sketch (Rev. 14.12.15.0).

The study of the design space was made on an Agilent 1100 series LC system equipped as above but using a quaternary instead of a binary pump as well as a diode array detector (DAD) instead of VWD.

The two-dimensional LC experiments were carried out on an Agilent 1290 Infinity II 2D-LC Solution (Agilent Technologies, Waldbronn, Germany). The first dimension (^{1}D) instrument was equipped with a quaternary pump, multisampler, column compartment and a VWD detector. The second dimension consisted of a binary pump, column compartment and a DAD detector. The first and second dimension was interfaced by a pressure release kit followed by a 2D-LC five position/ten-port valve (concurrently installed, active solvent modulation possible) connected to two 14-port multiple heart cutting valves with 6 sample loops (each 40 µL). For the experiments using active solvent modulation (ASM factor 5, split ratio 1:4), the 0.96-µL restriction capillary (85 × 0.12 mm) was installed. The system was controlled and the data were analyzed by using Open Lab CDS Rev. C.01.07SR3. Further analysis was done using LC-Image v2.7r3 LC × LC-HRMS (GC Image, LLC, Lincoln, Nebraska, USA).

4.3.3.3. 1D-Liquid Chromatographic Methods

The concentration of the vitamins in the test mixture was 0.1 mg/mL, except vitamin B_{12} (1.0 mg/mL) and vitamin A, D, E and K (0.025 mg/mL), dissolved in mobile phase.

Unless stated otherwise, for all 1D-LC experiments the flow rate was set to 1.0 mL/min, the temperature to 25 °C and the injection volume of the vitamin mixture was 10 µL. The vitamins were detected at 270 nm, except for vitamin A which was detected at 325 nm and vitamin E at 290 nm.

4.3.3.3.1. Screening of Elution Conditions (Scouting Runs)

Initially, the separation of fat- and water-soluble vitamins was examined under RPLC (Kinetex C8) and HILIC conditions (2-pyridylurea mixed-mode phase). To do so, the mobile phases consisted of an acetonitrile/water mixture, whereas mobile phase A contained 5% (v/v) acetonitrile and mobile phase B 95% (v/v). Both mobile phases contained 15 mM ammonium

acetate, the apparent pH was adjusted to 4.5 with acetic acid in the final mixture. An RP gradient (100% A to 100% B) and a HILIC gradient (100% B to 100% A) was run.

4.3.3.3.2. Design Space and Development of a Suitable Gradient

The further experiments were performed under HILIC conditions with the mixed-mode column for development of a suitable ^{1}D method. A design space was created consisting of different acetonitrile concentrations (95, 90 and 85% (v/v)), different buffer concentrations (5, 10 and 15 mM ammonium acetate) and different apparent pH values (4.5, 5.5 and 6.5, adjusted with acetic acid in the final mixture).

With the help of the design space a final gradient method was developed. The mobile phases contained 10 mM ammonium acetate and the pH was adjusted to 4.5 in the final mixture. The linear gradient was performed from 95 to 30% (v/v) acetonitrile in 10 min.

4.3.3.4. Two Dimensional Separation of Fat and Water-Soluble Vitamins

In the first dimension (HILIC using *N*-propyl-*N*′-2-pyridylurea-modified mixed-mode phase), a linear gradient from 100% B (ACN–H_2O; 95:5, v/v, containing 15 mM ammonium acetate (NH_4Ac) in total, apparent pH 4.5 adjusted in the mixture with acetic acid) to 100% A (ACN–H_2O, 30:70, v/v, containing 15 mM NH_4Ac in total, apparent pH 4.5 adjusted in the mixture with acetic acid) in 10 min was performed, with a subsequent 2-min hold at 100% A. Afterwards, the column was re-equilibrated for 8 min at 100% B.

The second dimension conditions (RP with Kinetex C8 column) are described in the corresponding discussion part. The fat-soluble vitamins were collected by high-resolution sampling and either transferred directly into the second dimension [ACN:H_2O (4:1, v/v), 0.1% FA in total], transferred and focused for 0.61 min by an isocratic elution step [ACN:H_2O (5:95, v/v), 0.1% FA in total] or transferred using active solvent modulation (ASM factor 5, threefold capillary flush for 0.61 min in total with (ACN:H_2O (5:95, v/v)) before starting the isocratic run. In case of the directly transferred fractions, the ^{2}D gradient time corresponds to the ^{2}D cycle time (6.1 min), whereas in case of the focused and/or the runs using active solvent modulation the ^{2}D gradient time is 6.71 min and focusing conditions are equilibrated until the ^{2}D cycle ends (7.0 min). The ^{2}D flow rate was 1.0 mL/min and the temperature was set to 60 °C.

4.3.4. Results and Discussion

4.3.4.1. Screening of Elution Conditions (Scouting Runs)

The investigated vitamin test mixture contains substances that cover a wide polarity range and are difficult to resolve in their entirety on either RPLC or HILIC stationary phases. On the other hand, they show a great structural diversity of functional groups being present for interactions with stationary phases in a chromatographic separation. In detail, the mixture contained the water-soluble acidic vitamins like ascorbic acid, folic acid, and nicotinic acid as well as basic ones like thiamine (Fig. 2). Furthermore, the amphoteric pyridoxine and the complex cyanocobalamine add to the structural complexity of the mixture leading to a wide range of polarities and charge state and thus to diverse chromatographic interactions driving the adsorption and partitioning behavior of these analytes. Table 1 summarizes some physicochemical properties of the tested vitamins which are decisive for their chromatographic retention characteristics in RPLC and HILIC.

Table 1: Physicochemical characteristics of the investigated fat- and water-soluble vitamins.

Name	pKa[a,d]	Log D[d]			Net charge[d]			IP[b,d]
		pH 4.5	pH 5.5	pH 6.5	pH 4.5	pH 5.5	pH 6.5	
Water-soluble Vitamins								
Thiamine (vitamin B_1)	5.54	-4.1	-3.41	-3.14	1.92	1.52	1.1	-
Riboflavin (vitamin B_2)	5.97	-0.93	-1.04	-1.54	-0.03	-0.25	-0.77	1.8
Nicotinic acid (vitamin B_3)	2.79 4.19	-0.49	-1.33	-2.25	-0.14	-0.65	-0.95	4.01
Pantothenic acid (vitamin B_5)	4.35	-1.69	-2.48	-3.44	-0.58	-0.93	-0.99	0.8
Pyridoxine (vitamin B_6)	5.58 9.4	-1,92	-1.28	-1	0.92	0.55	0.11	7.49
Biotin (vitamin B_7)	4.4	-0.16	-0.93	-1.86	-0.58	-0.93	-0.99	1.27
Folic acid (vitamin B_9)	0.84 2.12 3.38	-2.11	-3.94	-5.8	-1.69	-1.97	-2.07	2.64
Cyanocobalamine (vitamin B_{12})	4.17 4.32				0.4	0.06	0.01	8.44
Ascorbic acid (vitamin C)	4.36	-2.29	-3.08	-4.04	-0.58	-0.93	-0.99	1.29
Fat-soluble Vitamins								
Retinol palmitate (vitamin A)	-		11.62[c]		-	-	-	-
Cholecalciferol (vitamin D)	-		7.13[c]		-	-	-	-
Tocopherol (vitamin E)	-		10.51[c]		-	-	-	-
Menadion (vitamin K)	-		1.89[c]		-	-	-	-

[a] pK_a of functional groups, relevant for changes in the protonation status in the investigated pH range

[b] IP = isoelectric point

[c] depicted value = log P value, calculated with Marvin Sketch

[d] calculated with Marvin Sketch

The idea in this work was to examine the retention characteristics of vitamins on a new mixed-mode stationary phase [22] that in dependence on mobile phase pH can be either weakly positively charged (pH < 6.5) or negatively charged (pH > 6.5) (due to residual silanols). Dependent on mobile phase pH ionic interactions with either anionic (acidic) vitamins or cationic (basic) vitamins can be superimposed upon other types of interactions such as hydrogen bonding with urea group of the chromatographic ligand, π–π interactions and/or hydrophobic with the aromatic moieties (in particular under aqueous RP conditions). Mixed-mode phases are usually more flexible in method development as they may be often operated in different elution modes (e.g., RP, HILIC or ion-exchange elution mode). For this reason, in a first screening experiment we tested which of the two conditions, RPLC or HILIC, provides a more promising strategy for further method development. The results of a positive acetonitrile-

gradient elution (RPLC conditions) are shown in Fig. 3a and those of a negative acetonitrile-gradient elution (HILIC conditions) in Fig. 3b (both at pH 4.5). It becomes evident that the elution pattern in RPLC and HILIC scouting gradients is not in accordance to the log D calculated for pH 4.5 (Table 1) and is not simply following a reversal of the elution order expected from the hydrophilicity and/or lipophilicity of the compounds. Instead, a mixed-mode retention appears to be established that makes the two modes quite complementary. Overall, the HILIC elution conditions seem to give a better overall separation with less overlaps. The fat-soluble lipophilic vitamins elute unresolved at the front while the other substances are all close to baseline separated (Fig. 3b). In contrast, under RPLC conditions a number of peaks are unresolved in the early eluting part of the chromatogram and the lipophilic vitamins are still not separated (Fig. 3a) although they elute late in the chromatogram. It turns out that the ligand chain is too short and lipophilicity insufficient for a good RPLC behavior of the lipophilic vitamins on this phase. The HILIC separation mode was therefore selected to be further developed as ^{1}D separation.

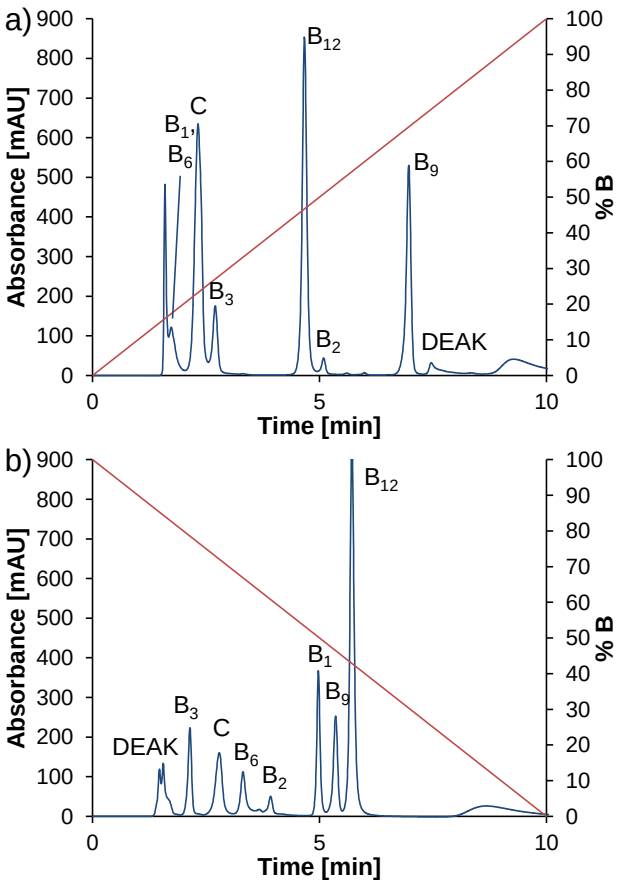

Fig. 3: Screening of chromatographic conditions utilizing **a** reversed phase and **b** hydrophilic interaction chromatography conditions on the 2-pyridylurea-modified mixed-mode stationary phase. Experimental conditions: mobile phase A: 5% ACN, 95% H_2O; mobile phase B: 95% ACN, 5% H_2O; containing both 15 mM NH_4Ac in total, pH 4.5 adjusted with acetic acid in the final mixture, gradient profile: **a** 0–100% B in 10 min, 100%B for 2 min, 100–0% B in 0.01 min, 0% B for 8 min; **b** 100–0% B in 10 min, 0%B for 2 min, 0–100% B in 0.01 min, 100% B for 8 min; 1.0 mL/min; 25 °C, 270 nm, inj. vol. 10 µL.

4.3.4.2. Design Space of ^{1}D HILIC Separation

A systematic study of the effect of the major experimental variables was undertaken under isocratic conditions. The idea was to study the impact of mobile phase conditions on retention of water-soluble vitamins under HILIC conditions and pinpoint the design space for this type of separation. The aim was also to get insight into the retention mechanism of these molecules on the current mixed-mode stationary phase that is more difficult to understand. Accordingly, this part of the work should outline the retention behavior of polar compounds on the presently investigated mixed-mode column under HILIC elution conditions. The results of the design-of-experiment (DoE) optimization with a full factorial design on 3 levels are given in the Supplementary (see Suppl. Fig. S1–S8 and Suppl Table S1).

4.3.4.2.1. Variation of Organic Modifier Content

As can be expected for a HILIC method, the acetonitrile content plays a major role on retention and this is underpinned by the coefficients plot shown in supplementary Fig. S2. Since the current mixed-mode phase has an aromatic (i.e., pyridyl) group and C3 linker connected via a urea functionality, it could be expected that the stationary phase shows some RP-type retention at low organic content. For this reason the effect of acetonitrile percentage on the retention was investigated over a wider range (pH 4.5). At acetonitrile contents higher than 60% a typical HILIC behavior is observed, i.e., retention factors steeply increase with the ACN content (Fig. 4). On the other hand, RP-type retention (i.e., increase with lower ACN content) is observed only for B_9 (folic acid), B_2 (riboflavin) and B_{12} (cyanocobalamine). It becomes evident that the lipophilicity of the pyridylurea ligand is low (note, at pH 4.5 the pyridyl ligand is partly charged further reducing the lipophilicity; pK_a = 3.88 as calculated by Marvin Sketch [22]). If we look closer at the elution order at high ACN percentage, we find out that it is different from what was expected from the calculated log $D_{4.5}$. Acidic folic acid (B_9) is stronger retained than the more hydrophilic basic thiamine (B_2). At pH 4.5 the pyridyl ring is protonated and can impose a weak anion-exchange retention increment. B_{12}, which possesses a negatively charged phosphate moiety is probably strongly retained for the same reason. Zwitterionic nicotinic acid (B_3) does not show this strong retention. Overall, it becomes apparent that a mixed-mode retention resulting from common HILIC behavior superimposed by attractive and repulsive ionic interactions provides a specific opportunity for a unique retention pattern on this 2-pyridylurea-modified mixed-mode phase.

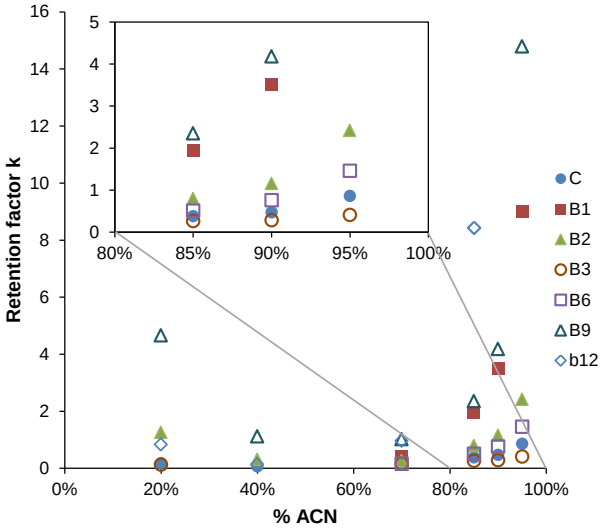

Fig. 4: Retention factors of vitamins on the 2-pyridylurea-modified mixed-mode stationary phase in dependence on acetonitrile percentage in the eluent buffered with 15 mM ammonium acetate at pH 4.5, adjusted in the final mixture with acetic acid. U-shaped curves for vitamin B9, B2, and B12 indicate hydrophobic interactions at low ACN content (in accordance to an RPLC mode) and dominance of hydrophilic interactions at high ACN content (in accordance to a HILIC mode).

4.3.4.2.2. Variation of Apparent pH

The surface charge of the 2-pyridylurea-modified mixed-mode phase was recently characterized by pH-dependent ζ-potential measurements [22]. They revealed positive surface charge below pH 6.5 and a soft weak anion-exchange capacity around pH 4–5. Due to residual silanols the surface gets negatively charged at pH above 6.5, leading to attractive ionic interactions with cationic species or moieties and repulsive electrostatic interactions with anionic species or moieties. Under current ACN-rich eluents, all analytes regardless of their charge character showed increased retention factors when the mobile phase pH was elevated from 4.5 to 6.5 (Fig. 5). This trend follows roughly the increasing dissociation degree of residual silanols between pH 4 and 6. With increased number of dissociated silanols the surface becomes more polar causing stronger HILIC retention. The 2-pyridylurea ligand seems to have only minor modulating effect.

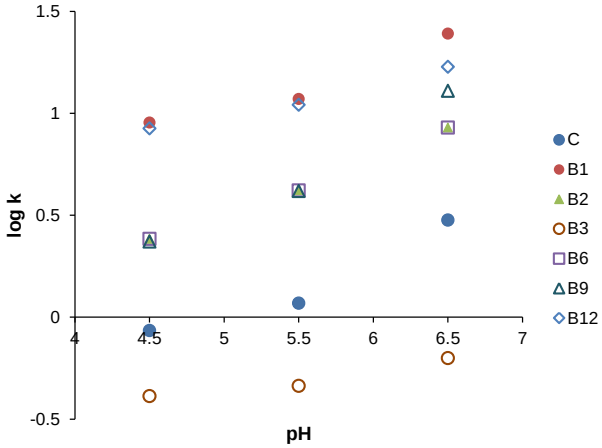

Fig. 5: Effect of the mobile phase pH on log *k* values on the 2-pyridylurea-modified mixed-mode stationary phase under HILIC conditions (95% ACN, 5 mM ammonium acetate).

4.3.4.2.3. Variation of Buffer Concentration

To illustrate the extent of ionic interactions, the buffer concentration in the eluent was varied (Fig. 6). The trends are given by plots of log *k* vs log buffer (ammonium acetate) concentration (in accordance to the stoichiometric displacement model). Such plots should give a linear trend line with negative slope for compounds with attractive ionic interactions (here at pH 4.5 anion exchange for acidic compounds) while the slope is expected to be positive for compounds for which repulsive ionic interactions are dominating (at pH 4.5 net positively charged analytes). Strong silanol interactions may mask the effect of the chromatographic ligand.

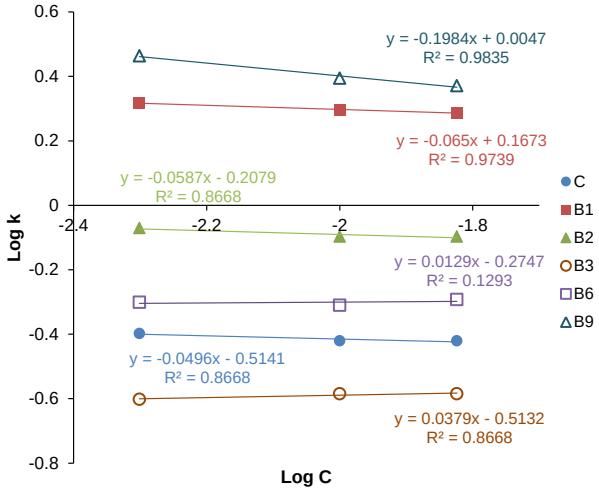

Fig. 6: Effect of ionic strength (log C) on retention factors (log *k*) in accordance to the stoichiometric displacement model (85% ACN, pH 4.5).

It can be seen that folic acid (B_9) is the only compound with a significant anion-exchange contribution (negative slope of ca. − 0.2; corresponds to the effective charge ratio of analyte and counterion). B_1, B_2 and C also reveal a slightly negatively charged slope (ca. − 0.1). While

this is understandable for ascorbic acid for which anion-exchange process can be expected, for B_1 (thiamine) it is more likely due to cation-exchange at the silanols. For the other compounds (B_3 and B_6), slightly positive slopes are observed and can be explained by absence of strong ionic interactions or very weak repulsive electrostatic interactions. Overall, this stationary phase imposes only soft ionic interactions on the given analytes and is mainly driven by HILIC retention mechanism under the selected conditions.

4.3.4.3. ^{1}D and ^{2}D Gradient Optimization

From above screening experiments and DoE study, useful conditions for the design of a selective comprehensive 2D-LC separation, which was found to be most promising solution to solve this problem of the simultaneous analysis of water- and fat-soluble vitamins, could be identified. Some further optimizations were then carried out for ^{1}D and ^{2}D gradients.

For the ^{1}D-HILIC gradient separation, gradient time, gradient steepness, and mixed buffer–acetonitrile gradients were tested as variables for optimization of the resolution of the water-soluble vitamins. The results are given in supplementary material (supplementary Fig. S9 to Fig. S11). Full baseline separation could be achieved when the ^{1}D gradient time was at least 10 min or larger (Suppl. Fig. S9) and gradient steepness was at least 35%B in 10 min (with initial %B always 5%, $t_G = 10$ min) (Suppl. Fig. S10). The effect of a superimposed buffer gradient upon the acetonitrile gradient was minor (Suppl. Fig. S11). For the water-soluble vitamins, an optimized HILIC separation with a full baseline separation could be achieved under the conditions shown in Fig. 7a.

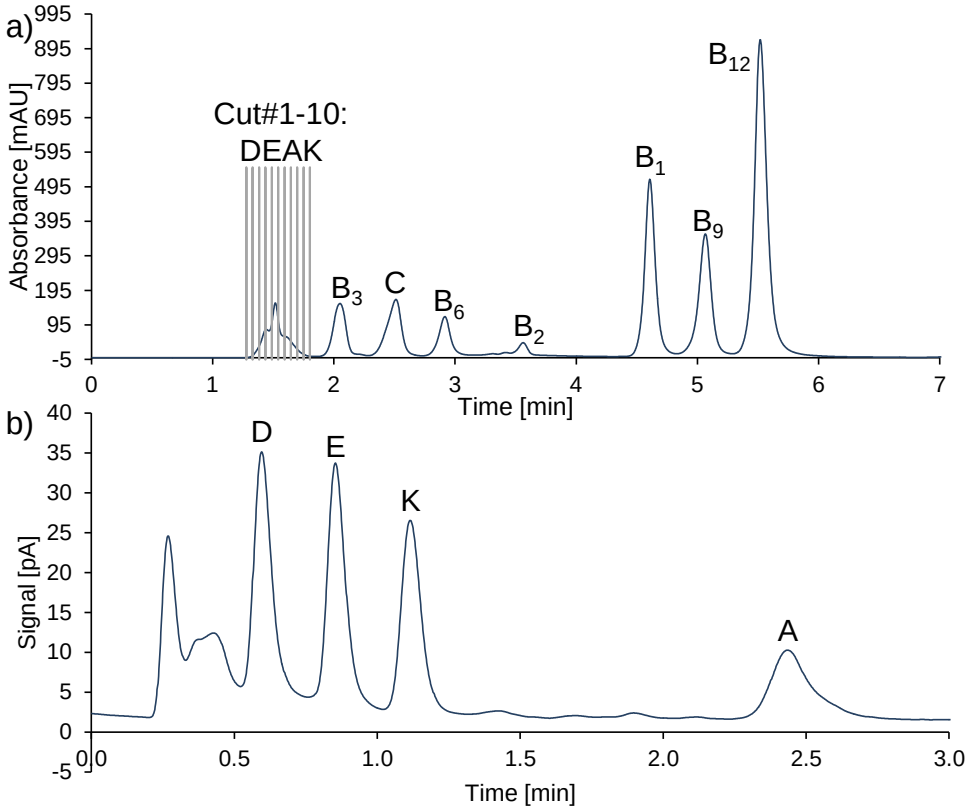

Fig. 7: Optimized [1]D (**a**) and [2]D (**b**) chromatograms of fat- and water-soluble vitamins. The cuts indicate the eluents of fat-soluble vitamins which were transferred to [2]D via high-resolution sampling. **a**[1]D: 2-pyridylurea-modified stationary phase, 5 µm, 100 Å, 150 × 4.6 mm; mobile phases: A: 30% ACN, 15 mM NH_4Ac in total, pH 4.5; B: 95% ACN, 15 mM NH_4Ac in total, pH 4.5; gradient: 100 to 0% B in 10 min, 2 min 0% B, 8 min re-equilibration 100% B, Inj. vol.: 10 µL; flow rate: 1.0 mL/min; 25 °C; 270 nm. **b**[2]D: column: Kinetex® 2.6 µm C8, 100 Å, 50 × 2.1 mm; mobile phase: ACN:H_2O (85:15, v/v), 0.1% FA, 1.0 mL/min; 60 °C; detection, CAD (charged aerosol detector); injection, 10 µL mixture of fat-soluble vitamins (note, in the final 2D-LC method isocratic conditions with slightly lower organic content, i.e., 80%B were used to shift the first peak farther away from t_0).

The early eluted fat-soluble vitamins were then separated in the [2]D by RPLC using a high-resolution sampling approach, also called selective comprehensive HILIC × RPLC. Since the fat-soluble vitamins differ sufficiently in their lipophilicity (log P values are listed in Table 1), the level of hydrophobic interactions occurring on a C8 phase is well suited for the baseline separation under optimized conditions. The goal of the optimization was therefore to accelerate the separations and keep the [2]D run time as short as possible. One has to consider that the [2]D runs of the various cuts are performed serially and therefore cumulatively contribute to the entire analysis time (see Electronic Supplementary Material Fig. S14). The speed at which the [2]D separation can be performed is therefore decisive for the overall analysis time.

A core–shell particle C8 column was therefore used because they allow faster separations as compared to sub-2 µm C8 columns of the same dimension. As a further optimization parameter, temperature was investigated. Suppl. Fig. S12 depicts chromatograms of the mixture of the fat-soluble vitamins at two distinct temperatures, 50 and 60 °C. It can be seen that this slight increase by 10 °C has a significant influence on the speed of separation with a reduction of run time for the [2]D separation from ca. 7 to ca. 5 min. 60 °C was hence maintained

as column temperature. Various gradients (from 70, 80 or 90% B to always 97%B in 4 min with a 1-min hold at 97%B before re-equilibration; B composed of acetonitrile with 0.1% formic acid) were tested (Suppl. Fig. S13). It turned out that for fast elution the %B should be between 80 and 90%. In order to save the re-equilibration time, an isocratic ^{2}D separation column temperature of 60 °C and a flow rate of 1 mL/min were finally adopted as optimal ^{2}D separation (Fig. 7b). It allows to finish the ^{2}D separation in about 3 min, as to keep the entire analysis time acceptable (see Electronic Supplementary Material Fig. S14) (vide infra).

4.3.4.4. 2D-LC with High Resolution Sampling of Fat-Soluble Vitamins

Neither the polar mixed-mode stationary phase with 2-pyridylpropylurea ligand nor RPLC with C8 core–shell column were capable to resolve the entire mixture of fat- and water-soluble vitamins. Hence, a two-dimensional LC approach was established. Only the early part of the ^{1}D HILIC chromatogram on the 2-pyridylpropylurea mixed-mode column which contained the coeluted fat-soluble vitamins was switched into a second dimension by a comprehensive sampling of ^{1}D eluates into ^{2}D RPLC. This mode of 2D-LC is called selective comprehensive HILIC × RPLC or simply high-resolution sampling. It should be noted that with a large loop a single fraction of the lipophilic vitamins could be switched onto the RP column. However, due to severe solvent incompatibility trap columns for refocusing should be used [25]. In our proof-of-principle high-resolution sampling method, a standard 2D-UHPLC system can be used on routine basis without changing loops or the setup. An easy handling of the quantitation is also offered by the Open Lab CDS Rev. C.01.07SR3 software which allows the identification of the peaks in the cuts and automatically sums up the peak area of a single compound.

Thus, the first dimension (mixed-mode column) was coupled to a second dimension (Kinetex C8 column) by a two position 4-port dual valve which was connected to two loop decks each one equipped with six 40-µL parking loops (Fig. 8a). Of those loops, 5 can be used to sample fractions, while the 6th loop must be free for mobile phase flow. Thus, 10 cuts across the unresolved DEAK peak (Fig. 7a), each of 40 µL eluate of ^{1}D separation, starting with sampling from 1.35 min in the ^{1}D HILIC run were made and analyzed by ^{2}D RPLC. Like already expected the directly transferred ^{1}D eluent caused broadened, distorted peaks in the second dimension when 100% loop fill was adopted (Fig. 9a). This distortion effect is usually especially prominent for high injection volumes (i.e., here 40 µL) and is due to mobile phase incompatibilities of ^{1}D (HILIC) and ^{2}D (RPLC) eluents. The sampled ^{1}D mobile phase represents the sample matrix of the ^{2}D separation and the high acetonitrile content of the HILIC eluates during sampling of the ADEK peak exhibits too strong elution strength in ^{2}D RPLC, in particular for the weakly

retained analytes (D, E, and K). In contrast, the highly lipophilic and strongly retained retinol palmitate (vitamin A) seems to get refocused on the C8 phase.

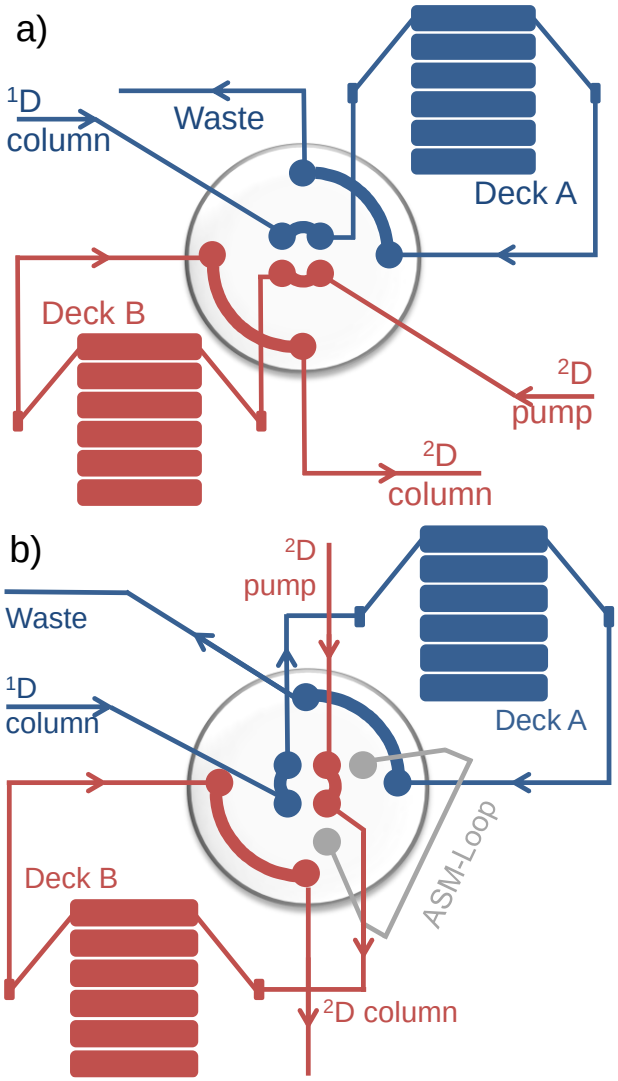

Fig. 8: Different valve types for the short time storage and transfer of the sampled first dimension into the second dimension **a** 4-port/2-position duo valve and **b** 10 port/4-position switching valve (offering the possibility for ASM) coupled to two 14-port/6-positions multiple heart cutting valves with 40-µL loops.

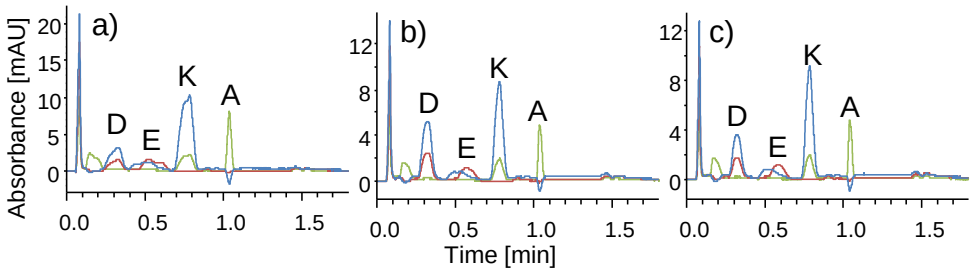

Fig. 9: Improvement of ^{2}D peak shape with decreasing loop fill level (**a** 100%, **b** 70% and **c** 60%) exemplarily shown on cut #5 of the high-resolution sampling of the HILIC × RPLC chromatographic system. ^{1}D: 2-pyridylurea-modified stationary phase, 5 µm, 100 Å, 150 × 4.6 mm; mobile phases: A: 30% ACN, 15 mM NH_4Ac in total, pH 4.5; B: 95% ACN, 15 mM NH_4Ac in total, pH 4.5; gradient: 100 to 0% B in 10 min, 2 min 0% B, 8 min re-equilibration 100% B, Inj.vol.: 10 µL; flow rate: 1.0 mL/min; column temperature, 25 °C; detection: UV 270 nm; time-based high-resolution sampling: 40 µL loops; sampling start at 1.35 min. ^{2}D: Kinetex C8, 2.6 µm, 100 Å, 50 × 2.1 mm; mobile phase: A: H_2O, 0.1% FA B: ACN, 0.1% FA; 0–0.5 min 80% B, from 0.5 to 1.0 min 80 to 97% B, from 1.0 to 1.33 min hold at 97%B, from 1.33 to 1.4 min to start conditions, then 0.3 min reequilibration. Flow rate: 2.0 mL/min; column temperature, 60 °C, detection: UV 270 nm (blue), 290 nm (red) and 325 nm (green).

The online coupling of HILIC and RPLC is a challenging exercise since mobile phase mismatch is a well-known problem [23, 24]. A number of solutions to the incompatibility problem have been suggested, e.g., trap columns for modulation [25], dilution of ^{2}D eluent with weak mobile phase using an additional pump, fixed-loop modulation [18] and others. Herein, we first tested partial loop fill which already showed limited advantageous effects on the ^{2}D peak shape [26]. We studied reduced filling levels of the parking loops from 100% to 70 and 60%. Indeed, the peak shape and peak width improved using a loop fill level of 70 and 60% exemplarily shown in the chromatograms of cut #5 in Fig. 9 (loop fill 70%, Fig. 9b and loop fill 60% in Fig. 9c). A disadvantage of this strategy was that the collection time of the peak in ^{1}D decreased leading to incomplete sampling of the peak at the rear end (100% loop fill level covers a peak width of 0.4 min, 60 and 70% only 0.24 and 0.28 min, respectively). Since the ^{1}D peak (peak width = 0.4 min) requires 100% loop fill in the first dimension (if the loop volumes are not increased) in order to avoid loss of analyte and sample disproportioning, an alternative strategy had to be used for comprehensive characterization of the fat-soluble vitamins.

Alternatively, peak focussing by an initial isocratic step at low organic modifier content of 5% B before an isocratic elution at 80% B was applied to reduce peak distortions due to mismatch of the ^{1}D sample solvent and the mobile phase. The resultant chromatograms are shown in Fig. 10c, f for cuts #3 and #7 in comparison to the chromatograms obtained with direct transfer which are depicted in Fig. 10b, e. It can be seen that the refocusing at low elution strength works well for the stronger retained analytes such as vitamin A, K and also vitamin E (Fig. 10c) but fails for early eluted vitamin D for which a peak splitting/double peak was observed (Fig. 10f).

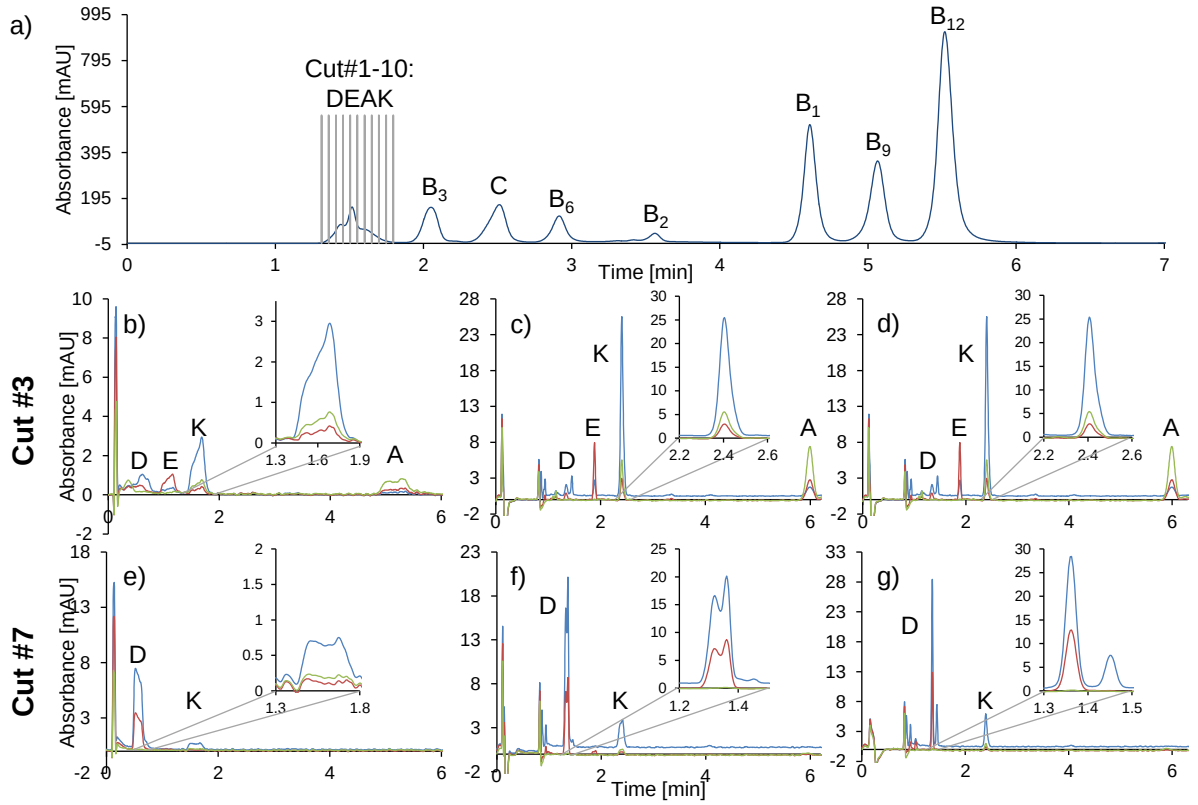

Fig. 10: Simultaneous analysis of fat- and water-soluble vitamins using time-based high-resolution sampling for comprehensive peak coverage of target analytes **a** ^{1}D chromatogram of the investigated vitamin mixture separated on the 2-pyridylurea-modified silica column (5 µm, 100 Å, 150 × 4.6 mm) under HILIC conditions and ^{2}D chromatograms [cut #3 (**b**–**d**) and #7 (**e**–**g)**] which were measured after direct transfer of the mobile phase used for elution in the second dimension (**b** and **e)**, after focusing for 0.61 min at 5% B (**c** and **f)** and after focusing 0.61 min at 5% B using active solvent modulation **d** and **g**. ^{1}D: conditions as specified in Fig. 7a. 40 µL loop; 100% loopfill (2.4 s); sampling start: 1.35 min, ^{2}D: column: Kinetex 2.6 µm C8, 100 Å, 50 × 2.1 mm; mobile phase: A: H_2O/ACN (1:4, v/v), 0.1% FA, 1.0 mL/min; 60 °C; 270 (blue), 290 (red) and 325 nm (green).

To overcome this problem, the active solvent modulation (ASM) valve (Fig. 8b) was activated and the corresponding chromatograms are given in Fig. 10d, g. The ASM valve allows four positions (Fig. 11) [18]. In Fig. 11, the valve switching beginning with the sampling in Deck A and ending with the analysis of Deck B is depicted. In Fig. 11 Pos.1a the ^{1}D eluent is transferred and sampled into the multiple heart cutting (MHC) loops of the Deck A ending with cut #5 in the sixth loop. Then the valve switches like it is shown in position 2. The new position enables on the one hand the sampling of further cuts in Deck B. On the other hand, the analysis of previously sampled cuts starts. The flow of the mobile phase of the second dimension is split in the valve. According to the installed ASM capillary (bypass capillary), the flow is divided into one part which transfers the sample from loop deck A and four parts which go through the ASM capillary, for example. Both flow streams are reunited in the valve and directed to the ^{2}D column. In this way, the cut is diluted before it is transferred to the ^{2}D column and the solvent mismatch is reduced. The number of ASM capillary flushes can be adjusted. Once the sampled volume is completely transferred, the ASM phase is finished and the valve switches to position 3 where the whole flow is led through the MHC loop. After finishing the analysis of this cut the

MHC valve switches to the other cuts (not shown) and the analysis starts in the same way with the ASM phase like already described. As soon as all the cuts stored in Deck A are analyzed, the valve switches to position 4 where the ASM phase of the last ^{1}D effluent sampled in the MHC loops starts. Afterwards, the valve returns to start position and the analysis without enabled ASM of Deck B is possible (position 1b).

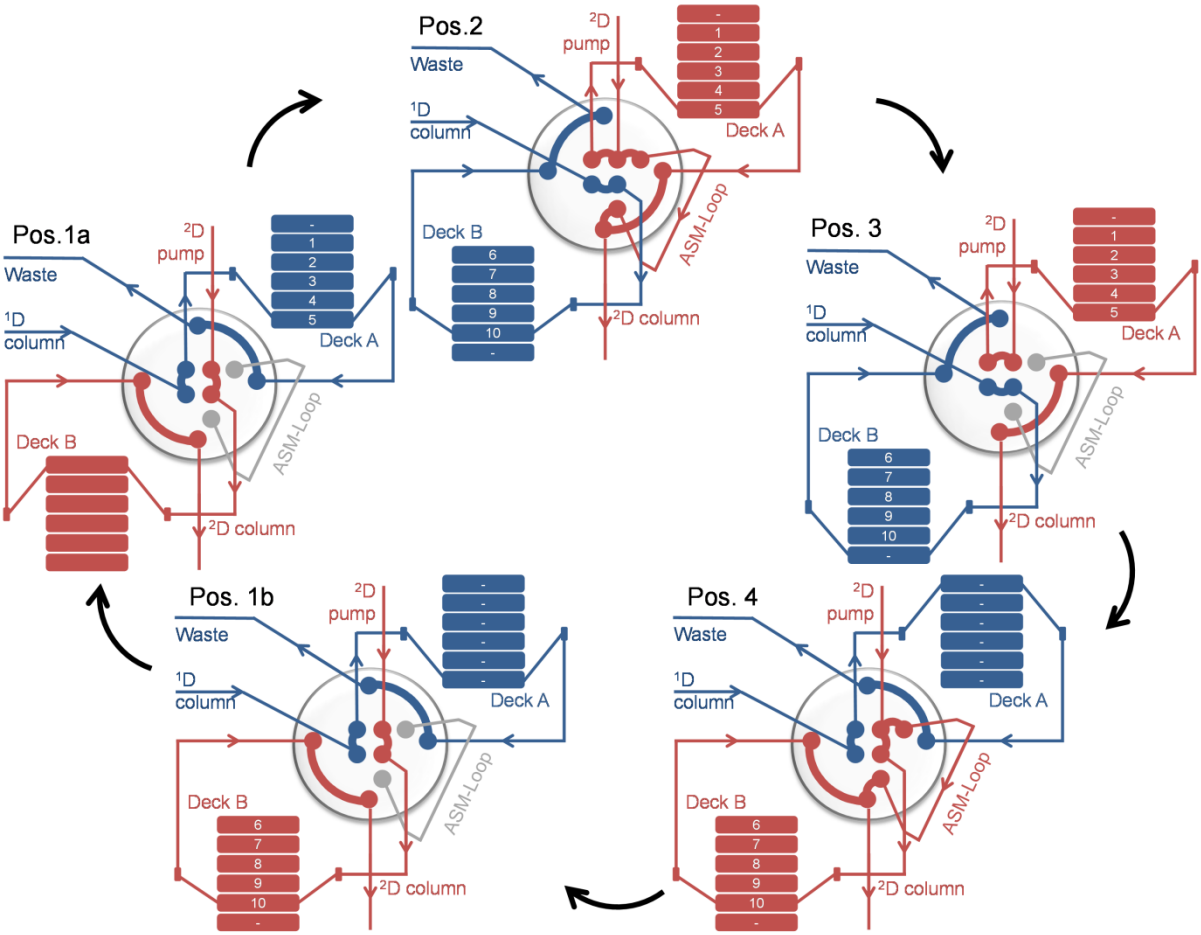

Fig. 11: Valve positions during the analysis of 10 cuts stored by high-resolution sampling with and without enabled active solvent modulation (ASM).

In general, the bypass dilutes the stored fraction before being transferred onto the ^{2}D column which gives a refocusing effect of the sample zone. The ASM factor is dependent on the installed ASM capillary. Herein, we used the smallest available ASM loop leading to the (largest) dilution factor 5. This is necessary because of the high elution strength of the composition of the ^{1}D eluent under RP conditions used in ^{2}D, as well as the lower tolerance of high injection volumes due to the column dimension in the second dimension (50 × 2.1 mm) [18]. In consequence, the mismatch of the start conditions in the second dimension and the solvent of the sample from ^{1}D decreases. In cut #3 vitamin A showed no further improvement

in efficiency (see Electronic Supplementary Material Table S2) by using the ASM valve (plate number N = 11,500) as compared to gradient refocusing without ASM (N = 10,100) because it is strongly retained (cf. Fig. 10d vs c). The same was observed for vitamin E. Vitamin K exhibits slightly higher efficiency with ASM in cut #3 (Electronic Supplementary Material Table S2). Finally, Vitamin D peak shape and efficiency was greatly improved and turned into a symmetric Gaussian peak with ASM (Electronic Supplementary Material Table S2). Additionally, the vitamin A peak was completely separated into a main peak and a peak of an impurity/degradation product in cut #7 with ASM (see different UV spectra shown in Electronic Supplementary Material Fig. S15) while only a shoulder was observed by gradient refocusing (cf Fig. 10g vs Fig. 10f). Overall, the positive effect of ASM is striking and can lead to significantly improved separations when HILIC is coupled to RPLC in 2D-LC high-resolution sampling.

The chromatographic traces of the cuts #1–10 from the high-resolution sampling can be reconstituted into a comprehensive chromatogram using LC×LC-image software (Fig. 12). Comparing the contour plots in Fig. 12b–d, it becomes clearly evident that the zones in Fig. 12c (gradient refocusing) and Fig. 12d (ASM) are sharp while they are extremely broad in Fig. 12b (direct transfer of HILIC fractions). In the contour plots of Fig. 12d, wavelength 270 nm, two peaks emerge with ASM which are not separated in the corresponding UV trace of Fig. 12c (gradient refocusing), underlining the advantage of ASM. Vitamin D is the first eluted of the two zones.

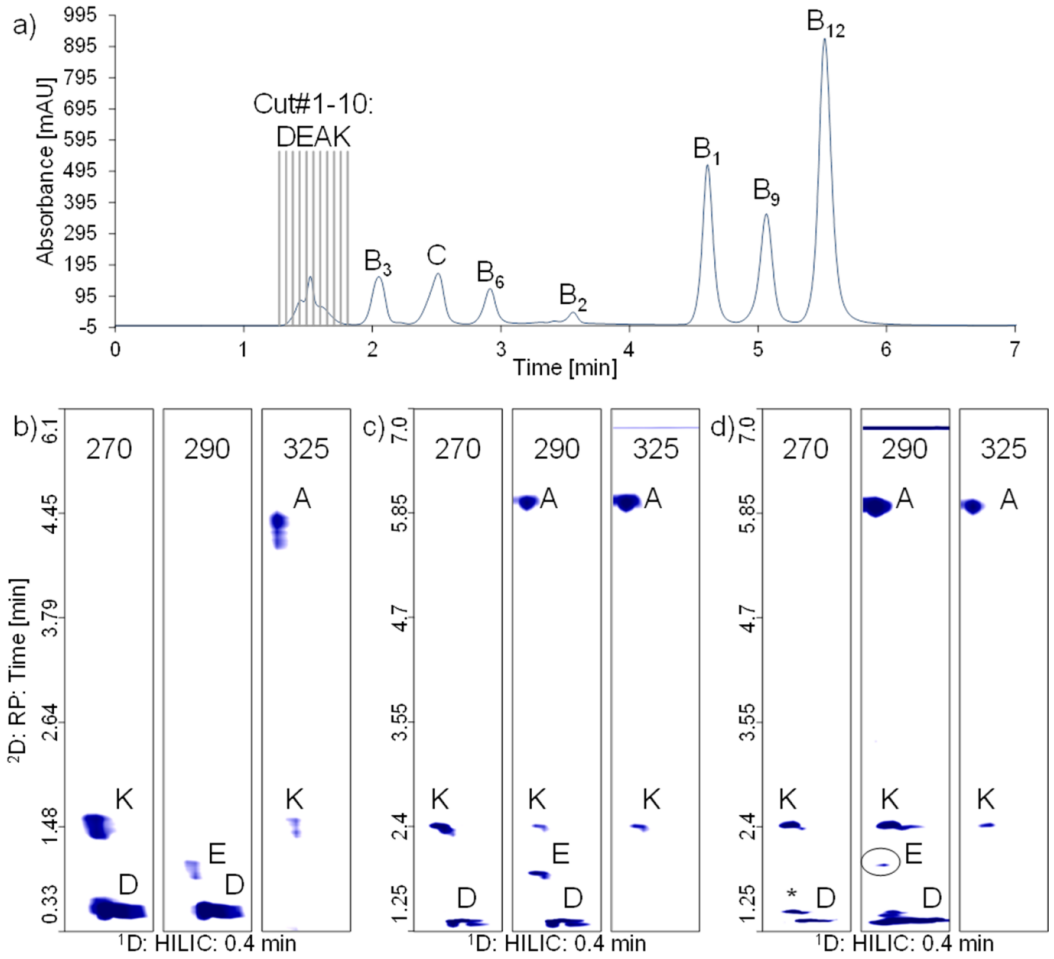

Fig. 12: Simultaneous analysis of fat- and water-soluble vitamins using time-based high-resolution sampling for comprehensive peak coverage of targeted analytes **a** ^{1}D chromatogram of the investigated vitamin mixture separated on the 2-pyridylurea column (5 µm, 100 Å, 150 × 4.6 mm) under HILIC conditions and the ^{2}D signal of the transferred fractions visualized with LC x LC software detected **b** after direct transfer, **c** after 0.61 min focusing at 5% B and **d** 0.61% at 5% B using active solvent modulation. Experimental conditions, same as specified in Fig. 10.

4.3.5. Conclusions

A selective comprehensive 2D-LC with a 2-pyridylurea-modified silica stationary phase operated in the HILIC mode in the first dimension and a RP C8 core–shell column in the second dimension allowed the simultaneous separation of fat- and water-soluble vitamins in a single analysis. The HILIC separation in ^{1}D enabled a baseline resolution of all water-soluble vitamins and the ^{2}D separation by RP C8 of all fat-soluble vitamins. The two separation modes were coupled to get a full separation of all analytes. Since only the fat-soluble vitamins remained unresolved in the ^{1}D, only the region of the chromatogram close to the void where the fat-soluble vitamins eluted was comprehensively sampled into the ^{2}D (high-resolution sampling, selective comprehensive 2DLC). Upon direct transfer of the collected ^{1}D-HILIC fractions into the ^{2}D-RPLC column, peaks were distorted and broad due to mobile phase incompatibility. Gradient refocusing starting the 2D gradient with very low modifier content has led to refocusing of the zones of late eluting peaks while early ones were still broad with some loss in resolution as exemplified for vitamin D. Using active solvent modulation, this problem could be solved and all peaks showed good peak shape and optimal resolution. 2D-LC hyphenating HILIC and RPLC is therefore a good option for the simultaneous separation of fat- and water-soluble vitamins. The method should be also applicable to quantitative analysis of vitamins in multivitamin supplements. For this purpose, like for the analysis of vitamins in food extracts or other more complex mixtures, elution conditions may need some adjustments. In this case, matrix components may coelute with the lipophilic components in the ^{1}D HILIC separation and will be switched into the ^{2}D where the lipophilic analytes can be resolved from matrix components. This is the topic of ongoing studies.

Acknowledgements: ML is grateful to Agilent Technologies for financial support through an Agilent Research Award. Stephan Buckenmaier (Agilent Technologies, Waldbronn, Germany) is gratefully acknowledged for technical support.

Funding: This study was funded by an Agilent Technologies Research Award (grant number Agilent Research Gift #4068).

Compliance with Ethical Standards

Conflict of Interest: Author ML has received a research grant from Agilent Technologies. Other authors declare no conflict of interest.

Ethical approval: This article does not contain any studies with human participants or animals performed by any of the authors.

4.3.6. References

[1] Papadoyannis IN, Tsioni GK, Samanidou VF (1997) Simultaneous determination of nine water- and fat-soluble vitamins after SPE separation and RP-HPLC analysis in pharmaceutical preparations and biological fluids. J Liq Chromatogr Relat Technol 20(19):3203–3231. https://doi.org/10.1080/10826079708000485

[2] Moreno P, Salvado V (2000) Determination of eight water- and fat-soluble vitamins in multi-vitamin pharmaceutical formulations by high-performance liquid chromatography. J Chromatogr A 870(1 + 2):207–215. https://doi.org/10.1016/S0021-9673(99)01021-3

[3] Zbanyszek W, Buszewski B (2002) Determination of different solubility vitamins in pharmaceutical preparations. II. Methods validation. J Liq Chromatogr Relat Technol 25(8):1243–1254. https://doi.org/10.1081/JLC-120004022

[4] Buszewski B, Zbanyszek W (2002) Determination of different solubility vitamins in pharmaceutical preparations. I. HPLC column switching. J Liq Chromatogr Relat Technol 25(8):1229–1241. https://doi.org/10.1081/JLC-120004021

[5] Phinney KW, Rimmer CA, Thomas JB, Sander LC, Sharpless KE, Wise SA (2011) Isotope dilution liquid chromatography-mass spectrometry methods for fat- and water-soluble vitamins in nutritional formulations. Anal Chem (Washington, DC, U S) 83(1):92–98. https://doi.org/10.1021/ac101950r

[6] Li HB, Chen F (2001) Simultaneous determination of twelve water- and fat-soluble vitamins by high-performance liquid chromatography with diode array detection. Chromatographia 54(3):270–273. https://doi.org/10.1007/bf02492256

[7] Klejdus B, Petrlová J, Potěšil D, Adam V, Mikelová R, Vacek J, Kizek R, Kubáň V (2004) Simultaneous determination of water- and fat-soluble vitamins in pharmaceutical preparations by high-performance liquid chromatography coupled with diode array detection. Anal Chim Acta 520(1):57–67. https://doi.org/10.1016/j.aca.2004.02.027

[8] Romain D, Nazanin A, Achim S, Michael L, Wolfgang L (2011) Simultaneous separation and analysis of water- and fat-soluble vitamins on multi-modal reversed-phase weak anion exchange material by HPLC-UV. J Sep Sci 34(7):761–772. https://doi.org/10.1002/jssc.201000793 doi

[9] Gentili A, Caretti F(2013) Analysis of vitamins by liquid chromatography. In Elsevier Inc., pp 477–517. https://doi.org/10.1016/B978-0-12-415806-1.00018-8

[10] Karazniewicz-Lada M, Glowka A (2016) A review of chromatographic methods for the determination of water- and fat-soluble vitamins in biological fluids. J Sep Sci 39(1):132–148. https://doi.org/10.1002/jssc.201501038

[11] Fanali C, D'Orazio G, Fanali S, Gentili A (2017) Advanced analytical techniques for fat-soluble vitamin analysis. TrAC Trends Anal Chem 87:82–97. https://doi.org/10.1016/j.trac.2016.12.001

[12] Santos J, Mendiola JA, Oliveira MBPP, Ibanez E, Herrero M (2012) Sequential determination of fat- and water-soluble vitamins in green leafy vegetables during storage. J Chromatogr A 1261:179–188. https://doi.org/10.1016/j.chroma.2012.04.067

[13] Tayade AB, Dhar P, Kumar J, Sharma M, Chaurasia OP, Srivastava RB (2013) Sequential determination of fat- and water-soluble vitamins in *Rhodiola imbricata* root from trans-Himalaya with rapid resolution liquid chromatography/tandem mass spectrometry. Anal Chim Acta 789:65–73. https://doi.org/10.1016/j.aca.2013.05.062.

[14] Taguchi K, Fukusaki E, Bamba T (2014) Simultaneous analysis for water- and fat-soluble vitamins by a novel single chromatography technique unifying supercritical fluid chromatography and liquid chromatography. J Chromatogr A 1362:270–277. https://doi.org/10.1016/j.chroma.2014.08.003

[15] Ni X, Xing X, Cao Y, Cao G (2014) Rapid analysis of water- and fat-soluble vitamins by electrokinetic chromatography with polymeric micelle as pseudostationary phase. J Chromatogr A 1370:263–269. https://doi.org/10.1016/j.chroma.2014.10.047

[16] Stoll DR, Carr PW (2017) Two-dimensional liquid chromatography: a state of the art tutorial. Anal Chem 89(1):519–531. https://doi.org/10.1021/acs.analchem.6b03506

[17] PB WJ, GA FG, J. SP (2018) Optimizing separations in online comprehensive two-dimensional liquid chromatography. J Sep Sci 41(1):68–98. https://doi.org/10.1002/jssc.201700863 doi

[18] Stoll DR, Shoykhet K, Petersson P, Buckenmaier S (2017) Active solvent modulation: a valve-based approach to improve separation compatibility in two-dimensional liquid chromatography. Anal Chem 89(17):9260–9267. https://doi.org/10.1021/acs.analchem.7b02046

[19] Pursch M, Wegener A, Buckenmaier S (2018) Evaluation of active solvent modulation to enhance two-dimensional liquid chromatography for target analysis in polymeric matrices. J Chromatogr A 1562:78–86. https://doi.org/10.1016/j.chroma.2018.05.059

[20] Stoll DR, Harmes DC, Staples GO, Potter OG, Dammann CT, Guillarme D, Beck A (2018) Development of comprehensive online two-dimensional liquid chromatography/mass spectrometry using hydrophilic interaction and reversed-phase separations for rapid and deep profiling of therapeutic antibodies. Anal Chem 90(9):5923–5929. https://doi.org/10.1021/acs.analchem.8b00776

[21] Lämmerhofer M, Richter M, Wu J, Nogueira R, Bicker W, Lindner W (2008) Mixed-mode ion-exchangers and their comparative chromatographic characterization in reversed-phase and hydrophilic interaction chromatography elution modes. J Sep Sci 31(14):2572–2588. https://doi.org/10.1002/jssc.200800178 doi

[22] Bäurer S, Polnick S, Sánchez-Muñoz OL, Kramer M, Lämmerhofer M (2018) N-Propyl-N′-2-pyridylurea-modified silica as mixed-mode stationary phase with moderate weak anion exchange capacity and pH-dependent surface charge reversal. J Chromatogr A 1560:45–54. https://doi.org/10.1016/j.chroma.2018.05.012

[23] Jandera P, Hájek T, Česla P (2011) Effects of the gradient profile, sample volume and solvent on the separation in very fast gradients, with special attention to the second-dimension gradient in comprehensive two-dimensional liquid chromatography. J Chromatogr A 1218(15):1995–2006. https://doi.org/10.1016/j.chroma.2010.10.095

[24] Stoll DR, O'Neill K, Harmes DC (2015) Effects of pH mismatch between the two dimensions of reversed-phase × reversed-phase two-dimensional separations on second dimension separation quality for ionogenic compounds—I. Carboxylic acids. J Chromatogr A 1383:25–34. https://doi.org/10.1016/j.chroma.2014.12.054

[25] Gargano AFG, Duffin M, Navarro P, Schoenmakers PJ (2016) Reducing dilution and analysis time in online comprehensive two-dimensional liquid chromatography by active modulation. Anal Chem 88(3):1785–1793. https://doi.org/10.1021/acs.analchem.5b04051

[26] Stoll DR, Sajulga RW, Voigt BN, Larson EJ, Jeong LN, Rutan SC (2017) Simulation of elution profiles in liquid chromatography—II: Investigation of injection volume overload under gradient elution conditions applied to second dimension separations in two-dimensional liquid chromatography. J Chromatogr A 1523:162–172. https://doi.org/10.1016/j.chroma.2017.07.041

4.3.7. Supplementary Material

4.3.7.1. Modeling of Responses with MODDE and Statistical Evaluation

The chromatographic data (retention factors) of the isocratic study on the influence of the various experimental factors were processed with MODDE 8.0.2 (Umetrics, Umea, Sweden) using Full Factorial (3 levels) Design.

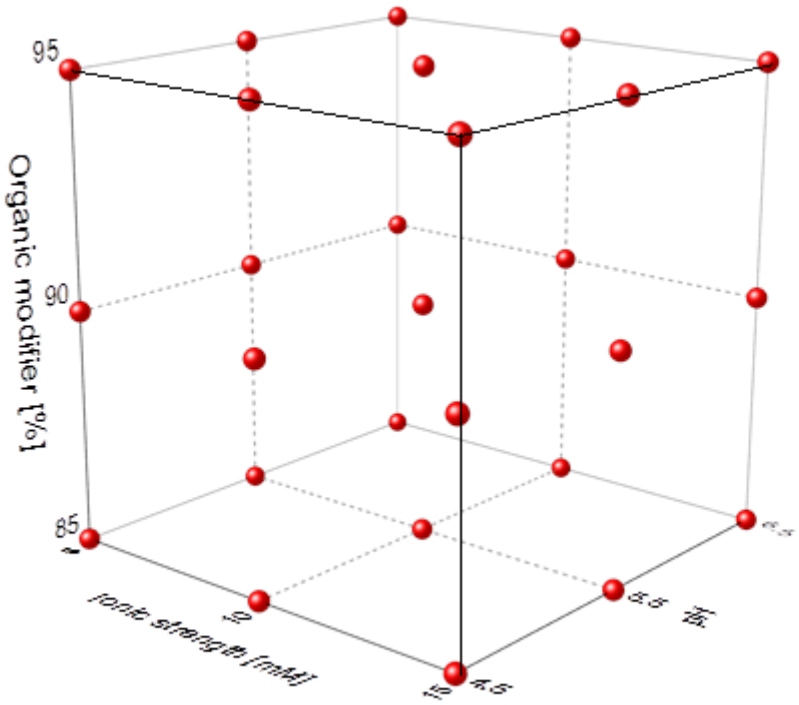

Fig. S1. Full factorial design (with 3 factors at 3-levels) used for the evaluation of the design pace under isocratic HILIC conditions.

To find out the effects of the three investigated factors (acetonitrile percentage, pH and buffer concentration) on the response, the following polynom function was used to model the response:

$$Y = b_0 + b_1X_1 + b_2X_2 + b_3X_3 + b_{11}X_1^2 + b_{22}X_2^2 + b_{33}X_3^2 + b_{12}X_1X_2 + b_{13}X_1X_3 + b_{23}X_2X_3 + b_{123}X_1X_2X_3 + \varepsilon$$

where Y is the response, Xi are the factors, including % ACN (modifier), mM NH_4Acetate (buffer) and pH, b0 is the intercept and the other bi are the coefficients, ε are the residuals.

This model was used to derive the coefficients by nonlinear curve fitting which then allowed to create contour plots.

In Table S1 the model statistics is summarized. The best model with PLS was obtained with 5 principal components. In this Table S1, R2 shows the model fit, while Q2 shows an estimate of the prediction quality, where 1 is perfect, 0 is similar predictive quality as the sample mean.

The models for retention factors B_3, B_6, C, B_2 have sufficient model fit (higher R2) and reasonable predictive quality (Q2 >0.5). The Summary List (Table S1) displays for each response also R2 Adjusted (R2 Adj.), the Standard Deviation of Y (SDY), the Residual Standard Deviation (RSD), and the number of experiments (N). As can be seen from Table S1, for the retention factors of B_1 and B_9 no model with a good fit could be obtained (R2 <0.9 and Q2 < 0.5) and therefore these models are discarded and not further discussed.

Table S1: Summary of multivariate optimization (PLS; optimal number of components, 5)

k	R2	R2 Adj	Q2	SDY	RSD	N
B_3	0.95990	0.93484	0.68202	0.12032	0.03071	27
B_6	0.97361	0.95711	0.79089	0.43893	0.09090	27
C	0.93547	0.89514	0.74720	0.71367	0.23111	27
B_2	0.95470	0.92638	0.68067	0.21173	0.57449	27
B_1	0.61677	0.37725	0.37911	0.79804	6.29774	27
B_9	0.49018	0.17154	0.18761	0.65098	5.92522	27

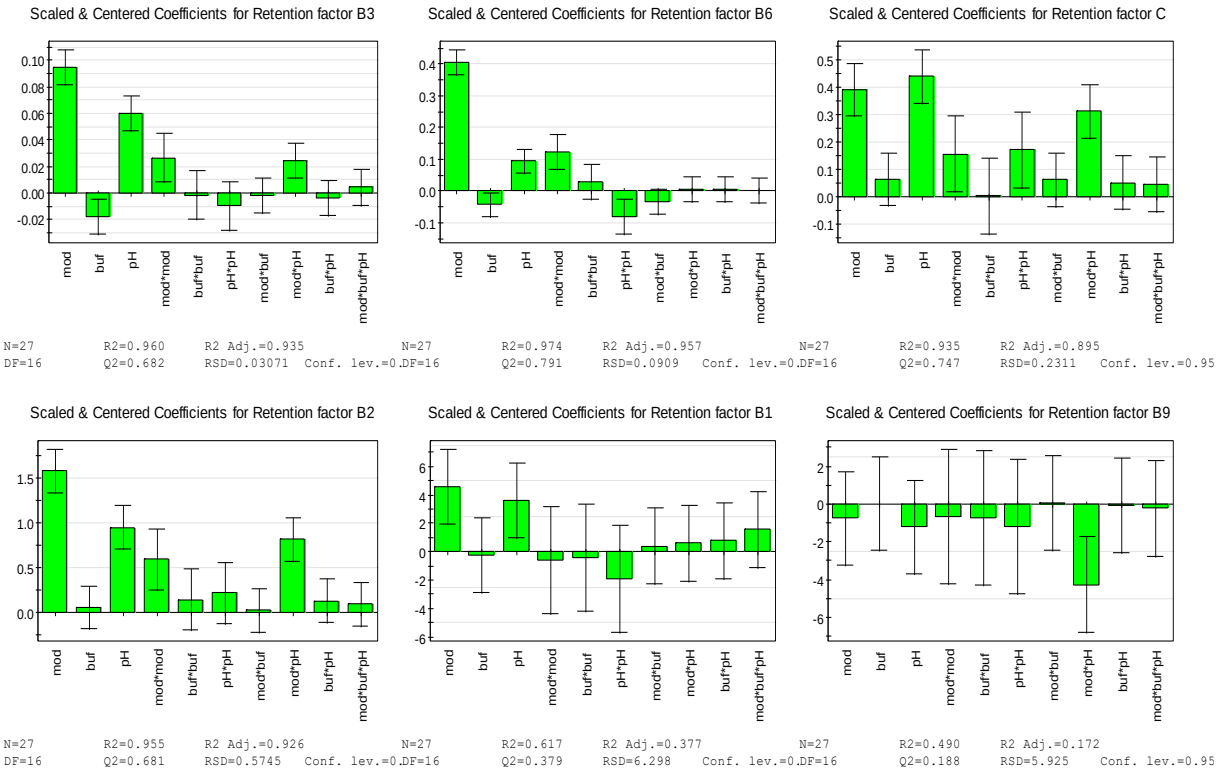

Fig. S2: Coefficient plots for retention factors (error bars are 95% confidence intervals).

Fig. S2 depicts the coefficient plots (scaled and centered coefficients with 95% confidence intervals as error bars), which illustrate the significance of the model terms. The most significant term for retention factors of vitamin B_3, B_6, and B_2 was the % ACN, for retention factor of vitamin C is pH. From error bars being larger than the respective coefficient, it can be derived that this term is not significant.

4.3.7.1.1. Contour Plots

The contour plots can be used to predict the response values. They show how retention factors *k* vary by the selected two factors while the third factor is kept constant. The dark regions (red) identify higher retention. It can be observed that at high pH and high modifier content a maximum retention factor for vitamin B_3, B_6, C, and B_2 is obtained. In addition, it seems that changing the buffer concentration has little effect on the retention for these vitamins.

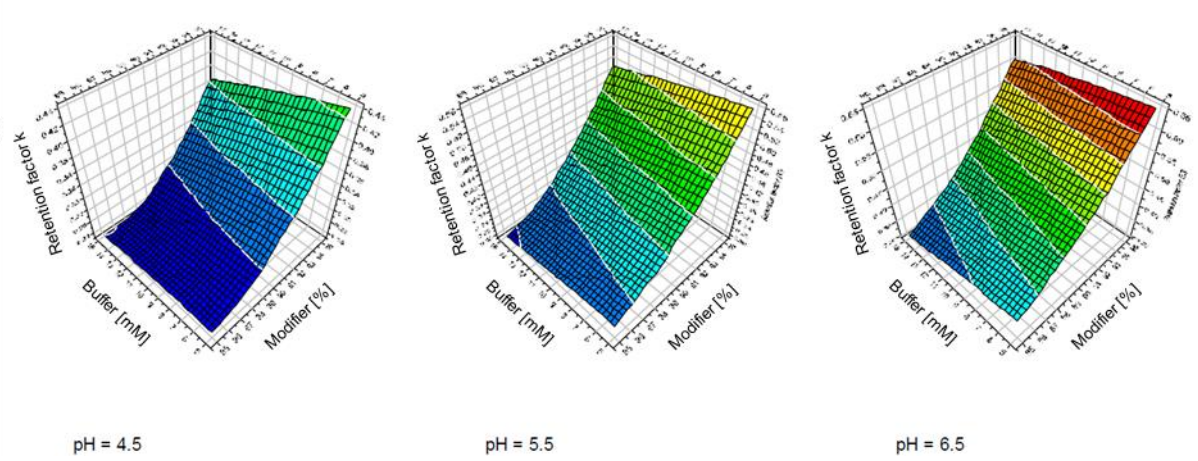

Fig. S3: Contour plots of retention factor for vitamin B_3 with respect to buffer concentration and percentage of modifier, where pH was held at 4.5, 5.5, 6.5 (buffer as variable to the left and modifier, i.e. acetonitrile, to the right)

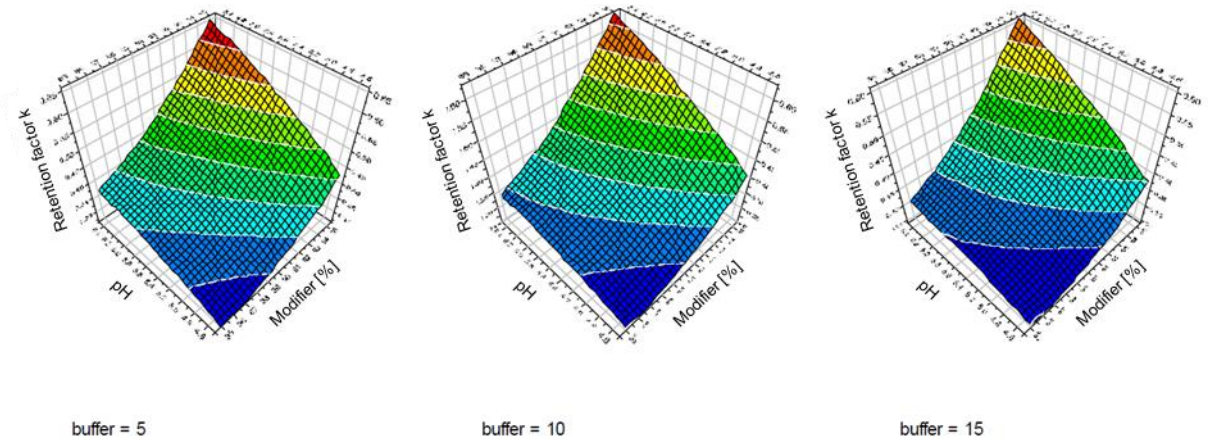

Fig. S4: Contour plots of retention factor for vitamin B_3 with respect to pH and percentage of modifier, where buffer concentration was held at 5, 10, 15mM (pH as variable to the left and modifier, i.e. acetonitrile, to the right)

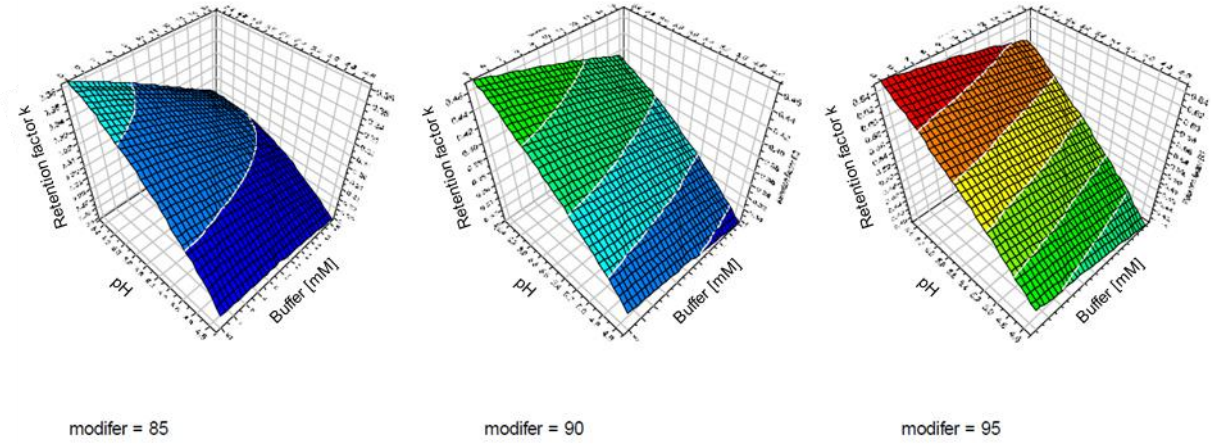

Fig. S5: Contour plots of retention factor for vitamin B_3 with respect to pH and buffer concentration, where percentage of modifier was held at 85, 90, 95% (pH as variable to the left and buffer to the right)

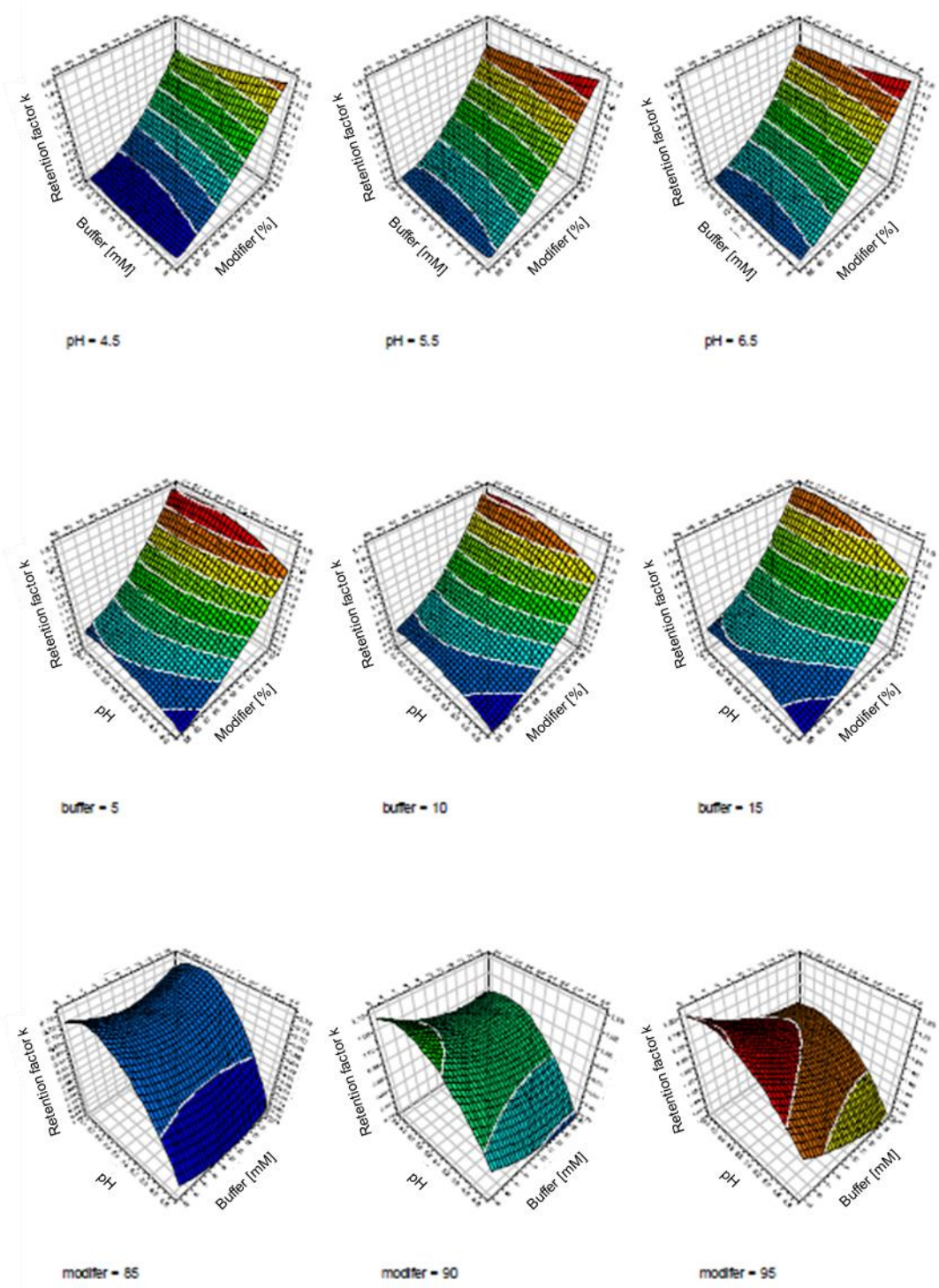

Fig. S6: Contour plots of retention factor for vitamin B_6 (top panel: buffer as variable to the left and modifier, i.e. acetonitrile, to the right; middle panel: pH as variable to the left and modifier, i.e. acetonitrile, to the right; bottom panel: pH as variable to the left and buffer to the right)

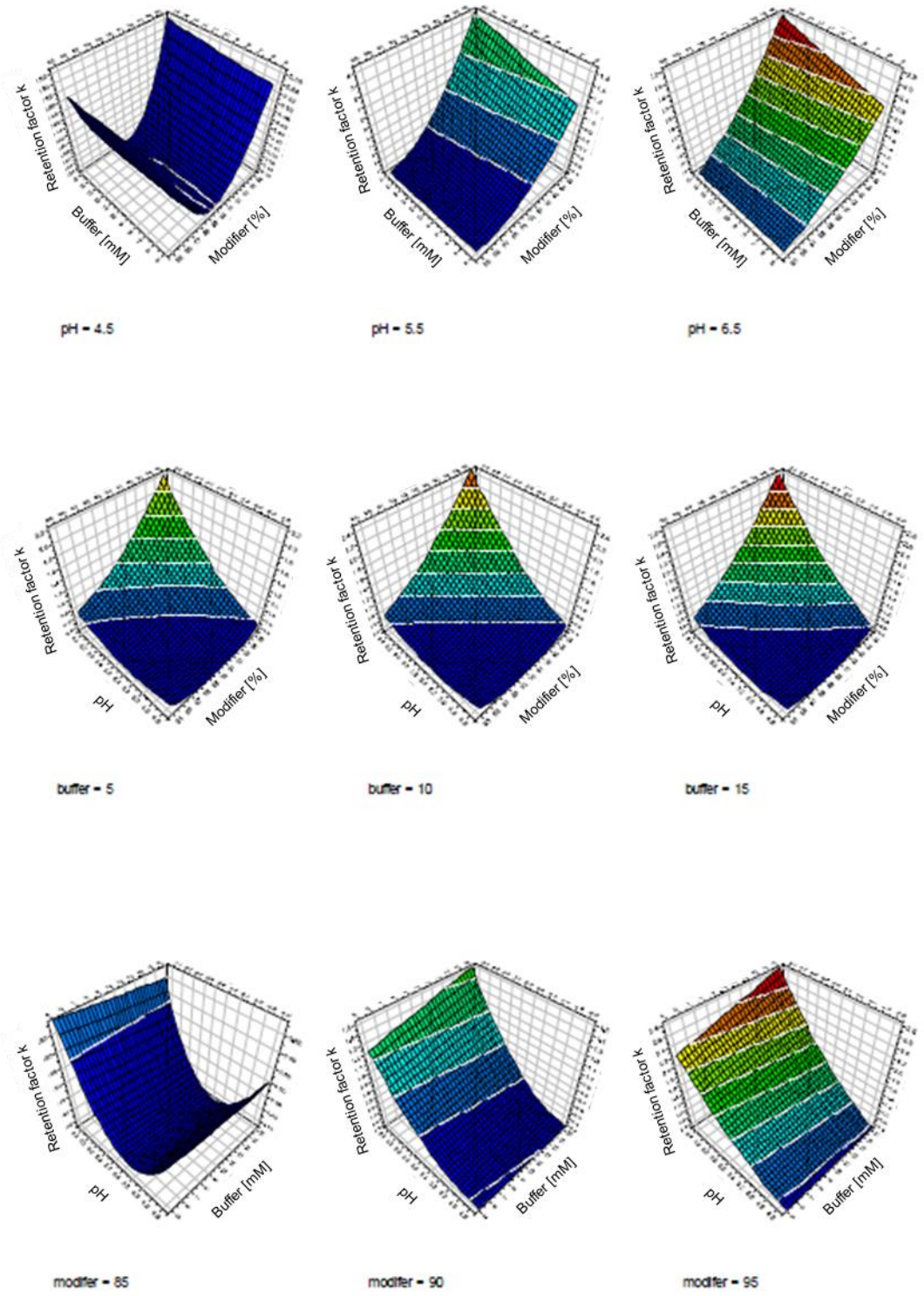

Fig. S7: Contour plots of retention factor for vitamin C (top panel: buffer as variable to the left and modifier, i.e. acetonitrile, to the right; middle panel: pH as variable to the left and modifier, i.e. acetonitrile, to the right; bottom panel: pH as variable to the left and buffer to the right)

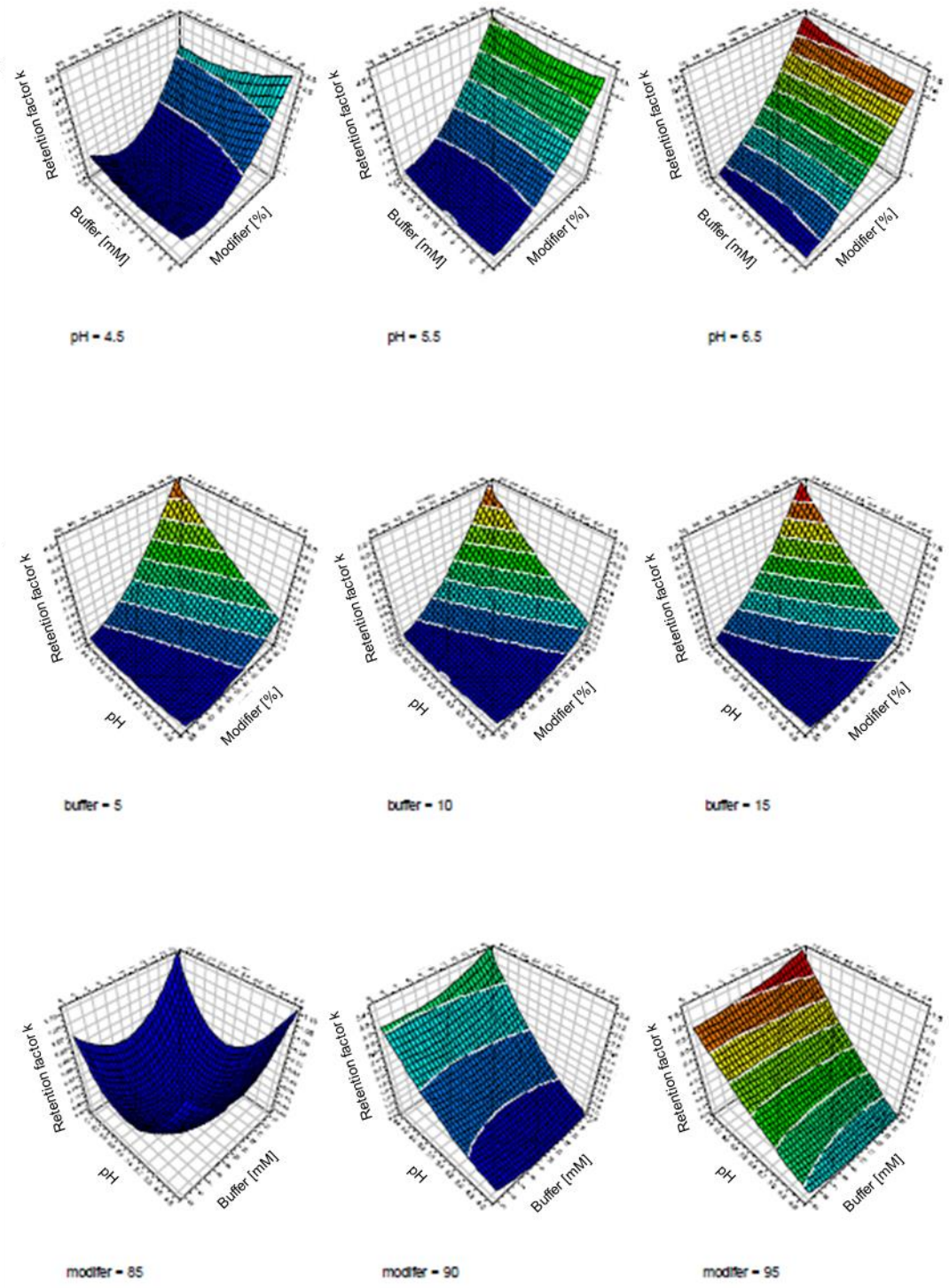

Fig. S8: Contour plots of retention factor for vitamin B_2 (top panel: buffer as variable to the left and modifier, i.e. acetonitrile, to the right; middle panel: pH as variable to the left and modifier, i.e. acetonitrile, to the right; bottom panel: pH as variable to the left and buffer to the right)

4.3.7.2. ^{1}D Gradient Optimization

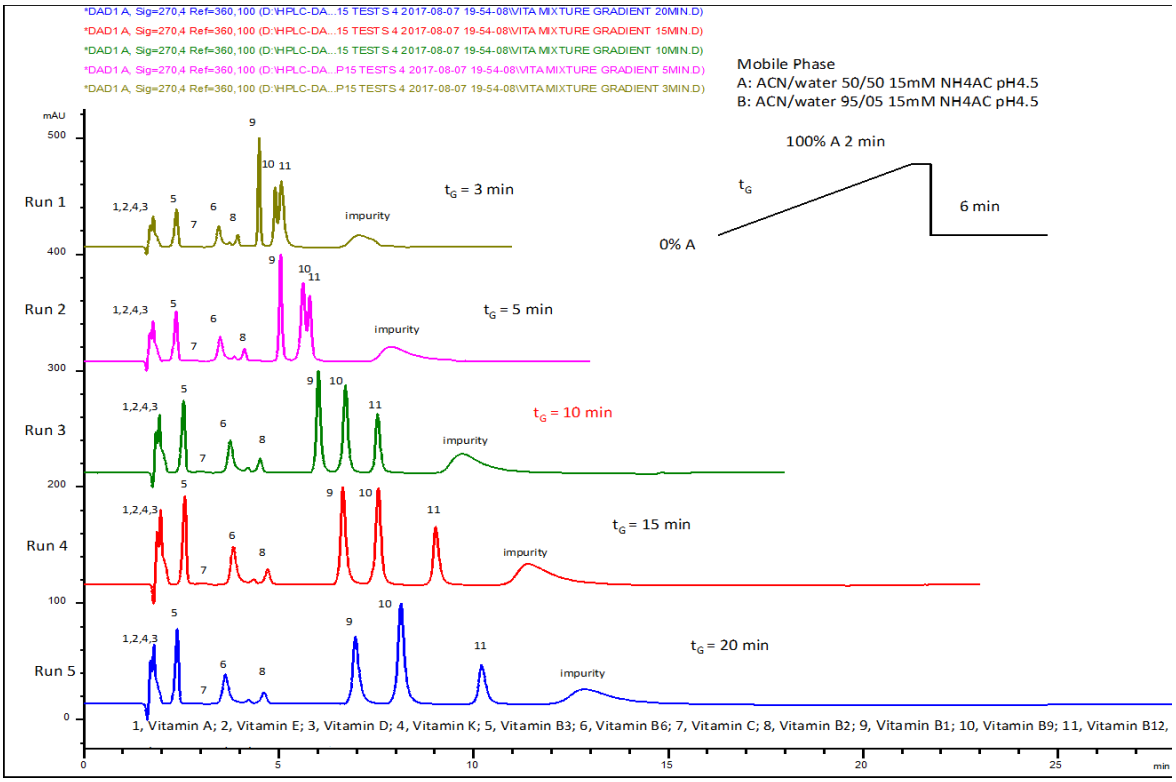

Fig. S9: Influence of the investigated HILIC gradient time on the retention and separation of the vitamins with constant pH and buffer concentration.

Experimental conditions: Mobile phase A: ACN/H_2O (1:1,v/v), 15 mM NH_4CH_3COO, apparent pH 4.5, adjusted with acetic acid, mobile phase B: ACN/H_2O (95:5,v/v), 15 mM NH_4CH_3COO, apparent pH 4.5 adjusted with acetic acid; 1 mL/min, 25 °C, 270 nm;
1, Vitamin A; 2, Vitamin E; 3, Vitamin D; 4, Vitamin K; 5, Vitamin B_3; 6, Vitamin B_6; 7, Vitamin C; 8, Vitamin B_2; 9, Vitamin B_1; 10, Vitamin B_9; 11, Vitamin B_{12}.

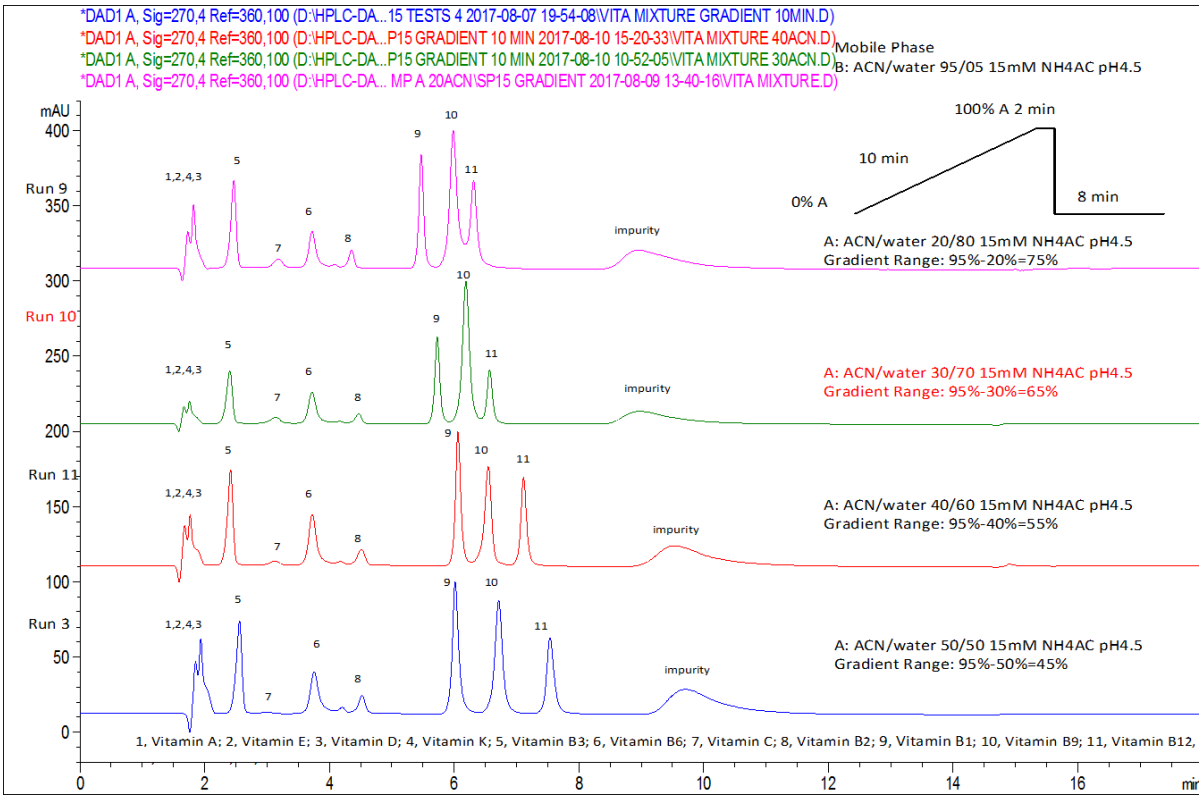

Fig. S10: Variation of the organic modifier gradient steepness and the influence on the separation of the vitamins.

Experimental conditions: Mobile phase A: pink: ACN/H_2O (2:8,v/v), green: ACN/H_2O (3:7,v/v), red: pink: ACN/H_2O (4:6,v/v), blue: pink: ACN/H_2O (5:5,v/v) 15 mM NH_4CH_3COO, apparent pH 4.5, adjusted with acetic acid, mobile phase B: ACN/H_2O (95:5,v/v), 15 mM NH_4CH_3COO, apparent pH 4.5 adjusted with acetic acid; gradient: 0-10 min 0 to 100% A, hold for 2 min 100% A followed by reequilibration for 8 min, 1.0 mL/min, 25 °C, 270 nm;
1, Vitamin A; 2, Vitamin E; 3, Vitamin D; 4, Vitamin K; 5, Vitamin B3; 6, Vitamin B_6; 7, Vitamin C; 8, Vitamin B_2; 9, Vitamin B_1; 10, Vitamin B_9; 11, Vitamin B_{12}.

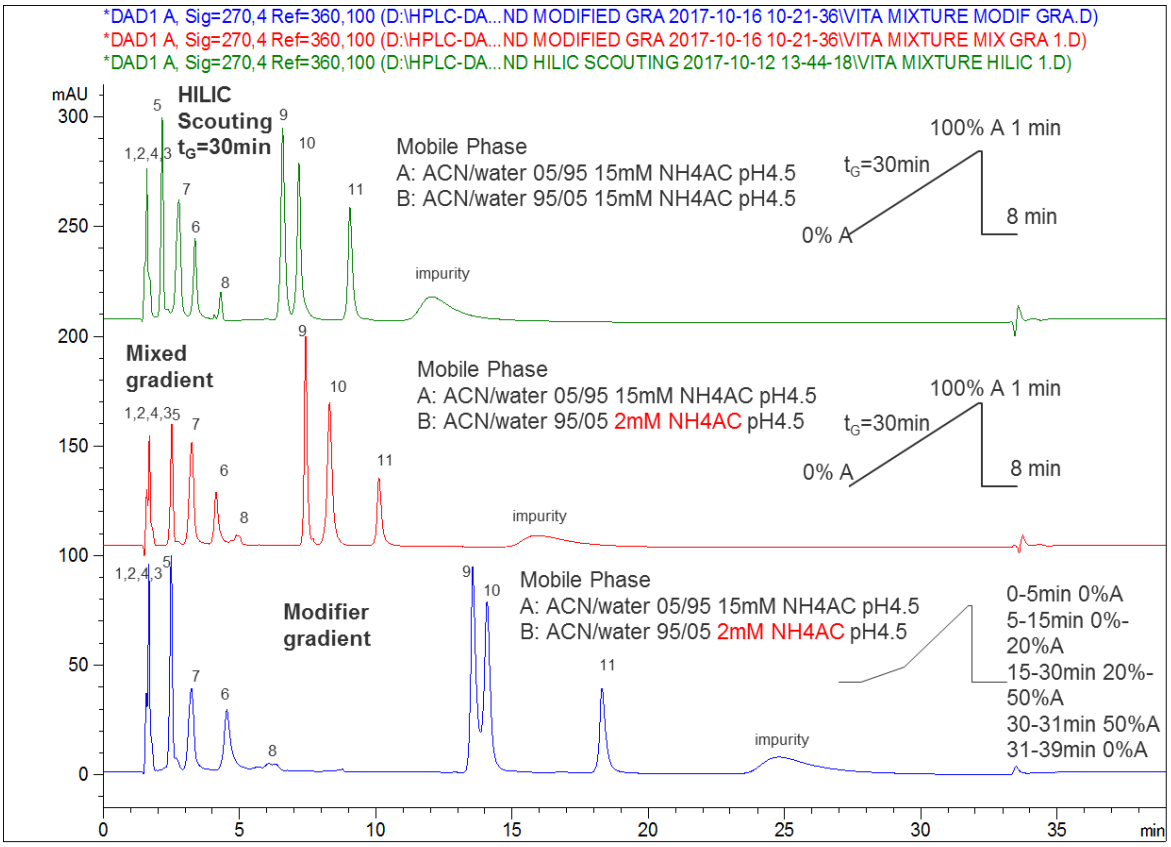

Fig. S11: Comparison of the differences in retention especially for vitamin B_1, B_9 and B_{12} using a linear organic modifier gradient (green) with a linear mixed organic modifier and buffer gradient (red) and a mixed step organic modifier and buffer gradient (blue).
Experimental conditions: Mobile phase A: ACN/H_2O (5:95,v/v), 15 mM NH_4CH_3COO, apparent pH 4.5, adjusted with acetic acid, mobile phase B: ACN/H_2O (95:5,v/v), green: 15 mM; red and blue: 2 mM NH_4CH_3COO, apparent pH 4.5 adjusted with acetic acid;
gradient: green and red: 0-30 min 0 to 100% A, hold for 1 min 100% A followed by reequilibration for 8 min; blue: 0-5 min 0% A, 5-15 min 0 to 20 % A, 15-30 min 20 to 50% A, hold for 1 min 50% A, followed by reequilibration for 8 min at 0% A, 1.0 mL/min, 25 °C, 270 nm;
1, Vitamin A; 2, Vitamin E; 3, Vitamin D; 4, Vitamin K; 5, Vitamin B_3; 6, Vitamin B_6; 7, Vitamin C; 8, Vitamin B_2; 9, Vitamin B_1; 10, Vitamin B_9; 11, Vitamin B_{12}.

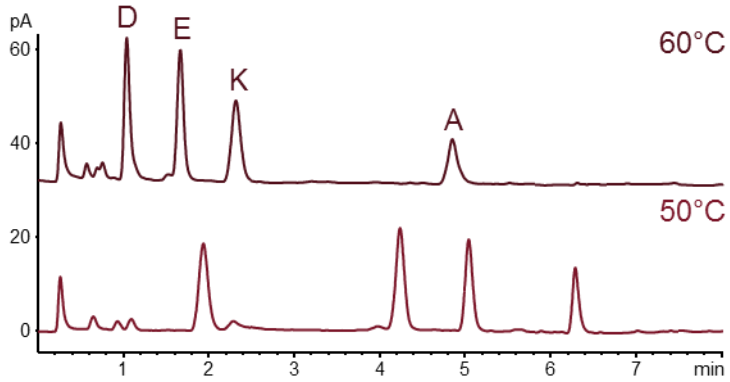

Fig. S12: Effect of temperature on ^{2}D RPLC separation on Kinetex C8 2.6 µm column (100 Å, 50 x 2.1 mm). Charged aerosol detector (CAD).

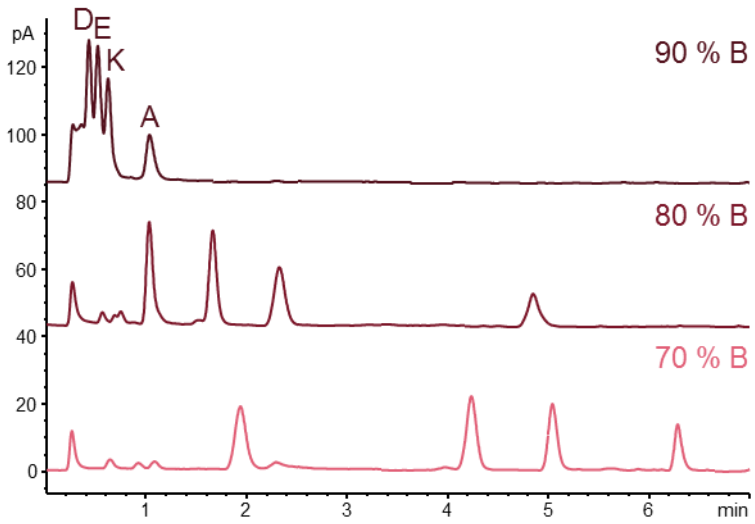

Fig. S13: Optimization of ^{2}D gradient. Agilent 1100 system; Column: Kinetex 2.6 µm C8 (100 Å, 50 x 2.1 mm); mobile phase: A: H_2O, 0.1 % FA B: ACN, 0.1 % FA; 2 min start conditions, to 97 % B in 4 min, hold 1 min, in 0.5 min to start conditions, 0.5 min reequilibration. Flow rate: 1.0 mL/min; 60°C; CAD.

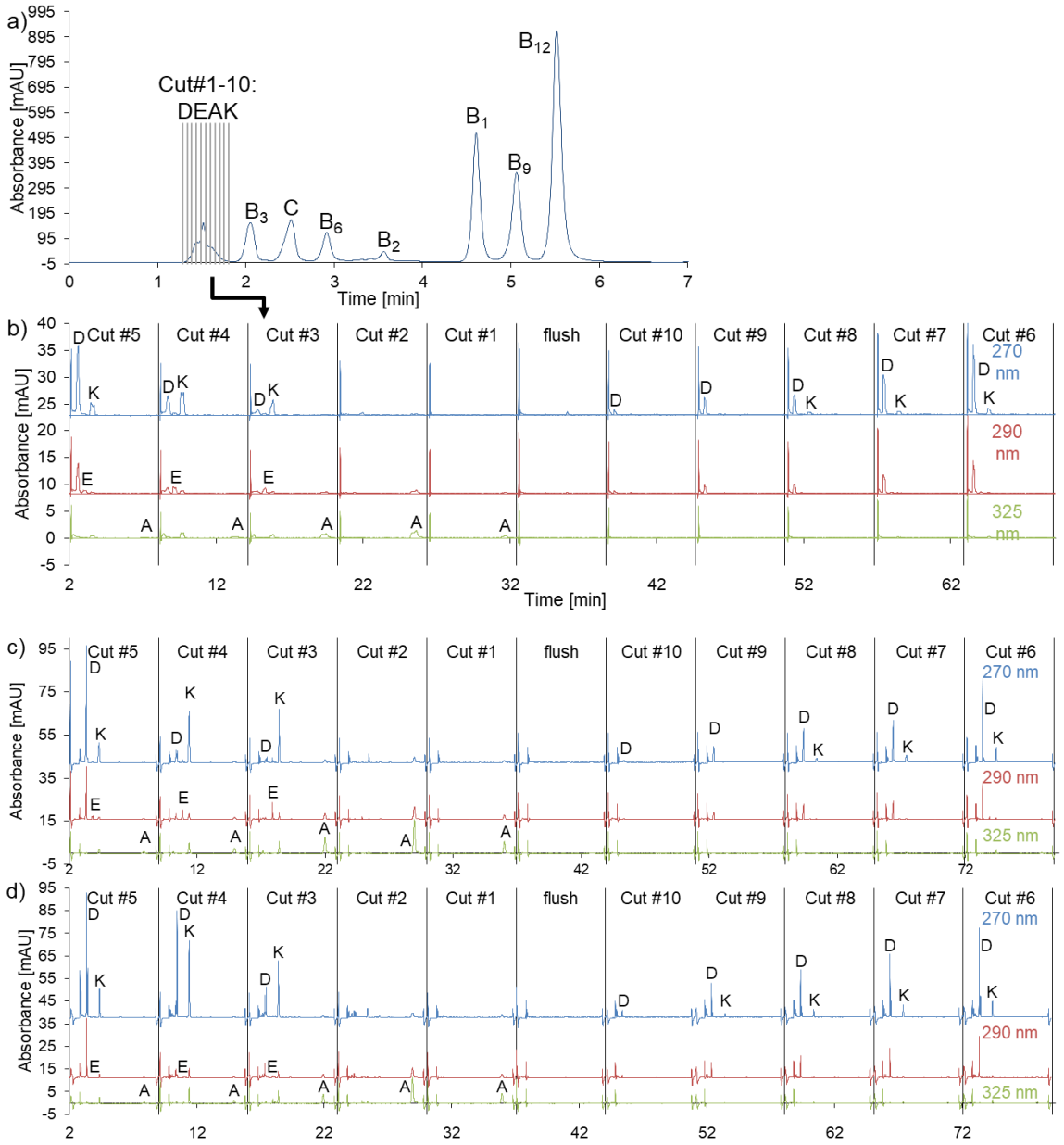

Figure S14: High Resolution Sampling of the fat-soluble vitamins which are not retained under HILIC conditions in the first dimension (a) and the UV signal of the cuts which are led directly into the second dimension (RP) (b), focussed for 0.61min at 5% ACN, 95 % H_2O, 0.1% FA in total (c) and combined focussing and transfering via active solvent modultion after high resolution sampling of the HILIC separation.

Experimental conditions: [1]D: 2-Pyridylurea stationary phase, 5µm, 100 A, 150 x 4.6 mm; mobile phases: A: 30 % ACN, 15 mM NH_4Ac in total, pH 4.5; B: 95 % ACN, 15 mM NH_4Ac in total, pH 4.5; Gradient: 100 to 0 % B in 10 min, 2 min 0 % B, 8 min reequilibration 100 % B Inj. vol.: 10µL; Flowrate: 1.0 mL/min; 25°C; 270 nm

Time based High Resolution Sampling: 40 µL Loop; sampling start: 1.35min, 100 % loopfill, ASM activated during the first 0.61 min at H_2O/ACN (95:5, v/v) , 0.1 % FA

[2]D: Column: Kinetex ® 2.6 µm C8, 100 A, 50 x 2.1 mm;
mobile phase: A mobile phase: A: H_2O/ACN (1:4, v/v) , 0.1 % FA, 1.0 mL/min; 60°C; 270, 290 and 325 nm.

4.3.7.3. Performance Evaluation of Refocusing and ASM

Table S2. Chromatographic data obtained for the three modes of modulation in the selective comprehensive HILIC × RPLC 2DLC approach.

	Vitamin	^{2}D Retention time [min]	FWHM[a] [min]	Asymmetry[b]	Symmetry[c]	N[d]	$R_{1/2}$[e]
	Cut #3						
Directly transferred	D	0.61	0.20	0.93	0.98	52	
	Unknown	Coelution with vitamin D					
	E	1.16	0.21	0.43	0.80	169	1.57[f]
	K	1.68	0.23	0.46	0.75	297	1.40
	A	5.29	0.48	0.73	0.88	674	6.00
focused	D	1.34	0.06	1.15	1.11	2776	
	Unknown	1.45	0.03	0.80	0.80	12942	1.40
	E	1.88	0.04	0.91	0.92	12277	6.37[f]
	K	2.40	0.06	1.36	1.15	8886	6.14
	A	5.99	0.14	0.90	0.94	10152	21.18
focused + ASM	D	1.34	0.03	0.91	1.08	11102	
	D*	1.97	0.03	0.73	0.95	23962	12.39
	E	1.46	0.03	0.80	0.77	13067	2.24[f]
	K	2.40	0.05	1.43	1.22	12796	13.95
	A	5.93	0.13	0.89	0.94	11527	23.12
	Cut #7						
Directly transferred	D	0.52	0.16	3.64	2.67	59	
	Unknown	Coelution with vitamin D					
	K	1.67	0.27	0.42	0.80	213	3.16
focused	D	1.36	0.08	0.33	0.70	1601	
	Unknown	Coelution with vitamin D					
	K	2.41	0.11	0.61	0.83	2653	6.50
focused + ASM	D	1.36	0.03	0.78	0.95	11385	
	Unknown	1.45	0.03	1.00	0.95	12889	1.71
	K	2.39	0.05	1.43	1.19	12690	15.24[g]

[b] FWHM = full width half maximum

[b] calculated: Asymmetry = b/a

[c] calculated: Symmetry = $(a_{0.05}+b_{0.05})/(2*a_{0.05})$

[d] calculated: N = $5.54*(t_R/FWHM)^2$

[e] calculated: R = $1.18*(t_{R2}-t_{R1})/(FWHM_1+FWHM_2))^2$

[f] Resolution between vitamin D and E

[g] Resolution between vitamin D and K

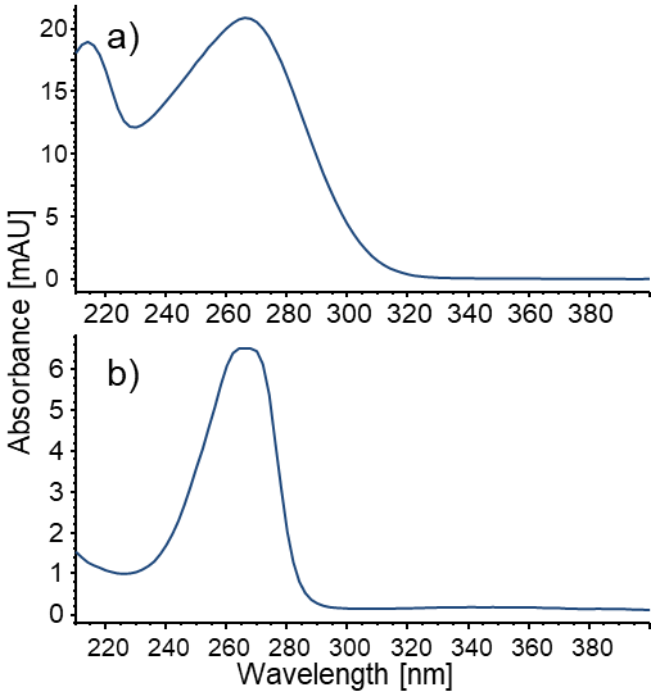

Fig. S15: UV Spectra of the two compounds that were separated using ASM before starting the analysis in the second dimension a) Vitamin D (retention time 65.922 min (complete signal)) and b) related compound (impurity) (retention time 66.011 min)

4.3.8. Corrigendum

Correction to: Simultaneous Separation of Water and Fat Soluble Vitamins by Selective Comprehensive HILIC × RPLC (High Resolution Sampling) and Active Solvent Modulation

Stefanie Bäurer [1], Wenkai Guo [1], Stefan Polnick[1], Michael Lämmerhofer [1] *

[1] Institute of Pharmaceutical Sciences, Pharmaceutical (Bio-)Analysis, University of Tübingen, Auf der Morgenstelle 8, 72076 Tübingen, Germany

Reprinted by permission from Springer Nature Customer Service Centre GmbH:
Springer Nature, Journal: Chromatographia:
Title: Correction to: Simultaneous Separation of Water and Fat Soluble Vitamins by Selective Comprehensive HILIC × RPLC (High Resolution Sampling) and Active Solvent Modulation,
S. Bäurer, W. Guo, S. Polnick, M. Lämmerhofer, Chromatographia 83 (2020) 1159.
DOI: 10.1007/s10337-020-03940-w

Correction to Chromatographia (2019) 82:167-180, https://doi.org/10.1007/s10337-018-3615-0

In this article, we depicted the structure of the investigated fat-and water-soluble vitamins in Fig. 2. Unfortunately, the published structure in Fig. 2 was vitamin K_3 (Menadione) instead of vitamin K_1 (Phytomenadione) (log P = 9.7, calculated with Marvin Sketch) which was actually used in the presented experiments.

Additionally, we want to clarify the final buffer concentration of the ^{1}D gradient method which was 15 mM ammonium acetate (pH adjusted to 4.5) as correctly stated in the respective Figure captions and the ^{2}D conditions used for the separations depicted in Fig. 10 (conditions as described in the Materials and Methods part are correct): Mobile phases: A: H_2O, 0.1% FA, B: ACN, 0.1% FA, isocratic separation at 80% B after direct transfer, focusing (5% B), and focusing (5% B) with ASM, respectively. The corresponding text is still correct.

4.4. Mixed-mode Chromatography Characteristics of Chiralpak ZWIX(+) and ZWIX(–) and Elucidation of their Chromatographic Orthogonality for LC×LC Application

*Stefanie Bäurer [a], Martina Ferri [a,b], Andrea Carotti [b], Stefan Neubauer [a], Roccaldo Sardella [b], Michael Lämmerhofer [a] **

[a] Institute of Pharmaceutical Sciences, Pharmaceutical (Bio-)Analysis, University of Tübingen, Auf der Morgenstelle 8, 72076 Tübingen, Germany

[b] Department of Pharmaceutical Sciences, University of Perugia, Via del Liceo 1, 06123 Perugia, Italy

Reprinted with permission from Analytica Chimica Acta, Volume 1093 (2020) Pages 168-179,
DOI: 10.1016/j.aca.2019.09.068

Graphical Abstract

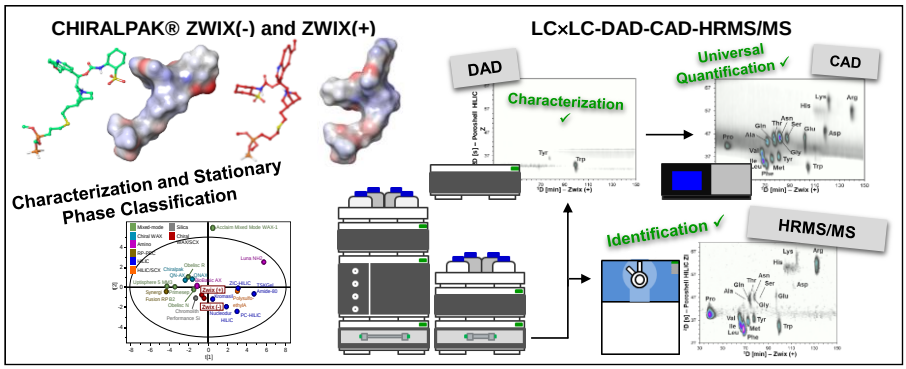

4.4.1. Abstract

Two-dimensional liquid chromatography requires orthogonal columns and/or separation principles in the first and second separation dimension. It is sometimes not straightforward to achieve. Chiral columns could expand the toolbox for 2D-LC, but are rarely exploited for this purpose, not least due to missing understanding of retention principles under non-chiral application conditions. To gain more insight, in this study Chiralpak ZWIX(+) and ZWIX(−), based on zwitterionic quinine and quinidine carbamate selectors, were carefully characterized by molecular dynamics simulations, lipophilicity/hydrophilicity measurements of selectors, pH-dependent ζ-potential determinations, and chromatographic characterization in RPLC and HILIC modes combined with unsupervised principal component analysis to extract classification of these columns in comparison to a number of commercial benchmarks (RP, HILIC and mixed-mode columns). The results showed that these chiral columns can be classified as mixed-mode chromatography phases with balanced lipophilic-hydrophilic surface character, excess of negative net charge due to sulfonic acid groups (in spite of weakly basic quinuclidine and quinoline rings), and multimodal applicability (RP, HILIC and polar organic elution modes). Orthogonality mapping in comparison to a number of modern HILIC and mixed-mode columns revealed that Poroshell HILIC-Z (with a zwitterionic ligand on 2.7 µm core-shell particles) can be beneficially combined as second dimension with the ZWIX column for comprehensive LC × LC. The online hyphenation of this 2D-LC system with complementary detection modalities including UV (DAD for chromophoric substances), charged aerosol detection (for universal detection and calibration of non-volatile analytes) and high-resolution mass spectrometry (ESI-QTOF-MS/MS for identification) provided an advanced method for comprehensive impurity profiling, applicable for instance for amino acid pharmaceutical products.

4.4.2. Introduction

Two-dimensional liquid chromatography gained recently strong impetus in the field of pharmaceuticals and biopharmaceuticals analysis as well as a number of other applications of LC including food and polymer analysis [1-10]. Its success in both maximizing effective peak capacities and providing enhanced selectivities for challenging analyte mixtures is largely related to the availability of orthogonal separations in first and second separation dimensions. The combination of two RP phases at distinct pH as well as of RPLC and HILIC modes have qualified as the most promising orthogonal separation modes in LC × LC [11]. The former combination is of advantage in terms of mobile phase compatibility upon [12-16] fraction transfer while the degree of orthogonality may be lower. The latter employs principally miscible

eluents in the two dimensions, but compatibility is seriously compromised by the fact the fraction sampled from the first dimension is a strong eluent in the second dimension leading to peak broadening, distorted peaks or even splitted peaks; the introduction of the active solvent modulation concept has relieved the problem a bit [17]. Mixed-mode chromatography [18-30] in one of the two dimensions could hold some promise as orthogonal LC mode as well but has been realized in few studies only [31]. Some researchers reported that chiral columns could be beneficially used for achiral separation problems as well [32], a strategy that is rarely considered by workers not much involved in chiral separations. In fact, since most chiral stationary phases contain both polar functionalities embedded in apolar domains they might be classified as mixed-mode phases per se in achiral applications i.e. separations not having enantiomer separations as the target focus. However, their general physicochemical properties in terms of hydrophilicity-lipophilicity balance (HLB) as well as their retention characteristics for pharmaceuticals or organic molecules in achiral applications is rarely reported in a systematic manner like is the case for RP phases [33] (e.g. based on hydrophobic subtraction model or United States Pharmacopoeia Product Quality Research Institute (USP PQRI) approach [34]). Only a few studies attempted to apply retention models to mixed-mode chromatography. However, the models were typically examined on a single MMC column [35-38], but not applied for comparison of a larger number of MMC phases. A systematic classification of mixed-mode phases [19,21] and of chiral columns regarding their mixed-mode character could widen their application range.

Along this line, we herein propose the use of two chiral columns, namely Chiralpak ZWIX(+) and Chiralpak ZWIX(−) [39] as potentially useful mixed-mode phases for achiral separations and in particular also as orthogonal separation principle in 2D-LC separations. The selectors ZWIX(+) and ZWIX(−) exhibit multiple interaction possibilities like hydrophobic moieties, polar embedded groups, a strong cation exchange site and a weak anion exchange site (see Fig. 1). The pK_a of the sulfonic acid, quinoline and quinuclidine nitrogens were calculated to be −0.97, 4.05 and 8.08, respectively (MarvinSketch 14.12.15.0, ChemAxon Ltd., Budapest, Hungary). In order to make these chiral columns more amenable for the design of 2D-LC separations, their physicochemical surface properties should be examined to allow their characterization and classification within the set of other polar RP, HILIC and commercial mixed-mode chromatography (MMC) phases. For this purpose, we adopt a molecular modelling approach to visualize the 3-dimensional structure of the chromatographic ligands indicating their binding clefts and steric interaction contributions, as well as their hydrophilic and hydrophobic surface domains. Followed is a pH-dependent lipophilicity and hydrophilicity measurement of the zwitterionic ligands by RPLC and HILIC, respectively, for the characterization of their HLB and regarding their differences with respect of the two diastereomers. Since the nominal net charge was expected to be largely zero due to positive-negative surface charge balance by mutual

compensation of anionic and cationic sites of the ligands, there was great interest in measuring the ζ-potential after immobilization of the chiral selectors on silica particles in order to figure out which is the prevailing surface charge under experimental conditions. Simple chromatographic tests were then carried out to allow for the unsupervised classification of the two chiral phases amongst a series of benchmarks (polar RP, HILIC, MMC) as outlined above by use of principal component analysis (PCA) using retention factors as independent variables. Last but not least, chromatographic orthogonalities were evaluated against a number of stationary phases of distinct classes for the LC × LC separation of amino acids. To indicate the practical utility of the resultant LC × LC method for the potential application of amino acid impurity profiling, this comprehensive two-dimensional LC method was combined with orthogonal detection modalities including UV (diode-array detector), CAD (charged aerosol detector) and high-resolution mass spectrometry (HR-MS/MS).

4.4.3. Materials and Methods

4.4.3.1. Materials

The columns Chiralpak ZWIX(+) (150 × 3 mm, 3 µm) and ZWIX(−) (150 × 4 mm, 3 µm) were obtained from Chiral Technologies (Illkirch, France). The surface structures of the silica-based zwitterionic chiral selectors are shown in Fig. 1. The Poroshell HILIC-Z column (50 × 3.0 mm, 2.7 µm) was from Agilent Technologies (Waldbronn, Germany).

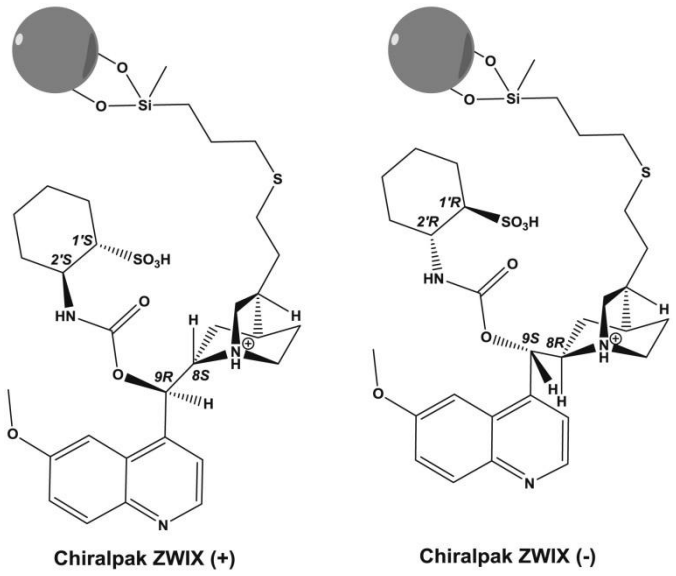

Fig. 1. Surface structure of the zwitterionic pseudo-enantiomeric stationary phases ZWIX(+) and ZWIX(−). Note, the stereochemistry is different for four out of seven asymmetric atoms. *1S*,*3R*, *4S* are identical in ZWIX(+) and ZWIX(−). Other configurations: ZWIX(+) (quinine-derived): *8S,9R,1"S,2"S*; ZWIX(−) (quinidine-derived): *8R,9S,1"R,2"R*.

Formic acid (FA), acetic acid (AA), histidine, tris-HCl, boric acid, hydrochloric acid, sodium hydroxide and potassium chloride for the determination of the ζ-potentials, as well as acetic acid, formic acid, ammonium acetate (NH_4AA), ammonium formate (NH_4FA) and ammonia used for the preparation of the mobile phases of the liquid chromatographic experiments (HPLC grade quality) were purchased from Sigma Aldrich (Merck, Munich, Germany). Acetonitrile HPLC grade (ACN) was from J.T.Baker (Deventer, Netherlands) and MS grade quality from Carl Roth (Karlsruhe, Germany). Water for HPLC and 2D-LC-DAD-CAD-MS was prepared from demineralized water by further purification using ElgaPurLab Ultra Purification system (Celle, Germany).

The analytes of the RP test butylbenzene (BuB), pentylbenzene (PeB), *N-tert*-butoxycarbonyl-prolyl-phenylalanine (Boc-Pro-Phe) and the reagents *O*,*O*-diethylthiochlorophosphate (DETCP) and triethylamine for the synthesis of *O*,*O*-diethylthiophosphate (DETP), for the

HILIC test (caffeine, theobromine, theophylline, adenosine, cytidine, guanosine, thymidine, uridine, ascorbic acid, nicotinic acid, pyridoxine, riboflavin, thiamine), the salts lithium bromide, potassium chloride, rubidium chloride and sodium chloride, as well as the void volume markers uracil, acetone and toluene were purchased from Sigma Aldrich (Munich, Germany). DETCP was hydrolyzed to DETP in the presence of an equimolar amount of triethylamine in a mixture of acetonitrile and water (75:25; v/v). Amino acids were from Sigma Aldrich and purchased from Merck.

4.4.3.2. Molecular Modelling Methods

The Maestro 11.4 graphical interface of the Schrödinger Suite 2017-4 (Schrödinger, LLC, New York, NY, 2017) was used. As reported in the previous work [40] the cubic box was built with a 30 Å side length. For a realistic reproduction of the stationary phase environment, four 3-mercaptopropyl-functionalized silanols (~1.97 mol m^{-2}), eight free silanols (~8.0 mol m^{-2}) and forty-five silicon atoms were considered for each grafted selector (SO) unit (~0.5 mol m^{-2}), at the base of the box. All the silicon atoms and their bonded hydrogen atoms in the base layer were set frozen during the molecular dynamics. A custom solvent of ACN/water (90:10; v/v) was created in house with the aid of the Packmol tool [41] and added to the simulation systems. The two simulations with the two CSP systems were performed in the canonical ensemble at 298 K. The temperature in the simulation cell was maintained constant through use of a Nosé-Hoover thermostat [42]. All the other parameters in the simulation study were left to default values in the Desmond Molecular Dynamics System (version 5.2, Schrödinger, LLC, New York, NY, 2017) present in the Schrödinger Suite 2017-4 [43-45]. A production run produced 3000 frames during the 1 μs dynamics, with an integration time of 2 fs. All the conformations of the two SOs were extracted by each frame and used to calculate three descriptors: the conformational energy of the SO (SELF-SO, in kcal mol^{-1}) to identify the energy minima, the Solvent Accessible Surface Area (SASA, in $Å^2$), the Polar Surface Area (PSA, in $Å^2$) and the Volume (in $Å^3$). The three latter surface descriptors were calculated by the Vega ZZ software [46,47].

4.4.3.3. ζ-Potential Determination by Electrophoretic Light Scattering (ELS)

The measurements of the electrophoretic mobility of the modified silica particles were carried out in a pH dependent manner with a Zetasizer NanoZS particle analyzer equipped with a Universal Dip Cell (Malvern Instruments, Herrenberg, Germany). For this purpose, modified silica particles were suspended at a concentration of 0.2 mg mL^{-1} in 10 mM KCl solutions containing 1 mM of the following buffers: formic acid/Na formate, acetic acid/Na acetate,

histidine, tris/tris-HCl, boric acid/Na-borate. The dip cell was tempered to 25 °C. The measurements were done in triplicates. The Von Smoluchowski equation was used for the calculation of the ζ-potentials.

4.4.3.4. Liquid Chromatographic Experiments

4.4.3.4.1. Instrumentation and Utilized Software

The chromatographic characterization of the ZWIX phases by 1D-LC was performed on an Agilent 1100 series LC system (Waldbronn, Germany) equipped with a degasser, quaternary pump, autosampler, thermostated column compartment and a diode array detector. In some experiments, the Agilent 1100 HPLC was coupled to a charged aerosol detector (CAD) (Corona VEO CAD, Thermo Fisher Scientific, Munich, Germany). The system was controlled, and the data was analyzed using OpenLab CDS ChemStation – Edition for LC & LC/MS System (Rev. B.04.03). The samples for the characterization under RP and HILIC conditions were analyzed on an Agilent 1290 series LC system from Agilent Technologies with the same setup except a binary pump.

The principal component analysis was done by SIMCA Multivariate Data Analysis Solution, Version 15.0.2.5959 from Sartorius Stedim Data Analytics AB (Umeå, Sweden) (level of significance: 95%, normalized in units of standard deviation, no weighting, autoscaled, centered).

The online full comprehensive 2DLC runs were performed on an Agilent 1290 Infinity II 2D-LC Solution. The first dimension (^{1}D) consisted of a flexible pump (G7104A), autosampler (G7167B) and column compartment (G7116B) followed by a pressure relief device (G4236-60010). For the coupling of ^{1}D and ^{2}D, a two-position four port dual valve with 40 µL sample loops was installed. In the second dimension (^{2}D), a high speed pump (G7120A) and a column compartment (G7116B) was used. The flow was split at the ratio of 1:11.6 using a QuickSplit Flow Splitter from ERC GmbH (Riemerling, Germany). The high flow stream was directed to a DAD (G7117B) (1 µL flow cell) connected in series (in-line) to the Corona Veo CAD, while the low flow stream was used for hyphenation to a Sciex TripleTOF 5600 + with a Duospray ion source (ESI interface). The 2D-LC system was controlled with Open Lab CDS Rev. C.01.07SR4 and the mass spectrometer with Analyst TF 1.7 software (AB Sciex, Darmstadt, Germany). The data were processed by LC-Image Version 2.7b3 LC × LC-HRMS from GC Image (Lincoln, NE, USA).

4.4.3.4.2. Chromatographic Conditions for 1D-LC

The mobile phases were prepared according to the conditions stated in the figure captions and/or in the Supplemental Material. The apparent pH ($_w^s pH$, measured in the hydro organic mixtures (s), calibrated in aqueous calibration solutions (w)) was adjusted in the final mixture. The flow rate was 1.0 mL min^{-1}, the temperature was 30 °C, the injection volume 5 µL and in case of UV detection the wavelength was 220 nm unless otherwise stated.

4.4.3.4.3. Analysis of Proteinogenic Amino Acids via LC × LC-DAD-CAD-ESI-QTOF-MS/MS

For the column screen (columns, their dimensions and suppliers are listed in Table S2), the mobile phases were a mixture of acetonitrile, water and aqueous 200 mM NH_4FA, pH 3.5 (A: 50:45:5, v/v/v; B: 90:5:5, v/v/v) except for Poroshell HILIC-Z and Chiralpak ZWIX(+) and ZWIX(−) (conditions compare Supplemental Material). After the initial holding period (for 5 min at 100% B), the linear 20 min long linear gradient from 100 to 0 %B started. After another 5 min hold at 0% B, the column was re-equilibrated for 10 min at 100 %B. The linear flow velocity was 1.18 mm s^{-1}, the thermostat was set to 40 °C, the injection volume was adjusted to the column dimension (5, 10 and 20, respectively). The ESI parameters were chosen as follows: GS1: 60 psi, GS2: 60 psi, CUR: 35 psi, ISVF 4000 V, TEM 500 °C. The QTOF was operated in positive mode (35–1000 *m*/*z*) and information-dependent acquisition (IDA) was used. A complete cycle comprised one survey scan (200 ms, CE: 5 V, DE: 100) and four product ion scans (20 ms, CE: 30 V, CES: 20 V, DE: 100) resulting in a cycle time of 330 ms.

For the online full comprehensive measurements, ZWIX(+) was used in the first dimension (^{1}D) and Poroshell HILIC-Z in the second (^{2}D). The ^{1}D mobile phases were A: H_2O, B: ACN, C: 200 mM NH_4FA/400 mM FA in MeOH/H_2O (98:2, v/v) and D: MeOH. After an initial isocratic period, the linear gradient started (organic modifier ACN: 75 to 0%, methanol: 23–78%, H_2O: 2–22% in 75 min) using a constant ionic strength (18.8 mM NH_4FA and 37.6 mM FA) at 20 °C. The detailed gradient profile regarding each channel can be found in Table S3. The injection volume was 5 µL (10 µg mL^{-1} of the proteinogenic amino acids in ACN/MeOH; 80:20, v/v). 36 µL of the ^{1}D eluent was collected per modulation and transferred into ^{2}D (cycle time: 1.2 min). In ^{2}D, the ^{1}D eluent was separated in a 0.6 min long gradient from 70 to 50% ACN at 20 mM NH_4FA, pH 3, followed by a hold period (0.1 min 50% B) and subsequently re-equilibrated for 0.3 min (detailed description can be found in the Supplemental Material). The ^{2}D effluent was split in the ratio of 1:11.6. As specified above for the column screening, the high flow stream was directed to DAD and CAD. The low flow stream was directed to the high-resolution mass spectrometer (QTOF). The settings were the same like already mentioned except for the ESI settings: GS1: 50 psi, GS2: 40 psi, CUR: 30 psi, ISVF 5500 V, TEM 450 °C.

4.4.4. Results and Discussion

4.4.4.1. Molecular Modelling

Molecular modelling can give valuable insights into 3-dimensional structural features and resultant physicochemical properties as evidenced by derived structural descriptors. Herein, it was particularly of interest to use it for the characterization/explanation of differences in hydrophilicity/lipophilicity of the two chromatographic surfaces with diastereomeric chromatographic ligands, if there are any, allowing hopefully reasonable interpretations of the retention profiles in RPLC and HILIC elution modes. Commonly employed structural descriptors such as log D fail for description of hydrophilicity/lipophilicity differences because in this concept the structural descriptor is calculated by a mere incremental approach which does not consider the 3D structure and therefore will provide identical results for stereoisomeric ligands like ZWIX(+) and ZWIX(−). To this end, structural descriptors accounting for interactive surface area, polarity and providing steric information, possibly indicating preferential binding clefts, were therefore considered to be helpful in the interpretation of the chromatographic results. Consequently, a molecular dynamics study was performed with the two distinct diastereomeric zwitterionic chromatographic ligands considering also the linker group and eight free silanols.

In order to assess the lipophilicity/hydrophilicity profile of the two zwitterionic chromatographic surfaces (Fig. 1), a conformational analysis was initially carried out. In Fig. 2 the favourable minimal energy conformations are depicted, which are to some extent different for ZWIX(−) (left, Fig. 2a) and ZWIX(+) (right; Fig. 2b), as expected for diastereomers. The mean molecular volumes were calculated for comparison, to support this claimed structural difference by a quantitative measure. Slightly different values were obtained with 668.46 ± 4.68 $Å^3$ for ZWIX(+) against 694.2 ± 4.47 $Å^3$ for ZWIX(−), respectively, indicating that the former has a slightly more compact conformations than the latter. The model also shows that the hydrophilic functionality (carbamate group) and ionic interaction sites are freely accessible for analytes. As these hydrophilic interaction sites are embedded between bulky groups they can be possibly supported (or, more in general, affected) by simultaneous hydrophobic and steric interactions, respectively, which are deemed to be favourable for a mixed-mode chromatography concept.

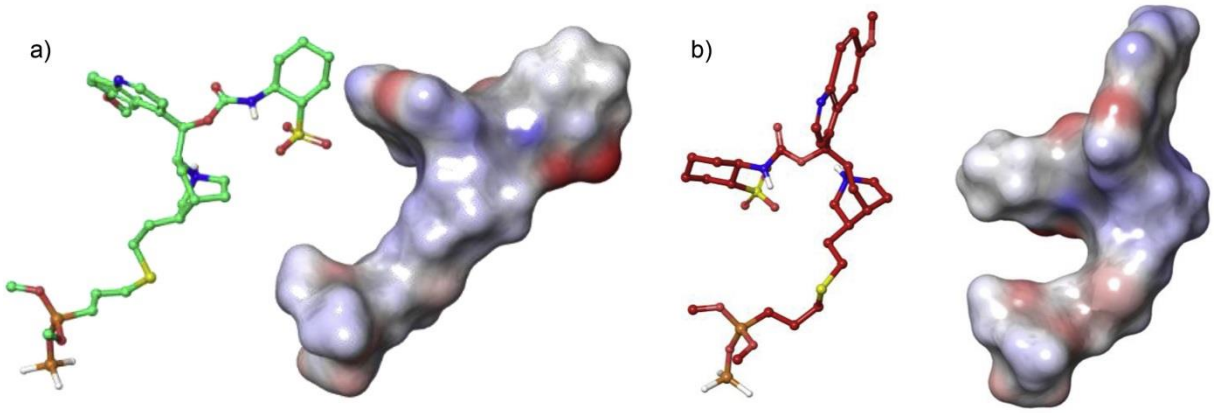

Fig. 2: Minima energy conformations of the ZWIX(+) (a) and ZWIX(−) (b) chromatographic ligands. Both selector molecules are displayed in ball and sticks and with the relative SASA. The ball and sticks are coloured with green and red carbon atoms for ZWIX(+) and ZWIX(−), respectively. ZWIX(−): SASA 1102.90 Å^2; Volume 676.98 Å^3; ZWIX(+): SASA 1124.10 Å^2; Volume 688.34 Å^3. (For interpretation of the references to colour in this figure legend, the reader is referred to the Web version of this article.)

Further information was obtained from the extent of exposure of the Polar Surface Area (PSA, in Å^2) in the two diastereomers. It was initially appraised on all the 3000 produced conformers. In this context, interested at studying the distribution of the measured PSA, intervals of 5 Å^2 were set (Fig. 3a). Interestingly, this analysis revealed negligible differences among the two diastereomers, with population values close to each other for the two diastereomeric ligands and similar distributions.

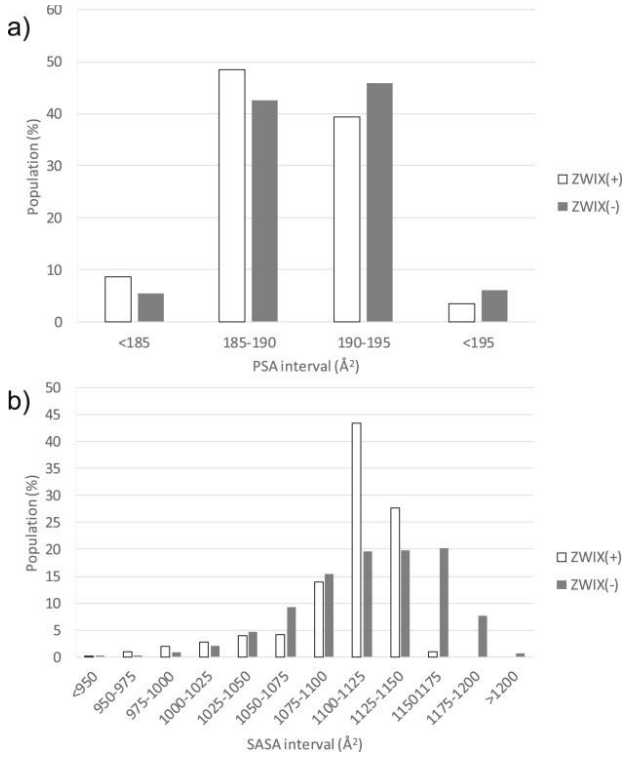

Fig. 3: a) Distribution of the PSA values (in Å^2) of the ZWIX(+) and ZWIX(−) selectors. In the y axis is reported the percentage of conformations (population) falling into a certain interval of surface values, while the ranges of polar surface area values are shown in the x axis. b) Distribution of the SASA values (in Å^2) of the ZWIX(+) and ZWIX(−) selectors. In the y axis is reported the percentage of conformations (population) falling into a certain interval of surface values, while the ranges of molecular surface area values are shown in the x axis.

Since the surface accessibility plays a significant role in chromatography, the Solvent Accessible Surface Area (SASA, in $Å^2$) was calculated as well. Smaller values were computed for the ZWIX(+) selector with respect to its ZWIX(−) diastereomer. Indeed, the former exhibits about 98% of the conformer population with SASA values < 1150 $Å^2$ while only 71.6% of conformers were classified into such categories by the latter (Fig. 3 b).

Overall, the *in silico* results revealed significant similarities and minor differences of the diastereomeric selectors. As a result of its smaller SASA and the comparable PSA, ZWIX(+) exposes a less extended hydrophobic area than ZWIX(−), thus ultimately resulting in a chromatographic ligand with a more pronounced polar feature as a whole. However, the modelling also shows that the ZWIX(−) has a more open interactive surface from which the analyte can more easily dissociate again after its binding. On contrary, ZWIX(+) appears to be more compact featuring narrower binding clefts which could be favourable for mixed-mode interactions. Driven by simultaneous attractive interactions and effective steric barriers precluding fast dissociation, it might be a more favourable mixed-mode ligand displaying generally stronger interactions.

4.4.4.2. Lipophilicity and Hydrophilicity Measurement of the Zwitterionic Selectors by RPLC and HILIC

Measurements of lipophilicity by RP-HPLC is a common strategy in drug discovery to characterize the lipophilic potential and membrane distribution of a molecule [48]. For rationalizing lipophilicity differences of ZWIX(+) and ZWIX(−) selectors and their relative propensity to allow for hydrophobic interactions in MMC, the two diastereomeric zwitterionic selectors were injected into RP C18 column under variable pH conditions (detailed experimental conditions see Suppl. Material). It can be seen in Fig. 4a that ZWIX(+) showed marginally higher retention, in general. Increased pH values lead to enhanced retention, thus increased lipophilicity, of both selectors whereas the selectivity for the selectors decreased slightly. Since the sulfonic acid is dissociated over the entire investigated pH range, the increase in retention and lipophilicity at higher pH is assumed to be largely due to the decreasing dissociation of the basic sites, i.e. quinoline (pK_a ~4.05) and quinuclidine (pK_a ~8.08). Higher buffer concentrations in the mobile phase, which may increasingly shield existing surface charges, gave the same trends (compare Supplemental Material Fig. S1).

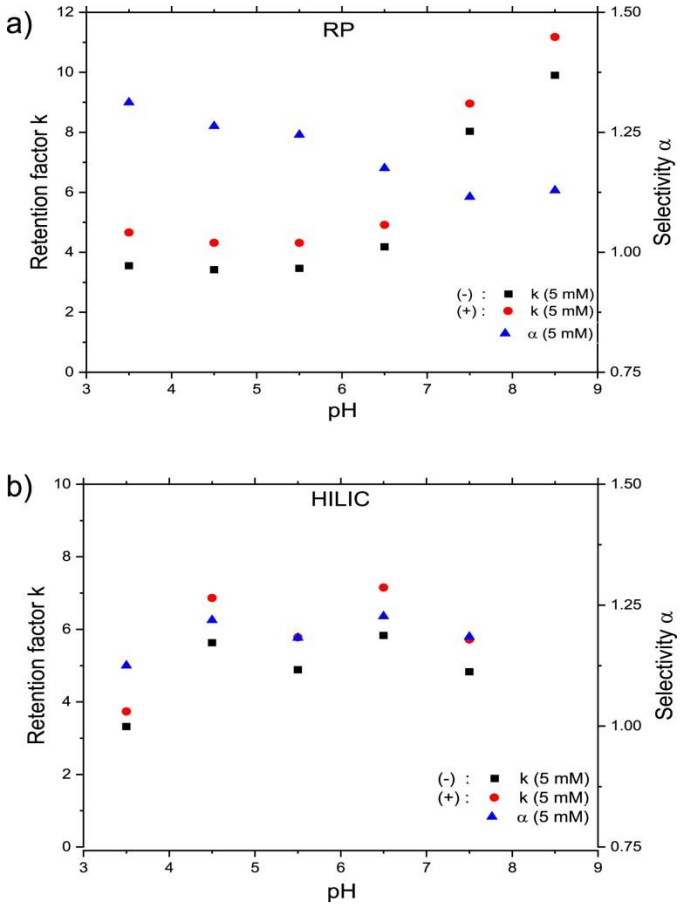

Fig. 4: Chromatographic lipophilicity (a) and hydrophilicity (b) measurements of the chromatographic ligands of ZWIX(+) and ZWIX(−) by RPLC (a) and HILIC (b).Experimental conditions: (a) Phenomenex Gemini (150 × 4.6 mm, 120 Å, 5 µm), mobile phase: MeOH/H_2O (1:1, v/v), (b) LiChrospher 100 Diol (250 × 4 mm, 100 Å, 5 µm) mobile phase: ACN/H_2O (9:1, v/v); buffers in (a) and (b): 5 mM NH_4FA (pH 3.5 and 4.5) or 5 mM NH_4AA (pH 5.5 to 8.5), apparent pH ($_w^s pH$) adjusted with FA in the hydroogranic mixture (pH 3.5 and 4.5), AA (pH 5.5 to 7.5) or NH_3 (8.5); flow rate, 1.0 mL min^{-1}; injection volume, 5 µL (ZWIX(+) and ZWIX(−) selectors dissolved at 0.1 mg mL^{-1}, in mobile phase); temperature, 40 °C; UV detection, λ = 245 nm.

Considering the amphiphilic nature of the current ZWIX type selectors, an extension to characterize their hydrophilicity under HILIC conditions (Diol column; see Suppl. Material for detailed conditions) was devised in analogy. Under HILIC conditions, ZWIX(+) was surprisingly also more strongly retained than ZWIX(−) (Fig. 4b) (for corresponding experiments with 20 mM buffer see Supplemental Material Fig. S1).

This unexpected behavior is somewhat difficult to understand; a reversed elution order compared to RPLC was expected because stronger retention in RPLC indicates higher lipophilicity and consequently lower retention was expected in HILIC. However, experiments reveal that the ZWIX(+) selector shows under both, RP and HILIC conditions, slightly stronger retention than the pseudo-enantiomeric ZWIX(−). This may indicate that the accessibility of the interaction sites differs somehow and/or conformational differences exist in distinct solvents which lead to exposure of different moieties at the interactive surface. Applying the reciprocity principle of molecular recognition, the ZWIX(+) selector should be the preferred selector for MMC both in RP as well as HILIC mode providing stronger retention in both elution modes.

4.4.4.3. Surface Charge Characterization by Determination of ζ-potentials of Modified Silica Particles

In chromatography, the surface charge of separation materials plays an important role for the analysis of charged compounds. The characterization of modified silica particles by determination of ζ-potentials in a pH-dependent manner already offered valuable information about the chromatographic behavior and applicability of MMC phases [18,19,24,49,50]. Suspended ionized particles in electrolyte solutions usually possess a non-abrasive layer of counter-ions (Stern layer) followed by an abrasive layer of mixed species at the surface. If an electric field is applied, the charged particles will start moving in the solution and a shear plane is formed. The potential at this shear plane is defined as the ζ-potential [51] and can be used to characterize the surface charge of the particles. In this particular case, the same ζ-potentials for both ZWIX(+) and ZWIX(−) are expected due to the similar selectors only differing in their stereochemistry (note: the stereochemistry is different for four out of seven asymmetric atoms; see caption of Fig. 1 for more details) and the same ligand coverage. Therefore, we studied the ζ-potentials of these silica gels and for comparison *tert*-butyl carbamoyl quinine-bonded silica (Chiralpak QN-AX) investigating different pH values at constant ionic strength of 10 mM KCl (Fig. 5).

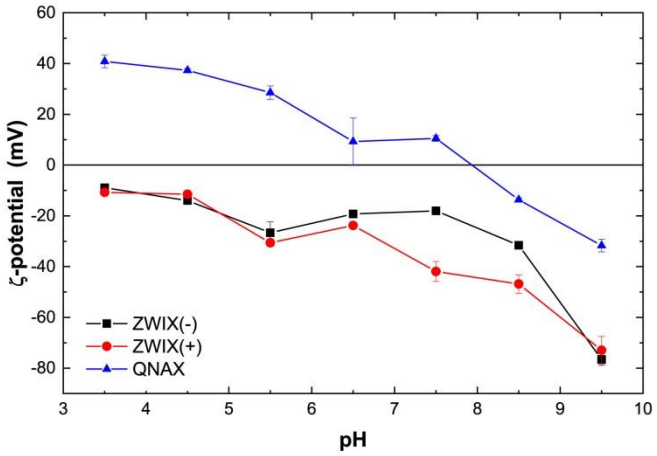

Fig. 5. Surface charge tendency of ZWIX(+) and ZWIX(−)-modified silica presented by ζ-potentials determined at different pH values.

The *tert*-butyl carbamoyl quinine modified silica particles (QNAX) showed positive ζ-potentials at low pH values dominated by the presence of tertiary amines (pk_a (quinuclidine) = 8.08, pk_a (quinoline) = 4.05 (Marvin) [49]. By increasing the pH ζ-potential slightly dropped but remained positive up to pH 7.5. This trend can be explained on the one hand by the weakly basic properties of the quinoline and quinuclidine nitrogens and on the other hand by the enhancing dissociation of residual surface silanol groups. The dominating influence of the latter forces the surface charge at pH values higher than 8 to negative values.

The introduction of an additional sulfonic acid moiety (pK_a = −0.97, calculated with Marvin Sketch) resulted in a negative offset of the ζ-potentials of around 30–50 mV for both ZWIX selectors. The general pH-dependency was similar for both diastereomeric ZWIX selectors (increasing pH led to declined values). This indicates that the negative polarity of the surface charge was mainly caused by the fully dissociated sulfonic acid while the net charge state was still influenced to some extent by the weak anion exchange increments. Comparing the calculated values for ZWIX(+) and ZWIX(−), no significant differences are revealed over a wide pH range except for pH values around 7.5. The slight difference could originate from the opposite configurations at the chiral centers at C8/C9 close to the quinuclidine nitrogen which could slightly influence the protonation of this interaction site i.e. its effective pK_a due to distinct electronic effects from the microenvironment. Interestingly, at very basic pH values, ZWIX(−) and ZWIX(+) showed the same surface charge probably due to domination of silanols at this pH.

Overall, it becomes evident that the ZWIX phases have a net negative character, different than expected. Obviously, charge balance from sulfonic acid and quinuclidine ring does not occur as expected, but there is an overall domination from the presence of the sulfonic acid group rendering these modified silicas slightly acidic.

4.4.4.4. Characterization of Ion Exchange Capability of Small Ions

The ability to cause retention of small solvated spherical inorganic ions is a property that depends strongly on surface chemistry and the surface charge state, respectively. It can be utilized as a complementary characterization approach of the surface charge compared to the above described ζ-potential determination. For this purpose, the counterion concentration-dependent retention of ionic analytes in accordance to the stoichiometric displacement model can be adopted which describes the linear relationship of the logarithmic retention factor *k* to the logarithm of the counterion concentration *C* [M] (Eq. (1)) and can serve for retention prediction [51]. The intercept K_z is a system-specific constant which describes the used ion exchange system, taking into account the dead volume t_0, the concentration of available ion exchange sites q_x [mol m^{-2}] in relation to the particle surface S [m^2 g^{-1}] and the ion exchange equilibrium constant *K* [L mol^{-1}] (Eq. (2)) [51]. The slope Z characterizes the ratio of the effective involved charges of analyte and counterions.

$$\log k = \log K_Z - Z \cdot \log C \quad (1)$$

$$K_Z = \frac{K \cdot q_x^Z \cdot S}{V_0} \quad (2)$$

Herein, we selected a homologous series of inorganic spherical solvated ions from the class of alkali metals and halide anions to probe electrostatic interactions. Since ZWIX phases can have both cation exchange as well as anion exchange capacity, it was of interest which one would prevail experimentally. In Fig. 6 the stoichiometric displacement model is applied to the retention data of alkali metal ions obtained from the chromatographic experiments with ZWIX(+) and ZWIX(−). The retention order for both columns follows the generally known pattern of the lyotropic series: $Li^+<Na^+<K^+<Rb^+$ [51]. The charge density drops with increasing atomic number within the group. As a result, the degree of hydration decreases and thus the electrostatic attraction that acts on the ion increases [52]. The cations show almost parallel straight lines in both cases. However, it becomes clear that in the case of ZWIX(+) the intercept is slightly higher than that of ZWIX(−). The trends prove the existence of cation exchange properties. Halide ions, on contrary, were not retained and thus not resolved being indicative for an experimentally net negative surface charge which is confirming the behavior measured by ELS.

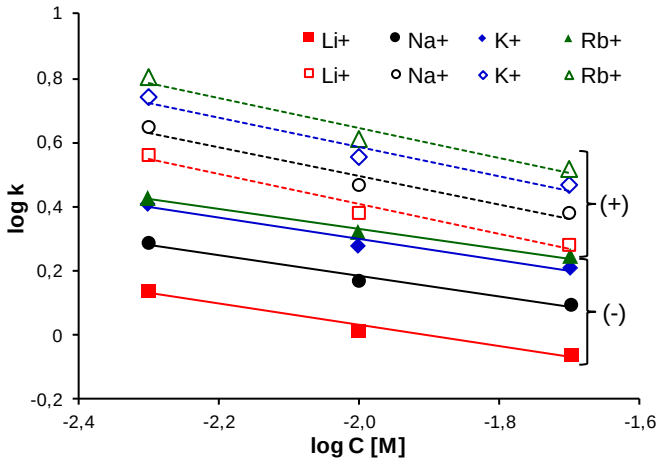

Fig. 6: Stoichiometric displacement model applied to the counterion concentration (ammonium) dependent retention of the lyotropic series of small inorganic cations at pH 7: Blue diamonds, K+; black circles: Na+; red squares: Li+; green triangles: Rb+; open symbols: ZWIX(+); closed symbols: ZWIX(−) Experimental conditions: ACN/H_2O (4:1, v/v), 5, 10 or 20 mM NH_4FA, pH unadjusted, 0.2 mL min^{-1}, T = 40 °C, injection volume 7 µL (10 mM of each cation), charged aerosol detection (CAD). (For interpretation of the references to colour in this figure legend, the reader is referred to the Web version of this article.)

4.4.4.5. Characterization of MMC Behaviour under RP and HILIC Conditions

The MMC capability of the columns ZWIX(+) and ZWIX(−) were tested under non-chiral RP conditions. The suitability of RP and MMC stationary phases can nicely be characterized by the selectivity for compounds only differing in a single methylene unit. Herein, the retention of homologous alkylbenzenes served for the characterization of hydrophobic interactions, especially the methylene selectivity. A test mix commonly used previously for characterizing methylene selectivity of mixed mode phases containing also some other compounds (DETP,

Boc-Pro-Phe) was used. The obtained chromatograms of the zwitterionic stationary phases were compared to the ones of a polar RP column Synergi Fusion RP. The retention data are summarized in Table S1 and the chromatograms are shown in Fig. 7 [21]. As expected, the polar RP column showed no retention for the polar acid DETP and only weak retention for the more hydrophobic acid Boc-Pro-Phe (Fig. 7a) (both additional part of a previously used test mix for mixed-mode phases) [21]. The zwitterionic stationary phases (Fig. 7b and c) revealed a similar behavior in spite of the quinuclidine WAX site. The sulfonic acid moiety and the net negative surface charge has led to low retention because of electrostatic repulsion. Overall, the ZWIX phases show reasonable MMC character as can be derived from the retention of aromatic alkanes (BuB, and PeB). Methylene selectivities $\alpha(CH_2)$ calculated for these compounds were 1.43 and 1.29 on ZWIX(+) and ZWIX(−), respectively. It indicates some potential to separate analytes by hydrophobic interactions in accordance to a MMC concept. For comparison, the polar RP phase Synergi Fusion RP (Fig. 7a) showed strong retention of BuB and PeB due to the occurring strong hydrophobic interactions with methylene selectivity $\alpha(CH_2)$ of 1.79 [21].

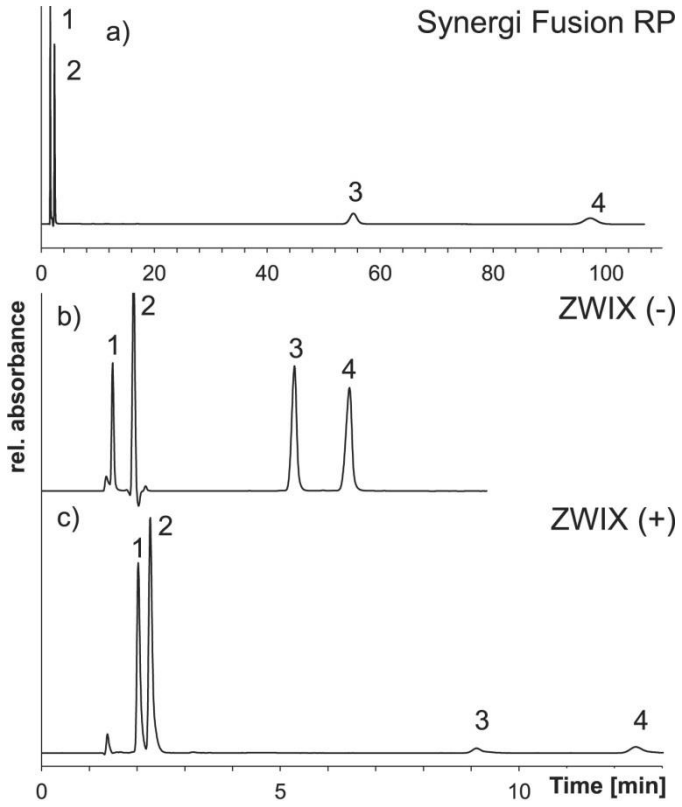

Fig. 7: Separation of alkylbenzenes and acids under RP conditions on a) Synergi Fusion RP, b) ZWIX(−) and c) ZWIX(+).
Solutes: 1, DETP; 2, Boc-Pro-Phe; 3, Butylbenzene (BuB); 4, Pentylbenzene (PeB). Mobile phase: ACN/H_2O (2:3, v/v), 0.29% AA (C_{tot} = 50 mM), apparent pH ($^{s}_{w}pH$) 6, adjusted with NH_3 in the hydroogranic mixture, lin. flow velocity: 1.7 mm s^{-1}, T = 25 °C, λ = 220 nm. Injection volume: 5 µL. Note, the concentrations of BuB and PeB were not the same for ZWIX(+) and ZWIX(−) because they were partly evaporated from the sample mixture.

MMC phases have been shown to possess multimodal applicability. Hence, due to the polar surface properties of ZWIX(+) and ZWIX(−), the retention behavior was additionally

investigated under HILIC conditions in comparison to the zwitterionic HILIC column ZIC-HILIC. A mixture of xanthines, nucleosides and vitamins served as model analytes. The chromatograms in Fig. 8 show the separation of nucleosides on ZWIX(+), ZWIX(−) and the reference column ZIC-HILIC. The retention data are listed in Tab S1. The elution order is similar for both columns (thymidine < uridine < adenosine < cytidine < guanosine), which is not corresponding to the log D values (adenosine < thymidine < uridine < guanosine < cytidine) like already reported previously for other HILIC columns [5]. The reference column showed an elution order switch of adenosine and uridine and in general a stronger retention of the nucleosides compared to the ZWIX columns as expected for a pure HILIC column. Aligning the chromatograms of ZWIX(+) and ZWIX(−), it can be seen that the selectivity for thymidine and uridine is slightly dropped on ZWIX(+) under the investigated experimental conditions. However, the nucleobases cytosine and guanosine are more strongly retained on ZWIX(+) than on ZWIX(−).

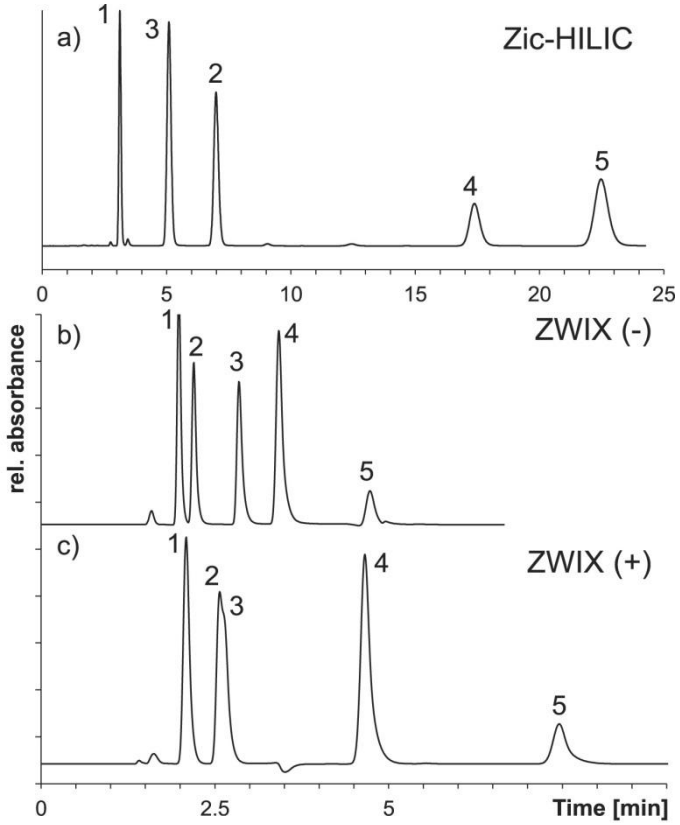

Fig. 8. Separation of nucleosides performed on the HILIC stationary phase ZIC-HILIC (a), ZWIX(−) (b) and ZWIX(+) (c) using HILIC conditions. Solutes: 1, thymidine; 2, uridine; 3, adenosine; 4; cytidine; 5; guanosine. Mobile phase: ACN/water (90:10, v/v) with 5 mM NH_4AA, lin. flow velocity: 1.7 mm s^{-1}, T = 25 °C, λ = 220 nm, injection volume: 2 µL.

The results clearly indicate that ZWIX(+) and ZWIX(−) columns have multimodal applicability and can be useful for MMC in various applications. Overall, the ZWIX(+) phase seems to be of advantage both for RP as well as HILIC mode applications.

4.4.4.6. Stationary Phase Classification by Multivariate Data Analysis

Unsupervised principal component analysis (PCA) is well suited to demonstrate similarities and differences of stationary phases in their retention profiles. A data set of retention factors of hydrophilic, lipophilic, neutral, basic and acidic analytes obtained on various (commercial) RP, HILIC, mixed-mode and chiral columns under HILIC and RP conditions were subjected to PCA [18-21,24,50]. The surface structure of the columns is depicted in Fig. S2. Multivariate analysis can be used to calculate a score plot (Fig. 9), which depicts columns with similar retention behavior in close proximity. The more different the retention behavior, the greater is the distance [18-21,24,50,53]. In this particular case, the two main components PC1 and PC2 describe approximately 68% of the variance in the data set. While the PC1 axis is a descriptor of the hydrophilicity, the PC2 axis represents the effective charge of the silica particles. Stationary phases with polar surfaces can be found at high PC1 values like the amino column Luna NH_2 and the HILIC columns ZIC-HILIC, Polysulfoethyl A, PC HILIC and the TSKGel Amide-80. The polar RP phase Synergi Fusion-RP shows the lowest score on the lipophilicity-hydrophilicity axis indicative for its apolar surface character. The MMC columns Uptisphere 5 MM3 (RP phase with quaternary ammonium endcapping) and Primesep B2 (RP/AX; suppl. Fig. S2) also showed a pronounced RP character and were therefore clustered together with the RP phase. The PC2 axis, on the other hand, is mainly characterized by the charge state of the surface of the separation materials. Mixed-mode anion exchange columns like Acclaim Mixed Mode WAX-1 are found at high PC2 values and net negatively charged phases like PC-HILIC at low PC2 values.

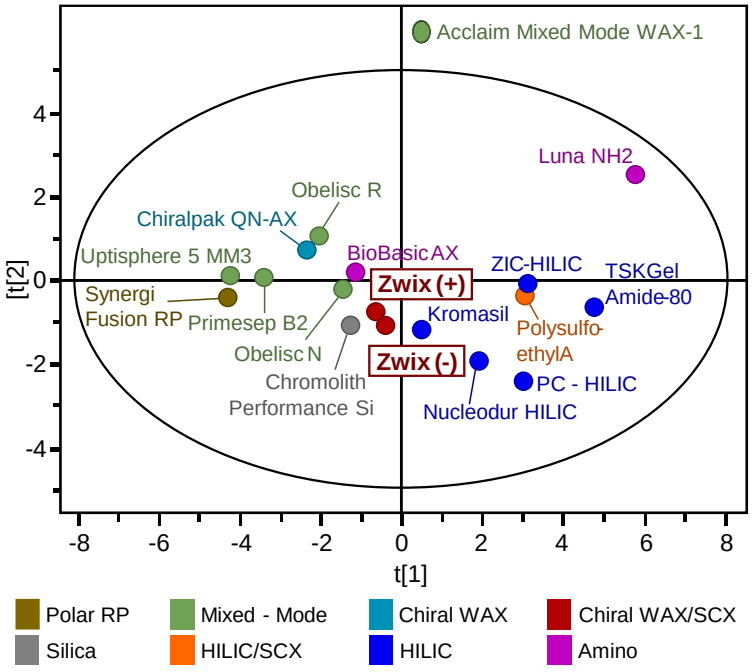

Fig. 9: Score plot of principal component analysis based on retention factor (*k*) of the RP and HILIC tests with several RP, HILIC, MMC and chiral stationary phases (for more details see suppl. material).

In accordance to the already discussed ζ-potentials, it is not surprising, that the ZWIX columns are located between negatively charged columns like bare (Kromasil) and monolithic silica (Chromolith Performance Si). It again highlights the dominating effect of the strongly acidic sulfonic acid moiety in the ligand molecule. This statistical projection shows slightly different locations for the two columns with diastereomeric ZWIX selectors that can be regarded as the result of the slightly different retention behavior and is in accordance with the *in silico* prediction and the other above discussed studies. On the polarity scale (PC1), they show intermediate hydrophilicity (balanced hydrophilicity-lipophilicity) being indicative for their mixed-mode character rather than classical HILIC behavior. Depending on the elution conditions, one of the respective chromatographic modes (RP- or HILIC-type) prevails making them a flexible tool.

4.4.4.7. Evaluation of the Orthogonality of ZWIX(+) and ZWIX(−) for LC × LC

Successful LC × LC separations rely on a proper column selection and, amongst others, sufficient orthogonality regarding their retention profiles in first and second separation dimension. General column characterization and classification systems like described in the previous chapters can be helpful concerning the preliminary column choice. In order to address specific analyte groups, column screens investigating the target compounds or similar ones (if the real target analytes of interest are not available) are necessary. Multiple approaches comprising statistical procedures like correlation coefficients, bin counting methods [11,13,54], fractional surface coverages like the convex hull method [55] and asterisk methods [12] were described to determine the degree of orthogonality. In our work, we were interested in establishing a complementary selectivity dimension for amino acid analysis by 2D-LC, being potentially useful for impurity profiling in amino acid formulations.

Due to the small analyte set, the comparison of ZWIX(+) and ZWIX(−) with commercial HILIC and mixed mode stationary phases can be conveniently performed by plotting normalized retention times [11] of the amino acids on the ZWIX columns against the ones on the investigated stationary phases in the two dimensional retention space. In Fig. 10 the orthogonality plots of ZWIX(+) (employed in polar organic elution mode) versus uncharged and zwitterionic HILIC and MMC stationary phases (in HILIC elution mode) are depicted. The corresponding figure for ZWIX(−) can be found in the Supplemental Material (suppl. Fig. S3). However, the comparison of ZWIX(+) and ZWIX(−) showed less related retention mechanisms than expected (Fig. 10a). Especially in case of the amino acids with charged residues, the correlation is low and a reasonable distribution in the chromatographic 2D-space can be found.

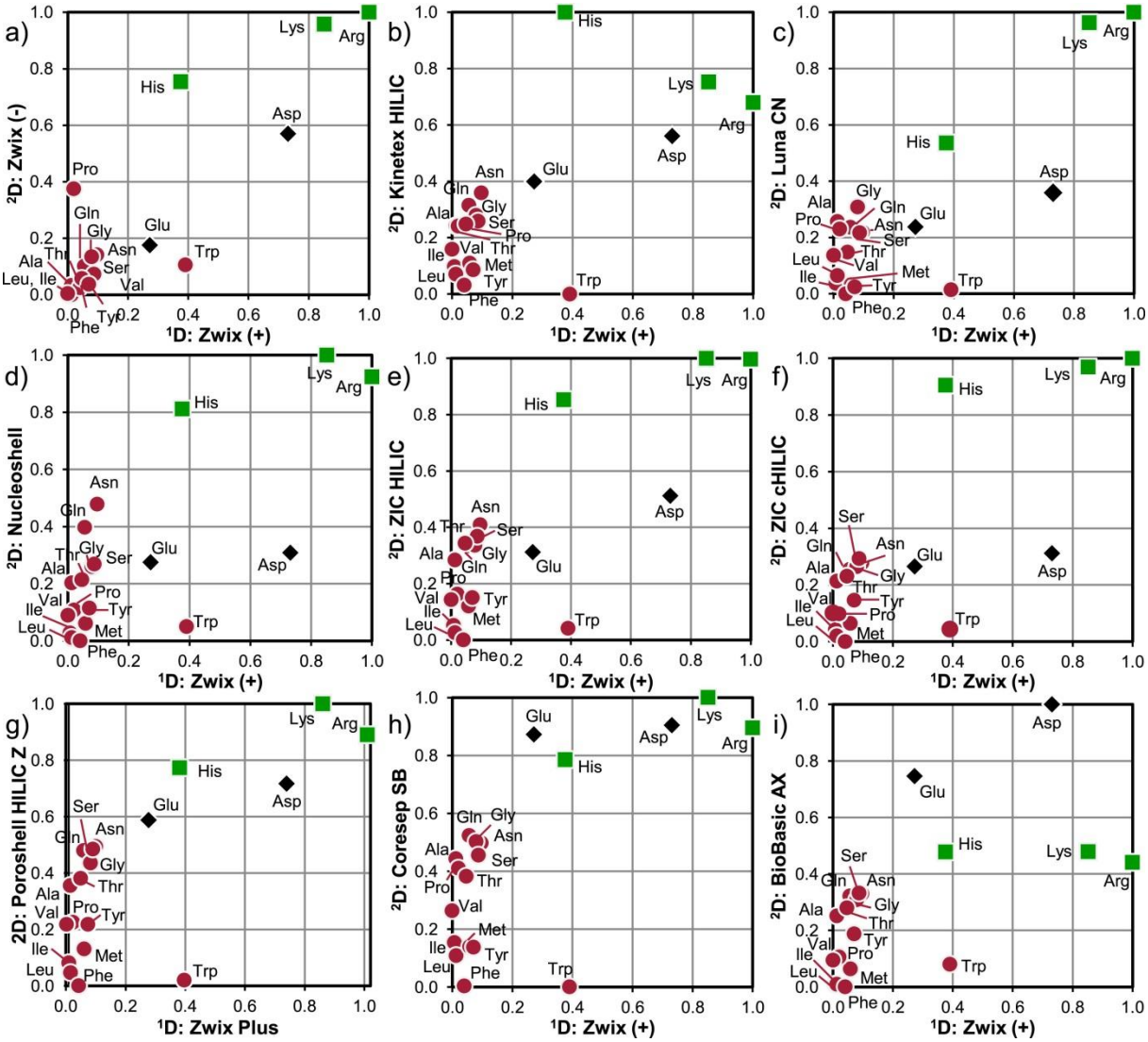

Fig. 10: Orthogonality plots of normalized retention times of proteinogenic amino acids in the two dimensional separation space with ZWIX(+) as ^{1}D column and commercial HILIC (b–g) and MMC columns (a, h-i) in ^{2}D under HILIC conditions. Screening conditions: A: ACN/H_2O/200 mM NH_4FA in the aqueous solution, pH 3.5 adjusted with ammonia (50:45:5, v/v/v), B: ACN/H_2O/200 mM NH_4FA in the aqueous solution, pH 3.5 adjusted with ammonia (90:5:5, v/v), linear flow velocity: 1.18 mm s^{-1}, T = 40 °C gradient: 0.0–5 min: 100 %B, 5–25 min: 0 %B, 25–30 min: 0% B, 30–30.1 min: 0–100 %B, 30.1–40 min: 100 %B, except Poroshell HILIC-Z and ZWIX(+) and ZWIX(−), detailed conditions can be found in the Supplemental Material. Red circles: polar and apolar amino acids, green squares: basic amino acids, black diamonds: acidic amino acids. (For interpretation of the references to colour in this figure legend, the reader is referred to the Web version of this article.)

In order to extend the chromatographic window for early eluted amino acids in the 2D retention space and to find the most promising complementary column to ZWIX, retention on the zwitterionic stationary phases (employed in polar organic mode) were plotted against bare silica stationary phases (Kinetex HILIC, Fig. 10b), with cyano phases like Luna CN (Fig. 10c), zwitterionic HILIC phases like Nucleoshell (Fig. 10d), ZIC-HILIC (Fig. 10e), ZIC-cHILIC (Fig. 10f) and Poroshell 120 HILIC-Z (Fig. 10g) as well as the mixed mode columns Coresep SB (Fig. 10h) and BioBasic AX (Fig. 10i) under HILIC conditions (pH 3.5). All investigated column combinations were able to sufficiently separate the basic and acidic amino acids. However, the amino acids with apolar and polar residues clustered together. The investigated

superficially porous columns Nucleoshell, Poroshell 120 HILIC-Z and Coresep SB showed the best selectivity for this analyte group in the 1D screening experiments.

For the online LC × LC experiments, ZWIX(+) in polar organic mode was combined with Poroshell HILIC-Z (50 × 3.0 mm) under HILIC conditions (Fig. 11). The combination of these complementary chromatographic modes (polar organic and HILIC) offered the possibility to avoid distorted peaks due to solvent mismatch issues. The short ^{2}D HILIC column allowed fast separations of the amino acids in about 60 s. Since the final application of the method is for impurity profiling, the 2D-LC system with its DAD in the ^{2}D (chromatogram in Fig. 11a) was additionally equipped with complementary detectors via a splitter (ratio 1:11.6), viz. a high-resolution mass spectrometer (ESI-QTOF) for identification (Fig. 11c) and a charged aerosol detector (CAD) for universal detection (of non-volatile compounds) (Fig. 11b) as well as preliminary quantitation as reported previously [56]. In the first and in the second dimension a mixed retention mechanism was observed. Amino acids with ionizable residues were strongly retained while the hydrophobic and polar amino acids were clustered, but separated in the early retention time window of the two dimensional analysis. It is clearly evident that in the case of an impurity profiling approach, the retention space not covered by the main amino acid constituents is available for the separation and detection of impurities. Such comprehensive LC × LC method with multiple complementary detection systems should be beneficial for advanced impurity profiling. Its application will be reported separately.

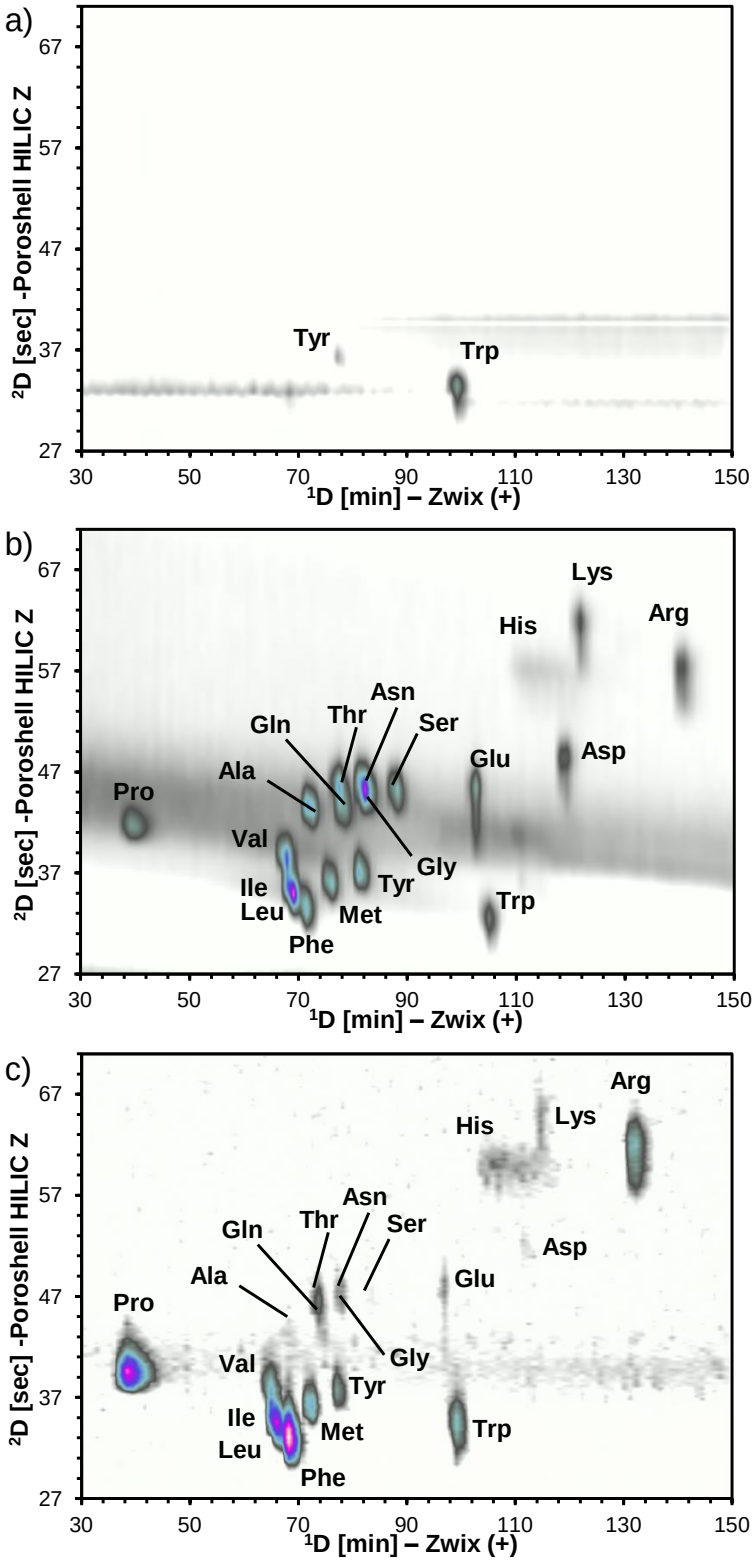

Fig. 11: Two dimensional separation of underivatized proteinogenic amino acids using ZWIX(+) in polar organic mode in ^{1}D and Poroshell 120 HILIC-Z under HILIC conditions and complementary detection in ^{2}D for comprehensive sample information. Therefore, the ^{2}D flow was split (1:11.6) to a DAD (λ = 280 nm) (a) followed by a charged aerosol detector (b) and a high resolution mass spectrometer (ESI-QTOF) (c) multiple selected ion chromatograms of proteinogenic amino acids). The detailed experimental conditions can be found in the Supplemental material.

4.4.5. Conclusions

Chiral columns could expand the tool box for 2D-LC. They can be often categorized as mixed-mode chromatography columns and frequently show chromatographic complementarity to both RP and HILIC columns. A better characterization of chiral stationary phases in view of achiral applications is therefore worthwhile. In this work, such beneficial utility was demonstrated for the two diastereomeric selectors of Chiralpak ZWIX(+) and ZWIX(−) columns which are well established for the separation of enantiomers. Herein, we focused on the characterization and elucidation of differences in non-chiral chromatography. While the *in silico* predicted polar surface areas were very similar, the solvent accessible surface areas (SASA), the molecular volumes and the minimal energy conformations indicated differences. Therefore, the pH-dependent study of the retention behavior of selector molecules under RP and HILIC conditions followed the same trend but indicated that the involved charges may play an important role. Hence, the surface charge of the ZWIX(+) and ZWIX(−) stationary phases were chromatographically characterized by separation of inorganic ions through application of the stoichiometric displacement model. A net negative surface charge was indicated which was confirmed by pH-dependent ζ-potential determinations. Principal component analysis of retention data from RP and HILIC elution modes acquired for ZWIX(+) and ZWIX(−) along with a variety of commercial RP, HILIC and mixed-mode phases allowed to classify the zwitterionic chiral stationary phases within the group of RP/SCX mixed-mode phases with slightly negative charge excess and balance hydrophilic-lipophilic surface character. Orthogonality plots for amino acids in comparison to a number of HILIC and mixed-mode phases were established and the Poroshell HILIC-Z column was then selected as ^{2}D column for LC × LC. By establishing such a comprehensive 2D-LC method in combination with complementary detectors (DAD, CAD and HR-MS/MS) a powerful method for comprehensive impurity profiling could be established.

Declaration of Competing Interest

The authors declare that they have no known competing financial interests or personal relationships that could have appeared to influence the work reported in this paper.

Acknowledgements

M. L. is grateful to Agilent Technologies for support of this research by an Agilent Research Award (#4068). M.L. is grateful to Pilar Franco from Chiral Technologies Europe (Illkirch, France) for providing Chiralpak ZWIX columns.

4.4.6. References

[1] F. Cacciola, P. Donato, D. Sciarrone, P. Dugo, L. Mondello,Comprehensive liquid chromatography and other liquid-based comprehensive techniques coupled to mass spectrometry in food analysis, Anal. Chem., 89 (2017), 414-429

[2] P. Jandera, J. Fischer, H. Lahovska, K. Novotna, P. Cesla, L. Kolarova, Two-dimensional liquid chromatography normal-phase and reversed-phase separation of (co)oligomers, J. Chromatogr. A, 1119 (2006), 3-10

[3] B.W.J. Pirok, A.F.G. Gargano, P.J. Schoenmakers, Optimizing separations in online comprehensive two-dimensional liquid chromatography, J. Sep. Sci., 41 (2018), 68-98

[4] B.W.J. Pirok, D.R. Stoll, P.J. Schoenmakers, Recent developments in two-dimensional liquid chromatography: fundamental improvements for practical applications, Anal. Chem., 91 (2019), 240-263

[5] M. Pursch, A. Wegener, S. Buckenmaier, Evaluation of active solvent modulation to enhance two-dimensional liquid chromatography for target analysis in polymeric matrices, J. Chromatogr. A, 1562 (2018), 78-86

[6] K. Sandra, M. Steenbeke, I. Vandenheede, G. Vanhoenacker, P. Sandra, The versatility of heart-cutting and comprehensive two-dimensional liquid chromatography in monoclonal antibody clone selection, J. Chromatogr. A, 1523 (2017), 283-292

[7] D.R. Stoll, P.W. Carr, Two-dimensional liquid chromatography: a state of the art tutorial, Anal. Chem., 89 (2017), 519-531

[8] D.R. Stoll, D.C. Harmes, G.O. Staples, O.G. Potter, C.T. Dammann, D. Guillarme, A. Beck, Development of comprehensive online two-dimensional liquid chromatography/mass spectrometry using hydrophilic interaction and reversed-phase separations for rapid and deep profiling of therapeutic antibodies, Anal. Chem., 90 (2018), 5923-5929

[9] P. Yang, W. Gao, T. Zhang, M. Pursch, J. Luong, W. Sattler, A. Singh, S. Backer, Two-dimensional liquid chromatography with active solvent modulation for studying monomer incorporation in copolymer dispersants, J. Sep. Sci., 42 (2019), 2805-2815

[10] S.H. Yang, J. Wang, K. Zhang, Validation of a two-dimensional liquid chromatography method for quality control testing of pharmaceutical materials, J. Chromatogr. A, 1492 (2017), 89-97

[11] M. Gilar, P. Olivova, A.E. Daly, J.C. Gebler, Orthogonality of separation in two-dimensional liquid chromatography, Anal. Chem., 77 (2005), 6426-6434

[12] M. Camenzuli, P.J. Schoenmakers, A new measure of orthogonality for multi-dimensional chromatography, Anal. Chim. Acta, 838 (2014), 93-101

[13] M. Gilar, J. Fridrich, M.R. Schure, A. Jaworski, Comparison of orthogonality estimation methods for the two-dimensional separations of peptides, Anal. Chem., 84 (2012), 8722-8732

[14] S.E. Porter, D.R. Stoll, S.C. Rutan, P.W. Carr, J.D. Cohen, Analysis of four-way two-dimensional liquid chromatography-diode array data: application to metabolomics, Anal. Chem., 78 (2006), 5559-5569

[15] X. Wang, D.R. Stoll, A.P. Schellinger, P.W. Carr, Peak capacity optimization of peptide separations in reversed-phase gradient elution chromatography: fixed column format, Anal. Chem., 78 (2006), 3406-3416

[16] M. Iguiniz, F. Rouviere, E. Corbel, N. Roques, S. Heinisch, Comprehensive two dimensional liquid chromatography as analytical strategy for pharmaceutical analysis, J. Chromatogr. A, 1536 (2018), 195-204

[17] D.R. Stoll, K. Shoykhet, P. Petersson, S. Buckenmaier, Active solvent modulation: a valve-based approach to improve separation compatibility in two-dimensional liquid chromatography, Anal. Chem., 89 (2017), 9260-9267

[18] S. Bäurer, S. Polnick, O.L. Sánchez Muñoz, M. Kramer, M. Lämmerhofer, N-Propyl-N'-2-pyridylurea-modified silica as mixed-mode stationary phase with moderate weak anion exchange capacity and pH-dependent surface charge reversal, J. Chromatogr. A, 1560 (2018), 45-54

[19] S. Bäurer, A. Zimmermann, U. Woiwode, O.L. Sánchez Muñoz, M. Kramer, J. Horak, W. Lindner, W. Bicker, M. Lämmerhofer, Stable-bond polymeric reversed-phase/weak anion-exchange mixed-mode stationary phases obtained by simultaneous functionalization and crosslinking of a poly(3-mercaptopropyl)methylsiloxane-film on vinyl silica via thiol-ene double click reaction, J. Chromatogr. A, 1593 (2019), 110-118

[20] A.F. Gargano, T. Leek, W. Lindner, M. Lämmerhofer, Mixed-mode chromatography with zwitterionic phosphopeptidomimetic selectors from Ugi multicomponent reaction, J. Chromatogr. A, 1317 (2013), 12-21

[21] M. Lämmerhofer, M. Richter, J. Wu, R. Nogueira, W. Bicker, W. Lindner, Mixed-mode ion-exchangers and their comparative chromatographic characterization in reversed-phase and hydrophilic interaction chromatography elution modes, J. Sep. Sci., 31 (2008), 2572-2588

[22] D. Sýkora, P. Řezanka, K. Záruba, V. Král, Recent advances in mixed-mode chromatographic stationary phases, J. Sep. Sci., 42 (2019), 89-129

[23] K. Zhang, X. Liu, Mixed-mode chromatography in pharmaceutical and biopharmaceutical applications, J. Pharm. Biomed. Anal., 128 (2016), 73-88

[24] A. Zimmermann, J. Horak, O.L. Sánchez Muñoz, M. Lämmerhofer, Surface charge fine tuning of reversed-phase/weak anion-exchange type mixed-mode stationary phases for milder elution conditions, J. Chromatogr. A, 1409 (2015), 189-200

[25] E.P. Nesterenko, P.N. Nesterenko, B. Paull, Zwitterionic ion-exchangers in ion chromatography: a review of recent developments, Anal. Chim. Acta, 652 (2009), 3-21

[26] L. Zhang, Q. Dai, X. Qiao, C. Yu, X. Qin, H. Yan, Mixed-mode chromatographic stationary phases: recent advancements and its applications for high-performance liquid chromatography, Trac. Trends Anal. Chem., 82 (2016), 143-163

[27] W. Bicker, M. Lämmerhofer, W. Lindner, Mixed-mode stationary phases as a complementary selectivity concept in liquid chromatography–tandem mass spectrometry-based bioanalytical assays, Anal. Bioanal. Chem., 390 (2008), 263-266

[28] L. Ding, Z. Guo, Z. Hu, X. Liang, Mixed-mode reversed phase/positively charged repulsion chromatography for intact protein separation, J. Pharm. Biomed. Anal., 138 (2017), 63-69

[29] J. Wei, Z. Guo, P. Zhang, F. Zhang, B. Yang, X. Liang, A new reversed-phase/strong anion-exchange mixed-mode stationary phase based on polar-copolymerized approach and its application in the enrichment of aristolochic acids, J. Chromatogr. A, 1246 (2012), 129-136

[30] Q. Jiang, W. Zhao, H. Qiu, S. Zhang, Silica-based phenyl and octyl bifunctional imidazolium as a new mixed-mode stationary phase for reversed-phase and anion-exchange chromatography, Chromatographia, 79 (2016), 1437-1443

[31] Z. Wei, Q. Fu, J. Cai, L. Huan, J. Zhao, H. Shi, Y. Jin, X. Liang, Evaluation and application of a mixed-mode chromatographic stationary phase in two-dimensional liquid chromatography for the separation of traditional Chinese medicine, J. Sep. Sci., 39 (2016), 2221-2228

[32] E.L. Regalado, C.J. Welch, Separation of achiral analytes using supercritical fluid chromatography with chiral stationary phases, Trac. Trends Anal. Chem., 67 (2015), 74-81

[33] R.K. Lindsey, B.L. Eggimann, D.R. Stoll, P.W. Carr, M.R. Schure, J.I. Siepmann, Column selection for comprehensive two-dimensional liquid chromatography using the hydrophobic subtraction model, J. Chromatogr. A, 1589 (2019), 47-55

[34] B. Bidlingmeyer, C.C. Chan, P. Fastino, R. Henry, P. Koerner, A.T. Maule, M.R.C. Marques, U. Neue, L. Ng, H. Pappa, L. Sander, C. Santasania, L. Snyder, T. Wozniak, HPLC column classification, Pharmacopeial Forum, 31 (2005), 637-645

[35] J.L. Dores-Sousa, J. De Vos, W.T. Kok, S. Eeltink, Probing selectivity of mixed-mode reversed-phase/weak-anion-exchange liquid chromatography to advance method development, J. Chromatogr. A, 1570 (2018), 75-81

[36] E. Lemasson, Y. Richer, S. Bertin, P. Hennig, C. West, Characterization of retention mechanisms in mixed-mode HPLC with a bimodal reversed-phase/cation-exchange stationary phase, Chromatographia, 81 (2018), 387-399

[37] B.W. Pirok, S. Pous-Torres, C. Ortiz-Bolsico, G. Vivó-Truyols, P.J. Schoenmakers, Program for the interpretive optimization of two-dimensional resolution, J. Chromatogr. A, 1450 (2016), 29-37

[38] B.W.J. Pirok, S.R.A. Molenaar, R.E. van Outersterp, P.J. Schoenmakers, Applicability of retention modelling in hydrophilic-interaction liquid chromatography for algorithmic optimization programs with gradient-scanning techniques, J. Chromatogr. A, 1530 (2017), 104-111

[39] C.V. Hoffmann, R. Pell, M. Lämmerhofer, W. Lindner, Synergistic effects on enantioselectivity of zwitterionic chiral stationary phases for separations of chiral acids, bases, and amino acids by HPLC, Anal. Chem., 80 (2008), 8780-8789

[40] R. Sardella, A. Macchiarulo, F. Urbinati, F. Ianni, A. Carotti, M. Kohout, W. Lindner, A. Peter, I. Ilisz, Exploring the enantiorecognition mechanism of Cinchona alkaloid-based zwitterionic chiral stationary phases and the basic trans-paroxetine enantiomers, J. Sep. Sci., 41 (2018), 1199-1207

[41] L. Martinez, R. Andrade, E.G. Birgin, J.M. Martinez, PACKMOL: a package for building initial configurations for molecular dynamics simulations, J. Comput. Chem., 30 (2009), 2157-2164

[42] S. Nosé, A unified formulation of the constant temperature molecular dynamics methods, J. Chem. Phys., 81 (1984), 511-519

[43] J.L. Banks, H.S. Beard, Y. Cao, A.E. Cho, W. Damm, R. Farid, A.K. Felts, T.A. Halgren, D.T. Mainz, J.R. Maple, R. Murphy, D.M. Philipp, M.P. Repasky, L.Y. Zhang, B.J. Berne, R.A. Friesner, E. Gallicchio, R.M. Levy, Integrated modeling program, applied chemical theory (IMPACT), J. Comput. Chem., 26 (2005), 1752-1780

[44] D.E. Shaw, A fast, scalable method for the parallel evaluation of distance-limited pairwise particle interactions, J. Comput. Chem., 26 (2005), 1318-1328

[45] D. Shivakumar, J. Williams, Y. Wu, W. Damm, J. Shelley, W. Sherman, Prediction of absolute solvation free energies using molecular dynamics free energy perturbation and the OPLS force field, J. Chem. Theory Comput., 6 (2010), 1509-1519

[46] A. Pedretti, L. Villa, G. Vistoli, VEGA: a versatile program to convert, handle and visualize molecular structure on Windows-based PCs, J. Mol. Graph. Model., 21 (2002), 47-49

[47] A. Pedretti, L. Villa, G. Vistoli, VEGA – an open platform to develop chemo-bio-informatics applications, using plug-in architecture and script programming, J. Comput. Aided Mol. Des., 18 (2004), 167-173

[48] K.L. Valkó, Lipophilicity and biomimetic properties measured by HPLC to support drug discovery, J. Pharm. Biomed. Anal., 130 (2016), 35-54

[49] O.L. Sánchez Muñoz, E. Pérez Hernández, M. Lämmerhofer, W. Lindner, E. Kenndler, Estimation and comparison of ζ-potentials of silica-based anion-exchange type porous particles for capillary electrochromatography from electrophoretic and electroosmotic mobility, Electrophoresis, 24 (2003), 390-398

[50] U. Woiwode, A. Sievers-Engler, A. Zimmermann, W. Lindner, O.L. Sánchez Muñoz, M. Lämmerhofer, Surface-anchored counterions on weak chiral anion-exchangers accelerate separations and improve their compatibility for mass-spectrometry-hyphenation, J. Chromatogr. A, 1503 (2017), 21-31

[51] J. Ståhlberg, Retention models for ions in chromatography, J. Chromatogr. A, 855 (1999), 3-55

[52] J.L. Pauley, Prediction of cation-exchange equilibria, J. Am. Chem. Soc., 76 (1954), 1422-1425

[53] M.R. Euerby, P. Petersson, Chromatographic classification and comparison of commercially available reversed-phase liquid chromatographic columns using principal component analysis, J. Chromatogr. A, 994 (2003), 13-36

[54] J.M. Davis, D.R. Stoll, P.W. Carr, Dependence of effective peak capacity in comprehensive two-dimensional separations on the distribution of peak capacity between the two dimensions, Anal. Chem., 80 (2008), 8122-8134

[55] G. Semard, V. Peulon-Agasse, A. Bruchet, J.P. Bouillon, P. Cardinael, Convex hull: a new method to determine the separation space used and to optimize operating conditions for comprehensive two-dimensional gas chromatography, J. Chromatogr. A, 1217 (2010), 5449-5454

[56] S. Schiesel, M. Lämmerhofer, W. Lindner, Comprehensive impurity profiling of nutritional infusion solutions by multidimensional off-line reversed-phase liquid chromatography×hydrophilic interaction chromatography–ion trap mass-spectrometry and charged aerosol detection with universal calibration, J. Chromatogr. A, 1259 (2012), 100-110

4.4.7. Supplemental Material

4.4.7.1. Lipophilicity and Hydrophilicity Measurement of the Zwitterionic Selectors by RPLC and HILIC

4.4.7.1.1. Material and Methods

The stationary phase was Phenomenex Gemini C18 (150 x 4.6 mm, 120 Å, 5 µm) and a LiChrospher 100 Diol (250 x 4 mm, 100 Å, 5µm). The mobile phases were a mixture of methanol and MilliQ water for the separation under RP conditions (1:1, v/v) and acetonitrile and MilliQ water for the separation under HILIC conditions (90:10, v/v). The pH was buffered using 20 mM ammonium formate (3.5 and 4.5) and ammonium acetate (5.5 to 8.5), respectively. The apparent pH was adjusted to 3.5, 4.5, 5.5, 6.5, 7.5 and 8.5 (only under RP conditions due to limited column stability of the HILIC column) using formic acid (pH 3.5 and 4.5), acetic acid (pH 5.5 to 7.5) or ammonia (8.5). The flow rate was 1.0 mL min^{-1}. The selector molecules ZWIX (+) and ZWIX(-) were diluted with mobile phase (0.1 mg mL^{-1} of each). 5 µL were analyzed at 40°C and 254 nm.

4.4.7.1.2. Results for Mobile Phases with 20 mM Buffer

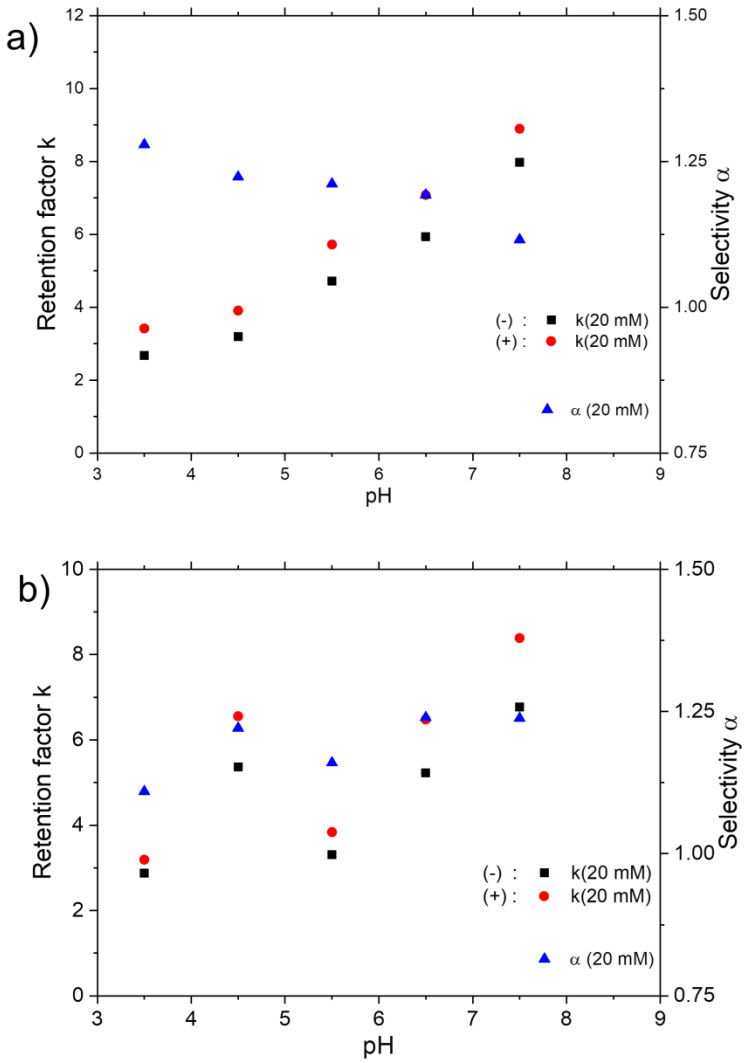

Fig. S1: Retention profiles of the diastereomeric selectors ZWIX(+) and ZWIX(-) dependent on pH under a) RP and b) HILIC conditions

4.4.7.2. Chromatographic Characterization under HILIC and RP Conditions for Column Classification

4.4.7.2.1. Material and methods

The stationary phases which were included in the test set for the evaluation of the chromatographic properties comprised all stationary phases depicted in Fig S2. For RP-HPLC separations, the mobile phase contained 40% (v,v) ACN, 60% (v,v) water and 0.29 % acetic acid (C_{tot} = 50 mM). The pH value was adjusted to 6 with ammonia. The HILIC measurements were carried out with the following mobile phases: For the xanthines the mixing ratio of ACN and water was 95:5 (v/v) and for the nucleosides and vitamins 90:10 (v/v). Ammonium acetate (5 mM) was used as buffer. The apparent pH was 8 and remained unadjusted. The analytes were dissolved in the mobile phase. The concentration of the analytes was 0.8 mg mL^{-1} (RP test) and 1.0 mg mL^{-1} (HILIC test). The injection volume was 5 µL (RP) and 2 µL (HILIC). The flow rate was 1.7 mm s^{-1}. The columns were thermostated to 25 °C. The detection wavelength was 220 nm. The void volume was determined using uracil (RP) and toluene (HILIC).

4.4.7.2.2. Results

Tab. S1: Overview of the chromatographic data obtained by the analysis of hydrophobic and acidic compounds under RP conditions and xanthines, nucleosides and vitamins under HILIC conditions on ZWIX(+) and ZWIX(-)

		ZWIX (-)					ZWIX (+)				
	Compounds	k	N	H	R[d]	α[d]	k	N	H	R	$\alpha_{1,2}$
RP[a]	DETP	0.09	4661	32.2			0.41	4477	33.5		
	Boc-Pro-Phe	0.41	5392	27.8	4.59[e]	4.73[e]	0.59	4677	32.1	1.98[e]	1.44[e]
	BuB	2.87	11898	12.6			5.35	10320	14.5		
	PeB	3.71	11823	12.7	5.35[f]	1.29[f]	7.68	10202	14.7	7.85[f]	1.43[f]
HILIC[b]	caffeine	0.30	4370	34.3			0.15	2322	64.6		
	theobromine	0.59	6760	22.2	3.64	1.93	0.45	4396	34.1	3.31	3.05
	theophylline	0.84	6738	22.3	2.97	1.42	0.62	4625	32.4	1.91	1.39
	thymidine	0.41	5856	25.6			0.41	4184	35.9		
	uridine	0.56	6184	24.3	2.00	1.37	0.73	4913	30.5	3.46	1.78
	adenosine	1.02	6895	21.8	5.26	1.83	0.78	5440	27.6	0.54	1.07
	cytidine	1.43	7046	21.3	3.83	1.40	2.14	7507	20.0	11.26	2.73
	guanosine	2.37	6807	22.0	6.70	1.65	4.02	8049	18.6	10.21	1.88
	pyridoxine	0.92	4640	32.3			0.53	2802	53.5		
	riboflavin	1.40	7653	19.6	4.26	1.51	2.51	2577	58.2	4.78	2.31
	ascorbic acid	n.d.[c]					2.29	2477	60.6	0.82	1.86
	nicotinic acid	1.94	7115	21.1	42.29	1.39	1.23	6273	23.9	4.80	0.91
	thiamine	5.78	761	197.1	6.86	2.98	10.27	8538	17.6	20.35	4.49

[a] Experimental conditions: ACN/H_2O (60:40, v/v), 50 mM acetic acid, pH 6 adjusted with ammonia

[b] Experimental conditions: xanthines: ACN/H_2O (95:5, v/v), vitamines and nucleosides: ACN/H_2O (90:10, v/v) 5 mM ammonium acetate, pH unadjusted

[c] n.d. = not detected

[d] Resolution and selectivity, respectively, refer to compound in the corresponding row and the previous eluting one if not otherwise stated

[e] Resolution and selectivity, respectively, of DETP and0 Boc-Pro-Phe

[f] Resolution and selectivity, respectively, of BuB and PeB

k, retention factor; *N*, plate number; *H*, theoretical plate height in µm; *R*, resolution; α, separation factor

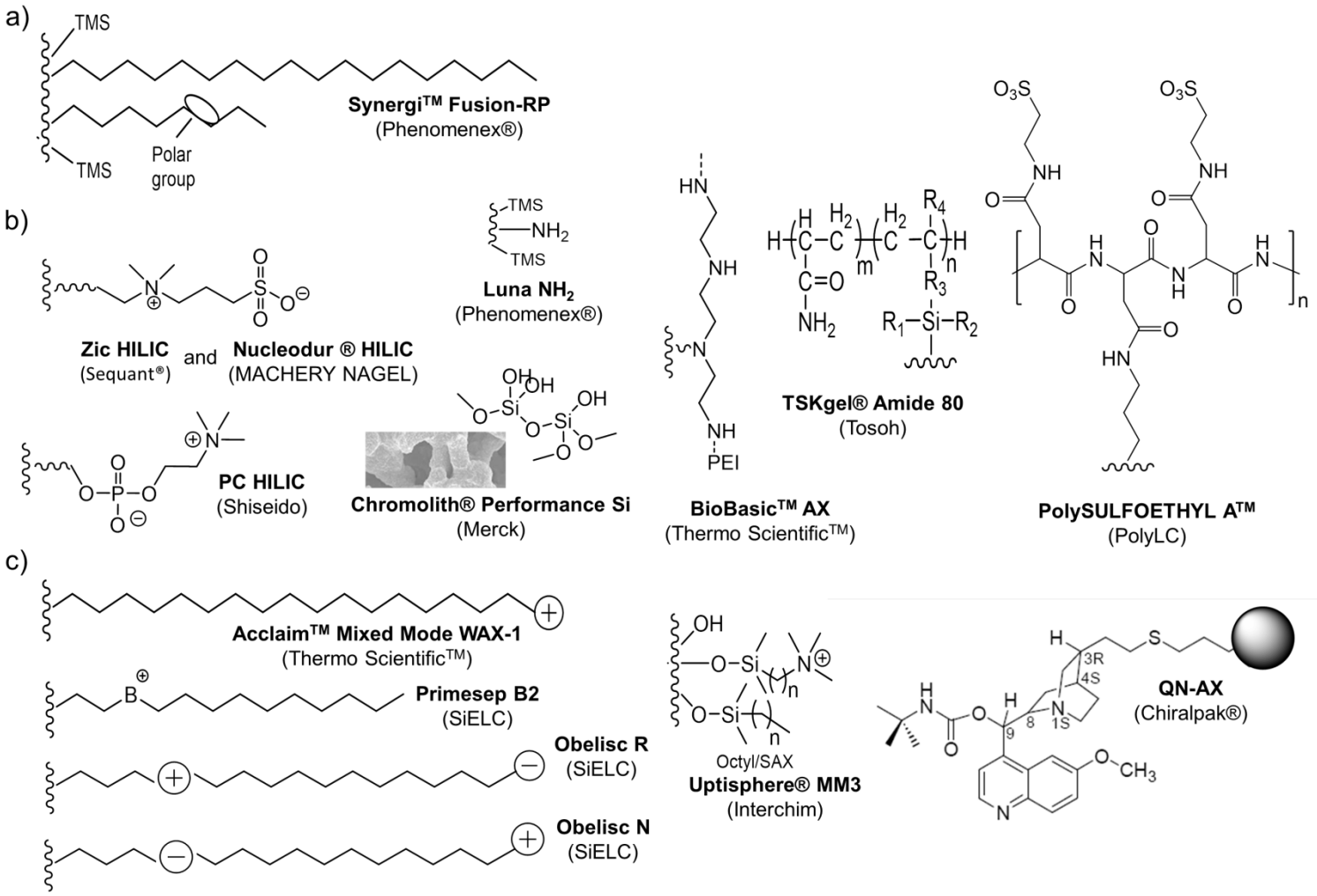

Fig. S2: Surface structure of investigated a) RP, b) HILIC and c) mixed mode stationary phases which were chromatographically evaluated for the principal component analysis.

4.4.7.3. Orthogonality Determination of ZWIX(+) and ZWIX(-) Compared to Commercially Available Stationary Phases

4.4.7.3.1. Material and Methods

Column Screen

Tab S2: Investigated columns including the dimension for the separation of proteinogenic amino acids.

Column	Dimension, Particle size
Phenomenex Kinetex HILIC	150 x 3.0 mm, 2.6 µm
Thermo Fischer, Biobasic AX	150 x 3.0 mm, 5µm
Agilent Technologies, Poroshell 120 HILIC Z	30 x 3.0 mm, 2.7 µm
Merck Sequant ZIC-HILIC	150 x 2.1 mm, 3.5 µm
Merck Sequant ZIC-cHILIC	100 x 2.1 mm, 3 µm
Macherey Nagel, Nucleoshell	50 x 4.6 mm, 2.7 µm
SIELC Coresep SB	50 x 4.6 mm, 2.7 µm
Chiralpak ZWIX(+)	150 x 3.0 mm, 3µm
Chrialpak ZWIX(-)	150 x 4 mm, 3 µm
Phenomenex Luna CN	150 x 4.6 mm, 3 µm

General experimental LC conditions:

Mobile phases:

A: ACN/H_2O/200mM NH_4FA in water, pH 3.5 adjusted with ammonia (50:45:5, v/v/v),

B: ACN/H_2O/200mM NH_4FA in water, pH 3.5 adjusted with ammonia (90:5:5, v/v), ,

Lin. flow vel.: 1.18 mm s^{-1}, T = 40°C

gradient: 0.0 - 5 min: 100 %B, 5 - 25 min: 0 %B, 25-30 min: 0 % B, 30 – 30.1 min: 0 - 100 %B, 30.1 - 40 min: 100 %B

Experimental LC conditions for Poroshell 120 HILIC-Z (30 x 3 mm, 2.7 µm):

Mobile phases:

A: 10 % 200 mM NH_4FA, pH 3 adjusted with FA, in H_2O;

B: 10 % 200 mM NH_4FA, pH 3 adjusted with FA, in ACN

Flow rate: 0.8 mL min^{-1}, T = 30 °C,

gradient: 0.0 – 10.0 min: 100-70 %B (compare legend), 10.0-10.1 min: 70-100% B, 10.1-15.0 min: 100 %B

Experimental LC conditions for ZWIX(+) (150 x 3 mm, 3 µm) and ZWIX(-) (150 x 4 mm, 3 µm):

mobile phases:

A: 9.4 mM NH_4FA in MeOH/ H_2O (98:2, v/v),

B: 9.4 mM NH_4FA in MeOH/ H_2O (49:51, v/v)

Flow rate: ZWIX (-): 0.45 mL min^{-1} , ZWIX (+): 0.28 mL min^{-1}, T = 30 °C, gradient: 0.0 – 18.0 min: 100 %B (compare legend), 18.0 – 40.0 min: 0 to 100 % B, 40.0-50.0 min: 100 %B, 50.0 - 50.2 min: 100 to 0 %B, 50.2 – 70.0 min: 100 %B [1]

ESI settings:

ESI settings: curtain gas (CUR) 35 psi, nebulizer gas (GS1) 60 psi, drying gas (GS2) 60 psi, source voltage (ISVF) 4000 V, source Temperature (T) 500 °C, the utilized gas was nitrogen,

The measurements were done in positive mode. Information dependent acquisition (IDA) was used. A TOF-MS scan (accumulation time 250 ms, scan window m/z: 35 to 1000, collision energy (CE) of 5 V, declustering potential (DP) 100 V, RF transmission m/z: 25 = 33%, 90 = 33 %, 290 = 34 %) was followed by four IDA experiments (accumulation time 50 ms, scan window m/z: 35 to 1000, collision energy (CE) of 30 V, declustering potential (DP) 100 V, RF transmission m/z: 25 = 50%, 90 = 50 %) resulting in a period cycle time of 500 ms.

Two Dimensional LC Experiments:

LC parameters:

^{1}D: ZWIX(+), 150 x 3 mm, 3 µm

A: H_2O, B: ACN, C: 200 mM NH_4FA / 400 mM FA in MeOH/H_2O (98:2, v/v) D:MeOH

Flow: 0.03 mL min^{-1}, 20°C, gradient profile: compare Tab S3.

Injection volume 5 µL (10 µg mL^{-1} AA in MeOH/ACN 20:80, v/v)

^{2}D: Poroshell HILIC-Z, 50 x 3 mm, 2.7 µm

A: 30% ACN, 20 mM NH_4FA, pH 3

B: 80% ACN, 20 mM NH_4FA, pH 3

Flow 1.0 mL min^{-1}, 30°C, gradient profile: compare Tab. S3.

40 µL Loops Modulation time 1.2 min, loop fill 90 %,

Tab S3: Investigated gradient profiles for the first and the second dimension. The mobile phases in the first dimension were: A: H_2O, B: ACN, C: 200 mM NH_4FA / 400 mM FA in MeOH/H_2O (98:2, v/v) D:MeOH and in the second: A: 30% ACN, 20 mM NH_4FA, pH 3 and B: 80% ACN, 20 mM NH_4FA, pH 3.

^{1}D							**^{2}D**	
Time [min]	**A [%]**	**B [%]**	**C [%]**	**D [%]**	**Flow [mL min^{-1}]**		**Time [min]**	**B [%]**
0	1.9	75	9.4	13.7	0.2		0	71.4
9	1.9	75	9.4	13.7	0.2		0.6	50
10	1.9	75	9.4	13.7	0.03		0.7	50
62	1.9	75	9.4	13.7	0.03		0.8	71.4
137	21.9	0	9.4	68.7	0.03		1.2	71.4
170	21.9	0	9.4	68.7	0.03			
172:2	1.9	75	9.4	13.7	0.03			
240	1.9	75	9.4	13.7	0.03			

After the column, the flow was split (1:11.6). The high flow path was directed to a DAD (λ = 280 nm) and a CAD veo (Thermo scientific). The low flow was directed to a high resolution mass spectrometer (Sciex QTOF 5600+) equipped with a DuoSpray Ionsource. The parameters were set as following.

MS parameter:

ESI settings: curtain gas (CUR) 30 psi, nebulizer gas (GS1) 50 psi, drying gas (GS2) 40 psi, source voltage (ISVF) 5500 V, source Temperature (T) 450 °C, the utilized gas was nitrogen,

The QTOF was operated in positive mode. Information dependant acquisition (IDA) was used as acquisition mode. One period cycle was 330 ms long and comprised a TOF-MS scan (accumulation time 200 ms, scan window m/z: 35 to 1000, collision energy (CE) of 5 V, declustering potential (DP) 100 V, RF transmission m/z: 25 = 33%, 90 = 33 %, 290 = 34 %) followed by four IDA experiments (accumulation time 20 ms, scan window m/z: 35 to 1000, collision energy (CE) of 30 V, declustering potential (DP) 100 V, RF transmission m/z: 25 = 50%, 90 = 50 %).

4.4.7.3.2. Results

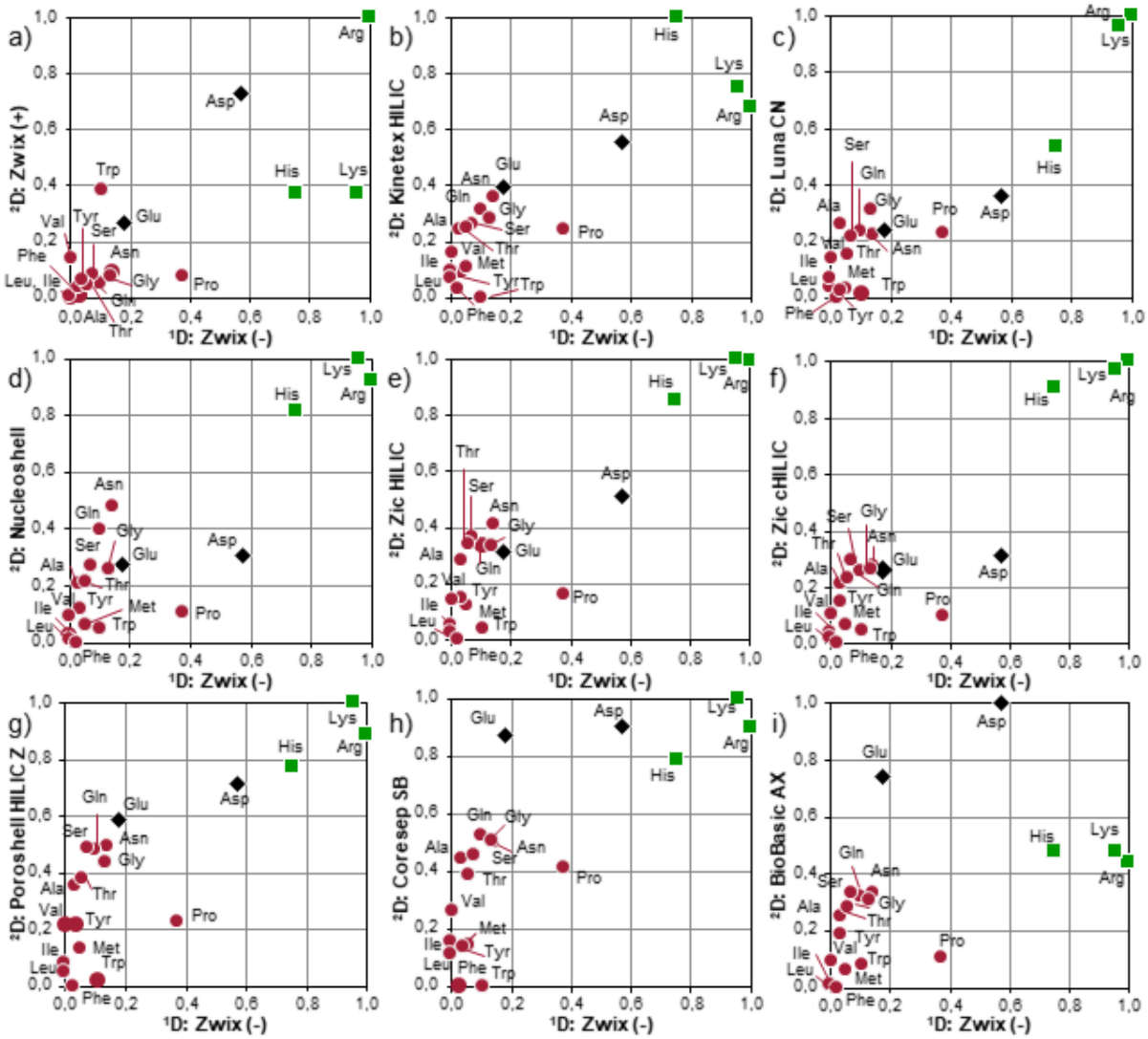

Fig. S3: Distribution of normalized retention times of proteinogenic amino acids in the two dimensional separation space of ZWIX(-) in ^{1}D and commercial HILIC (b-g) and mixed mode columns (a, h-i) in ^{2}D (normalized after Gilar [2]).

Screening conditions: compare Section 3.1.

Tab S4: Physicochemical properties of the investigated amino acids.

	pk_a (COOH)	pk_a (NH_4^+)	pk_a (3)	Isoelectric point (IP)	Log D (pH 3)	Net charge (pH 3)
Ala	2.47	9.48		5.98	-3.44	0.23
Arg	2.41	9.12	12.41	10.77	-6.4	1.3
Asn	2	8.43		5.22	-4.87	0.09
Asp	1.7	9.61	5.11	3.41	-4	0.04
Gln	2.15	9.31		5.73	-4.63	0.12
Glu	1.88	9.54	4.27	2.79	-3.77	-0.09
Gly	2.31	9.24		5.77	-3.95	0.17
His	1.85	9.44	6.61	7.69	-5.39	1.07
Ile	2.79	9.59		6.19	-2.24	0.38
Leu	2.79	9.52		6.15	-2.31	0.38
Lys	2.74	9.44	10.29	9.82	-7.17	1.12
Met	2.53	9.5		6.02	-2.93	0.25
Phe	2.47	9.45		5.96	-1.75	0.23
Pro	1.94	11.33		7.12	-3.16	0.45
Ser	2.03	8.93	15.17	5.7	-4.48	0.23
Thr	2.21	9	14.95	5.6	-4.08	0.14
Trp	2.54	9.4		5.97	-1.66	0.26
Tyr	2	9.19	9.79	5.51	-1.99	0.09
Val	2.72	9.6		6.16	-2.62	0.34

References

[1] J. Horak, M. Lämmerhofer, Stereoselective separation of underivatized and 6-aminoquinolyl-N-hydroxysuccinimidyl carbamate derivatized amino acids using zwitterionic quinine and quinidine type stationary phases by liquid chromatography-High resolution mass spectrometry, J Chromatogr A, 1596 (2019) 69-78.

[2] M. Gilar, P. Olivova, A.E. Daly, J.C. Gebler, Orthogonality of separation in two-dimensional liquid chromatography, Anal Chem, 77 (2005) 6426-6434.

4.5. Fragment-Based Design of Zwitterionic, Strong Cation- and Weak Anion-Exchange Type Mixed-Mode Liquid Chromatography Ligands and their Chromatographic Exploration

Martina Ferri [a,b #], Stefanie Bäurer [a #], Andrea Carotti [b], Marc Wolter [a], Belal Alshaar [a], Johannes Theiner [c], Tohru Ikegami [a,d], Caroline West [e], Michael Lämmerhofer [a,]*

[#] Shared first authorship

[a] Institute of Pharmaceutical Sciences, Pharmaceutical (Bio-)Analysis, University of Tübingen, Auf der Morgenstelle 8, 72076 Tübingen, Germany

[b] Department of Pharmaceutical Sciences, University of Perugia, Via del Liceo 1, 06123 Perugia, Italy

[c] "Mikroanalytisches Laboratorium", University of Vienna, Währinger Strasse 42, 1090, Vienna, Austria

[d] Department of Materials Synthesis, Faculty of Molecular Chemistry and Engineering, Kyoto Institute of Technology, Matsugasaki, Sakyo-ku, Kyoto 606-8585, Japan

[e] University of Orleans, Institute of Organic and Analytical Chemistry, CNRS UMR 7311, Rue de Chartres BP 6759, 45067 Orleans, France

Reprinted with permission from Journal of Chromatography A, Volume 1621 (2020) 461075, DOI: 10.1016/j.chroma.2020.461075

4.5.1. Abstract

The role of individual functional groups has been assessed with regard to surface charge and chromatographic retention. Coatings were prepared from various fragments of the chiral zwitterionic materials Chiralpak ZWIX(+) and ZWIX(-). The different chromatographic ligands allowed fine tuning of the surface charge. Chiralpak ZWIX phases showed strongly negative ζ-potentials over the entire pH-range. Zwitterionic congeners with quinuclidine and sulfonic acid moieties but lacking the quinolone ring in the ligand structure exhibited shifted ζ-potentials of around + 5 to 20 mV depending on the surrounding residues. Capillary electrophoretic mobilitiy measurements with the chromatographic ligands and molecular dynamics simulations were carried out to offer some explanation of these surface charge differences of the distinct zwitterionic stationary phases. The new mixed-mode phases were also chromatographically characterized by simple RP and HILIC tests. The results allowed their positioning within a large variety of different commercially available RP, HILIC and mixed-mode phases, which were evaluated as well, by multivariate data processing using principal component analysis. The new mixed-mode phases overall exhibit reasonable hydrophilicity-lipophilicity balance and enable retention of ionic compounds by additional ionic interactions through anion-exchange (WAX-type), cation-exchange (SCX-type) or both (RP/ZWIX-type). Hence, the new RP/ZWIX phases can be flexible tools for selectivity tuning in RP and HILIC separations.

4.5.2. Introduction

Mixed-mode chromatography (MMC) [1-7] has raised interest as an alternative LC separation mode to reversed-phase (RP) LC [8, 9] and hydrophilic interaction chromatography (HILIC) [10-12]. It combines distinct retention and separation principles, respectively, in one column. This can be accomplished by i) blending of distinct particles, e.g. RP particles and ion-exchangers (mixed bed), ii) mixing of chromatographic ligands with different retention principles on the same support (mixed-ligand), iii) distinct retention principles on one chromatographic ligand (mixed-mode ligand) [4]. Multimodality (e.g. applicability in RP, HILIC, cation exchange (CX), anion exchange (AX), ion-exclusion (IEC), hydrophobic interaction chromatography (HIC) [13]), orthogonality/complementarity to RP and HILIC, wider scope of application [2], enhanced flexibility in method development and optimization [13], and higher sample loading capacity compared to RP in preparative applications [14] are features of MMC phases. They have found applications for analysis of oligonucleotides [1, 15, 16], peptides [13, 14, 17-19], proteins [20], metabolites [2] and simultaneous analysis of pharmaceuticals and their counterions [4, 21], as well as for comprehensive analysis of natural products by multidimensional separations [22], and many more.

A number of distinct chromatographic modalities (i.e. retention principles) have been combined in MMC. For example, combination of size-exclusion with RP has been realized by so-called internal surface RP phases [23], HILIC with RP e.g. [24] or by the commercial column Acclaim Mixed-Mode HILIC-1 (from Thermo Fisher Scientific) [4]. Most commonly, however, ion-exchange is combined with RP or HILIC to yield RP/AX [1, 14, 16, 25-27], RP/CX [28], RP/ZWIX [29], HILIC/AX [30, 31], HILIC/CX [32], HILIC/ZWIX [33] phases (all available as either weak or strong ion-exchanger modalities). Trimodal phases combining e.g. cation-exchange, anion-exchange and RP have been proposed as well [4, 34, 35]. The combination of electrostatic repulsion with HILIC elution was termed ERLIC [36]. Many of the ionic liquid-derived LC phases [37] as well as several zwitterionic stationary phases [38] reported in the literature can also be classified as MMC phases. Further, more advanced mixed-mode phases have been proposed such as those combining chiral stationary phases with size exclusion principles (internal surface chiral stationary phase) [39, 40].

In general, chiral stationary phases can act per se as mixed-mode phases owing to their plurality of functional groups. Therefore, it is not surprising that they have been examined for challenging achiral applications [41-43]. In this work we explore the mixed-mode chromatography behavior of Chiralpak ZWIX(+) and ZWIX(-), i.e. cinchonan carbamate based chiral stationary phases decorated with cyclohexylsulfonic acid carbamate residues [44]. This chiral selector contains both anion (WAX) and cation exchanger (SCX) functionalities as well as hydrophobic moieties and can be classified as a RP/SCX/WAX trimodal mixed-mode phase (RP/ZWIX for short). To better understand the incremental contributions of the various interaction sites to the mixed-mode chromatography behavior, a fragment-based design was adopted to devise a series of structural analogs of this ZWIX-type MMC phase (Fig. 1). Thus, new RP/WAX, RP/SCX and RP/ZWIX type MMC phases were obtained which are characterized herein regarding their surface charge (pH-dependent ζ-potentials), multimodal applicability in RPLC and HILIC, hydrophilicity/lipophilicity balance (HLB) and anion- and cation-exchange capability. A benchmarking study was performed which allowed the classification of these phases among groups of commercial RP, HILIC and MMC phases. In addition, a molecular dynamics simulation was carried out to explain surface charge differences of the distinct zwitterionic stationary phases by conformational preferences of the different selectors.

4.5.3. Experimental

4.5.3.1. Materials

Chiralpak ZWIX(+) (150 × 3 mm ID, 3 µm) and ZWIX(-) (150 × 4 mm ID, 3 µm) were purchased from Chiral Technologies Europe (Ilkirch, France). The weak anion-exchange stationary phases QN-AX and QN were prepared as described elsewhere [45, 46]. Quinine, quincorine ((*2S,4S,5R*)-2-hydroxymethyl-5-vinyl-quinuclidine, QCI) and quincoridine ((*2R,4S,5R*)-2-hydroxymethyl-5-vinyl-quinuclidine, QCD) (all as free bases) were from Buchler (Braunschweig, Germany) (note, configurational descriptors are inconsistently used in the literature which may be confusing. The above terminology is identical to the CA index terminology (*1S,2S,4S,5R*)-5-ethenyl-1-azabicyclo[2.2.2]octane-2-methanol for quincorine, CAS registry number (RN) 207129-35-9, and (*1S,2R,4S,5R*)-5-ethenyl-1-azabicyclo[2.2.2]octane-2-methanol for quincoridine, CAS RN 207129-36-0).

The silica used for immobilization of the new chromatographic ligands was Daisogel 3 µm, 120 Å (DAISO Fine Chem GmbH, Düsseldorf, Germany). 3-Mercaptopropyl-modified silica was utilized for the immobilization of the chromatographic ligands and was synthesized as described previously [45]. 4-Nitrophenyl chloroformate, *N*,*O*-bis-(trimethylsilyl)acetamide (BSA), calcium hydride (CaH_2), taurine, 5-hexen-1-ol, 4-dimethylaminopyridine, and 3-mercaptopropyltrimethoxysilane were purchased from Sigma Aldrich (Munich, Germany). (*1R,2R*)- and (*1S,2S*)-*trans*-2-aminocyclohexane sulfonic acid (ACHSA) were kindly donated by Chiral Technologies Europe. Methanol (MeOH), hexane, diethyl ether, toluene and dichloromethane (DCM) used for the synthesis were technical grade and purchased from Brenntag (Essen, Germany). Acetonitrile (ACN) and methanol HPLC grade were used for HPLC analysis and ultrapure water was obtained by purification of demineralized water using Elga PureLab Ultra Purification System (Celle, Germany). Mobile-phase additives acetic acid, formic acid (FA), ammonium acetate (NH_4Ac) and trifluoroacetic acid (TFA) were of analytical grade (Sigma-Aldrich).

The analytes of the RP test, butylbenzene (BuB), pentylbenzene (PeB), *N-tert*-butoxycarbonyl-prolyl-phenylalanine (BocProPhe) and the reagents *O,O*-diethylthiochlorophosphate (DETCP) and triethylamine for the synthesis of *O,O*-diethylthiophosphate (DETP), and of the HILIC tests (theophylline (Tp), theobromine (Tb), uridine (U) and 2'-deoxyuridine (2dU), adenosine, cytidine, guanosine, thymidine, ascorbic acid, nicotinic acid, pyridoxine, riboflavin, thiamine), as well as the void volume markers 1,3,5-tri-*tert*-butylbenzene (TTBB) and toluene (for HILIC) were purchased from Sigma Aldrich (Munich, Germany).

4.5.3.2. Instrumentation and Software

The chromatographic tests were performed on an 1100 series HPLC instrument from Agilent Technologies (Waldbronn, Germany) equipped with a degasser, binary pump, column compartment with temperature control, a variable wavelength detector (VWD) and a charged aerosol detector (CAD, Thermo Scientific, Munich, Germany) or an Agilent Technologies LC MSD-SL ion-trap mass-spectrometer. Mobile phases for the chromatographic tests and other conditions are specified in respective figure captions.

Nuclear magnetic resonance (NMR) spectroscopy experiments were done on a Bruker Avance 400 MHz with methanol-d_4, DMSO-d_6, or $CDCl_3$ as solvents. The chemical shifts are described in ppm. The software MestReNova (Mestrelab Research, Santiago de Compostela, Spain) was used for data processing.

For chiroptical analysis, optical rotation (OR) was measured with an instrument from Anton Paar MCP 200 (Graz, Austria) at 589 nm (Na_{589}) using a 1 dm quartz cuvette with 1 mL volume.

Electrophoretic light scattering measurements for determination of the ζ-potentials were performed on a Zetasizer NanoZS particle analyzer equipped with a Universal Dip Cell (Malvern Instruments, Herrenberg, Germany). pKa values were calculated with Marvin Sketch (14.12.15.0). The software by SIMCA Multivariate Data Analysis Solution (Version 15.0.2.5959, Sartorius Stedim Data Analytics AB, Umeå, Sweden) was used for the principal component analysis with the following parameters: level of significance: 95 %, normalized in units of standard deviation, no weighting, autoscaled, centered.

4.5.3.3. Synthesis of the Chromatographic Ligands

The synthesis of the chromatographic ligands followed procedures as described for the ZWIX phases [44].

*General Procedure (A) for the synthesis of carbonate derivatives **1**, **2** and **3**:*

To a solution of the appropriate alcohol, quincoridine, quincorine or 5-hexen-1-ol, (8.97 mmol) in dry toluene (56 mL) 4-nitrophenyl chloroformate (1.8 g, 9.06 mmol) was added portionwise. A precipitate was quickly formed after addition of the chloroformate. To complete the reaction, it was stirred at room temperature for 16 hours. The precipitate was collected by filtration and washed with *n*-hexane (3 × 20 mL). The solid residue was dried under vacuum at room temperature for 16 hours. The desired product was used directly for the next step without further purification because of limited stability.

*(2R,4S,5R)-2-[(4-Nitrophenyloxycarbonyl)oxy]methyl)-5-vinylquinuclidin-1-ium chloride (**1**)*

Starting from quincoridine (1.5 g, 8.97 mmol) and 4-nitrophenyl chloroformate (1.8 g, 9.06 mmol) following the general procedure A, the desired product 1 was obtained as white solid (3.02 g, yield 91 %).

*(2S,4S,5R)-2-([(4-Nitrophenoxycarbonyl)oxy]methyl)-5-vinylquinuclidin-1-ium chloride (**2**)*

Starting from quincorine (1.5 g, 8.97 mmol) and 4-nitrophenyl chloroformate (1.8 g, 9.06 mmol) following the general procedure A, the desired product 2 was obtained as white solid (3.74 g, yield 100 %).

*Hex-5-en-1-yl (4-nitrophenyl) carbonate (**3**)*

Triethylamine (Et_3N) (5.4 mL, 38.85 mmol) was added to a solution of hex-5-en-1-ol (1.3 g, 12.95 mmol) in dry DCM (45 mL). Afterwards, the mixture was cooled to 0°C and 4-nitrophenyl chloroformate (2.9 g, 14.24 mmol) was added in one portion. The reaction was stirred at room temperature for 16 hours. Then, the reaction mixture was directly used for the next step without any purification step. An aliquot, however, was purified for characterization. For this purpose, the reaction was diluted with DCM and it was washed with aqueous 10% citric acid (3 × 20 mL) and aqueous saturated $NaHCO_3$ (3 × 20 mL). The organic phase was dried over Na_2SO_4, filtered and concentrated under reduced pressure. The desired product **3** was obtained as yellowish oil (3.46 g, 40% yield) and it was used directly for the next step. ^{1}H-NMR ($CDCl_3$, 400 MHz) δ 1.46-1.62 (m, 3H), 1.76-1.84 (m, 2H), 2.06-2.17 (m, 2H), 4.32 (t, Jt = 6.8 Hz, 1H), 4.96-5.08 (m, 2H), 5.78-5.88 (m, 1H), 7.40 (d, Jd = 9.2 Hz, 2H), 8.30 (d, Jd = 9.2 Hz, 2H).

General Procedure (B) for the synthesis of carbamate derivatives 4 – 9 (selectors of QCDRR (4), QCISS (5), QCDTAU (6), QCITAU (7), SS-ACHSA (8) and TAU (9)):

To a finely ground suspension of the appropriate 2-amino-1-sulfonic acid (5.96 mmol) in dry DCM (100 mL), BSA (4.4 mL, 17.88 mmol) was added dropwise. Then the mixture was stirred and heated to reflux (42°C) for 48 hours. After this time, the reaction was cooled to room temperature and the appropriate carbonate derivative (***1-3***) (2.20 g, 5.96 mmol) was added portionwise. Stirring of the reaction was continued for 16 hours at room temperature. Then the mixture was cooled to room temperature, quenched with MeOH (3 mL) and stirred for a few more minutes. The reaction was filtered in order to eliminate unreacted free amino sulfonic acid. The organic phase was concentrated under vacuum and the crude product was purified through further work up.

In detail, for compounds **4-7**, the main impurity, 4-nitrophenol, was removed by liquid-liquid extraction with basified water (saturated solution of NaHCO3, pH 8) and ethyl acetate. Then, the aqueous phase, which was produced after extraction with ethyl acetate, was firstly acidified

with HCl (3 mol/L) (pH adjusted to approx. 5/6), concentrated under vacuum and co-evaporated several times with ethanol (note, the product turned out to be too polar to be extracted from water with organic solvents; possibly salting out with ammonium or sodium sulfate could improve extraction yields but was not tested in this work). The product was then solubilized in DCM/MeOH. After that, it was filtered in order to eliminate inorganic salts and concentrated under vacuum. Finally, the product was dried under vacuum at room temperature over the weekend.

For compounds **8** and **9**, flash chromatography on RP phase (C18-modified silica, mobile phase methanol/water) was employed for further purification and removal of 4-nitrophenol.

4.5.3.4. Immobilization of the Ligands on Thiol-Modified Silica Particles

Typically 2.0 g of the thiol-modified silica gel were suspended in MeOH (8 mL), degassed and added to a solution of the chiral selector (0.3 mmol/g of silica, except for WAX-type QN phase 0.25 mmol/g) in MeOH (4 mL) under nitrogen. Then, azobisisobutyronitrile (AIBN 4 mM, 8 mg) was added to the mixture and it was heated to reflux (66°C) for 7 hours under nitrogen with mechanical stirring. The modified silica was isolated by filtration (glass filter funnel porosity 4) and washed with hot methanol (4 × 3 mL). It was dried in the vacuum oven at 65°C for 24 hours. The modified silica gels were subjected to elemental analysis and the results are given in Table 1.

Table 1. Elemental analysis data and selector coverages of the new mixed-mode stationary phases.

Chromatographic ligand (selector)	Class	C(%)	H(%)	N(%)	S(%)	Coverage (µmol/g)
QN	WAX	8.85	1.34	0.69	2.07	236
QCITAU	ZWIX	8.35	1.73	0.68	2.37	236
QCDTAU	ZWIX	8.03	1.69	0.61	2.35	211
QCISS	ZWIX	8.61	1.77	0.55	2.36	190
QCDRR	ZWIX	8.96	1.80	0.6	2.41	208
SS-ACHSA	SCX	5.81	1.32	0.32	2.50	199
TAU	SCX	5.63	1.41	0.23	2.71	146
Mean (of all SPs)						204
Standard deviation						31

The modified silica gels were finally slurry packed into stainless steel columns (150 × 3 mm ID).

4.5.3.5. ζ-Potentials

pH-Dependent ζ-potential determinations were carried out with a suspension of 0.2 mg/mL particles in 10 mM KCl solutions containing 1 mM of the following buffers: formic acid/sodium formate, acetic acid/sodium acetate, histidine (titrated with HCl to pH), tris/tris-HCl, boric acid/sodium borate. The dip cell was thermostated to 25°C. All measurements were performed in triplicates. The Von Smoluchowski equation (Supplementary, Equ. S1) was used for the calculation of the ζ-potentials.

4.5.3.6. Determination of Effective Electrophoretic Mobilities by CE

The effective mobility of the analytes was determined by capillary electrophoresis using a Hewlett Packard 3D Capillary Electrophoresis system (Agilent, Waldbronn, Germany) at different pH values. The background electrolytes were the same as described above for the ζ-potential measurements (10 mM KCl in 1 mM buffer solutions). Thiourea was used as EOF marker. Experiments were carried out in positive mode, applying a voltage of 15 kV, or in negative mode, applying a voltage of -10kV, respectively, using a bare fused-silica capillary (ID 50 µm) of 50.5 cm total length and 42.0 effective length. The temperature was adjusted to 20°C and detection was carried out at 210 nm for all analytes except for SS-ACHSA. For experiments with SS-ACHSA 0.5 mM sodium p-toluene sulfonate was added to the buffer systems and SS-ACHSA was detected by indirect UV detection at 200 nm (Ref. 235 nm). Hydrodynamic injection was performed by applying 50 mbar for 5 s. Preconditioning was done by flushing the capillary with 0.1 M NaOH for 2 min, followed by MilliQ water for 2 min and finally with the respective buffer for 3 min prior to each run. Postconditioning was done by flushing the capillary for 3 min with MilliQ water at the end of each run.

4.5.3.7. Molecular Modelling Methods

The Maestro 12.1 graphical interface of the Schrödinger Suite 2019-3 (Schrödinger, LLC, New York, NY) was used. As reported in the previous work [47] a cubic box was built with a 30 Å side length. For a realistic reproduction of the stationary phase environment, four 3-mercaptopropyl-functionalized silanols (~1.97 mol m^{-2}), eight free silanols (~8.0 mol m^{-2}) and forty-five silicon atoms were considered for each grafted selector (SO) unit (~0.5 mol m^{-2}), at the base of the box. All the silicon atoms and their bonded hydrogen atoms in the base layer were set frozen during the molecular dynamics. The box was solvated with water. The three simulations with the three CSP systems were performed in the canonical ensemble at 298 K. The temperature in the simulation cell was maintained constant through use of a Nosé-Hoover thermostat [48,49]. All the other parameters in the simulation study were left to default values

in the Desmond Molecular Dynamics System (version 5.9, Schrödinger, LLC, New York, NY) present in the Schrödinger Suite 2019-3 [50]. A production run produced 3000 frames during the 1 μs dynamics, with an integration time of 2 fs. All the conformations of the three simulated SOs, namely ZWIX(+), QCISS and QCITAU, were extracted by each frame and used to calculate different molecular properties. In particular, intramolecular salt-bridges (SB) and H-bonds (HB) were counted for each conformation analyzed, together with the relative conformational energy of the SO (SELF-SO, obtained subtracting the energy minima recorded along the trajectory by the energy of the frame, in kcal mol^{-1}), and the Polar Surface Area (PSA, in $Å^2$). The latter surface descriptor was calculated by the QikProp package (version 6.1, Schrödinger, LLC, New York, NY, 2019). A *k-mean* clustering protocol using KNIME 4.0 software (KNIME, Konstanz, Germany) was used on three numeric matrices containing the frame number, the SELF-SO and the distance measured between the sulfur atom of the sulfonic acid group and the nitrogen of the quinuclidinium moiety of each frame. Five clusters were set and plotted as a bubble graph.

4.5.4. Results and Discussion

4.5.4.1. Design, Synthesis of Ligands and Immobilization by Thiol-ene Click Reaction

The design of the new WAX-type, SCX-type and ZWIX-type MMC ligands is outlined in Fig. 1. It was based on the fragmentation of the Chiralpak ZWIX(+) (quinine-derived; *1S,3R,4S,8S,9R*) and ZWIX(-) (quinidine-derived; *1S,3R,4S,8R,9S*) selectors [44]. Leaving out the 2-sulfocyclohexyl residue of ZWIX(+) along with its carbamate moiety yielded a WAX-type ligand and quinine-based stationary phase, respectively. Its chiral separation capability was already described previously [45, 46, 51]. Replacement of the 2-sulfocyclohexyl moiety of ZWIX(+) by a *tert*-butyl carbamate residue gave the WAX-type ligand which is part of the commercial chiral stationary phase Chiralpak QN-AX and served as reference material in some of the following studies. ZWIX(+) and ZWIX(-) have a bulky, hydrophobic methoxyquinoline ring. Upon its removal, ligands retaining their zwitterionic nature, thus termed RP/ZWIX-type, were obtained. They have been synthesized from either quincorine (QCI) or quincoridine (QCD) (with configurations as in quinine and quinidine, respectively, but one stereogenic center less; see experimental section for specification of absolute configurations). WAX-type quincorine-derived ligands have been proposed as chemoaffinity type stationary phases for plasmid DNA isoform and topoisomer separations [52]. Through this structural change the resultant RP/ZWIX selectors, QCISS and QCDRR, lose their π-π-interaction capabilities and further a steric barrier which may significantly influence their conformational flexibility. By replacement of the 2-sulfocyclohexyl residue by a 2-sulfoethyl residue, taurine-derived zwitterionic RP/ZWIX-type MMC materials, termed QCITAU and QCDTAU, were obtained having four carbons less. Taurine-analogs of Chiralpak ZWIX have been reported by Lindner and coworkers as zwitterionic chiral stationary phases [44]. Taurine-derivatized polyaspartamide-modified silica is a commercial SCX-type stationary phase (Polysulfoethyl A) [53] frequently used as first dimension separation material in 2-dimensional peptide separations. In order to further explore the influence of the quinuclidine moiety of the QCI/QCD-derived RP/ZWIX phases on retention profiles and MMC behavior, respectively, it was replaced by 5-hexen-1-ol as O-carbamate residue resulting in SCX-type MMC ligands (SS-ACHSA and TAU) (Fig. 1). The synthesis of these RP/ZWIX and RP/SCX MMC ligands followed the procedures reported by Hoffmann et al. for ZWIX(+) and ZWIX(-) [44]. Reaction schemes can be found in the suppl. material and detailed protocols for ligand synthesis in the experimental part.

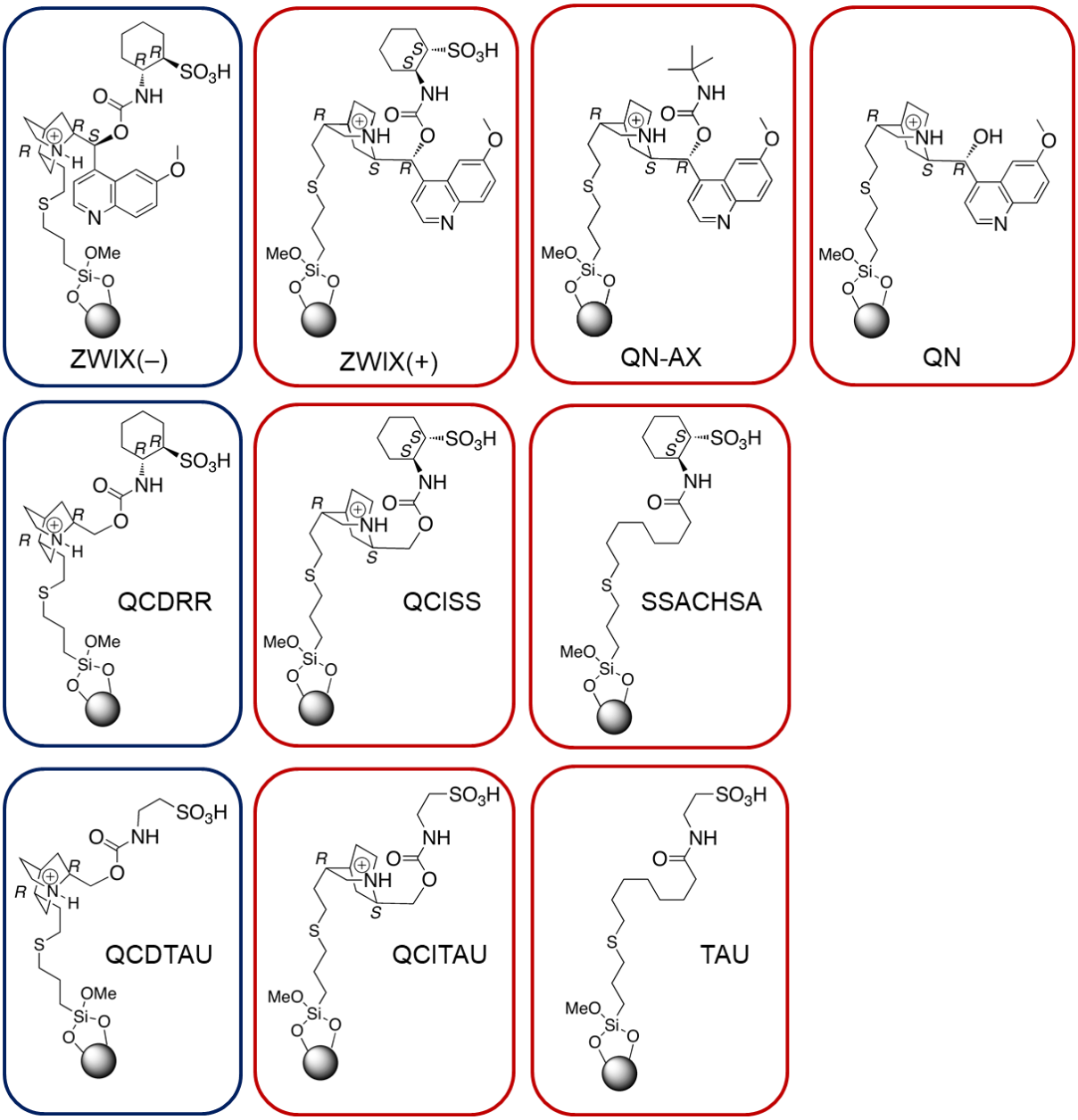

Fig. 1: Surface chemistries of the investigated zwitterionic, strong cation and weak anion-exchange type mixed-mode stationary phases.

All new MMC selectors were immobilized on 3-mercaptopropyl-modified silica (Fig. 1) following a well-established procedure which allows adjustment of dedicated selector coverages, whereby herein a ligand coverage of 200 µmol/g was targeted. Thiol-ene click reaction using thermal initiation and azobisisobutyronitrile (AIBN) as radical initiator was employed (see Experimental for details). In general, 68±16% of the ligand added to the reaction mixture was bonded to the thiol silica, as confirmed through elemental analysis. The detailed results of the elemental analysis and the calculated selector coverages are given in Table 1. It can be seen that all ligand coverages are in a comparable range (204±31 µmol/g; mean and standard deviation over all distinct phases listed in Table 1).

4.5.4.2. ζ-Potentials

In mixed-mode chromatography, the surface charge of the chromatographic particles under employed conditions plays a decisive role for the separation of charged compounds. It can be conveniently characterized by pH-dependent ζ-potential determinations using electrophoretic light scattering measurements as recently proposed [16, 26, 54-57]. Particles with charged surface suspended in electrolyte solutions (e.g. buffered mobile phases) build up an electrical double layer which consists of a uniform layer of counter-ions (Stern layer) followed by a heterogeneous layer of mixed ionic species at the surface. In this diffusive layer counterions are enriched as compared to the solution surrounding the solvated particle in which the ions are in equilibrium like in the employed background electrolyte solution. If an electric field is applied, the charged particles will start moving in the solution and a shear plane is formed on the solvated particle. The potential at this slipping plane is defined as the ζ-potential [58-60] and can be used to characterize the surface charge of the particles in presence of the given electrolyte solution. The particle radius of the investigated MMC materials is large compared to the thickness of the double layer, which can be characterized by the Debye length (1/κ), i.e. κr >> 1. For such cases, the Smoluchowski model for calculation of the ζ-potentials (see Suppl. Material chapter 2 for more details) is considered valid under the assumption that complications arising from particle porosity, surface conductance and surface roughness are negligible under the employed conditions. Since ionizable groups on the surface can change their dissociation state under different chromatographic conditions, determination of ζ-potentials over a wide pH-range typically employed in LC is most meaningful and was performed between pH 3.5 and 9.5 with 1 mM buffers in 10 mM KCl to keep ionic strength constant during all measurements. The results are depicted in Fig. 2.

The WAX-type QN and QN-AX phases behave quite similarly in terms of their ζ-potentials (Fig. 2a). They showed positive ζ-potentials at low pH values due to the presence of the tertiary amine of the quinuclidine ring (pK_a (QN/QN-AX) = 8.91/8.43, pK_a (QN/QN-AX) of quinoline = 4.06/4.08 as calculated with Marvin Sketch 14.12.15.0). In general, ζ-potentials of these WAX-type materials remained positive up to pH 7.5 and turned negative due to the dominating influence of residual silanols at pH above 8.

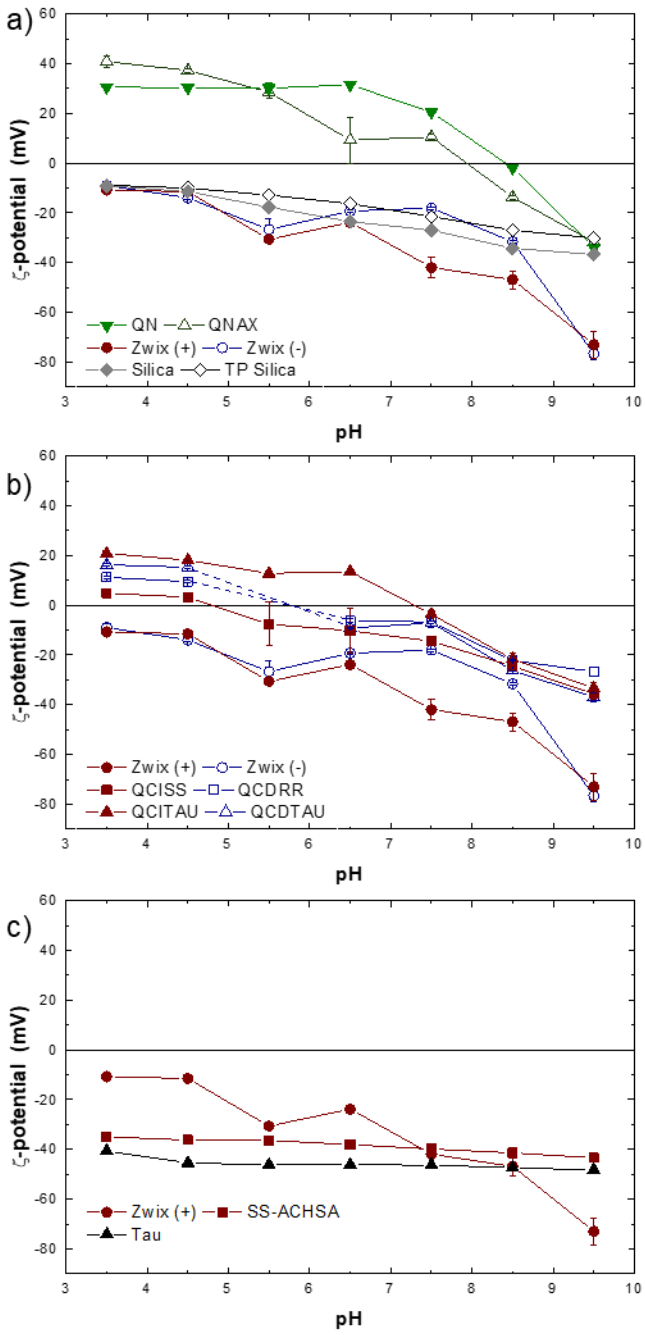

Fig. 2: ζ-Potentials determined in dependence of pH. (a) Cationic selectors (QN, QN-AX) in comparison to ZWIX(+), ZWIX(-) and supporting silica as well as thiol-modified silica, (b) all zwitterionic selectors in comparison, (c) anionic ligands in comparison to ZWIX(+).

The introduction of the sulfonic acid moiety (pK_a = -0.97, calculated with Marvin Sketch) of the 2-sulfocyclohexyl residue in ZWIX(+) and ZWIX(-) resulted in a significant negative offset of the ζ-potentials of around -30 to -50 mV thus adopting negative values over the entire pH range. It indicates a negative surface charge and demonstrates that it is mainly dominated by the fully dissociated sulfonic acid moiety. This is in line with former publications on zwitterionic stationary phases for HILIC, such as ZIC-HILIC [61], which have shown that these materials are cation-exchangers under low ionic strength conditions, i.e. at salt levels below 20 mM [62].

This observation has been often ascribed to the proximity of the anionic group (the sulfonate) of the ligand on the surface while the cationic moiety is shielded in the interior on these stationary phases. However, inversion of the cationic and anionic groups of the ligand, e.g. in ZIC-cHILIC did not lead to surface charge reversal; ZIC-cHILIC still exhibits negative ζ potential, albeit not as extreme as that of ZIC-HILIC [63, 64]. Fragmentation of the ZWIX selector was supposed to give additional insight.

Thus, Fig. 2b compares all the QCI/QCD-derived RP/ZWIX phases with Chiralpak ZWIX(+) and ZWIX-(-). By eliminating the quinoline ring of ZWIX(+) and ZWIX(-), respectively, furnishing quincorine- (QCI) and quincoridine-derived (QCD) MMC phases with 2-sulfocyclohexyl residue (QCISS and QCDRR) a significant positive shift in ζ-potentials of around +15 to +20 mM was observed yielding positive values in the pH range < 5. Above pH 5 the surface charge changed its sign and was still negative indicating that there is a pH-dependent charge reversal at mild conditions easily possible in these materials. Upon replacement of the 2-sulfocyclohexyl residue by a 2-sulfoethyl group furnishing QCITAU and QCDTAU a further but smaller positive shift of the ζ-potentials of around 5 to 15 mV was found. For the quincorine-derived taurine-based QCITAU, relatively stable ζ-potentials of around +20 mV were obtained in the pH range between 3.5 and 6.5. The ζ-potential of this material turned negative only above pH 7. Overall, it appears that group contributions are largely additive but there are some interesting delicate group effects which are not simple to explain. For instance, the absence or presence of the quinoline ring does not explain the large shift between ZWIX(+)/ZWIX(-) and QCI/QCD phases. It is hypothesized that due to the quinoline ring conformational freedom of the ZWIX selectors is constrained which presents this selector in an extended open conformation exposing the sulfonate moiety towards the outer surface of the particles and the positively charged quinuclidinium ring closer to the interior i.e. silica surface. Since 1:1 intramolecular ion-pair formation is not easily possible in this ligand due to constrained conformations, the surface is net negatively charged from the dominating effect of the surface sulfonate (SCX). On the other hand, absence of the quinoline ring gives the QCI- and QCD-derivative much larger conformational flexibility. This should enable much better intramolecular charge saturation by intramolecular ion-pair formation. Consequently, the sulfonate moiety gets less exposed to the surface leading to less negative or even positive ζ-potentials. The effect seems to be more pronounced in the corresponding QCI/QCD-TAU ligands in which the sulfonic acid side chain is less constrained compared to the sulfocyclohexyl side chain, thus favorable for intramolecular ion-pair formation and charge compensation.

Fig. 2c depicts the ζ-potentials of SCX-type MMC materials in comparison to ZWIX(+). The SCX-type MMC phases SS-ACHSA and TAU have a stable negative ζ-potential of around -40 mV over the entire pH range. On the contrary, the weak anion exchange moiety of ZWIX(+)

has a modulating effect which depends on the pH owing to its weakly basic quinuclidine group that changes its dissociation state over the investigated pH range.

Notably, the ζ-potentials (around pH 5) agree relatively well with the LSER d- terms recently measured by SFC on the same set of columns [65] which validates that the above presented ζ-potential measurements are representative also for the employed chromatographic situations. In general, the currently investigated MMC stationary phases differ not only in surface hydrophilicity/hydrophobicity but also in surface charge. Thus, a set of new mixed-mode ion-exchangers becomes available which will allow a fine tuning of separations due to their slightly distinct surface charge character.

4.5.4.3. Net Charge of Zwitterionic Selectors as Measured by Electrophoresis

To deconvolute the contribution of silica and of surface effects (selective ion accumulation effects on the surface) from the net charge of the chromatographic ligands, electrophoretic measurements of the ligands attached to thiol silica were performed in free solution by CE using the same background electrolyte (BGE) as for ζ-potential determinations. Fig. 3a shows the results of the determination of effective electrophoretic mobilities of the ligands in dependence on the pH of the BGE. The cationic ligands QN and QN-AX exhibit positive mobilities over the entire pH range (except for QN-AX at pH 9.5). The lower mobilities of QN-AX (with its *tert*-butylcarbamoyl residue) can be explained by a larger hydrodynamic radius. On the other hand, the anionic ligand SS-ACHSA has stable negative mobilities over the entire investigated pH-range, as expected. The ZWIX ligands possess positive mobilities in the pH range 3.5 to 4.5, negative mobilities in the pH range 7.5 to 9.5 and migrate with the electroosmotic flow (EOF) between pH 5.5 and 6.5. QCISS and QCITAU migrate with the EOF over the entire pH-range (Fig. 3a). These results seem to disprove that the excess negative charge of the ZWIX phases revealed by above ζ-potential measurements is due to excess negative charge on the zwitterionic selectors.

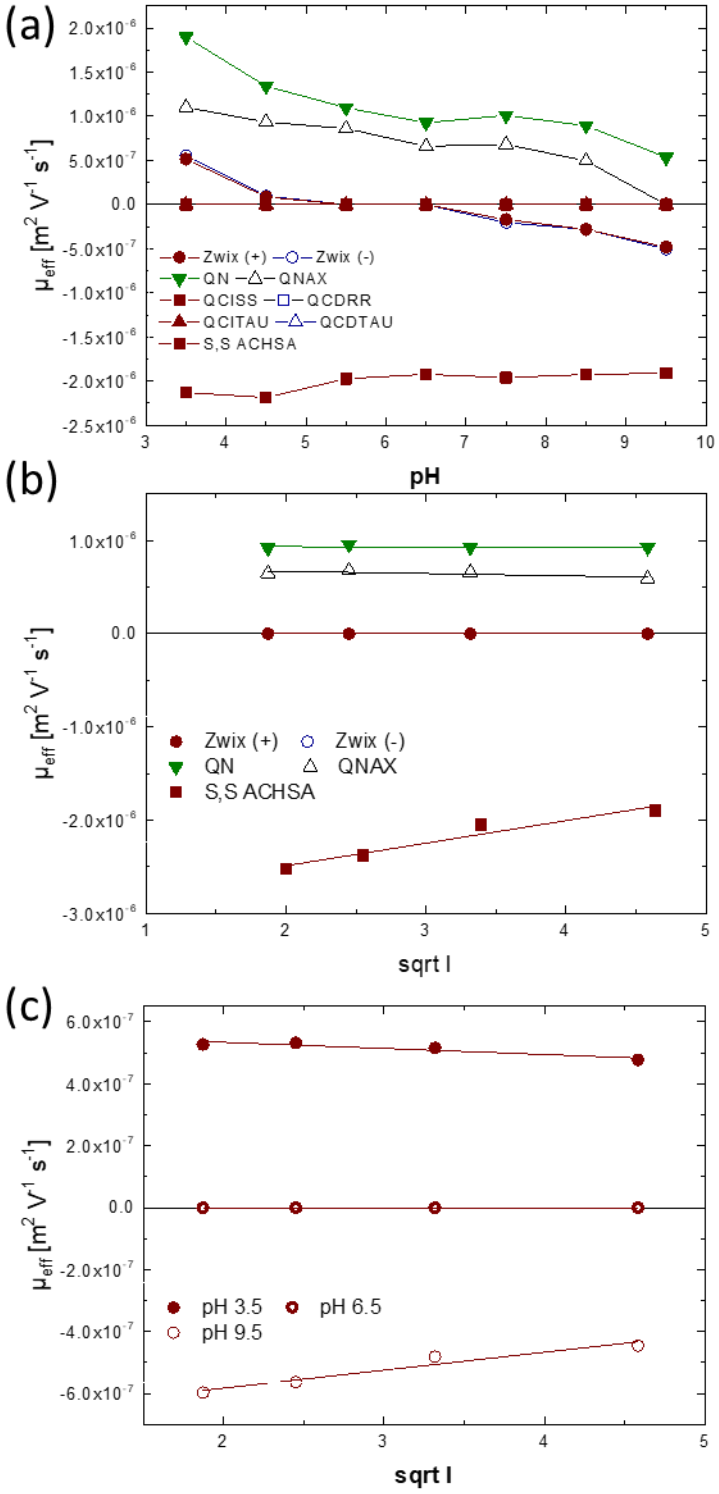

Fig. 3. Effective electrophoretic mobilities of ligands in free solution by CE using the same electrolytes as for ζ–potential measurements in Fig. 2 . (a) Effective mobilities at 10 mM KCl in 1 mM buffer, (b) selected ligands and their change in effective mobilities with ionic strength at pH 6.5, (c) effect of ionic strength on effective mobilities of ZWIX(+) at three different pH-values (3.5, 6.5 and 9.5).

The question then arises why differences in the ζ-potentials are observed between ZWIX(+), QCISS and QCITAU in spite of their same number and type of ionizable groups (always quinuclidinium and sulfonate) in the same bonding distance (always same 7 atom spacer between N^+ and sulfonate), respectively. A concept worth considering is the chaotropic effect.

It is known that the elution order in ion chromatography is from least to most chaotropic, i.e. chaotropes give stronger electrostatic interactions than kosmotropes [30]. Alpert has pointed out [66] that chaotropic ions are less well hydrated than are kosmotropic ions. This correlates with the strength of ionic interactions. This phenomenon also accounts for the worse retention of chaotropes in HILIC [30]. Chaotropic and kosmotropic effects are well described for inorganic ions but unfortunately our understanding of such lyotropic and solvation effects is not very well developed for organic molecules. It is therefore difficult to apply to the current situation but may play a role. Another effect, however, may be invoked as well. Materials with zwitterionic functional groups lose their ion-exchange capacity when the mobile phase contains a sufficiently high concentration of salt. The mechanism is that the concentration of potential counterions is high enough to titrate the charged groups of the bonding. Distinct ionic functionalities may be differently solvated and may have different affinities for counterions [30]. Pavel Nesterenko claimed in his work on ion chromatography media that cationic groups (amines) are titrated at significantly lower concentrations of salt than are anionic groups [38]. In fact, this would account for the net negative potential exhibited at low salt concentrations by both ZIC-HILIC, ZIC-cHILIC and related media such as current ZWIX materials; the amine groups (here quinuclidinium) are titrated by their counterions at lower salt concentrations than are the acidic groups (here, sulfonates). The low salt concentrations that is used herein for ζ-potential measurements would tend to accentuate this disparity. It is conceivable that the difference between ZWIX, QCISS and QCITAU can be explained in these terms notwithstanding the structural elements (quinuclidinium and sulfonate) being the same, just due to distinct solvation effects originating from different neighbor moieties. A disparity in polarity (and hydration) between the taurine ligand in QCITAU and the cyclohexylsulfonate ligand in QCISS could lead to the effect that they are titrated at different concentrations of counterions. Therefore, their charge potentials would differ at low concentrations of salt. However, it may be argued that if this is the case it should be visible by electrophoretic mobilities as well which were performed under the same conditions. Obviously, this is not the case, as can be seen from Fig 3a, i.e. the curve for ZWIX selectors; unlike ζ-potentials of the modified particles, effective mobilities of the mere ligands do not exhibit a negative sign over the entire pH range.

In order to have a deeper look into the ion titration effect, electrophoretic mobilities were measured at distinct ionic strengths (Fig. 3b and 3c). A convenient way to test for the ion titration effect, i.e. the change in effective charge with ionic strength, is to apply the Debye-Hückel-Onsager (DHO) limiting law of conductance and its transformation into mobilities [67]. In a simplified form it is written as a function of the ionic strength according to (Eq. 1)

$$\mu_{act,i} = \mu_{0,i} - A\sqrt{I} \quad (1)$$

wherein *A* is the Onsager slope, *I* the ionic strength, $\mu_{act,i}$ and $\mu_{0,i}$ are the actual and absolute electrophoretic mobilities at actual and zero ionic strength. For sake of simplicity, we report ionic strength effects for effective mobilities μ_{eff} which are related to $\mu_{act,i}$ by Eq 2

$$\mu_{eff} = \frac{\sum_{k=1}^{n} c_k \cdot \mu_{act,i} \cdot z_k}{c} \quad (2)$$

Wherein, for a compound with *n* ionic forms, c_k, z_i and *c* are the concentration and charge number of the kth ionic species and *c* the total concentration of the compound. Mobilities depend on the ion-solvent interactions which determine the size of the solvated ions and thus the Stokes radii for frictional resistance. They further depend, amongst other things, on ion-ion interactions between analyte ion and ionic species of the BGE which reduce the mobility in solutions with finite ionic strength relative to the limiting case at infinite dilution. These ion–ion interactions were initially described by the theory of Debye, Hückel and Onsager, based on the model of the ion cloud with the introduction of electrophoretic and relaxation effects (see Eq. 1). It was recently reported that the Onsager slope A of mobility vs $\sqrt{I}$ is linearly correlated with the solute charge. Herein, we use this relationship to get an idea whether the cationic site (quinuclidine) and anionic site (sulfonate) are titrated to different extents. The absolute values of effective mobilities at zero ionic strength depend on solvation effects and hydrodynamic radius and are not suitable parameters for such a comparison. However, the slope of the simplified Onsager Eq. 1 at pH 6.5 for individual selector moieties (QN and SS-ACHSA) might give some indication for this effect (note, in the zwitterionic ZWIX(+) selector the two contributions cancel out each other completely, giving 0 effective mobilities). K^+ and Cl^- have about the same hydrodynamic radius (K^+ 1.25 Å and Cl^- 1.20 Å, [68]) and same charge number; they should therefore be equivalent in strength for titrating respective counterions. The graphical results are given in Fig. 3b for pH 6.5. It can be seen that the ion-ion titration effect as revealed by the Onsager slope is stronger for the sulfonate compound (SS-ACHSA) than the quinuclidinium compound (QN), which does not support the idea that ammonium ions are titrated at lower concentrations than anions. The same trend is seen for the ZWIX(+) selector in Fig. 3c for different pH values (pH 3.5 and 9.5) which again shows that the ZWIX selector in its anionic form is stronger affected by titration with counterions than in its cationic form at pH 3.5. Unfortunately, the relevant zwitterionic selectors (ZWIX, QCISS, QCITAU) do not show any mobility at pH 6.5 (i.e. the opposite charges fully compensate each other) and therefore a direct proof of the counterion tirtration effect in zwitterionic selectors is not possible by this method. However, it can be concluded that other factors could play a role as well.

4.5.4.4. Molecular Modelling

The distinct surface charges of the zwitterionic phases under investigation, as measured by ζ-potentials, cannot be sufficiently explained by the immobilized functional groups alone and above considerations. Molecular modeling was therefore selected to support the hypothesis raised above that conformational differences and intramolecular ion-pairing are responsible for distinct surface net charges. In particular, molecular dynamics (MD) calculations were performed for three selectors: ZWIX(+), QCISS, QCITAU.

From the MDs, 3000 frames were extracted for each selector and individually analyzed counting the intramolecular salt-bridges (SB) and H-bonds (HB) present in that specific conformation, together with its PSA (polar surface area). The HB and SB measurement results are reported in a bar graph in Suppl. Material. From Suppl. Fig S19 it is possible to note that the sum of the intramolecular interactions (HB+SB) is larger for QCITAU (793) than ZWIX(+) (733), which in turn is larger than for QCISS (713). Comparing the exposed polar surface area of the selectors may give some idea about the compactness of the chromatographic ligand. Indeed, the mean polar surface area (PSA) is 142 (±2.9) $Å^2$ for ZWIX(+), 125.3 (±3.7) $Å^2$ for QCISS and 130.4 (±3.4) $Å^2$ for QCITAU. In general, QCITAU displays a high number of intramolecular interactions (HB+SB) and a quite low PSA exposed. On the other hand, QCISS has similar HB+SB value compared to ZWIX(+), but a lower PSA exposed. However, these data do not fully explain the trends in surface charge shown in Fig. 2.

For this reason, a different analysis was performed. Each of the three series of 3000 molecules, one for each SO trajectory, were clustered (k-mean) into 5 groups according to the frame relative conformational energies (SELF-SO) and the distance measured between the sulfur atom of the sulfonic acid group and the nitrogen of the quinuclidinium moiety. The results are shown in Fig. 4.

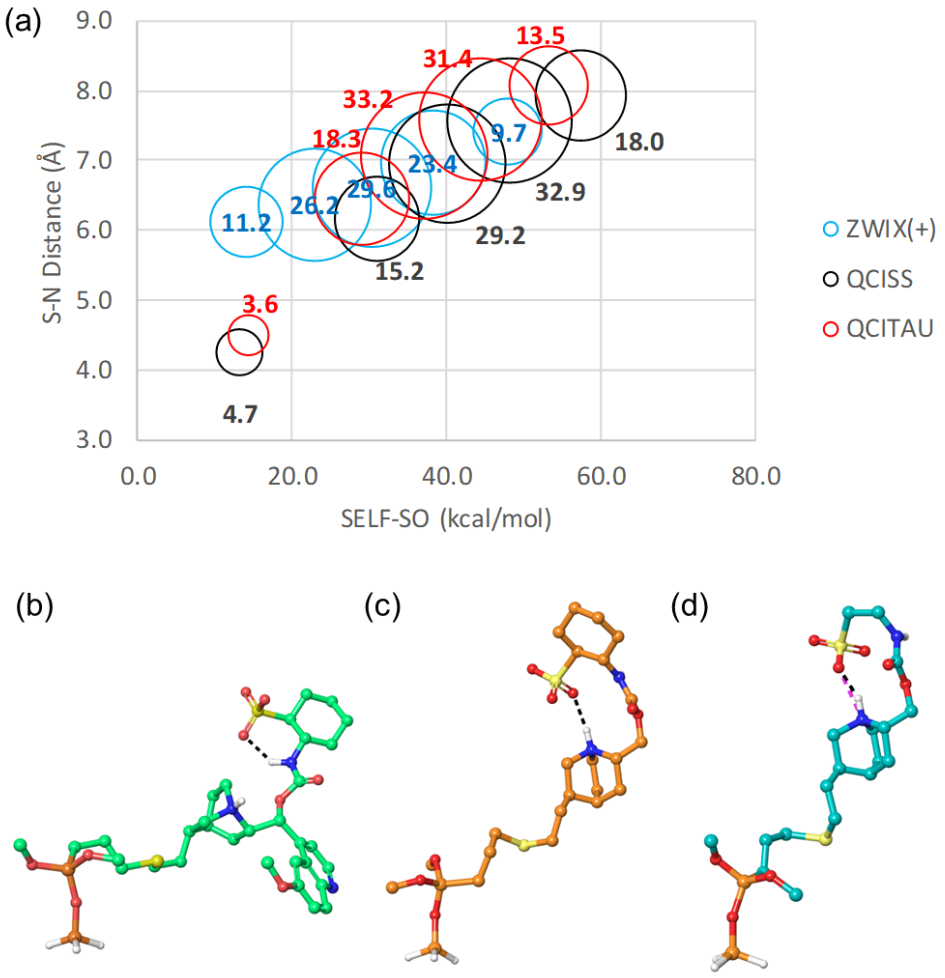

Fig. 4. Results of MD calculations of ZWIX(+), QCISS and QCITAU selectors: (a) Intramolecular distances between S of sulfonic acid and N of quinuclidinium moiety measured for the 3000 frames and grouped into 5 clusters, (b) exemplary conformer of the lowest energy cluster of ZWIX(+), (c) of QCISS and (d) of QCITAU.

Fig. 4a shows a scatter plot of the measured distance versus the relative conformational energies (calculated with Schrödinger Suite) in the form of a bubble graph (note, in particular, we used a utility aiming at the analysis of MD trajectories called Simulation Event Analysis that can monitor energies and interactions along time. Relative values were created by subtracting the minimum energy recorded for the examined selector from the values of all the frames). The size of the bubbles represents the cluster population. It can be seen that QCITAU and QCISS behave similarly, while ZWIX(+) shows significantly different profile. ZWIX(+) reveals exclusively conformers embedded by a long sulphur-nitrogen distance (>6.0 Å), indicating the presence of a very weak intramolecular electrostatic interaction. On the other hand, both QCITAU and QCISS exhibit favorable low energy clusters with short distance conformers (~4 Å between S and N) which is indicative for a strong intramolecular ion-pairing. The main difference that can be seen between QCITAU and QCISS clusters is that QCITAU displays barycenters characterized by 3-4 kcal/mol lower conformational energy distribution compared to that of QCISS. This outcome could indicate that, on average, conformers displaying short sulphur-nitrogen distances are energetically more stable (see Fig. 4a). Fig 4b-4d illustrate the

energy minima conformer for each selector, ZWIX(+) (Fig. 4b), QCISS (Fig. 4c) and QCITAU (Fig. 4d). Overall, these results support to some extent the above raised hypothesis that more favorable intramolecular ion-pairing may lead to less negative surface charge of the zwitterionic selectors by shielding the sulfonic acid group intramolecularly.

While this remains an unproven hypothesis, it may be worth to be considered as hypothesis for explanation of the ζ–potential differences of the distinct zwitterionic phases. In general, the set of data presented herein always explains some but not all effects observed.

Overall, three possible explanations have been presented: i) differential solvation and titration of cations and anions by respective counterions, ii) surface effects such as specific ion gradients due to more complex double layers, and iii) intramolecular charge neutralization by intramolecular ion-pairing to a characteristic extent when the conformational flexibility and solvation is altered by different structural elements due to other neighboring effects. Yet, finally it remains open which one is responsible for the observed ζ-potential shifts within the series of congeneric zwitterionic materials or whether all partially contribute to it.

4.5.4.5. Chromatographic Characterization

Simple test mixtures were injected in RP and HILIC elution mode to examine the multimodal applicability of the new MMC phases for i) RP-type separations, ii) HILIC utility, and iii) ion-exchange properties. The results will be mainly discussed in the form of chromatographic parameters of binary analyte combinations.

The surface lipophilicity and capability of the MMC phases to serve for LC separations based on lipophilicity differences of analytes in RP elution mode can be well expressed by the separation factors of an analyte pair differing by a methylene increment. Thus, butylbenzene (BuB) and pentylbenzene (PeB) were part of an RP test mixture along with two acids with different lipophilicity (DETP and BocProPhe). In general, $\alpha(CH_2)$ values of the new MMC phases ranged between 1.33 for the TAU RP/SCX phase and 1.47 for the QN RP/WAX phase. Thus, it can be concluded that the current MMC phases have moderate hydrophobicities and methylene selectivities as compared to RP phases (e.g. $\alpha(CH_2)$ of the polar RP phase Synergi Fusion RP is 1.79 [25]). On the other hand, this is characteristic for mixed-mode phases, being indicative of their hydrophilicity-lipophilicity balance, which makes them applicable in both RP and HILIC elution modes (*vide infra*). Exemplary chromatograms are given for QCITAU, QCISS and QN in Fig. 5 which documents that separations of analytes that differ just by a methylene increment are still feasible on these MMC phases. Peaks 3 and 4 are butyl- and pentylbenzenes; their retention and methylene selectivities increase in the order QCITAU < QCISS < QN. Also, the two acids elute in the order of their lipophilicity (DETP 1 < BocProPhe

2). However, as far as the anion-exchange capacity of the distinct MMC phases is concerned, there are significant differences. The general retentivity of the acids and anion-exchange capacity follows the same order as described for the ζ-potentials (*vide supra*): QN > QCITAU > QCISS (Fig. 5). The significantly higher anion-exchange retention increment of the QCITAU vs QCISS is remarkable as these two MMC phases differ just in a tetramethylene bridge which gives the former more conformational flexibility, obviously with some significant effect on net surface charge.

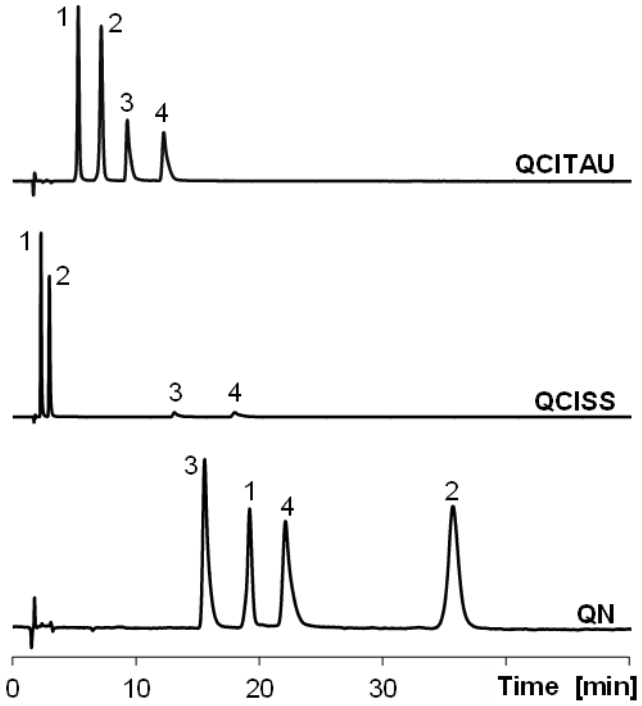

Fig. 5. Chromatographic characterization: Reversed-phase elution mode. Mobile phase: a mixture of ACN and H_2O (40:60, v/v), containing 50 mmol acetic acid in 1 L mobile phase, apparent pH 6, adjusted with ammonia in the polar organic mixture; Flow rate: 0.5 mL/min, 25 °C, 0.8 mg/mL of each analyte (1. DETP, 2. BocProPhe, 3. BuB, 4.PeB), injection volume: 5 µL, 220 nm

The HILIC applicability was characterized by a test mixture consisting of toluene (1), caffeine (2), theobromine (3), theophylline (4), 2-deoxyuridine (5), 5-methyluridine (6) and uridine (7) [69] (Fig. 6). In the chromatograms of Fig. 6 it can be seen that all of the tested new MMC phases can well baseline-resolve the peak pair uridine (7) and 2-deoxyuridine (5) indicating a good hydroxy group selectivity for all of them. The methyl group selectivity in HILIC significantly varied between the distinct phases. It was for instance better on QCDTAU than on QCDRR (both ZWIX-type MMC), TAU (SCX-type) and QN (WAX-type). Overall, QCDTAU showed the best separation in HILIC for this test mixture with a baseline separation of all seven peaks.

These results confirm the multimodal applicability of the current MMC phases in RP and HILIC elution modes. The chromatographic efficiencies of these mixed-mode ion-exchangers are, however, slightly lower than those of corresponding RP particles due to a slow adsorption-desorption kinetics (significant C-term from slow adsorption-desorption rate constants), in

particular for ionic analytes. This is in line with the general characteristics in terms of chromatographic efficiencies of ion-exchange processes.

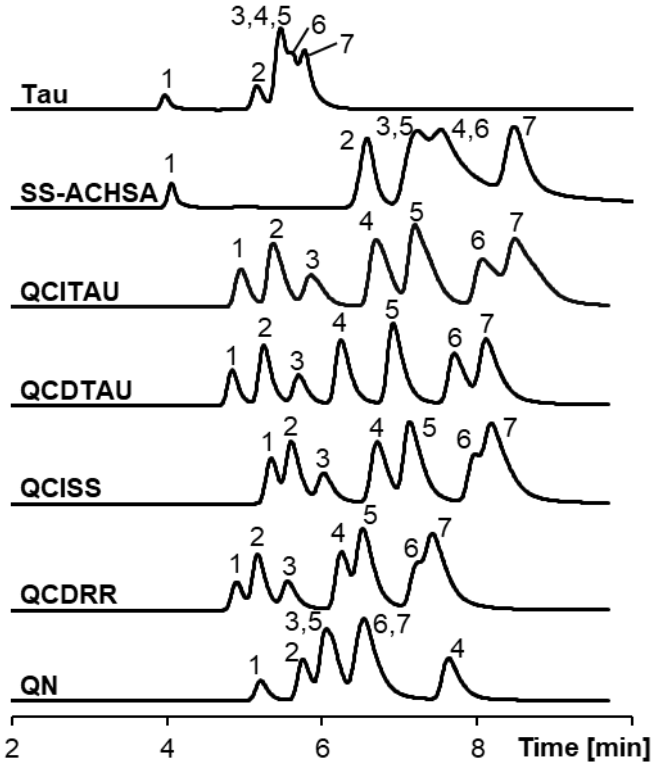

Fig. 6: Chromatographic characterization: HILIC elution mode. Mobile phase: 90 %(v) ACN / 10 % (v) aqueous 20 mM NH_4Ac (pH 4.7) solution, flow rate: 0.21 mL/min (linear flow velocity: 0.66 mm/s*), T=30°C, injection volume: 2µL, λ = 254 nm, 1. Toluene (1µL/mL), 2. Caffeine, 3. Theobromine, 4. Theophylline, 5. 2'-Deoxyuridine, 6. 5-Methyluridine, 7. Uridine (0.1 µg/mL), dissolved in ACN:H_2O (90:10; v/v). *[69]

4.5.4.6. Benchmark Study

The final question that was addressed in our study was related to the relative chromatographic characteristics compared to formerly described commercial and non-commercial mixed-mode phases as well as in comparison to popular HILIC phases.

The results are first discussed based on simple binary plots of chromatographic parameters [70]. Fig. 7 depicts a plot of surface acidity (as probed by the separation factor between theobromine, Tb, and theophylline, Tp) versus surface hydrophilicity as measured by the retention factor of uridine (both measured under HILIC conditions). Theophylline is weakly acidic while both theophylline and theobromine are dimethylxanthines with comparable hydrophilicity. If the surface is acidic, then Tp is less retained due to electrostatic repulsion effects. Again here it becomes evident that the quincorine- and quincoridine-based zwitterionic mixed-mode phases are less acidic than ZWIX(+) and ZWIX(-), as the points for QCITAU (16), QCDRR (17), QCISS (18) and QCDTAU (20) are placed lower on the y-scale of this acidity vs.

hydrophilicity plot than ZWIX(-) (33) and ZWIX(+) (34) (see Fig. 7). On the other hand, it is worthwhile mentioning that the latter are still less acidic than the popular zwitterionic sulfobetaine based ZIC-HILIC phase (1 and 2 in Fig. 7).

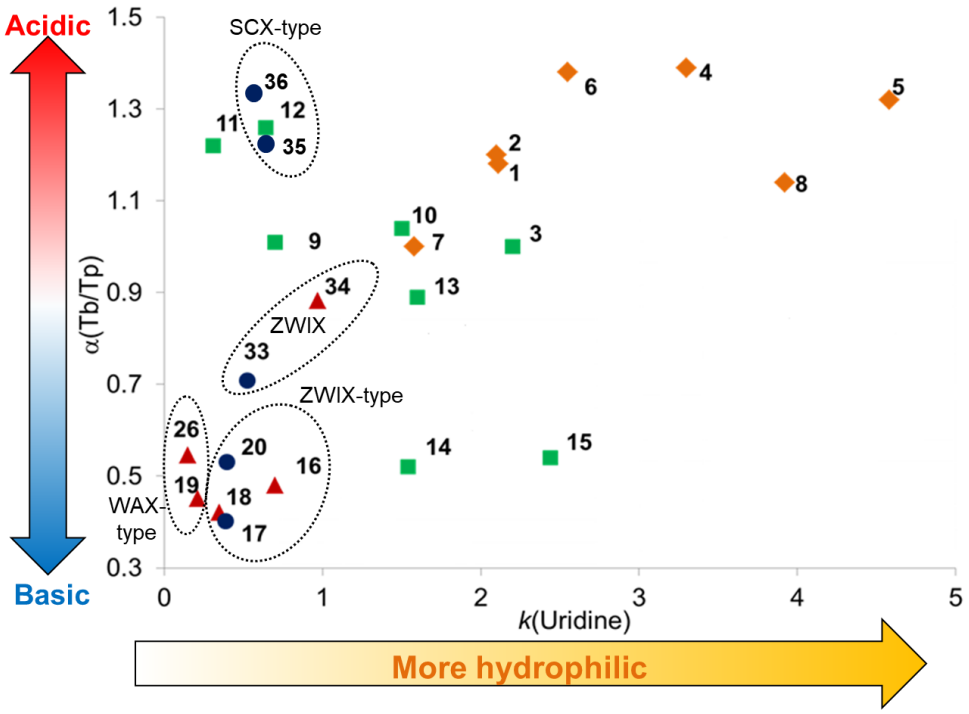

Fig. 7. Comparative visualization of acidic and basic surface properties of the tested stationary phases using the example of the selectivity of theobromine and theophylline (α(Tb/Tp) against their surface hydrophilicity measured on the retention of uridine (*k*(uridine). Chromatographic test conditions can be found in Supplemental Material 4.5.7.3.1 in accordance to ref.[25]. 1. ZIC-HILIC (5µm); 2. ZIC-HILIC (3.5 µm); 3. Nucleodur HILIC (3 µm); 4 TSKgel Amide-80 (5 µm); 5. TSKgel Amide-80 (3 µm); 6. XBridge Amide (3.5 µm); 7. PolySULFOETHYL A (3 µm); 8. PolyHYDROXYETHYL A (3 µm); 9. CYCLOBOND I (5 µm); 10. LiChrospher Diol (5 µm); 11. Chromolith Si; 12. HALO HILIC (2.7 µm); 13. COSMOSIL HILIC (5 µm); 14. Sugar-D (5 µm); 15. NH2-MS (5 µm); 16. QCITAU (3 µm), 17. QCDRR (3 µm); 18. QCISS (3 µm), 19. QN (3 µm), 20. QCDTAU (3 µm), 26. Chiralpak QN-AX, 33. ZWIX(-) (3 µm), 34. ZWIX(+) (3 µm); 35. TAU (3 µm); 36. SS-ACHSA (3 µm) Surface chemistries of other stationary phases are depicted in Suppl. Fig. S17 and S18.

Fig. 8 shows a plot of the methylene selectivity (from RP elution mode) indicating phase hydrophobicity against the retention factor of uridine (from HILIC) denoting the hydrophilicity of the stationary phase surface. Four clusters can be assigned: i) Cluster I: The commercial HILIC phases ZIC-HILIC, TSKgel Amide-80, Polysulfoethyl A and the amino phase Luna NH2 show strong retention of uridine but low methylene selectivity in RP due to their high hydrophilicity. ii) Cluster II: Chromolith Si and Biobasic AX are both hydrophilic as indicated by their low methylene selectivity. However, they show at the same time modest retention for uridine in HILIC mode. iii) Cluster III: A series of WAX-type mixed-mode phases all exhibit relatively high methylene increments (around 1.5 to 1.6) but are widely spread on the k(uridine) scale (hydrophilicity scale) in HILIC. The Acclaim Mixed-mode WAX-1 phase and a non-commercial N-undecenyl-3-aminoquinuclidine based RP/WAX phase (WAX AQ360) [25] also reveal reasonable retention for uridine and thus good HILIC behavior. They were even outperformed in terms of HILIC behavior by a similar N-undecenyl-2-dimethylaminoethylamide-bonded RP/WAX phase (WAX DMAE) [25]. iv) Cluster IV: The current zwitterionic MMC phases cluster together at low k(uridine) and intermediate levels of methylene selectivity. It demonstrates that these phases are not the best choice for HILIC separations of neutral compounds but may be quite useful for HILIC separations of charged (anionic, cationic and zwitterionic) analytes. They still show potential for RP-type separations of both neutral and ionic analytes.

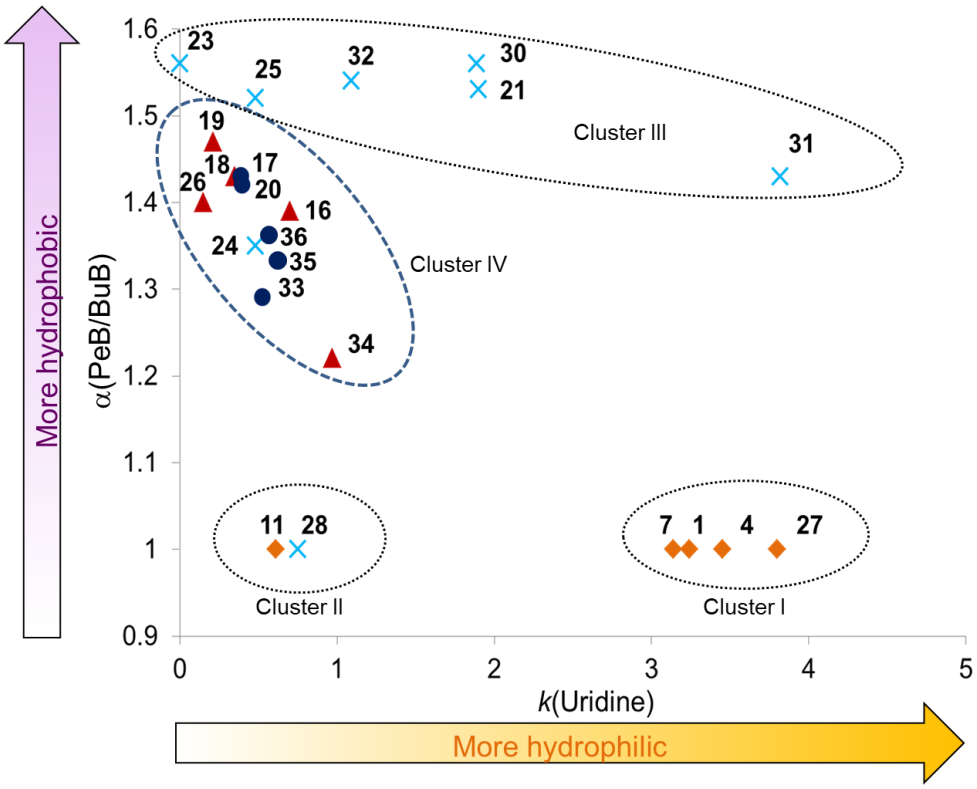

Fig. 8. Characterization of hydrophilic and hydrophobic surface properties (hydrophilic-lipophilic balance, HLB) based on the retention factor of uridine (*k*(uridine) and the methylene selectivity (α(PeB/BuB) of selected stationary phases. Chromatographic test conditions were as stated in Figure 5 for methylene selectivity (*α*(PeB/BuB)) and Figure 6 (*k*(uridine) in accordance to ref. [25] and can be found in the Supplemental Material sub-chapter 4.5.7.3.1. 1. ZIC-HILIC (5µm); 4 TSKgel Amide-80 (5µm); 7. Poly-SULFOETHYL (3 µm); 11. Chromolith Si; 16. QCITAU (3µm), 17. QCDRR (3µm); 18. QCISS (3µm), 19. QN (3µm), 20. QCDTAU (3µm), 21. Acclaim Mixed Mode WAX-1; 23. Primesep B2; 24. Obelisc R; 25. Obelisc N; 26. Chiralpak QN-AX, 27. Luna NH2; 28. BioBasic AX; 30. WAX AQ360; 31. WAX DMAE; 32. WAX BAMQO 33. ZWIX (-) (3µm), 34. ZWIX (+) (3µm); 35. TAU (3µm); 36. SS-ACHSA (3µm). Surface chemistries of stationary phases can be found in the Supplemental Material Suppl. Fig. S17 and S18.

This is underpinned by Fig. 9 which shows a plot of log k of nicotinic acid (mostly retained due to anion exchange retention) vs log k of thiamine (mainly due to cation exchange) under HILIC conditions. WAX-type QN phase has pronounced anion-exchange capacity while SCX-type TAU and ACHSA are classified as cation-exchangers as expected. The zwitterionic mixed-mode phases of this work are in the middle of a diagonal line between the SCX-type and WAX-type phases. They have moderate anion and moderate cation exchange capacity. The ZWIX(-) phase is shifted on the cation exchange scale to larger values, indicating again its stronger acidic character as compared to the quincorine- and quincoridine-derived zwitterionic MMC phases. Furthermore, it is striking that there is a slight shift to higher cation-exchange character when the quincorine (QCI) moiety in the zwitterionic MMC phases is exchanged for the quincoridine moiety (QCD) (Fig 9).

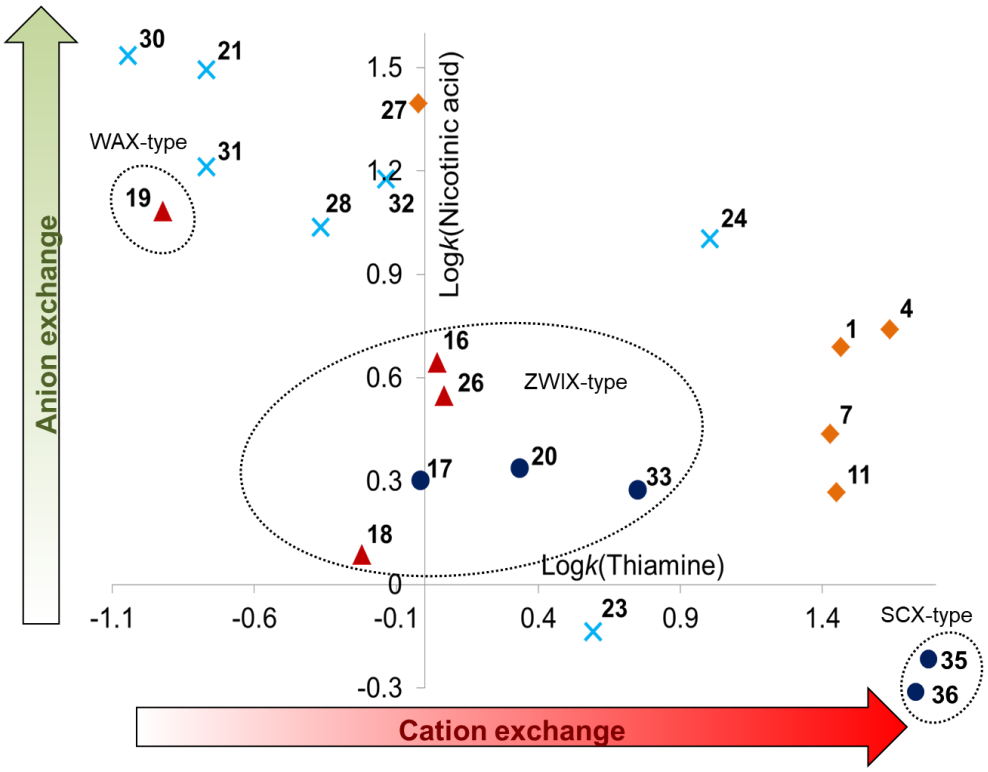

Fig. 9: Chromatographic categorization of the surface charge properties of the investigated mixed-mode columns: Anion-exchange as measured by log *k* for nicotinic acid and cation-exchange as determined by log *k* of thiamine. Conditions and stationary phase chemistries can be found in the Supplemental Material Chapter 4.5.7.3.1 (analysis of vitamins). Labels (numbers) as defined in Fig. 6 and 7.

Last but not least, a principal component analysis (PCA) was performed to classify the columns along with commercial RP, HILIC and mixed-mode phases. Retention factors of the chromatographic test mixture of the RP test (Fig 5), of nucleosides from a HILIC test, purines in HILIC mode, and vitamins in HILIC mode as factors (variables) were subjected to PCA. The score plot of the first two principal components PC1 and PC2 is shown in Fig. 10. PC1 and PC2 explain 51.1% and 18.3 % of the variance in the data, both together 69.4%. Columns with similar retention behavior are located on this score plot in close proximity. The more different the retention behavior, the greater is the distance from each other. In this particular case, the PC1 axis is a descriptor of the hydrophilicity, the PC2 axis represents the effective charge of the modified silica particles. Stationary phases with polar surfaces can be found at high PC1 values (e.g. HILIC phases like Luna NH2, ZIC-HILIC, Polysulfoethyl A, PC-HILIC and TSKGel Amide-80). On the opposite end of the PC1 axis, stationary phases with a predominantly apolar surface are found, like the polar RP phase Synergi Fusion-RP or the mixed-mode phase Uptisphere 5 MM3 which is an RP phase with quaternary ammonium endcapping. Mixed-mode phases such as Primesep B2, Obelisc R and N, including the current zwitterionic MMC phases, are located in the middle of the PC1 axis, indicative of their hydrophilicity-lipophilicity balance (see Fig. 10). The PC2 axis, in contrast, primarily quantifies the effective charge state of the surface of the stationary phases. Mixed-mode anion exchange columns like Acclaim Mixed Mode WAX-1 are found at high PC2 values and net negatively charged phases like PC-HILIC

at low (i.e. negative) PC2 values. The current mixed-mode phases are aligned on PC2 in accordance to the ζ-potentials measured at around pH 7.5. The WAX-type QN phase has the highest score, then the WAX-type QN-AX, followed by the zwitterionic quincorine and quincoridine MMC phases (QCITAU, QCDTAU, QCDRR, QCISS). ZWIX(+) and ZWIX(-) are already on the negative scale i.e. they have acidic excess on the surface. SCX-type SS-ACHSA and TAU have the lowest score on PC2 and thus the most acidic character, as expected.

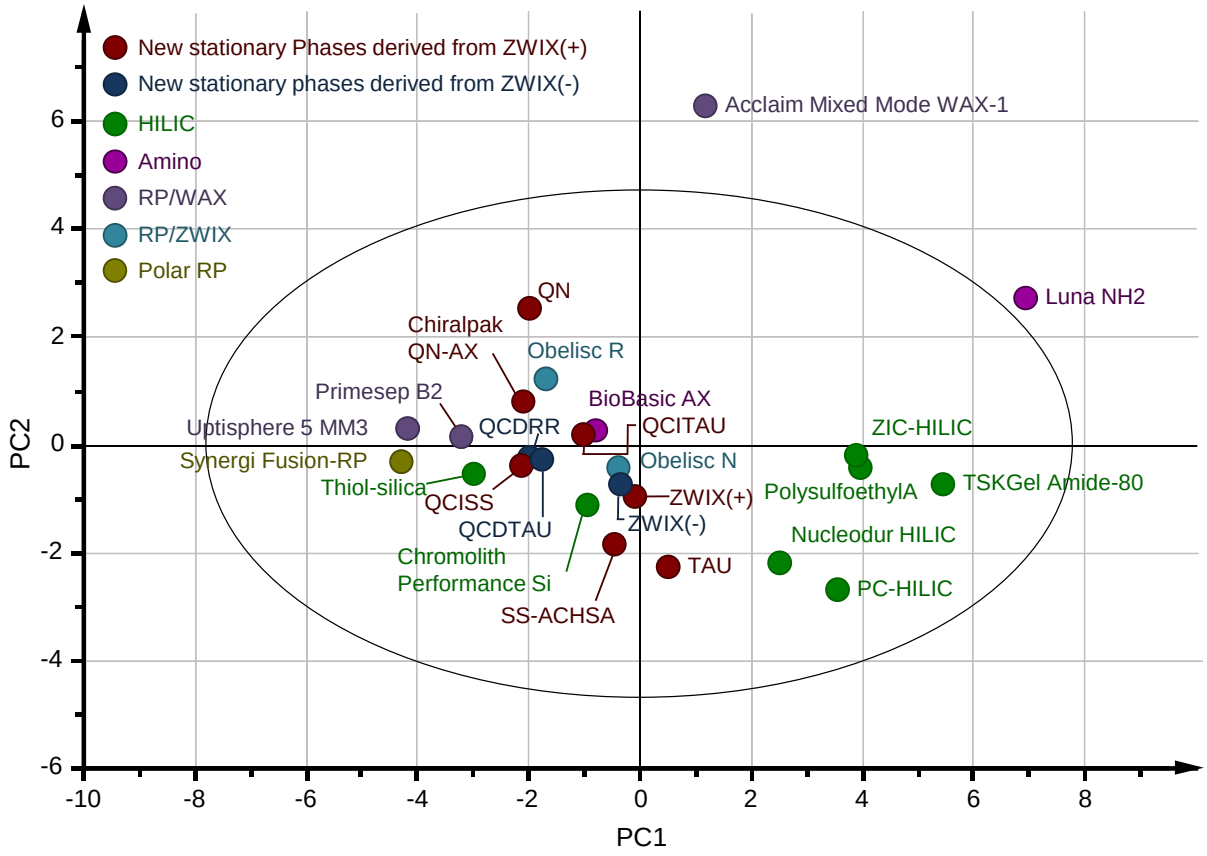

Fig. 10. Benchmarking study by principal component analysis (PCA): Score plot of first two principal components. Chromatographic conditions and evaluated stationary phases can be found in the Supplementary Material.

It can be concluded that PCA is a useful tool to characterize and classify stationary phases. It confirms what was discussed before by ζ-potentials and binary chromatographic plots. The new set of MMC stationary phases span a reasonably wide surface character and represent a useful supplement to the toolbox of stationary phases. To document their utility in practical applications will be the topic of future works.

4.5.5. Conclusions

A series of new silica-based stationary phases for mixed mode chromatography have been synthesized in this study. They were obtained by a fragment-based design through incremental fragmentation of the chromatographic ligand of the commercial chiral columns Chiralpak ZWIX(+) and ZWIX(-). These chiral stationary phases consist of a zwitterionic chromatographic ligand and show MMC behaviour. They exhibit utility for achiral separations with selectivity orthogonal to that of RP and HILIC phases. The removal of certain structural elements of these zwitterionic selectors has led to RP/ZWIX, RP/WAX and RP/SCX-type MMC phases with modulated surface charge and hydrophilicity/lipophilicity. They showed sufficient methylene selectivity under RP elution conditions for RP-type separations as well as enough retention for neutral polar compounds under HILIC conditions to allow for multimodal applicability. Besides, the RP/ZWIX phases possess both moderate anion- and cation-exchange capacity with low retentivity which could be advantageous in practical applications especially under mild elution conditions such as those required for ESI-MS detection. Their practical utility is currently being elucidated and will be reported elsewhere.

Declaration of Competing Interest

The authors declare that they have no known competing financial interests or personal relationships that could have appeared to influence the work reported in this paper.

CRediT Authorship Contribution Statement

Martina Ferri: Investigation, Formal analysis, Visualization, Writing - original draft, Writing - review & editing. **Stefanie Bäurer**: Data curation, Formal analysis, Investigation, Supervision, Writing - original draft, Writing - review & editing. **Andrea Carotti**: Methodology, Visualization, Writing - review & editing. **Marc Wolter**: Investigation, Writing - original draft. **Belal Alshaar**: Investigation. **Johannes Theiner**: Investigation. **Tohru Ikegami**: Conceptualization, Methodology, Supervision, Writing - review & editing, Funding acquisition. **Caroline West**: Conceptualization, Methodology, Writing - review & editing. **Michael Lämmerhofer**: Conceptualization, Methodology, Supervision, Writing - review & editing, Resources.

Acknowledgements

We are grateful to Pilar Franco from Chiral Technologies Europe for providing the Chiralpak ZWIX columns and the trans-ACHSA enantiomers. This research was partially supported by the Ministry of Education, Science, Sports and Culture, Grant-in Aid for Scientific Research (C), Japan, 2017-2019 (17K05900, Tohru Ikegami)

4.5.6. References

[1] L.W. McLaughlin, Mixed-mode chromatography of nucleic acids, Chem. Rev., 89 (1989) 309-319.

[2] W. Bicker, M. Laemmerhofer, W. Lindner, Mixed-mode stationary phases as a complementary selectivity concept in liquid chromatography-tandem mass spectrometry-based bioanalytical assays, Anal. Bioanal. Chem., 390 (2008) 263-266.

[3] L. Zhang, Q. Dai, X. Qiao, C. Yu, X. Qin, H. Yan, Mixed-mode chromatographic stationary phases: Recent advancements and its applications for high-performance liquid chromatography, TrAC Trends in Analytical Chemistry, 82 (2016) 143-163.

[4] K. Zhang, X. Liu, Mixed-mode chromatography in pharmaceutical and biopharmaceutical applications, J Pharm Biomed Anal, 128 (2016) 73-88.

[5] L. Wang, W. Wei, Z. Xia, X. Jie, Z.Z. Xia, Recent advances in materials for stationary phases of mixed-mode high-performance liquid chromatography, TrAC, Trends Anal. Chem., 80 (2016) 495-506.

[6] E. Lemasson, S. Bertin, P. Henning, E. Lesellier, C. West, Mixed Mode Chromatography - A Review, Supplement to LCGC Europe / LCGC North America, 30 (2017) 22-33.

[7] D. Sykora, P. Rezanka, K. Zaruba, V. Kral, Recent advances in mixed-mode chromatographic stationary phases, J Sep Sci, 42 (2019) 89-129.

[8] L.R. Snyder, J.W. Dolan, D.H. Marchand, P.W. Carr, The hydrophobic-subtraction model of reversed-phase column selectivity, Adv. Chromatogr. (Boca Raton, FL, U. S.), 50 (2012) 297-376.

[9] B. Bidlingmeyer, C.C. Chan, P. Fastino, R. Henry, P. Koerner, A.T. Maule, M.R.C. Marques, U. Neue, L. Ng, H. Pappa, L. Sander, C. Santasania, L. Snyder, T. Wozniak, HPLC Column Classification, Pharmacopeial Forum, 31 (2005) 637–645.

[10] A.J. Alpert, Hydrophilic-interaction chromatography for the separation of peptides, nucleic acids and other polar compounds, J Chromatogr, 499 (1990) 177-196.

[11] P. Hemstroem, K. Irgum, Hydrophilic interaction chromatography, J. Sep. Sci., 29 (2006) 1784-1821.

[12] P. Jandera, P. Janas, Recent advances in stationary phases and understanding of retention in hydrophilic interaction chromatography. A review, Anal. Chim. Acta, 967 (2017) 12-32.

[13] M. Laemmerhofer, R. Nogueira, W. Lindner, Multi-modal applicability of a reversed-phase/weak-anion exchange material in reversed-phase, anion-exchange, ion-exclusion, hydrophilic interaction and hydrophobic interaction chromatography modes, Anal. Bioanal. Chem., 400 (2011) 2517-2530.

[14] R. Nogueira, M. Laemmerhofer, W. Lindner, Alternative high-performance liquid chromatographic peptide separation and purification concept using a new mixed-mode reversed-phase/weak anion-exchange type stationary phase, J. Chromatogr. A, 1089 (2005) 158-169.

[15] R. Bischoff, L.W. McLaughlin, Mixed-mode chromatographic matrices for the resolution of transfer ribonucleic acids, J Chromatogr, 317 (1984) 251-261.

[16] S. Baeurer, A. Zimmermann, U. Woiwode, O.L. Sanchez Munoz, M. Kramer, J. Horak, W. Lindner, W. Bicker, M. Laemmerhofer, Stable-bond polymeric reversed-phase/weak anion-exchange mixed-mode stationary phases obtained by simultaneous functionalization and crosslinking of a poly(3-mercaptopropyl)methylsiloxane-film on vinyl silica via thiol-ene double click reaction, J Chromatogr A, (2019).

[17] B.Y. Zhu, C.T. Mant, R.S. Hodges, Mixed-mode hydrophilic and ionic interaction chromatography rivals reversed-phase liquid chromatography for the separation of peptides, J. Chromatogr., 594 (1992) 75-86.

[18] C.T. Mant, R.S. Hodges, Mixed-mode hydrophilic interaction/cation-exchange chromatography (HILIC/CEX) of peptides and proteins, J. Sep. Sci., 31 (2008) 2754-2773.

[19] C. Liu, P. Bults, R. Bischoff, J. Crommen, Q. Wang, Z. Jiang, Separation of deamidated peptides with mixed-mode chromatography using phospholipid-functionalized monolithic stationary phases, J. Chromatogr. A, 1603 (2019) 417-421.

[20] L. Ding, Z. Guo, X. Liang, Z. Hu, Mixed-mode reversed phase/positively charged repulsion chromatography for intact protein separation, J Pharm Biomed Anal, 138 (2017) 63-69.

[21] K. Zhang, L. Dai, N.P. Chetwyn, Simultaneous determination of positive and negative pharmaceutical counterions using mixed-mode chromatography coupled with charged aerosol detector, J. Chromatogr. A, 1217 (2010) 5776-5784.

[22] J. Xu, X. Zhang, Z. Guo, J. Yan, L. Yu, X. Li, X. Xue, X. Liang, Orthogonal separation and identification of long-chain peptides from scorpion Buthus martensi Karsch venom by using two-dimensional mixed-mode reversed phase-reversed phase chromatography coupled to tandem mass spectrometry, Analyst (Cambridge, U. K.), 138 (2013) 1835-1843.

[23] I.H. Hagestam, T.C. Pinkerton, Internal surface reversed-phase silica supports for liquid chromatography, Anal. Chem., 57 (1985) 1757-1763.

[24] Z. Guo, Y. Jin, T. Liang, Y. Liu, Q. Xu, X. Liang, A. Lei, Synthesis, chromatographic evaluation and hydrophilic interaction/reversed-phase mixed-mode behavior of a "Click beta-cyclodextrin" stationary phase, J Chromatogr A, 1216 (2009) 257-263.

[25] M. Laemmerhofer, M. Richter, J. Wu, R. Nogueira, W. Bicker, W. Lindner, Mixed-mode ion-exchangers and their comparative chromatographic characterization in reversed-phase and hydrophilic interaction chromatography elution modes, J Sep Sci, 31 (2008) 2572-2588.

[26] A. Zimmermann, J. Horak, O.L. Sánchez Muñoz, M. Laemmerhofer, Surface charge fine tuning of reversed-phase/weak anion-exchange type mixed-mode stationary phases for milder elution conditions, J Chromatogr A, 1409 (2015) 189-200.

[27] J. Wei, Z. Guo, P. Zhang, F. Zhang, B. Yang, X. Liang, A new reversed-phase/strong anion-exchange mixed-mode stationary phase based on polar-copolymerized approach and its application in the enrichment of aristolochic acids, Journal of Chromatography A, 1246 (2012) 129-136.

[28] X. Cai, Z. Guo, X. Xue, J. Xu, X. Zhang, X. Liang, Two-dimensional liquid chromatography separation of peptides using reversed-phase/weak cation-exchange mixed-mode column in first dimension, J Chromatogr A, 1228 (2012) 242-249.

[29] A.F. Gargano, T. Leek, W. Lindner, M. Laemmerhofer, Mixed-mode chromatography with zwitterionic phosphopeptidomimetic selectors from Ugi multicomponent reaction, J Chromatogr A, 1317 (2013) 12-21.

[30] M.E.A. Ibrahim, C.A. Lucy, Mixed mode HILIC/anion exchange separations on latex coated silica monoliths, Talanta, 100 (2012) 313-319.

[31] M.-X. Chen, Z.-Y. Cao, Y. Jiang, Z.-W. Zhu, Direct determination of glyphosate and its major metabolite, aminomethylphosphonic acid, in fruits and vegetables by mixed-mode hydrophilic interaction/weak anion-exchange liquid chromatography coupled with electrospray tandem mass spectrometry, J. Chromatogr. A, 1272 (2013) 90-99.

[32] X. Dong, A. Shen, Z. Gou, D. Chen, X. Liang, Hydrophilic interaction/weak cation-exchange mixed-mode chromatography for chitooligosaccharides separation, Carbohydr Res, 361 (2012) 195-199.

[33] A. Shen, X. Li, X. Dong, J. Wei, Z. Guo, X. Liang, Glutathione-based zwitterionic stationary phase for hydrophilic interaction/cation-exchange mixed-mode chromatography, J Chromatogr A, 1314 (2013) 63-69.

[34] X. Liu, C.A. Pohl, HILIC behavior of a reversed-phase/cation-exchange/anion-exchange trimode column, J. Sep. Sci., 33 (2010) 779-786.

[35] A.A. Kazarian, M.R. Taylor, P.R. Haddad, P.N. Nesterenko, B. Paull, Single column comprehensive analysis of pharmaceutical preparations using dual-injection mixed-mode (ion-exchange and reversed-phase) and hydrophilic interaction liquid chromatography, J. Pharm. Biomed. Anal., 86 (2013) 174-181.

[36] A.J. Alpert, Electrostatic repulsion hydrophilic interaction chromatography for isocratic separation of charged solutes and selective isolation of phosphopeptides, Anal Chem, 80 (2008) 62-76.

[37] X. Shi, L. Qiao, G. Xu, Recent development of ionic liquid stationary phases for liquid chromatography, J. Chromatogr. A, 1420 (2015) 1-15.

[38] E.P. Nesterenko, P.N. Nesterenko, B. Paull, Zwitterionic ion-exchangers in ion chromatography: A review of recent developments, Anal Chim Acta, 652 (2009) 3-21.

[39] F. Gasparrini, G. Cancelliere, A. Ciogli, I. D'Acquarica, D. Misiti, C. Villani, New chiral and restricted-access materials containing glycopeptides as selectors for the high-performance liquid chromatographic determination of chiral drugs in biological matrices, J. Chromatogr. A, 1191 (2008) 205-213.

[40] H. Wang, D. Xu, P. Jiang, M. Zhang, X. Dong, Novel restricted access chiral stationary phase synthesized via atom transfer radical polymerization for the analysis of chiral drugs in biological matrices, Analyst (Cambridge, U. K.), 135 (2010) 1785-1792.

[41] B. Zhang, R. Soukup, D.W. Armstrong, Selective separations of peptides with sequence deletions, single amino acid polymorphisms, and/or epimeric centers using macrocyclic glycopeptide liquid chromatography stationary phases, Journal of Chromatography A, 1053 (2004) 89-99.

[42] E.L. Regalado, C.J. Welch, Separation of achiral analytes using supercritical fluid chromatography with chiral stationary phases, TrAC Trends in Analytical Chemistry, 67 (2015) 74-81.

[43] F. Ianni, F. Blasi, D. Giusepponi, A. Coletti, F. Galli, B. Chankvetadze, R. Galarini, R. Sardella, Liquid chromatography separation of α- and γ-linolenic acid positional isomers with a stationary phase based on covalently immobilized cellulose tris(3,5-dichlorophenylcarbamate), Journal of Chromatography A, (2019) 460461.

[44] .V. Hoffmann, R. Pell, M. Laemmerhofer, W. Lindner, Synergistic Effects on Enantioselectivity of Zwitterionic Chiral Stationary Phases for Separations of Chiral Acids, Bases, and Amino Acids by HPLC, Analytical Chemistry, 80 (2008) 8780-8789.

[45] A. Mandl, L. Nicoletti, M. Laemmerhofer, W. Lindner, Quinine- versus carbamoylated quinine-based chiral anion exchangers: A comparison regarding enantioselectivity for N-protected amino acids and other chiral acids, Journal of Chromatography A, 858 (1999) 1-11.

[46] U. Woiwode, M. Ferri, N.M. Maier, W. Lindner, M. Laemmerhofer, Complementary enantioselectivity profiles of chiral cinchonan carbamate selectors with distinct carbamate residues and their implementation in enantioselective two-dimensional high-performance liquid chromatography of amino acids, Journal of Chromatography A, 1558 (2018) 29-36.

[47] R. Sardella, A. Macchiarulo, F. Urbinati, F. Ianni, A. Carotti, M. Kohout, W. Lindner, A. Peter, I. Ilisz, Exploring the enantiorecognition mechanism of Cinchona alkaloid-based zwitterionic chiral stationary phases and the basic trans-paroxetine enantiomers, J Sep Sci, 41 (2018) 1199-1207.

[48] W.G. Hoover, Canonical dynamics: Equilibrium phase-space distributions, Physical Review A, 31 (1985) 1695-1697.

[49] S. Nose, A unified formulation of the constant temperature molecular dynamics methods, The Journal of Chemical Physics, 81 (1984) 511-519.

[50] D.E. Shaw, A fast, scalable method for the parallel evaluation of distance-limited pairwise particle interactions, J Comput Chem, 26 (2005) 1318-1328.

[51] C. Rosini, C. Bertucci, D. Pini, P. Altemura, P. Salvadori, Cinchona alkaloids for preparing new, easily accessible chiral stationary phases. I. 11-(10,11-Dihydro-6'-methoxycinchonan-9-ol)-thiopropylsilanized silica, Tetrahedron Lett., 26 (1985) 3361-3364.

[52] M. Mahut, W. Lindner, M. Laemmerhofer, Molecular Recognition Principles and Stationary-Phase Characteristics of Topoisomer-Selective Chemoaffinity Materials for Chromatographic Separation of Circular Plasmid DNA Topoisomers, J. Am. Chem. Soc., 134 (2012) 859-862.

[53] A.J. Alpert, P.C. Andrews, Cation-exchange chromatography of peptides on poly(2-sulfoethyl aspartamide)-silica, J. Chromatogr., 443 (1988) 85-96.

[54] O.L. Sanchez Munoz, E. Perez Hernandez, M. Laemmerhofer, W. Lindner, E. Kenndler, Estimation and comparison of ζ-potentials of silica-based anion-exchange type porous particles for capillary electrochromatography from electrophoretic and electroosmotic mobility, Electrophoresis, 24 (2003) 390–398.

[55] B. Buszewski, S. Bocian, E. Dziubakiewicz, Zeta potential determination as a new way of stationary phases characterization for liquid chromatography, J. Sep. Sci., 33 (2010) 1529-1537.

[56] U. Woiwode, A. Sievers-Engler, A. Zimmermann, W. Lindner, O.L. Sanchez Munoz, M. Laemmerhofer, Surface-anchored counterions on weak chiral anion-exchangers accelerate separations and improve their compatibility for mass-spectrometry-hyphenation, J Chromatogr A, 1503 (2017) 21-31.

[57] S. Baeurer, S. Polnick, O.L. Sanchez Munoz, M. Kramer, M. Laemmerhofer, N-Propyl-N'-2-pyridylurea-modified silica as mixed-mode stationary phase with moderate weak anion exchange capacity and pH-dependent surface charge reversal, J Chromatogr A, 1560 (2018) 45-54.

[58] J. Stahlberg, Retention models for ions in chromatography, J. Chromatogr. A, 855 (1999) 3–55.

[59] A.V. Delgado, F. Gonzalez-Caballero, R.J. Hunter, L.K. Koopal, J. Lyklema, Measurement and interpretation of electrokinetic phenomena, J. Colloid Interface Sci., 309 (2007) 194-224.

[60] A.V. Delgado, F. Gonzalez-Caballero, R.J. Hunter, L.K. Koopal, J. Lyklema, S. Alkafeef, E. Chibowski, C. Grosse, A.S. Dukhin, S.S. Dukhin, K. Furusawa, R. Jack, N. Kallay, M. Kaszuba, M. Kosmulski, R. Noremberg, R.W. O'Brien, V. Ribitsch, V.N. Shilov, F. Simon, C. Werner, A. Zhukov, R. Zimmermann, Measurement and interpretation of electrokinetic phenomena: (IUPAC technical report), Pure Appl. Chem., 77 (2005) 1753-1805.

[61] W. Jiang, K. Irgum, Covalently Bonded Polymeric Zwitterionic Stationary Phase for Simultaneous Separation of Inorganic Cations and Anions, Analytical Chemistry, 71 (1999) 333-344.

[62] C. West, E. Auroux, Deconvoluting the effects of buffer salt concentration in hydrophilic interaction chromatography on a zwitterionic stationary phase, Journal of Chromatography A, 1461 (2016) 92-97.

[63] W. Jiang, G. Fischer, Y. Girmay, K. Irgum, Zwitterionic stationary phase with covalently bonded phosphorylcholine type polymer grafts and its applicability to separation of peptides in the hydrophilic interaction liquid chromatography mode, Journal of Chromatography A, 1127 (2006) 82-91.

[64] Z.-Y. Wu, J. Liu, H. Shi, P.J. Marriott, The retention behaviour of amino acids in hydrophilic interaction liquid chromatography on zwitterionic stationary phases, Journal of Separation Science, 36 (2013) 2217-2222.

[65] A. Raimbault, C.M.A. Ma, M. Ferri, S. Bäurer, P. Bonnet, S. Bourg, M. Laemmerhofer, C. West, Cinchona-based zwitterionic stationary phases: Exploring retention and enantioseparation mechanisms in supercritical fluid chromatography with a fragmentation approach, J Chromatogr A, accepted (2019).

[66] A.J. Alpert, Effect of salts on retention in hydrophilic interaction chromatography, Journal of Chromatography A, 1538 (2018) 45-53.

[67] A. Jouyban, E. Kenndler, Theoretical and empirical approaches to express the mobility of small ions in capillary electrophoresis, ELECTROPHORESIS, 27 (2006) 992-1005.

[68] F. Foret, L. Krivankova, P. Bocek, Capillary Zone Electrophoresis (Electrophoresis Library) Hardcover, Second Edition ed., VCH Publishing, October, 1993.

[69] Y. Kawachi, T. Ikegami, H. Takubo, Y. Ikegami, M. Miyamoto, N. Tanaka, Chromatographic characterization of hydrophilic interaction liquid chromatography stationary phases: Hydrophilicity, charge effects, structural selectivity, and separation efficiency, J. Chromatogr. A, 1218 (2011) 5903-5919.

[70] T. Ikegami, Manuscript will be submitted soon.

4.5.7. Supplementary Materials

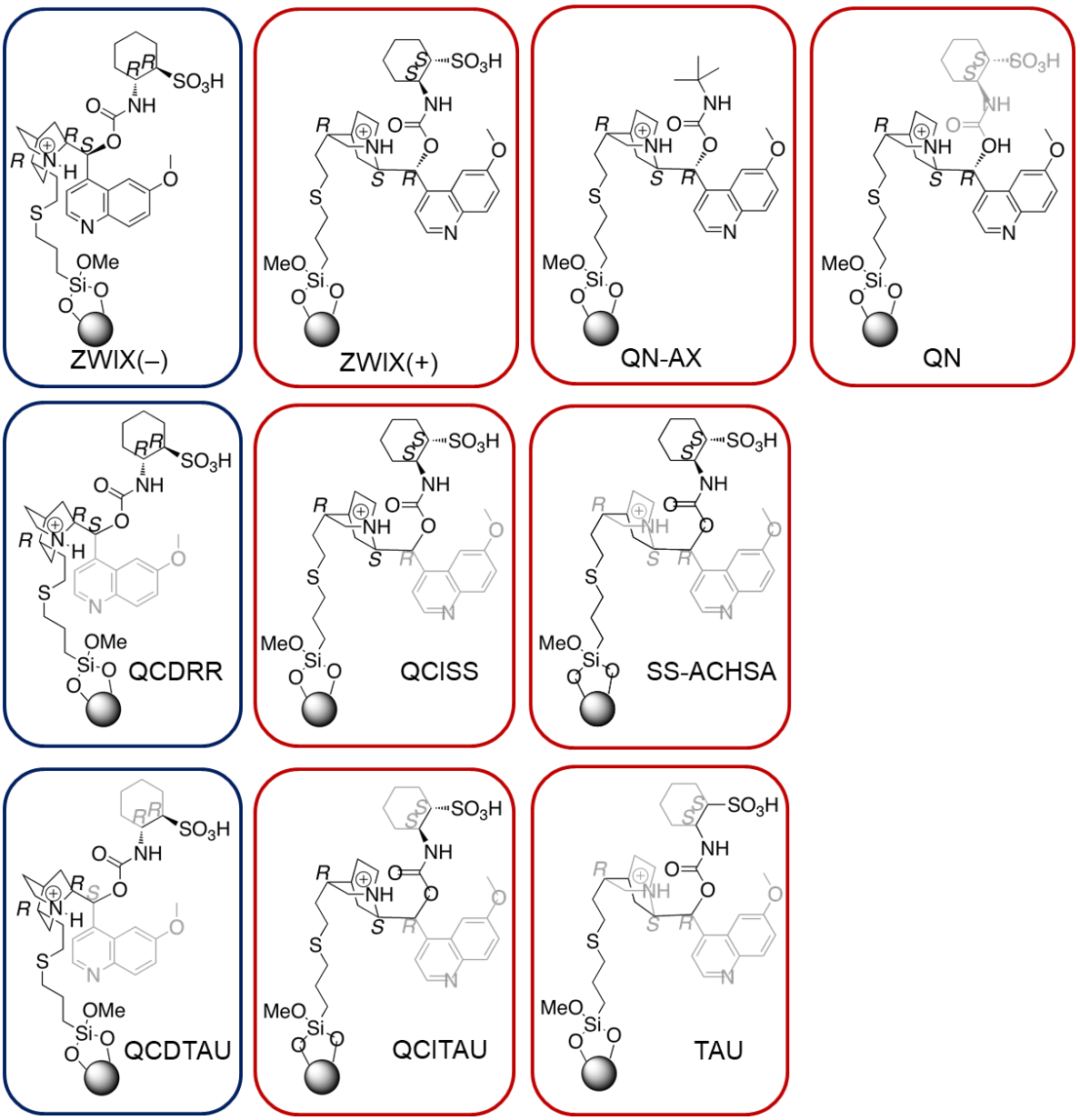

Scheme 1. Selector structures of this work with removed parts indicated in light grey. Blue frame means configurations derived from quinidine and red frame configurations derived from quinine.

4.5.7.1. Synthesis of Mixed-mode Stationary phases and their Characterization

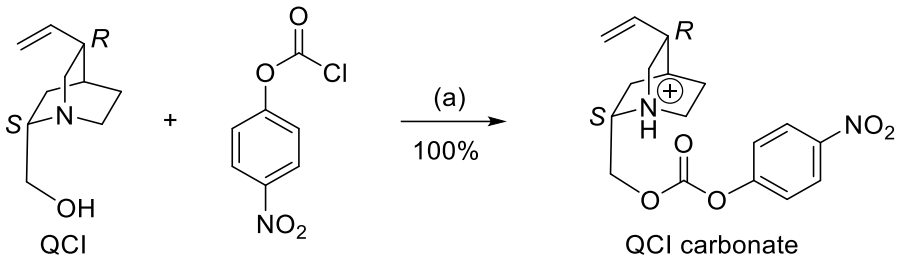

Fig. S1. Synthesis of (*2S,4S,5R*)-2-((((4-nitrophenoxy)carbonyl)oxy)methyl)-5-vinylquinuclidin-1-ium chloride QCI carbonate. Reagents and conditions: (a) Toluene, r.t., 16h.

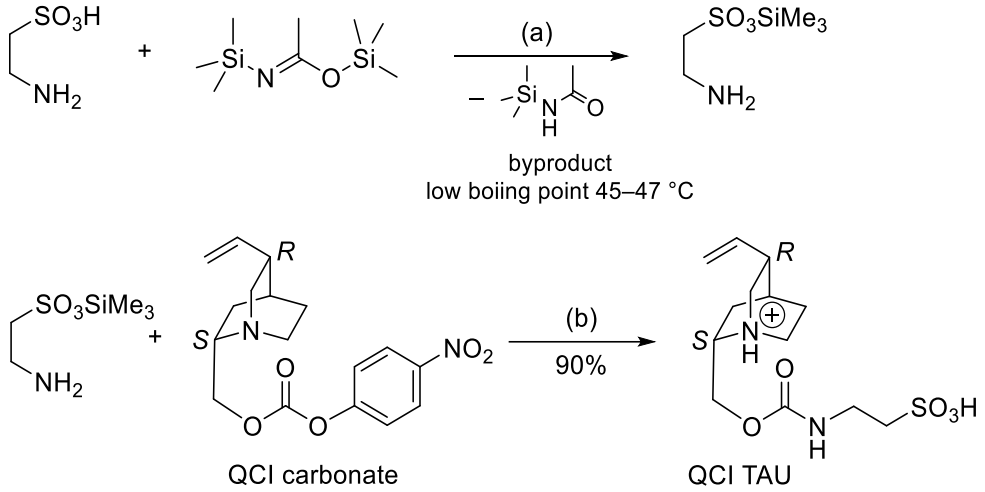

Fig. S2. Synthesis of (*2S,4S,5R*)-2-((((2-sulfoethyl)carbamoyl)oxy)methyl)-5-vinylquinuclidin-1-ium (QCITAU). Reagents and conditions: (a) CH_2Cl_2, BSA, reflux 48h. then (b) CH_2Cl_2, r.t., 16h.

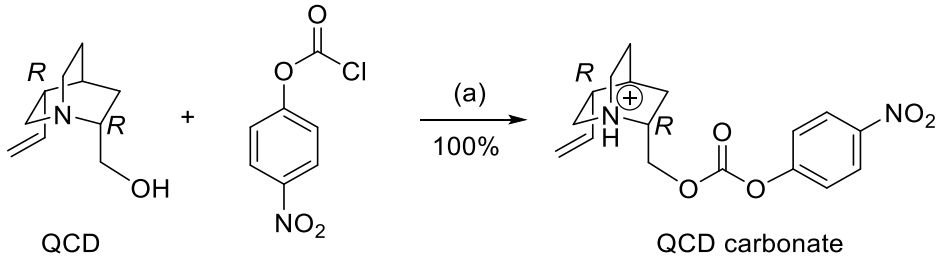

Fig. S3. Synthesis of (*2R,4S,5R*)-2-((((4-nitrophenyl)carbamoyl)oxy)methyl)-5-vinylquinuclidin-1-ium chloride QCD carbonate. Reagents and conditions: (a) Toluene, r.t., 16h.

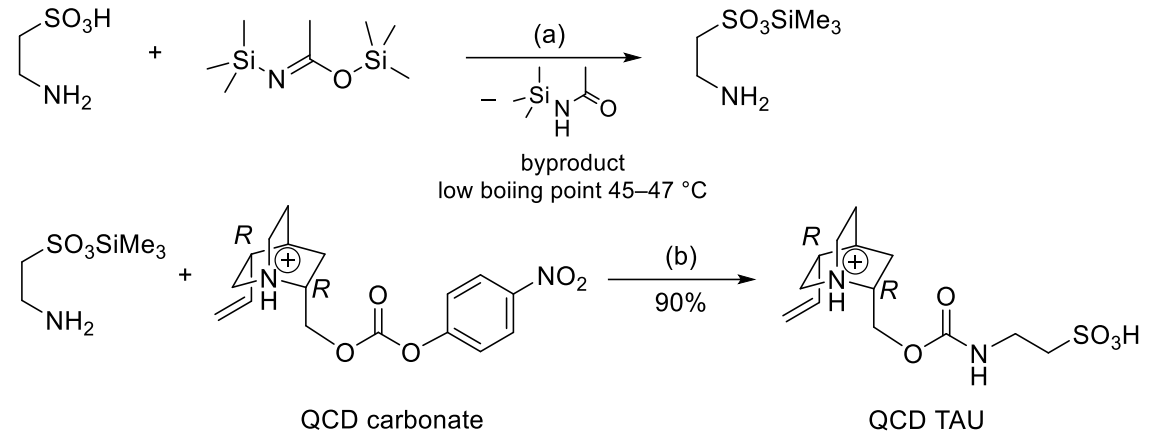

Fig. S4. Synthesis of (*2R,4S,5R*)-2-((((2-sulfoethyl)carbamoyl)oxy)methyl)-5-vinylquinuclidin-1-ium chloride (QCDTAU). Reagents and conditions: (a) CH_2Cl_2, BSA, reflux 48h. then (b) CH_2Cl_2, r.t., 16h.

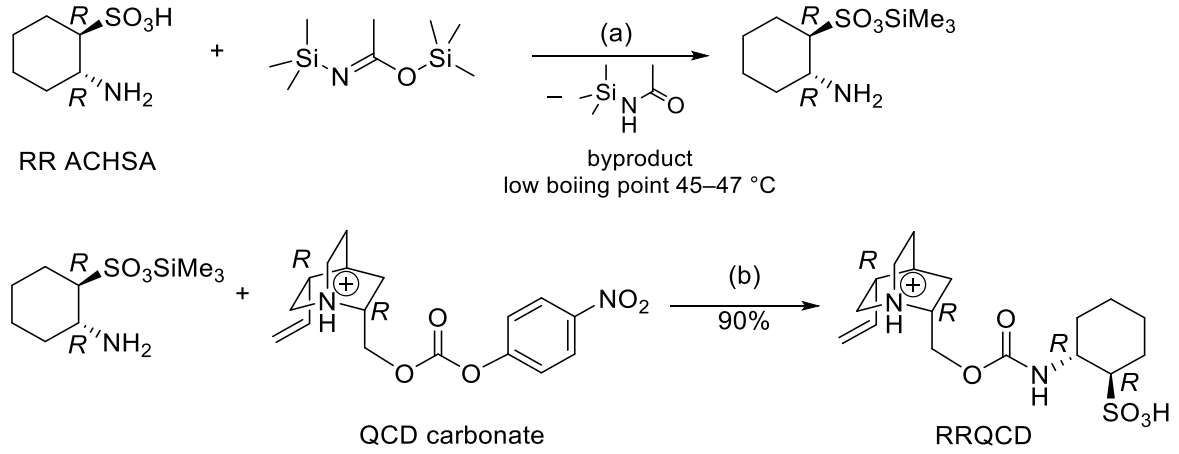

Fig. S5. Synthesis of (*2R,4S,5R*)-2-(((((1R,2R)-2-sulfocyclohexyl)carbamoyl)oxy)methyl)-5-vinylquinuclidin-1-ium chloride (RRQCD). Reagents and conditions: (a) CH_2Cl_2, BSA, reflux 48h, then (b) CH_2Cl_2, r.t., 16h.

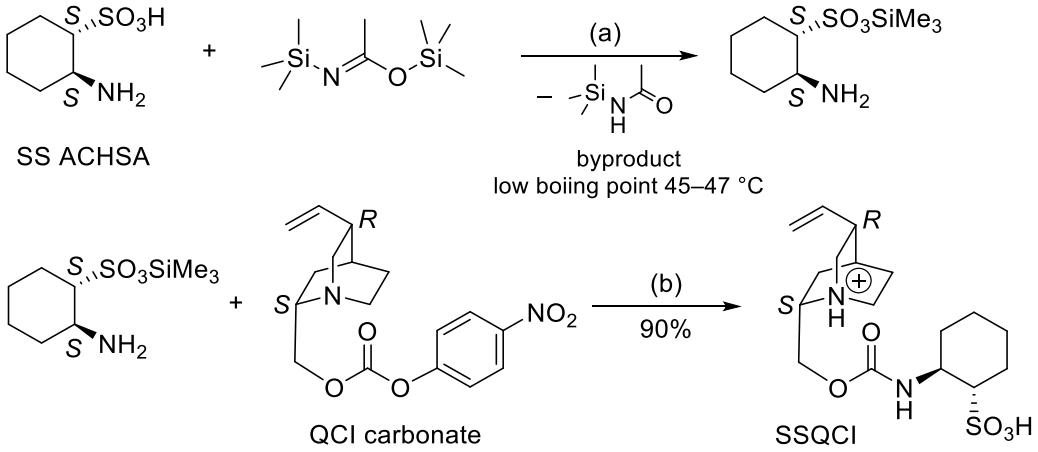

Fig. S6. Synthesis of (2S,4S,5R)-2-(((((1S,2S)-2-sulfocyclohexyl)carbamoyl)oxy)methyl)-5-vinylquinuclidin-1-ium (SSQCI). Reagents and conditions: (a) CH2Cl2, BSA, reflux 48h, then (b) CH2Cl2, r.t., 16h.

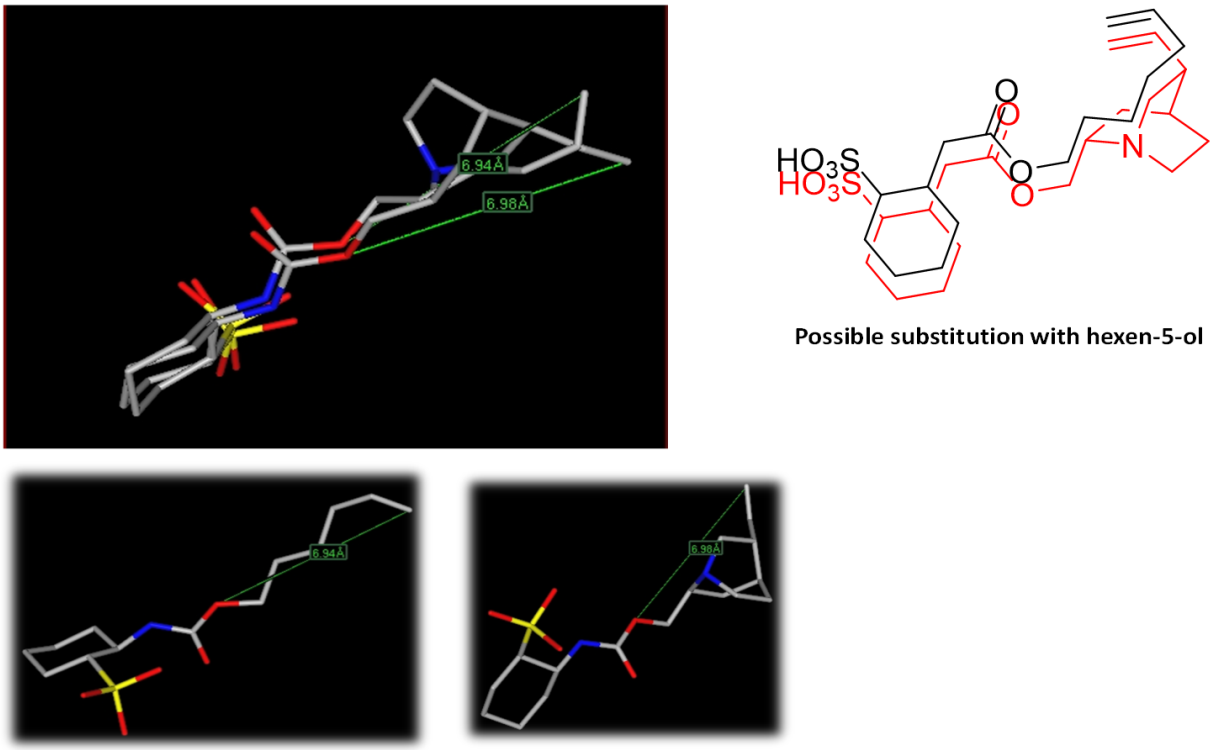

Fig. S7. 3D-alignment using MarvinSketch 14.12.15.0 of new derivative with hexen-5-ol chain and the quinuclidine precursor.

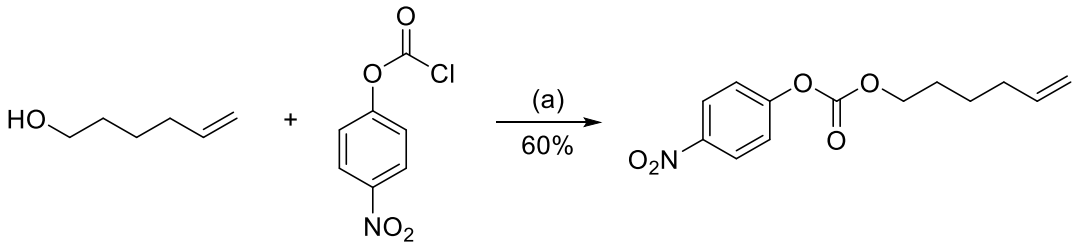

Fig. S8. Synthesis of hex-5-en-1-yl (4-nitrophenyl) carbonate. Reagents and conditions: (a) CH_2Cl_2, Et_3N, 0°C then r.t., 16h.

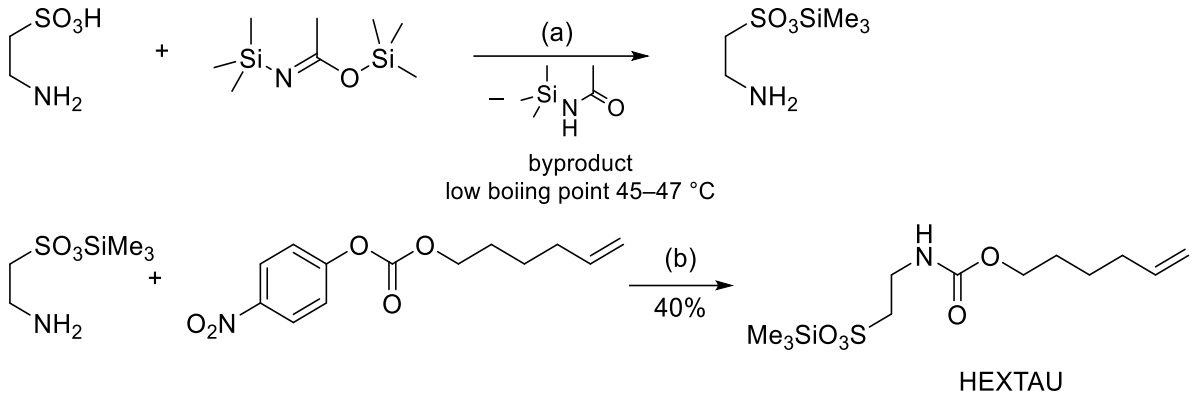

Fig. S9: Synthesis of 2-(((hex-5-en-1-yloxy) carbonyl) amino)ethane-1-sulfonic acid (HEXTAU) , Reagent and conditions: (a) CH_2Cl_2, BSA, reflux 48h, then (b) CH_2Cl_2, r.t., 16h.

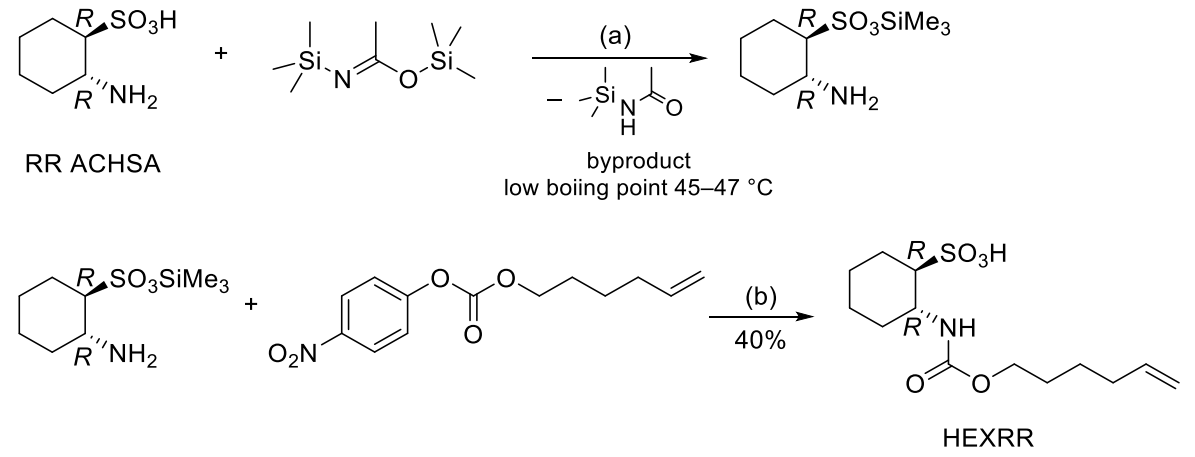

Fig. S10. Synthesis of (*1R,2R*)-2-(((hex-5-en-1-yloxy)carbonyl)amino)cyclohexane-1-sulfonic acid (HEXRR). Reagents and conditions: (a) CH_2Cl_2, BSA, reflux 48h, then (b)CH_2Cl_2, r.t., 16h.

4.5.7.1.1. Detailed Characterization of the Synthesized Selectors

*(2R,4S,5R)-2-{[(((1R,2R)-1-Sulfocyclohexyl)carbamoyl)oxy]methyl}-5-vinylquinuclidin-1-ium chloride (QCDRR, **4**)*

Starting from RR-ACHSA (1.07 g, 5.96 mmol) and **1** (2.20 g, 5.96 mmol) following the general procedure **B**, the title compound **4** was obtained as yellowish oil (2.7 g, yield 90%).

Specific rotation: + 15.77 (10 mg/mL in MeOH)

^{1}H-NMR (CD_3OD, 400 MHz): δ 1.24-1.37 (m, 3H), 1.49-1.64 (m, 3H), 1.78-1.80 (m, 2H), 1.89-1.92 (m, 2H), 2.03-2.11 (m, 4H), 2.35 (d, J_d = 13.6 Hz, 1H), 2.56 (td, J_t = 12.4 Hz, J_d = 4.0 Hz, 1H) 2.82 (q, J_q = 8 Hz, 1H), 3.36-3.39 (m, 3H), 3.50-3.54 (m, 1H), 3.81.3.85 (m, 2H), 5.23-5.29 (m, 2H), 5.91-6.00 (m, 1H) ppm.

^{13}C-NMR (CD_3OD, 100.6 MHz): δ 20.94, 22.90, 24.41, 24.91, 26.28, 27.41, 33.49, 36.56, 45.03, 50.50, 56.71, 59.31, 60.64, 63.14, 116.16, 136.71, 155.43 ppm.

HRMS (ESI-QTOF, negative mode): m/z calcd for $C_{17}H_{27}N_2O_5S$ $[M-H]^-$, 371.1641; found, 371.1630; HRMS (ESI-QTOF, positive mode): m/z calcd for $C_{17}H_{29}N_2O_5S$ $[M+H]^+$, 373.1797; found, 373.1814

*(2S,4S,5R)-2-{[(((1S,2S)-1-Sulfocyclohexyl)carbamoyl)oxy]methyl}-5-vinylquinuclidin-1-ium (QCISS, **5**)*

Starting from SS-ACHSA (1.07 g, 5.96 mmol) and **2** (2.20 g, 5.96 mmol) following the general procedure **B**, the title compound **5** was obtained as yellowish oil (2.3 g, yield 90%).

Specific rotation: + 20.00 (10 mg/mL in MeOH)

^{1}H-NMR (CD_3OD, 400 MHz): δ 1.28-1.41 (m, 4H), 1.45-1.57 (m, 1H), 1.78-1.80 (m, 2H), 1.89-1.91 (m, 2H), 1.97-1.99 (m, 2H), 2.08-2.11 (m, 1H), 2.15-2.24 (m, 1H), 2.33-2.37 (m, 1H), 2.56 (td, J_t = 10.8 Hz, J_d = 4 Hz, 1H), 2.80-2.87 (m, 1H), 3.14-3.22 (m, 1H), 3.28-3.30 (m, 1H), 3.58-3.65 (m, 3H), 3.81-3.92 (m, 2H), 5.24-5.31 (m, 2H), 5.93-6.00 (m, 1H) ppm.

^{13}C-NMR (CD_3OD, 100.6 MHz): δ 21.17, 23.45, 24.42, 24.92, 26.16, 27.42, 33.53, 36.70, 40.72, 50.53, 52.67, 56.75, 61.27, 63.13, 115.94, 137.70, 155.15 ppm.

HRMS (ESI-QTOF, negative mode): m/z calcd for $C_{17}H_{27}N_2O_5S$ $[M-H]^-$, 371.1641; found, 371.1619; HRMS (ESI-QTOF, positive mode): m/z calcd for $C_{17}H_{29}N_2O_5S$ $[M+H]^+$, 373.1797; found, 373.1795

*(2R,4S,5R)-2-{[((2-Sulfoethyl)carbamoyl)oxy]methyl}-5-vinylquinuclidin-1-ium chloride (QCDTAU, **6**)*

Starting from taurine (0.746 g, 5.96 mmol) and **1** (2.20 g, 5.96 mmol) following the general procedure **B**, the desired product **6** was obtained as yellowish oil (2.25 g, yield 90%).

Specific rotation: + 29.7 (10 mg/mL in MeOH)

^{1}H-NMR (CD_3OD, 400 MHz): δ 1.60-1.67 (m, 1H), 2.01-2.11 (m, 4H), 2.81-2.84 (m, 1H), 2.91 (t, J_t = 5.20 Hz, 1H), 2.97-3.01 (m, 1H), 3.36-3.54 (m, 4H), 3.65-3.85 (m, 2H), 4.16-4.47 (m, 2H), 5.22-5.29 (m, 3H), 5.91-6.00 (m, 1H) ppm.

^{13}C-NMR (CD_3OD, 100.6 MHz): δ 21.03, 22.89, 26.31, 36.64, 36.92, 51.13, 56.73, 59.32, 60.76,´61.12, 116.49, 136.64 ppm.

HRMS (ESI-QTOF, negative mode): m/z calcd for $C_{13}H_{21}N_2O_5S$ $[M-H]^-$, 317.1171; found, 317.1165; HRMS (ESI-QTOF, positive mode): m/z calcd for $C_{13}H_{23}N_2O_5S$ $[M+H]^+$, 319.1328; found, 319.1321

*(2S,4S,5R)-2-{[((2-Sulfoethyl)carbamoyl)oxy]methyl}-5-vinylquinuclidin-1-ium (QCITAU, **7**)*

Starting from taurine (0.746 g, 5.96 mmol) and **2** (2.20 g, 5.96 mmol) following the general procedure **B**, the desired product **7** was obtained as a yellowish oil (1.73 g, yield 90%).

Specific rotation: + 6.77 (10 mg/mL in MeOH)

^{1}H-NMR (CD_3OD, 400 MHz): δ 1.31-1.44 (m, 1H), 2.00 (m, 2H) 2.06-2.25 (m, 2H), 2.88 (m, 1H), 2.92 (t, J_t = 4 Hz, 1H), 3.00 (t, J_t = 8 Hz, 1H), 3.22-3.28 (m, 2H) 3.54-3.69 (m, 4H), 3.74-3.85 (m, 1H), 4.22-4.39 (m, 2H), 5.26 (t, J_t = 12 Hz, 2H), 5.94-6.03 (m, 1H) ppm.

^{13}C-NMR (CD_3OD, 100.6 MHz): δ 21.26, 23.44, 26.10, 36.71, 36.91, 49.85, 51.12, 52.71, 56.61, 61.46, 116.05, 137.60 ppm.

HRMS (ESI-QTOF, negative mode): m/z calcd for $C_{13}H_{21}N_2O_5S$ $[M-H]^-$, 317.1171; found, 317.1169; HRMS (ESI-QTOF, positive mode): m/z calcd for $C_{13}H_{23}N_2O_5S$ $[M+H]^+$, 319.1328; found, 319.1309

*(1S,2S)-2-{[(Hex-5-en-1-yloxy)carbonyl]amino}cyclohexane-1-sulfonic acid (SS-ACHSA, **8**)*

Starting from SS-ACHSA (1.00 g, 5.58 mmol) and **3** (2.05 g, 7.76 mmol) following the general procedure **B**, the title compound **8** was obtained as yellowish oil (0.4 g, yield 40%).

^{1}H-NMR (CD_3OD, 400,MHz): δ=8.24 (bp,OH), 5.81 (m,5H), 4.95 (dd,2H), 3.99 (d,2H), 3.32 (m,1H), 2.36 (m,1H), 2.10 (m,2H), 1.83 (m,2H), 1.65 (m,2H), 1.51 (m,2H), 1.51 (m,2H), 1.51 (m,2H), 1.35 (m,2H) ppm

^{13}C-NMR (CD_3OD, 400,MHz):δ=164.39, 140.11, 115.35, 63.98, 51.25, 49.25, 46.51, 36.62, 33.19, 28.60, 25.12, 25.09, 22.87 ppm

HRMS (ESI-QTOF, negative mode): m/z calcd for $C_{13}H_{22}NO_5S$ $[M-H]^-$, 304.1219; found, 304.1225

*2-{[(Hex-5-en-1-yloxy)carbonyl]amino}ethane-1-sulfonic acid (TAU, **9**)*

Starting from taurine (1.30 g, 10.10 mmol) and **3** (2.05 g, 7.76 mmol) following the general procedure **B**, the title compound **9** was obtained as yellowish oil (0.25 g, yield 20 %).

^{1}H-NMR (DMSO-d6, 400 MHz): δ 9.24 (bp, OH), 6.56 (bp, NH), 5.78 (m, 5H), 4.90 (dd, 2H), 3.90 (t, 3H), 3.25 (m, 2H), 2.58 (m, 2H), 2.047 (m, 2H), 1.53 (m, 2H), 1.37 (m, 2H) ppm.

^{13}C-NMR (DMSO-d6, 100MHz): δ 164.43, 138.94, 115.37, 63.79, 51.08, 46.22, 37.62, 28.60, 25.09 ppm.

HRMS (ESI-QTOF, negative mode): m/z calcd for $C_9H_{16}NO_5S$ $[M-H]^-$, 250.0749; found, 250.0742

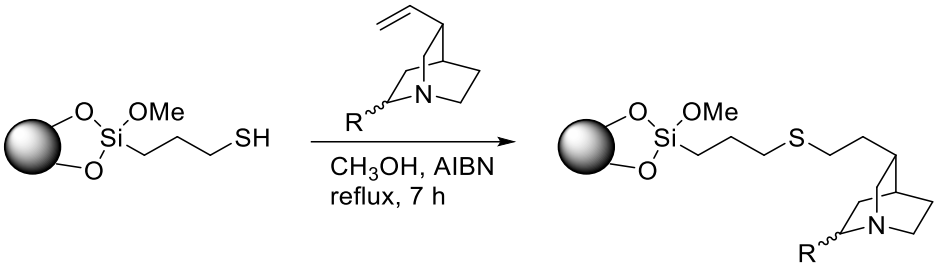

Fig. S11: Synthesis scheme for the immobilization of the selectors.

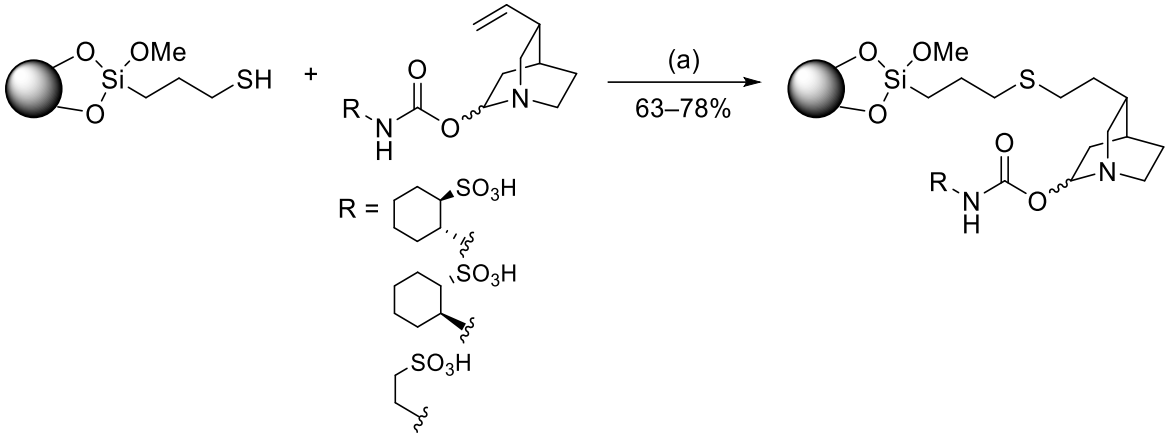

Fig. S12: Thiol-ene-click reaction to obtain immobilized derivatives. Reagents and conditions: a) MeOH, AIBN, reflux, 7h.

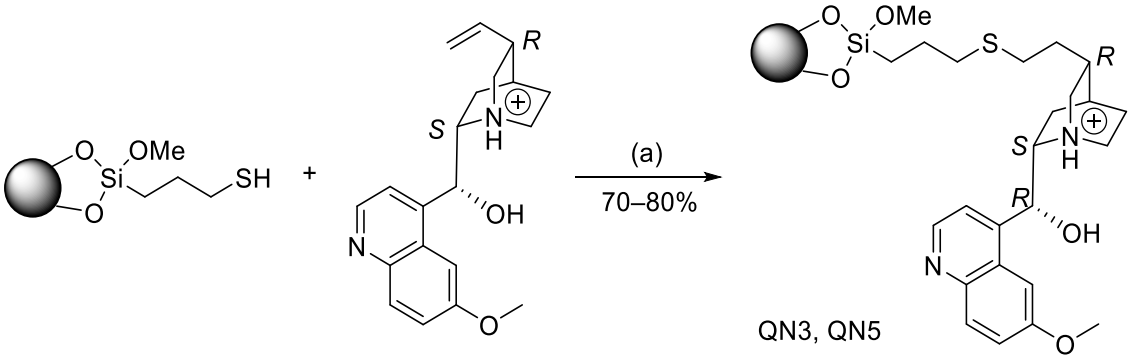

Fig. S13. Thiol-ene-click reaction to obtain immobilized derivative (QN3, QN5). Reagents and conditions: a) MeOH, AIBN, reflux, 7h.

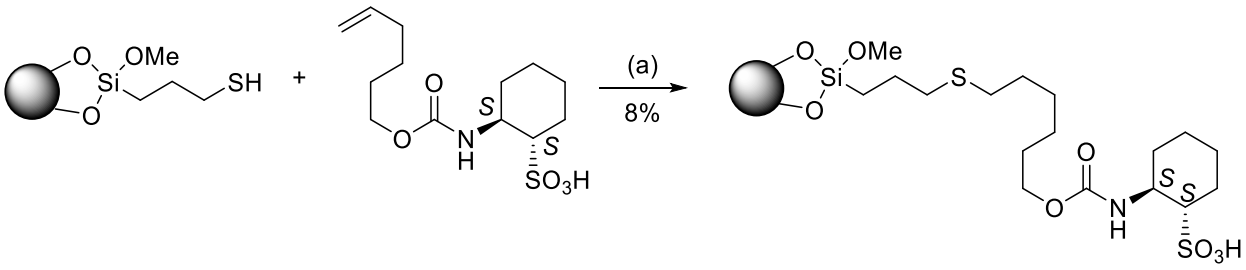

Fig. S14. Thiol-ene-click reaction to obtain immobilized derivative. Reagents and conditions: a) MeOH, AIBN, reflux, 7h.

4.5.7.1.2. Synthesis Control by MS Analysis

The chromatographic separation for the structure elucidation was performed on a Kinetex C18, 50 x 2.1 mm, 2.7 µm column (Phenomenex, Torrance, CA, USA). The measurement was carried out with 0.1% FA in acetonitrile and water with the following gradient profiles. The gradient, which was used for structure elucidation via UHPLC-QTOF-MS/MS (Agilent 1290 UHPLC instrument coupled to Triple TOF 5600+ from Sciex with CTC Pal autosampler), started at 5% B and increased to 95% B in 4.0 min and to 99% B in additional 0.5 min, followed by re-equilibration with 5% B for 1.5 min. The electrospray (ESI) settings were chosen as follows: curtain gas (CUR): 30, Ion Source Gas 1 (GS 1): 50 and Ion Source Gas 2 (GS 2): 40, IonSpray Voltage Floating (ISVF) 4500 and temperature was 500 °C. The QTOF was operated in negative mode and the m/z range 30 to 2000 was scanned. The TOF experiment had an accumulation time of 100 ms and was combined with 20 TOF MS2 experiments using information dependent acquisition (IDA) leading to a period cycle time of 551 ms.

4.5.7.1.3. Characterization of Modified Silica Gels by FTIR-Spectroscopy

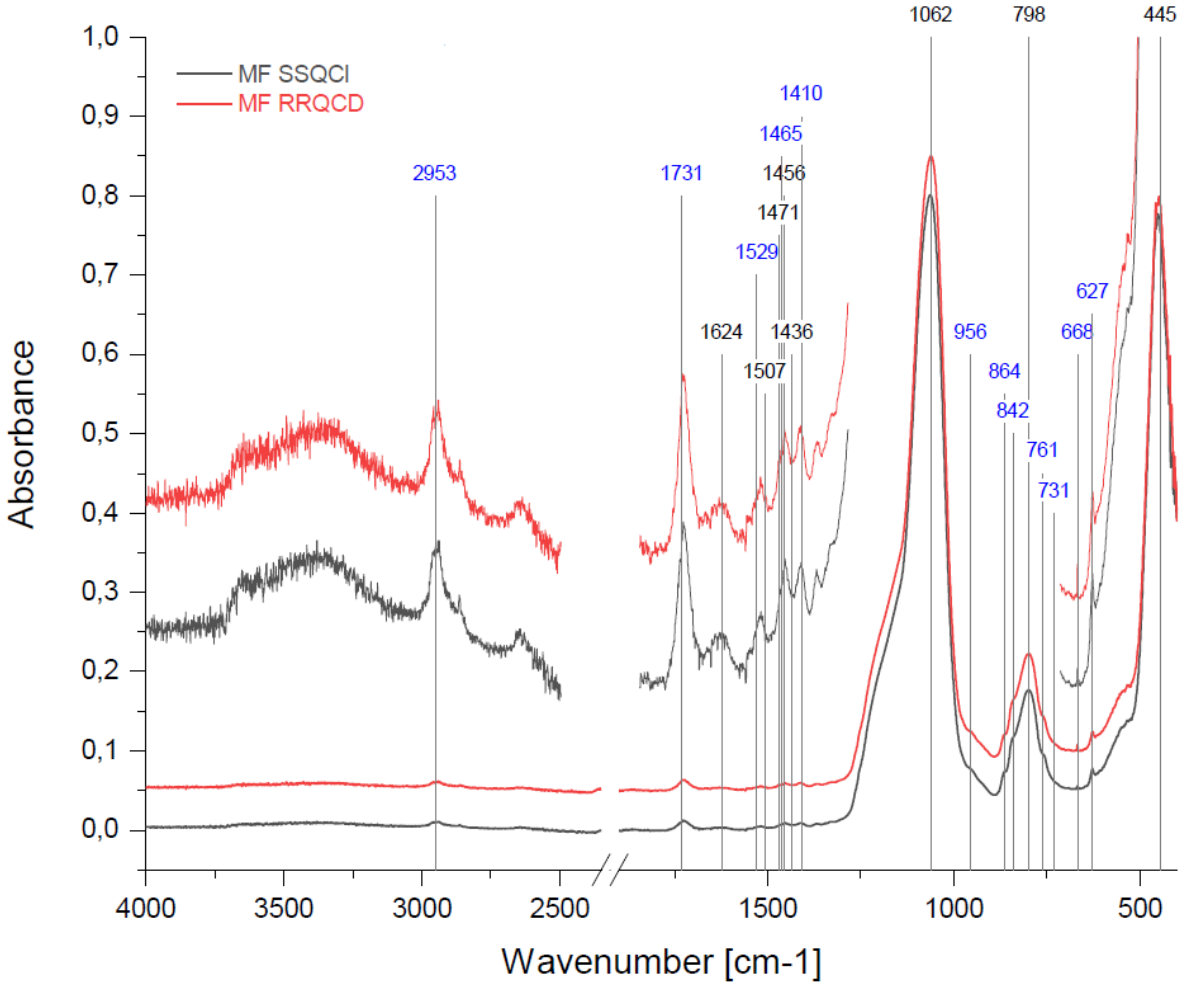

Fig. S15. FTIR spectra of the two RP/ZWIX MMC phases QCISS (black) and QCDRR (red). The IR-band at 1731 cm-1 is the C=O stretching vibration of the carbamate group and indicates successful immobilization of the corresponding zwitterionic ligands.

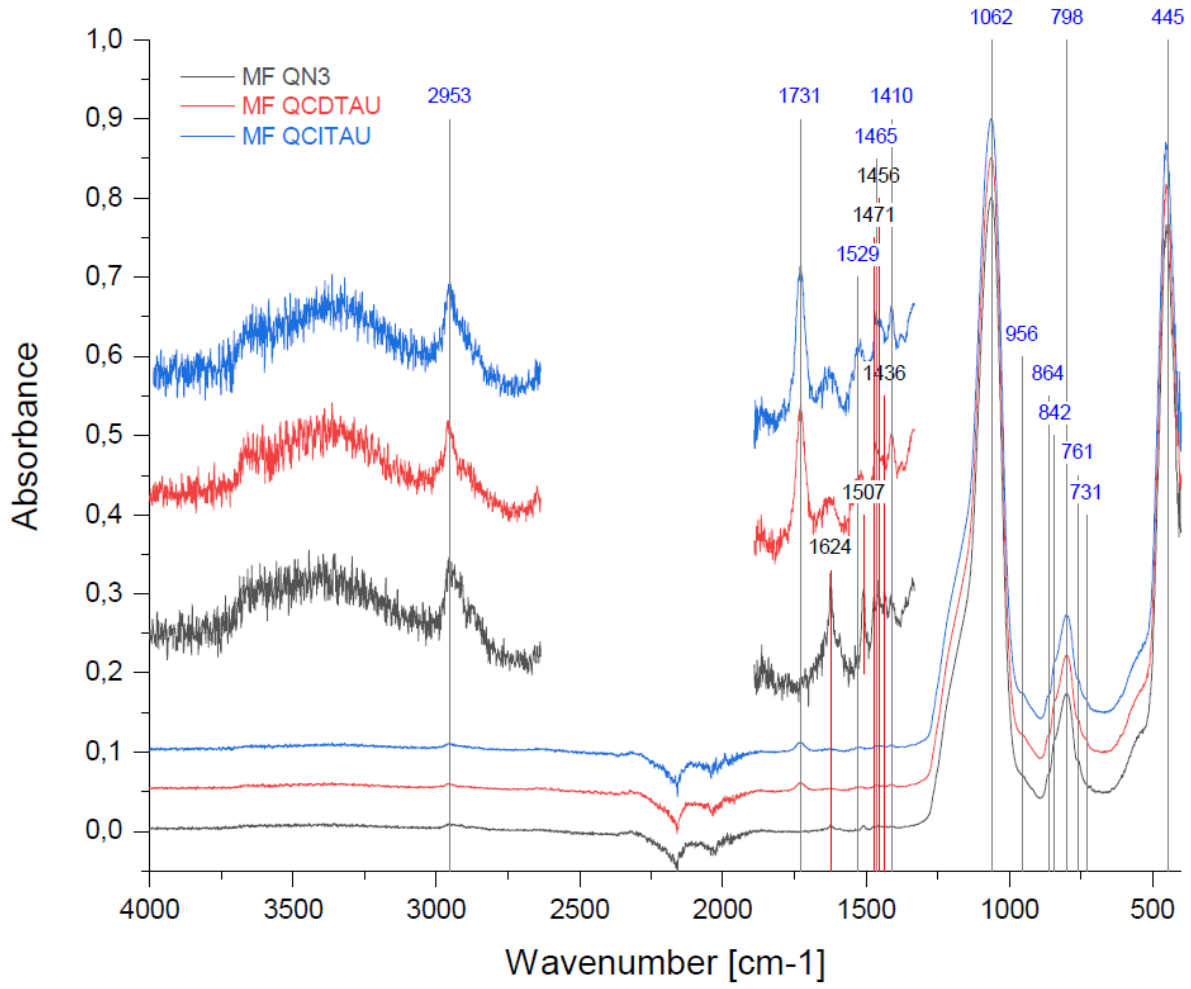

Fig. S16. FTIR spectra of the two RP/ZWIX MMC phases QCITAU (blue) and QCDTAU (red) as well as of the WAX-type QN phase (black). The IR-band at 1731 cm^{-1} is the C=O stretching vibration of the carbamate group and indicates successful immobilization of the corresponding zwitterionic ligands while this band is absent for QN which has no carbamate group. The band at 1624 cm^{-1} of the QN material indicates the C=C stretching vibration of the quinoline ring which is absent in the zwitterionic QCITAU and QCDTAU.

4.5.7.2. ζ-Potential Determination

Helmholtz-Smoluchowski equation:

$$\mu_E = C\frac{\varepsilon_0 \cdot \varepsilon_r \cdot \zeta}{\eta} \qquad \text{Equ. S1}$$

μ_E: mobility of a particle

C: The constant C becomes 2/3 for $\kappa r<0.1$ (κ, Debye parameter; κ^{-1}, Debye length) (Hückel approximation) and 1 for $\kappa r>100$ (Smoluchowski approximation).

ε_R: relative permittivity

ε_0: permittivity of vacuum

η: viscosity

4.5.7.3. Chromatographic Characterization under HILIC and RP Conditions for Column Classification

4.5.7.3.1. Material and Methods

The stationary phases which were included in the test set for the evaluation of the chromatographic properties comprised all stationary phases depicted in Fig S2. The RP-HPLC separations were carried out using a mobile phase consisting of ACN/H_2O (2:3, v/v) and 0.29 % acetic acid (C_{tot} = 50 mM). The apparent pH value was adjusted to 6 with ammonia in the polar organic mixture. The mobile phases of the HILIC measurements consisted as follows: The organic modifier ACN was mixed with water in the ratio 95:5 (v/v) for the analysis of xanthines and 90:10 (v/v) for the nucleosides and vitamins, containing ammonium acetate (5 mM referred to the total volume) as buffer. The pH was not adjusted and remained at approximately 8 in the polar organic mixture. The mobile phase was used for dissolving the analytes. For the RP test the concentration was 0.8 mg mL^{-1} (injection volume 5 µL) and for the HILIC tests 1.0 mg mL^{-1} (injection volume 2 µL). The flow rate was 1.7 mm s^{-1} at 25°C. The detection wavelength was 220 nm. The void volume was determined with uracil (RP) and toluene (HILIC).

4.5.7.3.2. Commercial Columns of Benchmarking Study

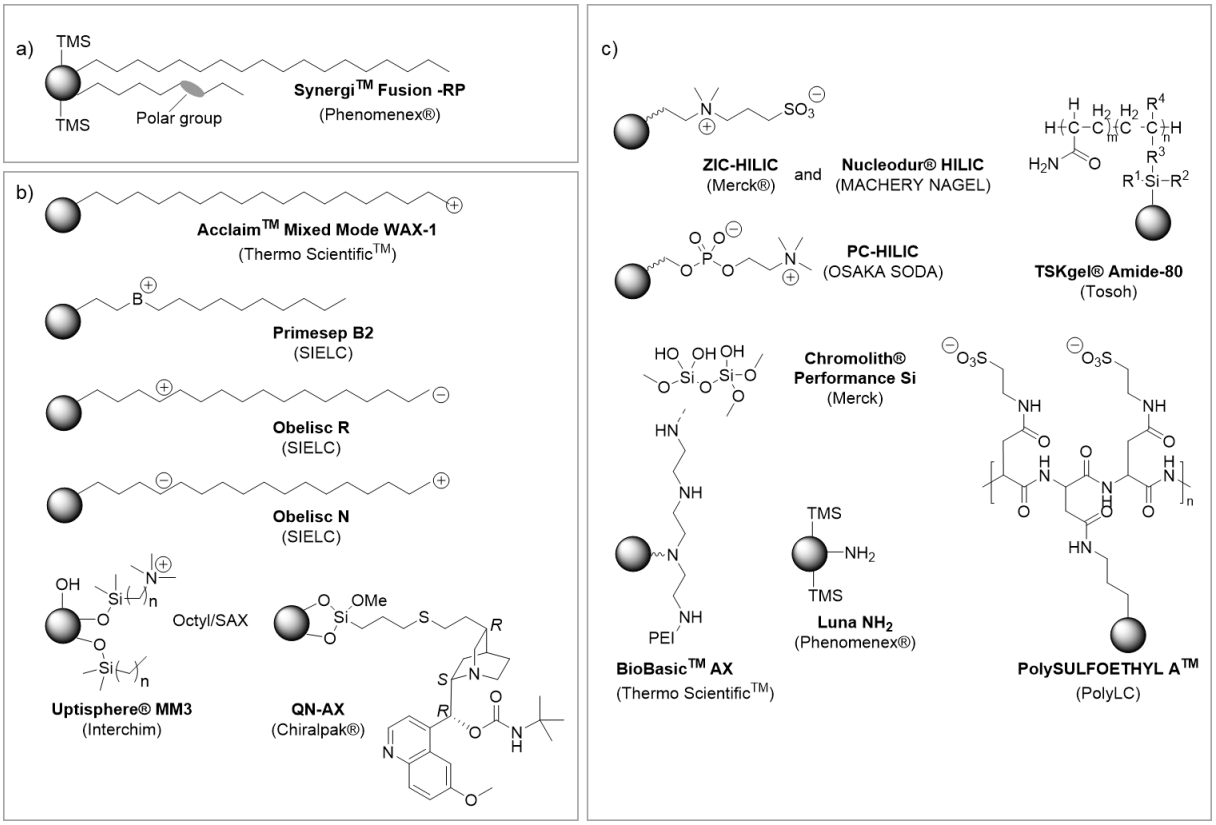

Fig. S17: Surface structure of investigated a) RP, b) mixed mode and c) HILIC stationary phases which were chromatographically evaluated for the principal component analysis.

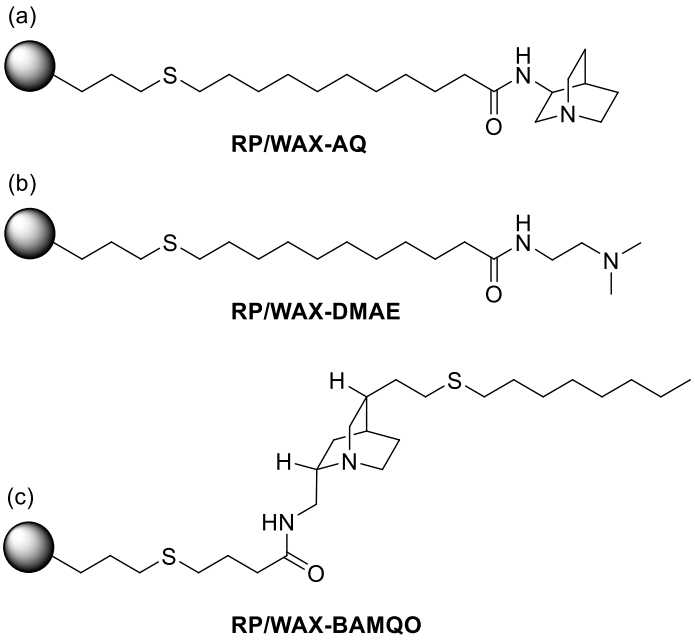

Fig. S18: Surface structures of investigated non-commercial RP/WAX mixed mode phases.

4.5.7.4. Molecular Modeling

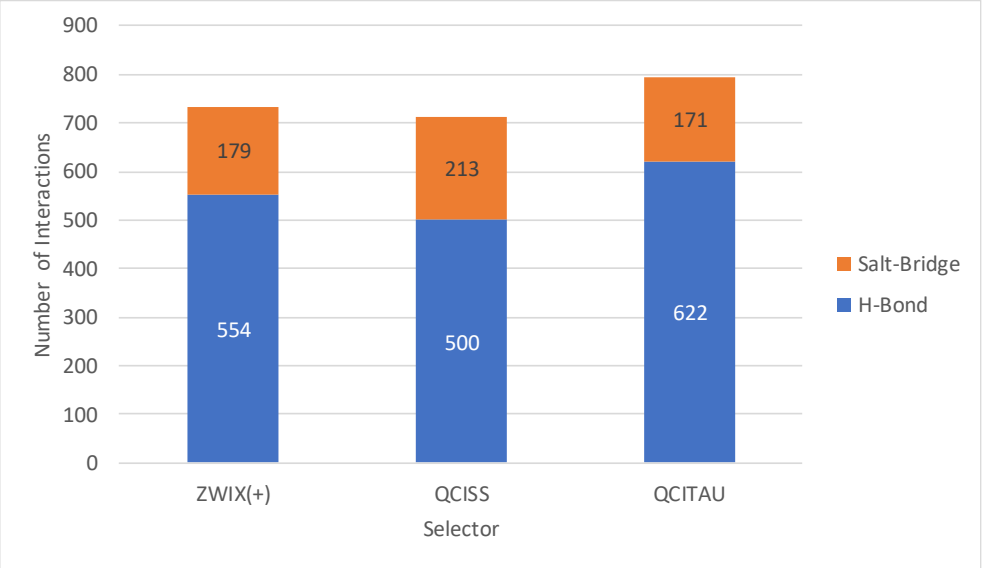

Fig. S19: Intramolecular interaction count (salt-bridges and H-bonds) measured for all the 3000 conformations extracted for each selector by the molecular dynamics trajectories. The single contribution of each interaction type is also reported inside the bar.

5. Acknowledgements

Foremost, I would like to express my deepest gratitude to my supervisor Prof. Dr. Michael Lämmerhofer for giving me the opportunity to work on these interesting research topics under his guidance. I want to thank for the numerous scientific discussions, the advice and the outstanding mentoring. Furthermore, I appreciated the possibility to attend advanced trainings and conferences.

Moreover, I would like to thank Prof. Dr. Stefan Laufer for the second supervision and Jun.-Prof. Dr. Matthias Gehringer for the review of this doctoral thesis.

I want to thank Prof. Dr. Carolin West, Prof. Dr. Tohru Ikegami, Prof. Dr. Wolfgang Lindner, Prof. Dr. Orlando L. Sánchez-Muñoz, Assoc. Prof. Dr. Andrea Carotti, Assoc. Prof. Dr. Roccaldo Sardella, Dr. Wolfgang Bicker, Dr. Markus Kramer, Dr. Martina Ferri and Johannes Theiner for the successful collaboration.

Additionally, I want to thank Dr. Jeannie Horak and Dr. Stefan Neubauer who were always willing to help theoretically and practically with their experience in analytical chemistry. Additionally, I want to thank my former colleagues Dr. Aleksandra Zimmermann, Dr. Stefan Polnick, Dr. Ulrich Woiwode, Belal Alshaar and Wenkai Guo and my current colleague Marc Wolter who worked together with me on projects presented in this work.

Many thanks to my current colleagues Dr. Adrian Sievers-Engler, Dr. Bernhard Drotleff, Christian Geibel, Marc Wolter, Kristina Dittrich, Ryan Karongo, Ece Aydin, Peng Li, Feiyang Li, Simon Jaag, Xiaoqing Fu and Matthias Olfert and my former colleagues Corinna Sanwald, Dr. Jörg Schlotterbeck, Dr. Carlos Caldéron-Castro, Maglorzata Cebo, Dr. Markus Höldrich, Dr. Siyao Lui and Mike Kaupert for the interesting discussions and the time we spent together in the laboratory in the past years.

Additionally, I am grateful for the help of Eveline Wachendorfer and Ingrid Straub who supported in administrative concerns.

Furthermore, I want to thank my friends and my family, in particular, my mother Bianka, who supported and encouraged me without restriction during my studies but also during this PhD thesis, my sister Denise and brother Nico who motivated and supported me.